THÈSE DE DOCTORAT

présentée et soutenue publiquement à

L'UNIVERSITE DE LILLE

Ecole doctorale des Sciences Pour l'Ingénieur (EDSPI)

pour obtenir le grade de

DOCTEUR

Spécialité: Mécanique Energétique Matériaux

par

Neeraj Kumar MANDLEKAR

Integration of wood waste to develop multifunctional fully biobased textile structure

Intégration des déchets de bois pour développer une structure textile multifonctionnelle entièrement biosourcée

---

Thèse en cotutelle avec l'Université de Soochow (Chine)

Soutenue le 26 septembre 2019 devant la commission d'Examen composée de:

Fouad LAOUTID	Chargé de Recherche, Materia Nova, Belgique	Rapporteur
Henri VAHABI	Maitre de Conferences, Université de Lorraine, France	Rapporteur
Gaelle FONTAINE	Professeur des Universités, ENSC- Lille, France	Président
Vanessa FIERRO	Directeur de Recherche, IJL-UMR CNRS, France	Examinateur
Fabien SALAUN	Professeur, ENSAIT-GEMTEX, France	Directeur de thèse
Jinping GUAN	Professeur, Soochow University, China	Co-directeur de thèse

Integration of wood waste to develop multifunctional fully biobased textile structure

Ph.D. Thesis defended at

L'UNIVERSITE DE LILLE

Ecole doctorale des Sciences Pour l'Ingénieur (EDSPI)

by

Neeraj Kumar MANDLEKAR

in partial fulfilment of Erasmus Mundus joint Doctorate program: SMDTex – *Sustainable Management and Design for Textiles*

in collaboration with

ENSAIT, GEMTEX – Laboratoire de Génie et Matériaux Textiles, France
University of Lille – Department of Materials and Mechanics, France
Politecnico di Torino – Department of Chemical Engineering, Italy
Soochow University – Department of Textile Engineering, China

Abstract

This thesis work was developed within the Erasmus Mundus SMDTex (sustainable management and design for textile) project, which aims to promote sustainable processes and materials for designing the textile. In this context, it has been chosen to study valorization of low-cost industrial lignin as additive in designing the flame retardant (FR) system for polyamide 11 (PA) to develop biobased textile structure. The main focus of this thesis work is to consider lignin as carbon source and introduce in a textile structure in combination with phosphinate FR. In the primary study, chemically different industrial (e.g., Domsjo lignosulphonate (LL) and Domtar kraft (DL)) and laboratory grade (e.g., Low sulphonate kraft (LS) and Alkali kraft (KL)) lignins were incorporated in PA by extrusion to investigate the char forming ability and fire retardant behaviour of the prepared binary blends. TG analyses showed a slow degradation of sulphonated lignin (LL and LS) blends due to the evolution of less organic products and the presence of sulphonate groups in LL and LS was responsible for the formation of a thermally stable higher amount of char residue. Unlike sulphonated lignins, the presence of kraft lignins (DL and KL) generate a lower amount of char residue due to the presence of less thermally stable lignin subunits that produce more volatile products during degradation. In addition, cone calorimeter tests showed the introduction of sulphonated lignins significantly reduced the peak of the heat release rate (PHRR) and of the total heat release (THR), and a noticeable increase in the final char residue was observed with an increased lignin content of 20 wt%.

In the next approach, lignin was exploited as carbon source in combination with commercially available phosphinate FR (i.e., ZnP and AlP). To achieve this objective, a preliminary study carried out with laboratory grade lignin (LS) combined with ZnP to investigate the thermal stability and fire performance as well as the possible synergy between lignin and ZnP and with the polymer matrix. The results obtained in this study permitted to

continue further, the practical implementation of lignin and multifilament production. In the next step, flame retarded blends were developed with direct addition of low-cost industrial lignins (LL and DL) with phosphinate FR. For the systematic understanding, various FR formulations were developed by varying the lignin and FR loading and characterized.

Thermal decomposition analysis showed that the presence of lignin decreases the initial decomposition temperature ($T_{5\%}$), but the maximum decomposition temperature (T_{max}) shifts to higher temperature region, at this stage the formation of phenolic, carbonyls, hydrocarbons and CO_2 along with phosphinate compounds occurs. Meanwhile, in the condensed phase thermally stable aromatic charred layer is formed because of lignin decomposition and phosphate compounds formation due to the presence of phosphinate metal salt. A higher amount of char residue is obtained when LL combined with ZnP/AlP as compared to the DL and ZnP/AlP blends. It is assumed that, during decomposition of LL, the sulfonate compounds release SO_2 and transformed into thermally stable Na_2SO_4, hence giving rise to the stable char residue.

The fire properties were assessed by cone calorimeter tests revealed that the combination of lignin and phosphinate FR significantly reduced the PHRR and other fire-related parameters due to the formation of a protective char layer. The presence of lignin not only improve the fire retardancy but also reduced the evolution of carbon monoxide (CO). More enhanced fire retardant properties were obtained with LL and ZnP/AlP combination reaches to 10 wt% in ternary blends, which not only promotes char formation but also confer the stability to char in the condensed phase. Furthermore, the most enhanced forced combustion results were obtained with LL and AlP (in particular, PA_{80}-LL_{10}-AlP_{10}).

Multifilament yarns were successfully produced for PA-DL-ZnP and PA-LL-ZnP combinations. However, the blends of AlP with lignin were not spinnable because of low compatibility and dispersion level of AlP in the polymer. Optical microscopy and tensile tests were performed to study the physical properties of multifilaments. A double layer (interlock structure) knitted fabrics were developed to evaluate fire behaviour analysis on fabric samples.

In summary, this work confirms that industrial lignin can be directly used in the polymer matrix and offers the possibility of developing biobased fire retardant textile. The concept of developing biobased flame retardant composite and the textile structure was an attempt to reduce the dependency on oil-based resources and to develop the non-halogenated flame retardant with the favorable environmental profile. It was possible to gain the biobased character up to 90 wt% in the final product.

Résumé

Ce travail de thèse a été réalisé dans le cadre du projet Erasmus Mundus SMDTex (Sustainable Management and Design for Textile), qui vise à promouvoir des procédés et des matériaux durables pour la conception du textile. Dans ce contexte, il a été choisi d'étudier la valorisation de la lignine industrielle à faible coût en tant qu'additif retard au feu (FR) du polyamide 11 (PA) afin de développer une structure textile biosourcée. L'objectif principal de cette thèse est de considérer la lignine comme source de carbone carbone permettant de créer un bouclier protecteur (char) sous l'effet d'un flux thermique et de l'introduire dans une structure textile en combinaison avec du phosphinate (agent FR)

Dans un premier temps, deux lignines industrielles (lignosulfonate de Domsjo (LL) et Domtar kraft (DL) de qualités différentes) et deux deux lignines de qualité laboratoire (kraft à faible teneur en sulfonate (LS) et alkali kraft (KL)) ont été incorporées par extrusion au PA afin de comparer leur propriété FR et leur aptitude à la formation de char. Les analyses thermogravimétriques des mélanges binaires ont montré que la lente dégradation des lignines sulfonée (LL et LS) et la présence de leur groupe sulfonate entraîne la formation d'une quantité supérieure de résidu carboné thermiquement stable. Contrairement aux lignines sulfonées, la présence de lignines kraft (DL ou KL) génère une quantité plus faible de résidu carboné en raison de la présence de sous-unités de lignine moins stables thermiquement qui produisent des produits plus volatils lors de la dégradation. En outre, des tests au calorimètre à cône ont montré que l'introduction de lignines sulfonées réduisait de manière significative le pic de dégagement de chaleur (PHRR) et le dégagement total de chaleur (THR), et qu'une augmentation notable du résidu carboné était observée avec un taux de 20% en poids de lignine.

Dans un deuxième temps, la lignine a été exploitée en tant que source de carbone en combinaison avec du phosphinate de zinc (ZnP) ou d'aluminium (AlP) disponibles dans le commerce. Pour atteindre cet objectif, une étude préliminaire a été réalisée avec la lignine de

laboratoire LS combinée à du ZnP, afin d'étudier la stabilité thermique et les performances au feu, ainsi que les synergies possibles entre la lignine, le ZnP et le PA. Dans l'étape suivante, des mélanges ignifugés ont été développés avec l'addition directe de lignines industrielles à faible coût (LL et DL) et d'agents ignifuges phosphinatés. Pour la compréhension systématique, diverses formulations de FR dans le PA ont été développées en faisant varier le taux de charge en lignine et en FR et ont été caractérisées.

L'analyse de la décomposition thermique a montré que la présence de lignine abaisse la température initiale de décomposition ($T_{5\%}$) compte tenu de la décomposition de la lignine qui débute à une plage de température inférieure avec l'évolution de composés thermiquement moins stables, et la température maximal de décomposition (T_{max}) est déplacée à une plage de température plus élevée, car à ce stade se produit la formation de composés phénoliques, carbonylés, hydrocarbures et de CO_2, ainsi que de composés phosphinates. Pendant ce temps, il se forme dans la phase condensée une couche carbonée aromatique thermiquement stable, en raison de la décomposition de la lignine et de la formation de composés phosphates issus de la décomposition du sel métallique de phosphinate. On obtient une plus grande quantité de résidu carboné lorsque la LL est combiné avec ZnP/AlP par rapport aux mélanges de DL et ZnP/AlP. Il est supposé que, lors de la décomposition de la LL, les composés sulfonates libèrent du SO_2 et se transforment en Na_2SO_4 thermiquement stable, donnant ainsi lieu au résidu de carbonisation stable.

Les propriétés au feu ont été évaluées par un calorimètre à cône. Les essais ont révélé que la combinaison de lignine et d'agents ignifuges phosphinatés réduisait de manière significative le PHRR et autres paramètres liés au feu de par la formation d'une couche carbonée protectrice. La présence de lignine améliore non seulement la résistance au feu, mais réduit également le dégagement de monoxyde de carbone (CO). Des propriétés ignifuges améliorées ont été obtenues avec la combinaison LL et ZnP/AlP atteignant 10% en poids dans les mélanges ternaires, par la formation d'une couche carbonée thermiquement résistante et efficace pour protéger le reste de la phase condensée. De plus, les meilleurs comportements au feu pour le PA ont été obtenus avec les mélanges LL et AlP, en particulier, avec 10% en masse de chaque charge.

Des multifilaments ont été produits avec succès pour les combinaisons PA-DL-ZnP et PA-LL-ZnP. Toutefois, les mélanges de AlP avec de la lignine n'étaient pas filables en raison de la faible compatibilité et du faible niveau de dispersion du AlP dans le polymère. Des observations au microscopie optique et des tests de traction ont été réalisés pour étudier les propriétés physiques des multifilaments. Des structures tricotées (interlock) ont été produites à partir des différents multifilaments pour évaluer leur comportement au feu.

En résumé, ces travaux confirment que la lignine industrielle peut être directement utilisée dans la matrice polymère et offre la possibilité de développer un textile ignifuge biosourcé, réduisant ainsi la dépendance vis-à-vis des ressources fossiles. Il est possible d'obtenir le caractère biosourcé jusqu'à 90% en poids dans le produit final.

中文摘要

本研究工作依托Erasmus Mundus SMDTex (纺织品可持续管理和设计)项目展开，旨在促进纺织品设计过程中工艺和材料的可持续性。在此背景下，本论文选用成本较低的工业化木质素作为添加剂提高聚酰胺11的阻燃性能，从而实现木质素的高值化利用。本论文主要利用木质素作为炭源与阻燃剂次膦酸盐结合提高纺织材料的阻燃性能。文中首先通过挤出法将化学结构不同的工业木质素(i.e., Domsjo lignosulphonate (LL) and Domtar kraft (DL))和实验室用木质素(low sulphonate kraft (LS) and Alkali kraft (KL))与聚酰胺分别共混挤出双组分混合物，并探究双组分复合物的成炭性和阻燃性能。热分析结果表明，磺化木质素(LL和LS)在加热过程中释放的有机物质较少，且磺化基团的存在使得LL和LS具有较高的残炭量，因此磺化木质素复合材料的热分解较为缓慢。与磺化木质素不同，木质素硫酸盐DL和KL中热稳定的木质素结构较少，在加热过程中产生较多的挥发性物质，因此木质素DL和KL的加入导致复合材料成炭较少。此外，磺化木质素的加入可明显降低材料的热释放速率(PHRR)和热释放总量(THR)，并提高材料的残炭量。

接着，采用木质素作为炭源与商业化的阻燃剂次膦酸盐(如ZnP和AlP)相结合提高材料的阻燃性能。因此，在前期实验中利用实验室用木质素(LS)与ZnP相结合制备阻燃体系，并对复合材料的热稳定性、阻燃性能以及木质素、ZnP和基质材料间可能存在的协同效应进行探究。根据上述研究的结果进行下一步木质素和复丝的实际生产。随后，通过直接添加低成本的工业木质素(LL和DL)与次膦酸盐阻燃剂制备阻燃复合材料。通过改变木质素和次膦酸盐阻燃剂的添加比例对阻燃体系的阻燃性能进行系统的探究。

热分析结果表明，木质素的存在导致材料的初始热分解温度($T_{5\%}$)降低，因为木质素的初始分解温度较低，分解产生热稳定性低的化合物，最大热分解时对应的温度(T_{max})向高温区域移动，而在此阶段木质素分解产生一系列酚类、羰基化合物、碳氢化合物、CO_2和磷酸盐化合物。与此同时，木质素和次膦酸金属盐分解生成磷酸盐化合物，导致固相中产生热稳定性高的芳香炭层。与DL和ZnP/AlP共混物相比，LL和ZnP/AlP共混物的残炭量更高，因为LL的磺酸基在热分解过程中释放SO_2并转化成热稳定的Na_2SO_4，促进热稳定残炭的形成。

通过锥形量热仪测试对材料的阻燃性能进行评价，结果表明由于保护性炭层的形成，木质素和次膦酸盐阻燃剂相结合可明显降低材料的最大热释放速率和其它火灾危险性相关参数。木质素的存在不仅改善了材料的阻燃性能，也降低了一氧化碳的释放。当LL和ZnP/AlP阻燃体系的添加量为10wt%时可促进热稳定性残炭的形成，复合材料可获得较高的阻燃性能。此外，当LL和AlP相结合作为阻燃体系时，复合材料(特别是PA_{80}-LL_{10}-AlP_{10})阻燃性能的提高更为明显。

本研究成功地制备了PA-DL-ZnP和PA-LL-ZnP复合尼龙丝。但由于AlP在聚合物中的相容性和分散性较低，AlP与木质素的共混物无法用于纺丝。利用光学显微镜和拉伸试验对复合丝的物理性能进行探究。通过制备双层(互锁结构)针织物以评价相关纺织材料的阻燃性能。

综上，本研究证明工业木质素可直接与聚合物混合，并为生物基阻燃纺织材料的开发提供可能。生物基阻燃复合材料和纺织材料的开发有助于降低对石油资源的依赖，有助于开发环境友好型的无卤阻燃剂。最终产品的生物基特征可高达90 wt%。

Acknowledgments

PhD study through SMDTex program was one of the most memorable journeys of my life. I would like to thank all of them who helped me directly or indirectly. First of all, I would like to express my gratitude to my supervisors and co-supervisors from all three mobility; Prof. Fabien Salaun, Dr. Stephene Giraud, Dr. Francois Rault and Dr. Aurelie Cayla from ENSAIT-GEMTEX, who guided me to the right direction, to begin with, this research. It is greatly fortunate for me to have them as the advisor of the Ph.D thesis. I would also like to thank Prof. Giulio Malucelli and Fabio Cuttica for providing lab facility for fire characterization at Politecnico di Torino. I would also like to thank Prof. jinping Guan and Prof. Yan Chen for their research guidance not only in Soochow University but also in previous mobilities. I would like to express my thanks to all the staff of ENSAIT and the GEMTEX, in particular to Guillaume Lemort and Sabine for their technical support. I would like to sincerely thanks to Marie Hombert for helping to go through non-technical issues during my first mobility in ENSAIT, Roubaix, France.

Furthermore, I would like to express my thanks to Dr. Hans Grundberg and Dr. Kristina from Domsjo Fabriker AB, Sweden and Dr. Christian Hubsch from UPM Biochemicals for kindly providing industrial lignin for this research project. Special thanks to my SMDTex colleagues, Jagadish Roy, Vijay Kumar, Sohail Yasin, Tarun Agarwal, Parag Bhavsar, Sweta Iyer for having a technical conversation and discussing our research. I would appreciate and thanks to friends whom I met during my PhD journey, Hossein, Maria, Sheenam, Melissa, Edwin, Ajinkya, Matia, Yuyang, Justin and Dr. Hong 😊

Last but not least, deepest gratitude to my family! Thanks to my lovely wife Sujata and adorable son Atharva, for accompanying and supporting me. Thanks to my parents for their endless and unconditional understanding, encouragement and love.

Table of Content

List of abbreviation

ABS	Acrylonitrile Butadiene Styrene
AEL	Alkaline enzymatic lignin
AL	Acidolytic lignin
AlP	Aluminium diethyl phosphinate
AMLR	Average mass loss rate
APP	Ammonium polyphosphate
ARHE	Average rate of heat emission
DL	Domtar kraft lignin
DSC	Differential scanning calorimetry
dTG	Derivative thermogravimetry
EDX	Energy dispersive X-rays
EHC	Effective heat combustion
FR	Flame retardant
FRs	Flame retardants
FTIR	Fourier transform infrared
HRR	Heat release rate
IL	Ionic liquid
KL	Kraft lignin
LL	Lignosulphonate lignin
LOI	Limiting oxygen index
LPMC	Lignin-based phosphate melamine
LS	Low sulphonate alkali lignin
MARHE	Maximum average rate of heat emission
MC	Melamine Cyanurate
MCAPP	Microencapsulated ammonium
MFI	Melt flow index
MMLR	Maximum mass loss rate
MPP	Melamine Polyphosphate

OM	Optical microscopy
OMMT	Organically modified montmorillonite
PA	Polyamide 11
PA 6,6	Polyamide 6,6
PA6	Polyamide 6
PBS	Polybutylene succinate
PBT	Polybutylene terephthalate
PET	Polyethylene terephthalate
PHB	Polyhydroxy butyrate
PHRR	Peak of heat release rate
PLA	Polylactic acid
PMMA	Polymethylmethacrylate
POSS	Polyhydral Oligomeric Silsequioxane
PP	Polypropylene
PU	Polyurethane
SEA	Specific extinction area
SEM	Scanning electron microscopy
TG	Thermogravimetric
TGA	Thermogravimetric analysis
THR	Total heat release
TSR	Total smoke release
TTI	Time to ignition
ZnB	Zinc borate
ZnP	Zinc bis-diethyl phosphinate

List of symbols

ΔH_c	Enthalpy of crystallization
ΔH_m	Enthalpy of fusion
µm	Micrometer
$T_{5\%}$	Temperature at 5% weight loss
T_c	Temperature of crystallization
T_m	Melting temperature
T_{max}	Temperature of maximum rate of weight loss
T_{max1}	First degradation temperature in TGA in air
T_{max2}	Second degradation temperature in TGA in
X_c	Degree of crystallinity

List of figures

List of Tables

List of chemical schemes

GENERAL INTRODUCTION

General introduction

Nowadays, polymers are found everywhere in our day to day life, mainly because of their relatively low cost, ease of manufacture, and superior properties. The use of these polymers has already replaced many traditional materials, such as wood, leather, metal, glass, and textile. As a consequence of the development of polymers, several natural fibres have been replaced by synthetic fibres made from polyolefins, polyester, and polyamide. Augmentation of these different polymers are used not only for apparel and structural applications but also in various high-value products, such as antibacterial, reinforcing structures for composites, intelligent textile, insulation for buildings, implants for medical, protection against fire risk, and so forth. However, most polymers, due to their organic nature, easily burn when exposed to heat or flame. This hazard slows down the expanding use of synthetic fibres in some applications where stringent fire regulation and safety level must be followed. As indicated by the information from National Fire Protection Association (NFPA) (Everts Ben, 2018), in 2017 the public fire departments in the U.S. reacted to 1,319,500 fires that caused 3.400 civilian deaths, 14,670 civilian injuries, and an expected $23 billion damage in direct property.

Polyamide 11 (PA), another fiber-grade polyamide is currently available in the market along with polyamide 6 (PA6) and polyamide 6,6 (PA66) fibres. It has been produced from renewable resources for more than half a century under the trade name Rilsan® by Arkema Inc., France. PA finds specific applications in automotive, aerospace, sports applications, and textile industries. However, low flame retardant (FR) properties and extended dripping of PA limits its potential applications in textile industries. So, the development of flame retardant PA is one of the prime interest of researchers.

For a long time, flame retardants (FRs) have been incorporated to these textile materials to increase the chances of survival against fire or flame by preventing its propagation. A large group of flame retardant (FR) additives available today consists mainly in organic and inorganic compounds based on halogens, nitrogen, phosphorus, sulphur, metals (mainly aluminum and magnesium). Halogenated FRs are widely used and very efficient to enhance fire retardant properties of textile materials, represents a cost-effective technology for flame retarding a broad range of polymers (Morgan and Gilman, 2012). However, due to the toxicity and environmental scrutiny, the use of halogenated flame retardants has been globally avoided and restricted. For example, some of the brominated flame retardants have been phased out of the US market voluntarily, while the European Union (EU) has also restricted their use (BSEF, 2014). In 2009, three BFRs products were forbidden: penta- and octa-bromodiphenyl ether and hexa-bromocyclododecane and included in the list of persistent organic pollutants (POPs) (United Nations Industrial Development Organization, 2012). To address these problems, the general trend in chemistry is slowly shifting towards the use of biobased additives. In the context of using biobased resources, specific attention has been given to lignocellulosic feedstock and lignin can be considered as carbon source and/or charring agent. The worldwide consumption of FRs amount reached about 2.25 million tons per year in 2018 (IHS Consulting, 2017), it represents a real market opportunity for the valorization of lignin (Figure 0.1)

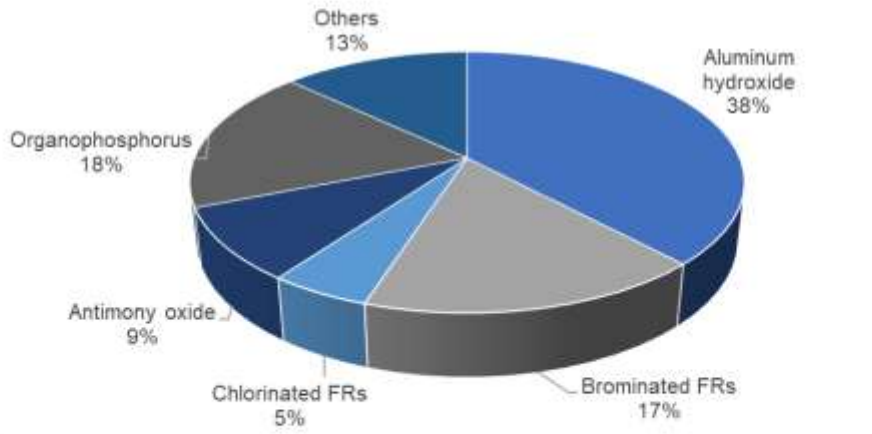

Figure 0.1. Global flame retardants market by additives (Source: IHS Consulting 2017, adopted from FLAME RETARDANTS-ONLINE web page link https://www.flameretardants-online.com/).

Next to cellulose, lignin is the second most abundant polymer from biomass and the primary one as far as aromatic subunit are considered (Calvo-Flores and Dobado, 2010). In particular, industrial lignin is produced as a by-product of wood pulping and papermaking industries, and not a resource which needs a specific production. Besides, taking into account that biosphere contains 3 x 10^{11} tons of lignin which is increasing annually. For the sustainable utilization of bioresources, major efforts have been put forward in the last few decades to use lignin as a material. Lignin, being a polyphenolic macromolecule, can be used in several ways for different applications. Its highly aromatic chemical structure leads to confer various functional properties such as the UV resistance, antioxidant, and the fire retardancy.

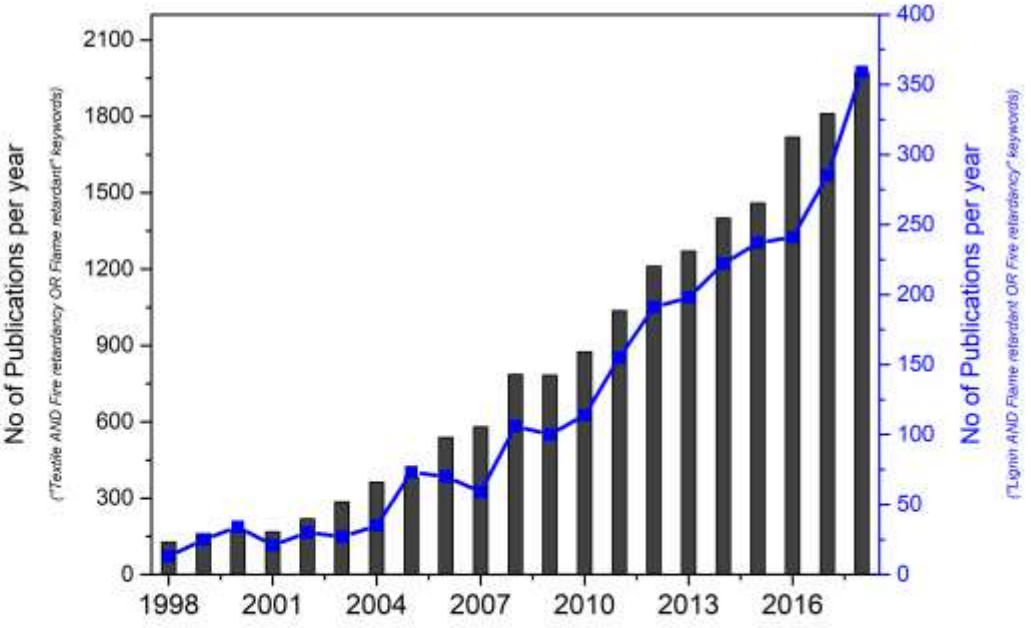

Figure 0.2. Numbers of publications per year in last 20 years for FR textile (keywords "Textile *AND* Fire retardancy *OR* Flame retardant") and Lignin (keywords "Lignin *AND* Flame retardant *OR* fire retardancy"). *Source: Web of science, May 2019.*

As shown in Figure 0.2, the growth in the number of publications in flame retardant textile has been increased due to advancement in science. Additionally, the use of halogenated FR additives decreased in the last few decades due to the regulation laid by governmental authorities pertaining to environmental concerns and sustainable solutions. In the pursuit of non-halogenated FR alternatives, lignin has received much attention as a biobased FR additive because of its char forming ability after thermal decomposition. This is reflected by the significantly growing number of scientific publications shown in Figure 0.2. The char formation also provides barrier properties against heat and oxygen diffusion in condensed phase and reduce the heat release rate of the polymeric material during degradation steps (Mouritz et al., 2006). This charring competency is particularly important for developing effective FR systems, and during the combustion, this charring FR systems act by creating an insulating layer at the surface of the burning material, resulting in the improvement of its fire behaviour by diminishing both the thermal and oxygen diffusion, as well as the volatilization of combustible products. It is reported that the presence of lignin can effectively enhance the flame retardancy of thermoplastic polymers such as PP, PBS, ABS, PET (Canetti and Bertini, 2009a; De Chirico et al., 2003; Ferry et al., 2015; Song et al., 2011). In addition, the FR effect of lignin can be enhanced by its combination with other FR additives (Lu et al., 2018; Réti et al., 2008).

In the last decades, phosphinates were developed and commercialized; several phosphinate structures were studied and published thereafter. As metal salts of phosphinates, they belong to a novel class of environmentally friendly and non-halogen phosphorus-based flame retardants for thermoplastic polymers. The most used phosphinate salt known in engineering thermoplastics are the dialkylphosphinate ones. In particular, aluminium diethyl phosphinate (AlP) and zinc bis-diethyl phosphinate (ZnP) are the most widely used: they were found to be very effective flame retardants especially for polyesters and polyamides. Therefore, it will be interesting to combine lignin and phosphinates (AlP/ZnP) with PA to increase biobased character in resulting blends.

Research framework and thesis outline

This PhD thesis discusses the development of the biobased fire retardant textile structure. The primary focus of this thesis work was to consider lignin as carbon source and introduce in a textile structure in combination with phosphinate FR during extrusion. This PhD project under the framework of SMDTex program aims to focus on the sustainability of management and design for textiles, concerning the environment, society, and human factors. This thesis work was carried out at three different universities, ENSAIT- GEMTEX, France; Politecnico di Torino, Italy and Soochow University, China. The key objective of this project was valorization of lignin as FR additive (charring agent) along with the supplementary objectives to minimize the loading of the phosphinate FR in the formulation and to increase the heat barrier effect of the material in fire conditions.

The PhD thesis is organized into five different chapters. Chapter one deals with state of the art, describing the flame retardancy of polymers and different FR additives used in polyamides followed by the general view on lignin as biobased material its extraction and applications as additive in various polymeric systems. In addition, the FR applications of lignin in thermoplastic polymers are reviewed in detail. Finally, the existing solutions for flame retarding PA and their limitations are briefly described.

The second chapter presents the materials, methodology and characterization techniques adopted in this study. The key components such as polymer matrix and additives, i.e., lignin and phosphinate used in this thesis, are discussed in detail followed by the method of compounding, melt spinning, and fabric production. Besides, the various characterization methods for analyzing the blends, the characterization techniques for the evaluation of the thermal stability, decomposition behaviour, flammability performance and fire retardant behaviour are also described.

The third chapter deals with the primary objective of the project. Chemically different lignins are selected and are combined with the PA by extrusion. Prepared formulations are investigated by TGA in order to evaluate the effect of lignin and its loading amount on the thermal degradation and the char-forming ability of PA/lignin blends, without any chemical modification and pretreatment. In addition, the FR properties resulted by direct addition of lignin are analyzed using vertical flame spread and cone calorimetry experiments.

The fourth chapter presents the supplementary approach of the project. The lignin is exploited as carbon source in combination with commercially available phosphinates FR (namely, ZnP and AlP). Prior to the exploitation of proposed objective, the primary study is carried out using laboratory grade lignin combined with ZnP to investigate the thermal stability and fire performance as well as the possible synergy between lignin and ZnP and with the polymer matrix. The outcome obtained in the primary study allowed to proceed further, for the practical application of lignin and multifilament production, low-cost industrial lignins are directly incorporated with commercial phosphinate FR. The ternary blends are developed by extrusion and characterized by microscopic technique to identify the dispersion of additives in a polymer matrix, additionally the thermal decomposition study conducted in the presence of nitrogen and air atmosphere is discussed. Furthermore, plate samples are prepared in order to evaluate the fire retardant behaviour of these combinations.

In the last chapter, the ternary blends of industrial lignin and phosphinates were selected for the development of multifilament yarns and textile structure in view of the main aim of this thesis work. Various parameters are optimized to facilitate the implementation of blends by melt spinning. Multifilaments are characterized by mechanical testing and the dispersion of additives in fibre is also evaluated by microscopic technique. The knitted fabric structure is produced to study the fire behaviour in fabric form.

General conclusion based on results and discussion in previous chapters is presented. At the end, the future work of this study will be drawn from different parts of the thesis that would need further investigation.

References

BSEF, 2014. EU Member States asked to voluntarily monitor some brominated flame retardants in food [WWW Document]. URL http://www.bsef.com/news/eu-member-states-asked-to-voluntarily-monitor-some-brominated-flame-retardants-in-food/ (accessed 11.9.18).

Calvo-Flores, F.G., Dobado, J.A., 2010. Lignin as Renewable Raw Material. ChemSusChem 3, 1227–1235. https://doi.org/10.1002/cssc.201000157

Canetti, M., Bertini, F., 2009. Influence of the lignin on thermal degradation and melting behaviour of poly(ethylene terephthalate) based composites. https://doi.org/10.1515/epoly.2009.9.1.596

De Chirico, A., Armanini, M., Chini, P., Cioccolo, G., Provasoli, F., Audisio, G., 2003. Flame retardants for pp based on lignin. Polym. Degrad. Stab. 79, 139–145.

Everts Ben, 2018. Fire Loss in the United States During 2017.

Ferry, L., Dorez, G., Taguet, A., Otazaghine, B., Lopez-Cuesta, J.M., 2015. Chemical modification of lignin by phosphorus molecules to improve the fire behavior of polybutylene succinate. Polym. Degrad. Stab. 113, 135–143. https://doi.org/10.1016/j.polymdegradstab.2014.12.015

IHS Consulting, 2017. The flame retardants market [WWW Document]. URL https://www.flameretardants-online.com/flame-retardants/market (accessed 5.15.19).

Lu, W., Li, Q., Zhang, Y., Yu, H., Hirose, S., Hatakeyama, H., Matsumoto, Y., 2018. Lignosulfonate / APP IFR and its flame retardancy in lignosulfonate- based rigid polyurethane foams. J. Wood Sci. 64, 287–293. https://doi.org/10.1007/s10086-018-1701-4

Morgan, A.B., Gilman, J.W., 2012. An overview of flame retardancy of polymeric materials: application, technology, and future directions. Fire Mater. https://doi.org/10.1002/fam

Mouritz, A.P., Mathys, Z., Gibson, A.G., 2006. Heat release of polymer composites in fire. Compos. Part A Appl. Sci. Manuf. 37, 1040–1054. https://doi.org/10.1016/j.compositesa.2005.01.030

Réti, C., Casetta, M., Duquesne, S., Bourbigot, S., Delobel, R., 2008. Flammability properties of intumescent PLA including starch and lignin. Polym. Adv. Technol. 19, 628–635.

https://doi.org/10.1002/pat.1130

Song, P., Cao, Z., Fu, S., Fang, Z., Wu, Q., Ye, J., 2011. Thermal degradation and flame retardancy properties of ABS/lignin: Effects of lignin content and reactive compatibilization. Thermochim. Acta 518, 59–65. https://doi.org/10.1016/j.tca.2011.02.007

United Nations Industrial Development Organization, 2012. UNIDO´s work in the area of Persistent Organic Pollutants (POPs).

1. STATE OF THE ART

1.1. Introduction

This chapter presents a state of the art on the valorization of lignin and specifically of fire retarding applications. The flame retardancy of polymeric materials and the additives used to enhance FR performance and the additive route, i.e., the incorporation of FR additives into polymer melt is largely reviewed. Furthermore, char promoting FRs are presented as non-halogenated environmentally friendly alternatives, more attention is given to the detailing of phosphinate FR additives. The use of lignin as an abundant renewable resource from lignocellulosic biomass is presented as a promising biobased additive for fire retardant applications in various synthetic and biobased thermoplastic polymers. Lignin can also be combined with environmentally friendly non-halogen phosphorus-based FRs in designing the FR system. Therefore, the literature survey is important to gain knowledge of lignin as material, its structure, extraction processes, and applications as additive. In brief context, the literature survey is providing the properties of lignin as FR additive. Finally, existing FR solutions to flame retarded PA in bulk are discussed and their limitations to be used in fibre application. In the end, the research framework and outline of the thesis is presented.

FR textiles find applications not only for protective clothing but also in various areas where fire protection is crucial, for example, home furnishing, public transports, covering for buildings. Thus, the need for FR textiles has been recognized for many years. From a historical point of view, the first patent with FR use was described by Obadjah Wyld (1735) focusing mainly on textile and paper. Gay-Lussac (1821) suggested a combination of ammonium phosphate, ammonium chloride, and borax to increase the fire retardancy of textiles used in French theaters. The most significant development occurred post World War II period, especially with the advancement in polymer chemistry that revolutionized the textile industry and enabled far greater use of textile in home and public places, with a significant increase in their fuel loading and fire hazard. The first synthetic fibre with intrinsic FR properties was meta-aramid from aromatic polyamide family produced by Dupont under the trade name Nomex® in the 1960s. Different classes of FR compounds have been developed and commercialized to treat various fibre and meet the specific FR requirements of the textile material. For example, organophosphorus and nitrogen-containing durable FR finish (Proban®, Rhodia) was developed in the 1950s, which was used to impart a durable FR treatment to cotton and other cellulosic fibres and blends. Several brominated FRs compounds developed during this period are restricted due to their environmental impact. Indeed, the industrial growth of flame retardant fibres and textiles continue to be governed by legislation and regulation, which define the required levels of fire retardancy specific to the application sectors. Horroks presented a historical perspective to reflect the challenges posed by the current socio-economic environment with the underlying research challenges addressed during the previous 70 years (Horrocks, 2011). Up to 1970 – 1980s, FRs studied and developed in this period still holds business necessity (Weil and Levchik, 2008a).

FR textiles can be developed using different methods. The selection of fibres having inherently FR property can be directly used for designing textile structure. High-performance polymers are fundamentally non-combustible and have high mechanical strength. Nevertheless, their lack of comfort and high cost of manufacturing limit their direct use in conventional applications, although, they can be used in combination with other fibres. Chemical modification of polymer chain by FR compound was used to achieve flame retardancy in commercial PET fibre by incorporation of reactive comonomeric organophosphorus units in the main chain, for example, Trevira® CS and HEIM®. Reactive finishing method is used to achieve high levels of durability as they either polymerize within the fibre surface or react with functional groups in the fibre-forming polymer backbone. The reactive treatment, as Pyrovatex® and Proban® are the two most famous processes for cellulose with resistance to washing. The direct incorporation of flame retardants in the molten polymer is another simplest way to develop fire retardant fibres. This method is very useful for thermoplastic polymers. However, problems of compatibility may occur at the high temperatures used during melt-spinning of polymers.

1.2. Polymer flame retardancy

1.2.1. The combustion process in general

The ignition or flaming combustion is a gas-phase thermo-oxidative process. A schematic of the combustion process and the flaming phenomenon is shown in Figure 1.1. Combustion is a multistep process; thus, before undergoing flaming combustion, a substance like a polymer or fabric exposed to a heating source, first degrades, giving rise to combustible volatiles that can mix together with atmospheric oxygen, and fuel a flame, when the system reaches to a critical concentration, ignition occurs. Part of the released heat of the flame is given back to the heat source, which increases the net heat transfer rate of the material, if sufficient heat is transferred to the surface, it may cause further degradation, and a self-sustaining combustion cycle can be promoted, and the material starts burning.

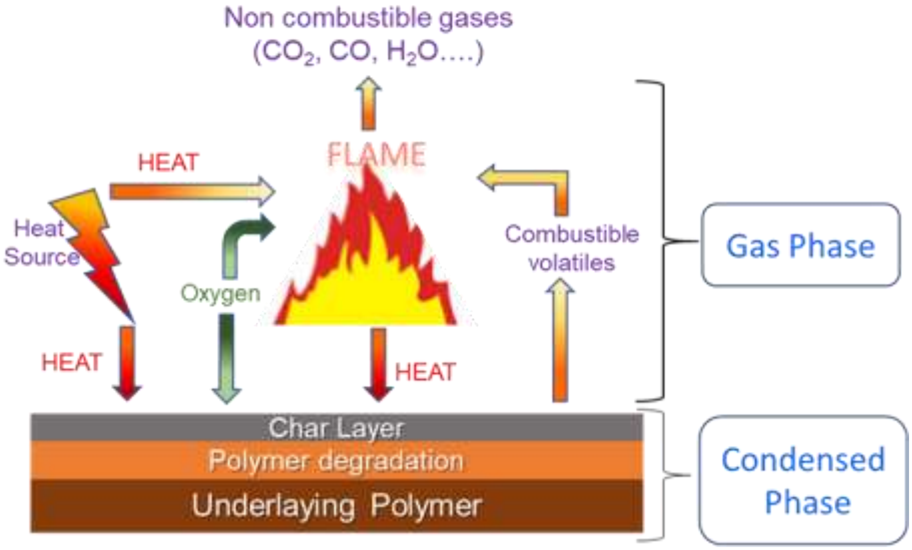

Figure 1.1. Combustion process and flame spread phenomena.

1.2.2. Flame retardants mode of action

The term “Flame retardants” refer to a variety of substances that are added to flammable materials to prevent fire from starting or spreading of fire and provide longer escape time. The most of FR substances developed in between 1950 and 1980s are still commercial significance to decrease the fire hazards of a material. The Fire Triangle or combustion triangle in Figure 1.2 shows a requirement of three elements: heat, fuel, and an oxidizing agent (usually oxygen) to propel the fire. Theoretically, FR substances act by taking away one or more elements of combustion: oxygen, heat, and fuel.

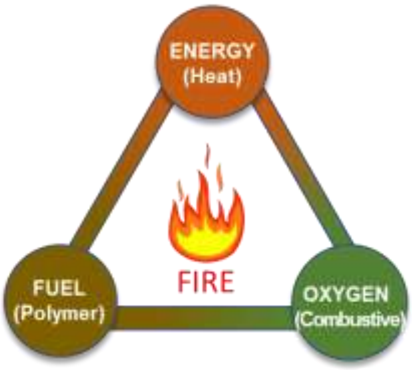

Figure 1.2. The fire triangle.

The aim of any FR system is to prevent or suppress the combustion process by interfering in any particular phase of the burning process, i.e., during ignition or fire spread, decomposition or even heating. They are intended to interrupt the phenomenon occurring in the ‘’fire triangle’’, by acting either chemically or physically, in the gas or condensed phase. A simple schematic illustration of the self-sustaining polymer combustion cycle is presented in Figure 1.3. Any FR act to break this cycle, and thus extinguish the flame or reduce the combustion rate, according to one of the following ways (Price et al., 2001):

- By dropping the heat released to below that is required for self-standing combustion

- By changing the pyrolysis process to reduce the amount of evolving flammable species. It increases the formation of less flammable volatiles or char layer which also acts as a barrier between the polymer and the flame ('a')
- By separating the flame from the oxygen/air source ('b')
- By incorporating substances into the polymer formulations which will evolve bromine or chlorine atoms if the polymer is heated to near the ignition temperature. Chlorine and particularly bromine atoms are very effective flame inhibitors ('c')
- By reducing the heat flow back to the polymer to counteract further pyrolysis. This can be achieved by the addition of a heat sink, e.g., aluminium oxide trihydrate (ATH), $Al(OH)_3$ which decomposes endothermically or by creating a barrier, e.g., the ceramic layer, char or intumescent coating, formed when the polymer is exposed to fire conditions ('d')
- By developing inherently flame retarded polymer systems

Based on the above consideration, all FRs show their activity in gas phase mechanism or condensed phase mechanism proposed for FR behaviour by which FRs may function.

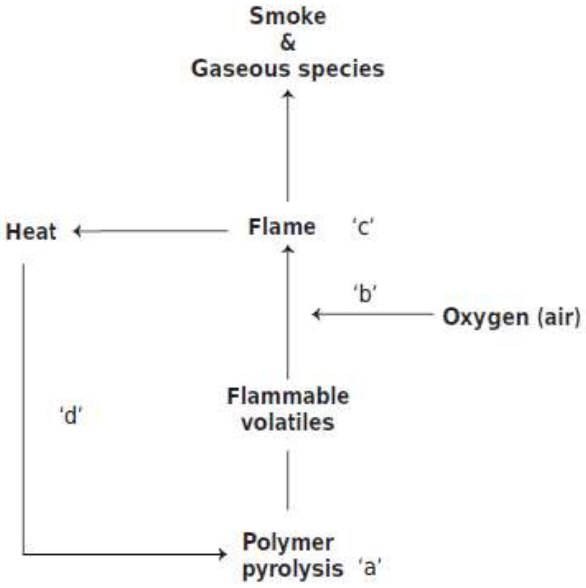

Figure 1.3. Schematic illustration of the potential mode of FR action (Price et al., 2001).

Gas Phase Mechanism

- This consists of the dilution of flame feeding gases by non-flammable ones or heat sink effect whereby the heat is prevented from returning to the polymer. Examples of such flame retardants include metal hydroxide releasing water, or nitrogen-based compounds generating ammonia (Cullis et al., 1991).
- This also takes place if flame evolution is influenced by species that inhibit the chain reaction of the flame. Such 'inhibitors' are radical species that are generated due to the presence of FR species. Halogen-containing (more specifically organobromine and organochlorine compounds) and some phosphorus-based compounds are involved in such mechanism (Cullis et al., 1991).

Condensed phase Mechanism

- Through physical cooling of the matrix by adding the fillers which decompose endothermically during combustion (e.g., metal hydroxide, carbonates, alumina hydrate, etc.). This effect is generally associated with a ceramization effect, whereas heat is prevented from returning to the polymer (Bourbigot et al., 1999).
- The creation of a protective layer, some additives can show 'intumescence' phenomenon when exposed to heat, results in an expanded carbonaceous shield (char) on its surface. This char acts as a physical barrier that can limit the transfer of fuel, heat, and oxygen between the flame and polymer. For example, P and N containing flame retardants such as ammonium polyphosphate, melamine polyphosphate, etc. (Bourbigot et al., 2004).

The different ways given above is an overview of the flame retardancy principles. Nevertheless, the discussed processes state that some generic flame retardants function occurs in more than one mode simultaneously with one dominating.

1.2.3. Flame retardant classification

Based on the incorporation method, flame retardants can be categorized into two categories.

- **Additive flame retardants**

In this method, FR additives are directly combined with a molten polymer by extrusion or melt compounding. The mechanical and thermal stresses are applied to the mixture when combined in a molten way to ensure a physical or chemical interaction between the two materials. This method has several advantages, for instance, easy handling and processing, it is the easy way to process thermoplastic polymers at a lower cost, and no additional chemicals are required. It also offers the possibility to implement a wide choice of raw materials with adaptable load rates. However, this process has some limitations, for example, the processing temperature of the polymer should not exceed the degradation temperature of additive to be incorporated. The particle size of the additives can lead to rheological changes in the melt, and at high loading content, significant reduction in the mechanical properties is observed.

Halogen-containing FR compounds have been used for a long time due to their excellent flame resistance performance (Arias, 2001; de Wit, 2002; Green, 1996). Nevertheless, due to global restriction towards the use of halogenated compounds their use is limited. As non-halogenated alternatives, intumescent FR additives have attracted much attention not just because of the fact that they are more environmentally friendly than traditional halogen-containing FRs, but also as they have high FR efficiency (Bourbigot et al., 2004; Levchik et al., 1992; Sakharov et al., 2014). This method has also been used to prepare polymer nanocomposites. Nanoparticles can be employed alone or in combination with intumescent FR additives like APP. Kashiwagi et al. (2004) investigated the use of MMT for fire retardancy performance. Synergistic effects have been observed when MMT was used with zinc borate (Shanmuganathan et al., 2007). Didane et al. used the same approach with POSS and ZnP in PET (Didane et al., 2012b).

- **Reactive flame retardants**

Fire retardancy can be accomplished by incorporating a reactive FR molecule in the main chain of the polymer by copolymerization or grafting. In this method, FR agents are not physically linked, as in the majority of mixtures prepared in the additive route but are chemically bound. One of the major advantages of chemical modification is that it avoids alterations in the physical and mechanical properties of the functionalized polymer. Indeed, the amounts of FR used are relatively low and the choice of functional monomers can be done in such a way that they have an optimal affinity with the flame retarding polymer.

Derivatives based on 9,10-dihydro-9-oxa-10-phosphaphenantrene-10-oxide (DOPO) are well known as reactive comonomer for various polymers. Liu et al. (2013) used DOPO grafted on maleic anhydride, which reacted with the terminal hydroxy group of PBT matrix. On adding 20 wt % DOPO-MAH, LOI increased from 20.9 to 25.7 and the UL-94 V-0 rating was achieved, whereas the tensile and flexural properties were notably improved. Li et al. grafted DOPO to SiO_2 particles to increase the thermal resistance of PA6 composites (Li et al., 2016). Recently, Negrell et al. (2016) used DOPO and Itaconic acid (DOPO-ITA) to prepare novel PA11/DOPO-ITA co-polyamide with phosphorus containing pendent group. Fire tests suggested that the presence of at least 5 wt% of DOPO enhanced the flame retardancy effect and leading to high oxygen index (LOI 40) and V-0 rating in UL94 test. The incorporation of DOPO-ITA had a limited (or negligible) influence on HRR, peak of HRR was rather constant.

1.2.4. Halogenated flame-retardant additives

Halogenated FR technology has been used since the 1930s, which makes it an established, savvy technology for flame retarding a broad range of polymers. Organochlorine and organobromine are used in majority, particularly, organobromine compounds by far the most commonly used (Cusack et al., 1997; Klein et al., 2009). These compounds mainly act by flame inhibition. During polymer decomposition, highly reactive free radical species such as

$H^{\bullet}$ and $OH^{\bullet}$ are formed (Scheme 1.1), which continue combustion by a cascade chain mechanism in the gas phase (Wilkie and Morgan, 2010). The flame retardant (RX) breaks down these exothermic chain reactions, and an active halogen radical ($X^{\bullet}$) reacts with the polymeric chain to form the halogen halide (HX) that is used to trap the high energy radicals ($H^{\bullet}$ and $OH^{\bullet}$) present in the flame.

Breakdown of flame retardant (RX) and polymer (RH)

$$RX \rightarrow R^{\bullet} + X^{\bullet}$$

$$X^{\bullet} + RH \rightarrow R^{\bullet} + HX$$

Flame retardation through radical trapping

$$HX + H^{\bullet} \rightarrow H_2 + X^{\bullet}$$

$$HX + HO^{\bullet} \rightarrow H_2O + X^{\bullet}$$

Scheme 1.1. Quenching mode of halogen-based FRs release in the gas phase (Wilkie and Morgan, 2010).

These exceptional bond strengths make halogen-based flame retardants firmly vapor phase flame retardants since the halogens show their activity in the vapor phase. The performance of halogens as FRs is rated as follows: I > Br > Cl > F. This trend of halogen FRs indicates that iodine compounds are most effective, but they thermally decompose at low temperature. On the other hand, Fluorine compounds are inherently non-combustible, but practically they are not used because of the high thermal stability of C-F bonds. This explains that bromide compounds have a higher FR efficiency than chlorine compounds. This can be explained by the thermal stability of C-Br bond which is perfect for preventing fires. The bond is stable enough for environmental exposure and yet unstable enough that heat can break the bond, releasing the bromine under fire conditions to inhibit combustion free radical reactions (Clarke, 1999; Hastie, 1973). Halogenated FRs in some cases used with synergists, for example, antimony oxide, zinc borate, or other phosphorus chemistry, as these different components help to make the halogens more efficient in the vapor phase (Levchik and Weil, 2000). Antimony oxide is well known synergistic for halogen compounds. The former is not volatile but antimony oxyhalide (SbOX) and antimony trihalide (SbX_3) formed in the condensed phase, by reaction with the halogenated flame retardant, are volatile. They facilitate the transfer of halogen and antimony into the gas phase where they function. Antimony oxide flame retardants are therefore usually used indirectly in the form of antimony trichloride ($SbCI_3$) or antimony tribromide ($SbBr_3$). These forms are very effective FRs at typical flame temperatures.

For the last few decades, there has been a constant trend in FR polymer industry to move from halogenated “Flame Retarded Polymers” towards non-halogenated alternatives. Some of the reasons for this are linked to toxic effects and environmental concerns of the halogenated additives (Birnbaum and Staskal, 2004; Darnerud, 2003). Besides, in the course of combustion, they instigate an increase in smoke and corrosive gases, and they are persistent environmental pollutants if they migrate out of the polymer matrix. Some of these products can impact human fertility or fetal mental health and can even cause cancer. Three halogenated products are presently prohibited: hexa-bromocyclododecane (HBCD) and penta- and octa-bromo-diphenyl ether (PBDPE, OBDPE) (Morgan and Gilman, 2012). In order to address these issues, attention must be devoted to the development of halogen-free flame-retardant additives.

1.2.5. Char promoting flame retardants

FR systems that promote the formation of a protective char layer on the surface of the burning substance are among the most promising environmentally friendly strategies for replacing halogenated flame retardants. Thus, research of new char promoting flame retardants was focused around finding ways to increase this char forming tendency. The char-forming ability of a polymer can be increased with FR additive and/or by changing its molecular structure (Alongi et al., 2015). These polymeric substances more often produce a highly conjugated system of aromatic structures, during thermal degradation; this char transforms into a highly cross-linked structure at a higher temperature. The formation of conjugated char during thermal degradation can play several roles in fire retardancy; it might limit the amount of fuel available; it might also act as a physical barrier against heat transmission and diffusion of oxygen towards the polymer. In this context, the intumescent approach, i.e., charring and foaming of the burning polymer have been broadly adopted for flame retardant applications, since it is described by a low environmental impact. The schematic illustration of the mode of action of classical intumescence process is shown in Figure 1.4. On heating, intumescent flame retardants produce a foamed cellular charred layer on the surface of the polymer and the formation of charring layer decelerates the mass and heat transfer between the condensed and gaseous phases (Camino et al., 1984a, 1984b; Feng et al., 2013).

Basically, the intumescent material consists of three components: (i) an acid source (e.g., ammonium phosphates or polyphosphates, which release phosphoric acid); (ii) a char former (e.g., pentaerythritol, polysaccharides, and lignin, which is dehydrated by acid source to form a char); and (iii) a blowing agent (e.g., guanidine and melamine, which decomposes into non-flammable gases). Upon heating, the acid source releases a mineral acid, which catalyzes the dehydration reaction of the char former that leads to the formation of a carbonaceous structure when the blowing agent decomposes into non-flammable gases. Acid should be released at a temperature below the decomposition temperature of the charring agent and dehydration of charring agent should occur around the decomposition temperature of the polymer. Moreover, the intumescent coating has been in use for more than 50 years (Roy Choudhury, 2017; Weil and Levchik, 2008b), while the incorporation of intumescent substance in polymeric bulk is a comparatively recent approach (Alongi et al., 2015).

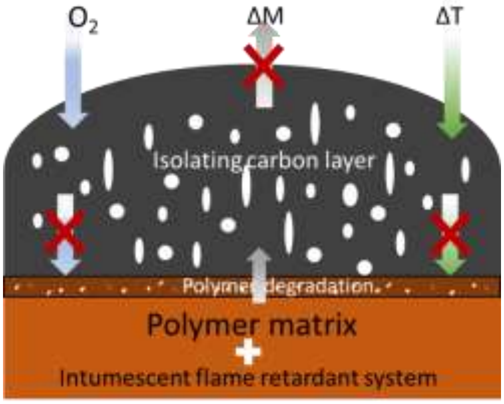

Figure 1.4. Mode of action of the intumescent system.

1.2.5.1. Phosphorus-based flame retardants

Phosphorous containing flame retardants are widely used as an alternative solution of halogenated FRs (Sakharov et al., 2014; Salmeia et al., 2016; Schwarzer et al., 2018). Phosphorus-based FRs include inorganic and organic phosphates, phosphonates, and phosphinates as well as red phosphorus (as a pure element); which includes an inclusive range of phosphorus compounds in all possible oxidation states from 0 to +5 (Scheme 1.2). Moreover, the phosphorus concentration in these compounds differs widely from 100% (red P) to about 10% (phosphates) and does not associate to the FR efficiency of the specific molecule (Hörold, 2014). This indicates that the FR effect of phosphorus products involves one or more mechanism.

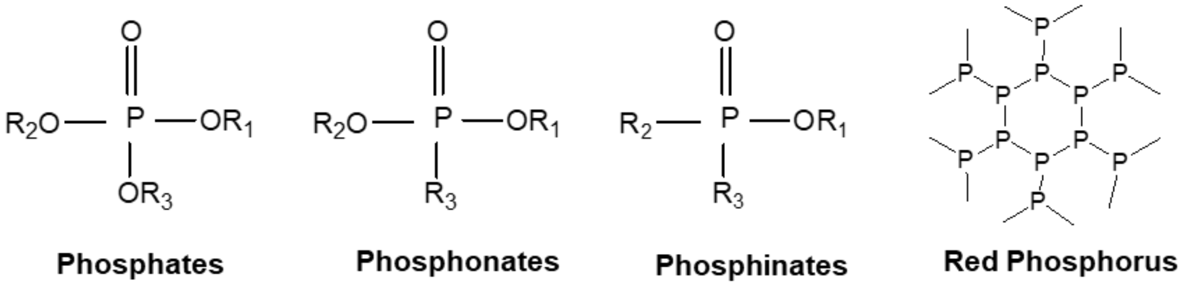

Scheme 1.2. Structure of different organophosphorus FR species.

Phosphorus-based FRs can act in both the gaseous and the condensed phases. In the gas phase, phosphorus exhibits flame inhibition through radical trapping; while, in the condensed phase, it results in the formation of aromatic char or inorganic residue inhibiting the pyrolysis process essential to fuel the flames. The activity of phosphorus depends on the FR used as well as on the chemical construction of the polymer matrix and on its interaction with other additives. Phosphorus species are particularly effective in matrices containing heteroatoms (mainly, O & N). Through thermal decomposition and oxidation, generally release phosphate or phosphoric acid. The latter can condense into pyro-, then meta-, and finally polyphosphoric acids at higher temperatures, thus releasing water, the reaction in the condensed phase leads to the char formation, which is acting as a barrier against heat, oxygen and mass transfer.

Phosphorus-based FRs can also volatilize and act in the gas phase. For the first time, Hastie and Bonnell suggested the mechanism of radical scavenging by phosphorus molecule (Hastie and Bonnell, 1980). In this case, the volatile species can form active radicals ($HPO_2^\bullet$, $HPO^\bullet$ and $PO^\bullet$) which act as scavengers for the flame radicals $H^\bullet$ and $OH^\bullet$ thus quench exothermic combustion reaction (Scheme 1.3). Combination of phosphorus-based additives with nitrogen-containing products like melamine cyanurate, melamine phosphate or melamine polyphosphate exhibits high performance because of synergistic effects (Jenewein et al., 2002).

$$\begin{aligned}
&HPO_2^\bullet + H^\bullet \rightarrow PO + H_2O\\
&HPO_2^\bullet + H^\bullet \rightarrow PO_2 + H_2\\
&HPO_2^\bullet + OH^\bullet \rightarrow PO_2 + H_2O\\
&PO^\bullet + H^\bullet + M \rightarrow HPO + M\\
&PO^\bullet + OH^\bullet + M \rightarrow HPO_2 + M
\end{aligned}$$

Scheme 1.3. Mechanism of radical scavenging by phosphorus flame retardants (Levchik, 2007).

The requirement for polyamides is stringent owing to high processing temperatures, sensitive to degradation caused by possible acids and the need for long term dimensional stability have eliminated most of the known phosphorus-based flame retardants apart from thermally stable ones.

1.2.5.2. Phosphinate flame retardant

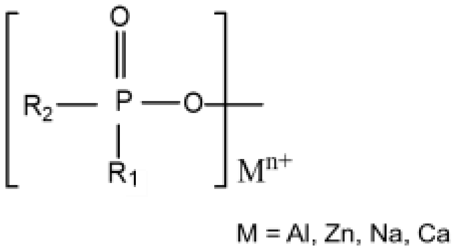

Figure 1.5. A general structure of metal phosphinate.

The use of phosphinates as flame retardants for textiles was first patented in the 1950s by DuPont (Kvalnes et al., 1954). However, their use in polyester and polyamide was first patented in the 1970s 1970s (Aoyama et al., 1976; Racky et al., 1972). Several phosphinate structures have been studied and published thereafter (Figure 1.5), and their mechanism of decomposition have been elucidated for most of them.

In 1976, Hoechst patented various formulations based on the use of phosphinate salt of metal cations such as Na^+ or Zn^{2+} (Noetzel S and Herwig W, 1974). They were the first phosphinate metal salts to be patented. Between 1980 and 1995, several studies and patents have reported the use of phosphinic ester structures and other novel phosphinate-containing polymeric structures. Moreover, in 1996, Hoechst patented the use of calcium and aluminum salt of monophosphinic acids as FR for PET and PBT (Kleiner et al., 1996). The development of such formulation in polyamide was also patented in 1997 (Kleiner et al., 1997). At the beginning of the 2000s, Clariant included phosphinate salt in its brand Exolit®, as new Exolit OP compounds, then joining existing polyphosphates based flame-retardant. Thanks to the number of patents involving the various phosphinate structures, many compounds were developed, for specific applications; for instance, OP1230 and OP1240 (aluminum diethylphosphinate) which count among the most studied phosphinates.

The most used phosphinate salt known in engineering thermoplastics are the dialkyl phosphinate ones, especially the aluminum-based salts. They have shown a high level of efficiency in polyamide and polyester. With 20 wt% content of aluminium phosphinate (AlP) in glass fibre reinforced PBT, V-0 ranking in UL94 test was reported (Elke Schlosser et al., 2003; Elke Jenewein et al., 2002; Nass and Wanzke, 2001). In glass fibre reinforced PA6, AlP also gives a similar FR property. A synergistic effect has been emphasized between AlP and MC (Braun and Schartel, 2008) or MPP (Braun et al., 2007). Synergism between AlP and modified clay can also be found in the literature (Samyn and Bourbigot, 2012); in the same line, the other mineral particles such as aluminum trihydrate (Duquesne et al., 2013) were also studied with AlP. The several combinations of alkyl phosphinates with synergists compounds lead to a variety of possible uses, processing temperature ranges, and synergistic effects (promoting char formation, cooling the matrix in combination with gas-phase activity). AlP has been extensively used in flame retardant systems such as polyurethane (PU) (Lorenzetti et al., 2012), polymethylmethacrylate (PMMA) (Laachachi et al., 2007) and polyamide 6,6 (PA6,6) (Braun et al., 2007).

On the other hand, ZnP has been widely used as FR in polyesters for textile applications because of its fusible characteristic with spinning temperature (Didane et al., 2012b, 2012a; Vannier et al., 2009). However, they show satisfactory flame-retardant properties only on rather a high loading of about 30 wt% (Kleiner et al., 1998). Phosphinate loading was conceivably reduced in the presence of synergistic or catalytic compounds. In this context, Didane et al. exploited the synergism between ZnP and POSS for manufacturing the flame retardant PET fibres (Didane et al., 2012c). It was found that the addition of synergistic agents can enhance the ZnP efficiency, by reducing its required loading in the polymer matrix. Furthermore, Vannier et al. proposed the combination of ZnP and polyhedral Oligomeric Silsesquioxane (POSS) in PET, and thoroughly investigated the species formed during decomposition and improved flame retardant features (Vannier et al., 2008); in another study, synergism was found between ZnP and nitrogen-containing additives like melamine cyanurate (MC) and melamine polyphosphate (MPP) (Braun et al., 2008).

The mode of action of Al and Zn diethyl phosphinate salts was investigated in glass fibre reinforced PBT (Braun et al., 2008). The authors reported that phosphinate salts evolved during a main degradation step diethyl phosphinic acid in the gas phase while forming metal terephthalates in the condensed phase. In a second minor decomposition step, the terephthalates evolve into benzene and CO_2 while phosphinates remaining in the condensed phase oxidized, releasing ethene (from the cleavage of ethylenic groups attached to phosphorus) and aluminum phosphate is formed in the condensed phase (Figure 1.6).

As a result, metal phosphates and a relatively small amount of carbonaceous char are yielded in the final residue. The char acts as an adhesive for glass fibres and increases the mechanical stability of the residue, providing additional protection against the transfer of flammable volatiles to the gas phase during combustion. There is a slight difference existing between Zn and Al phosphinate. Lower carbonaceous char is obtained in the residue with Zn salt. Thus, the residue presents poor mechanical properties and does not act as an effective barrier against mass transfer. This behaviour partially explains the lower efficiency of the zinc salt as compared to the Al salt based systems (Braun and Schartel, 2008).

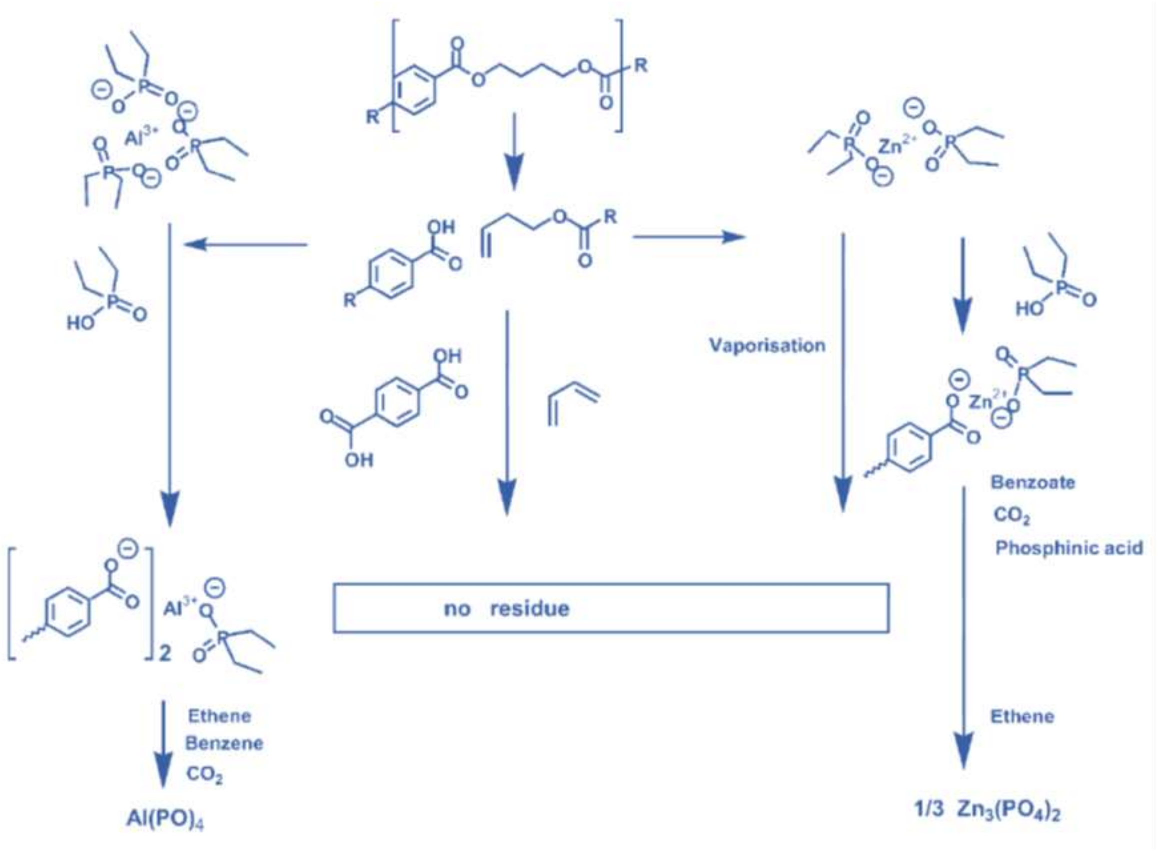

Figure 1.6. Decomposition pathway of the formulation PBT/Al or Zn phosphinate (Braun et al., 2008).

In PA6, the mechanism of action of aluminum diethylphosphinate was also investigated by Braun et al. (2010) . It was found that the carbonyl functional groups of the polymer chain are polarized by the presence of AlP, which enhances the intramolecular cyclization and thus the depolymerization of PA6 into Ɛ-caprolactam. The complexation of AlP by the polymer chain further lead to the formation of a charred structure at the end of the decomposition, comprising aluminum phosphates and carbonaceous residues.

In another study by Braun et al., aluminum phosphinate was also combined with MPP. In these cases, it was shown that MPP and AlP exhibit synergistic effects in the gas phase. A strong gas phase action was observed upon the fire, combining the effects of melamine and phosphinic acid (Braun et al., 2010). However, Samyn et al. demonstrated that no reaction between the additives or the additives and the PA6 was observed in the condensed phase despite the char promotion highlighted (Samyn and Bourbigot, 2012).

As a conclusion, it is shown that the dialkylphosphinates can act in both gas and condensed phase. However, a strong effect in the gas phase (illustrated by UL94 and LOI results) was proposed. In PBT and PA6, AlP was shown to affect the decomposition reactions of the polymer, leading to a stabilization of the residues in the condensed phase.

Due to limitations of existing intumescent additives and environmental concerns, research and development of new intumescent flame retardants have been focused on finding ways towards the development of biobased materials. Flame retardants based on biobased resources are attracting great interest, due to their availability and the growing awareness of environmental issues linked to the increased use of fossil feedstock. Furthermore, it is believed that the use of materials based on renewable resources can reduce the carbon footprint in our environment.

1.3. Lignin as biobased material

1.3.1. Lignin as wood component

Lignin is one of the natural occurring macromolecules in plants and trees. It constitutes 15-30 % dry weight of wood plants together with cellulose and hemicellulose (Saake and Lehnen, 2007). Its primary function in the plant cell is to provide mechanical strength and prevent any mechanical shock. Lignin is the second most abundant polymer from biomass after cellulose, and the main one based on aromatic subunits, its availability on Earth is more than 300 billion tons, which is even increasing exponentially every year. Alternatively, industrial lignin is primarily a byproduct of the wood pulping and paper making industries; its amount is estimated to be 70 million tons/year around the world (Laurichesse and Avérous, 2014; Tribot et al., 2019). However, less than 2 % is recovered for utilization as a chemical product, and the rest is considered as waste and primarily burnt for recovering energy. These applications include medium and small-scale markets such as additives, dispersant, and binders for various industrial applications. The reason for under exploitation of lignin in industries is that its structure and molecular weight are not defined, which differ with each other to a large extent depending on the botanical source, extraction process and the presence of impurities: these changing properties are the main obstacle to industrial valorization. Therefore, the comprehensive utilization of lignin remains a challenge. However, taking into account its high abundance in the biosphere and the growing interest for sustainable and environmentally friendly development, the scientific community has attracted more attention to explore the use of lignin. Therefore, significant efforts are put on lignin research to standardize the use and find suitable applications. The creation of international cooperation such as the EUROLIGNIN project illustrates the interest in lignin (R.J.A. Gosselink et al., 2004). Moreover, the concept of biorefinery emerged, and high-value lignin becomes available to a large extent (Langan et al., 2014). Many efforts have been made to increase the use of lignin into value-added applications (Agrawal et al., 2014; Naegele et al., 2016; Nicolas Smolarski, 2012; Thunga et al., 2014; Windeisen and Wegener, 2012). The use of lignin as a chemical product is now an important part of applications and will become more significant in the upcoming years. Indeed, the lignin market is expected to reach 985.5 million dollars in 2023 (Market Research Store, 2015).

1.3.2. Lignin basic structure

The lignocellulosic biomass is composed of three major components: cellulose (35–83%), hemicellulose (0–30%) and lignin (1–43%) on the basis of dry weight (Lin and Dence, 1992). Lignin contributes a key role in wood plants, regulating fluid flow, adding strength and structure to the cell wall and protecting against biochemical forces by preventing the enzymatic degradation of other components (Boerjan et al., 2003). Lignin has a complex structure created by a three-dimensional cross-linked network whose base unit is phenylpropane, instigating from three phenolic precursors (monolignols) known as sinapyl, p-coumaryl, and coniferyl alcohols, respectively. The phenolic subunits that originate from these monolignols are called p-hydroxyphenyl (H, from coumaryl alcohol), guaiacyl (G, from coniferyl alcohol) and syringyl (S, from sinapyl alcohol) moieties (Figure 1.7). The combination of these three monomers leads to a highly branched polyphenolic polymer with a three-dimensional structure. Lignin composition and content depend on the plant species and its environment; for example, hardwood lignins consist primarily of G and S units and traces of H units, whereas softwood lignins mostly comprise G units, with low levels of H units (Doherty et al., 2011). The variation of lignin composition is more prominent in hardwoods than in softwoods.

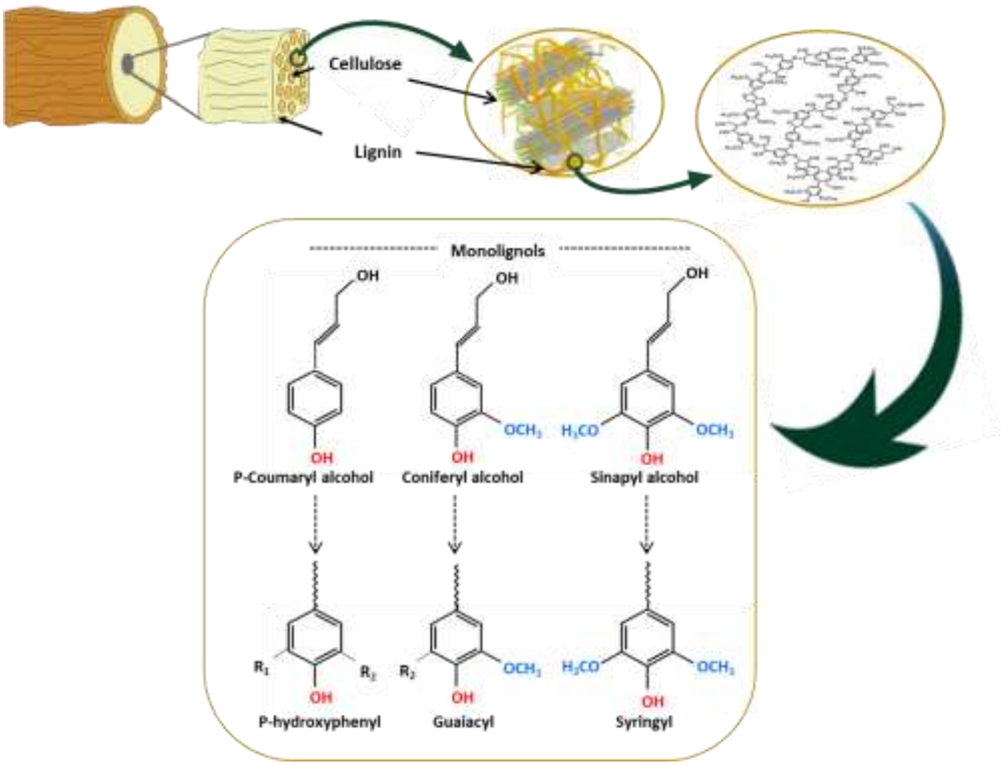

Figure 1.7. The three main precursors of lignin (monolignols) and their corresponding structures.

During the biological lignification process, the monolignols units are linked together via coupling reactions to form a complex three-dimensional molecular structure (Scheme. 1.4), which is particularly complex to explain. Sjöström et al. developed the model to draw lignin structures with the relative proportions of each monolignols and linkage types (Sjöström Eero, 1993). Whetten et al. investigated the most common types of bonds linking the monomers together and concluded that at least 20 different linkages are present in a common lignin structure (Whetten Ross et al., 1998). Generally, the β-O-4, α-O-4, β-5, 5-5, O-5, β-1, and β-β linkages are the most common bonds (Windeisen and Wegener, 2012). The most abundant lignin interunit linkage is the β-O-4 ether type of linkage, comprising about 50% of the interunit linkages in lignin (Dorrestijn et al., 2000; Ralph et al., 2004).

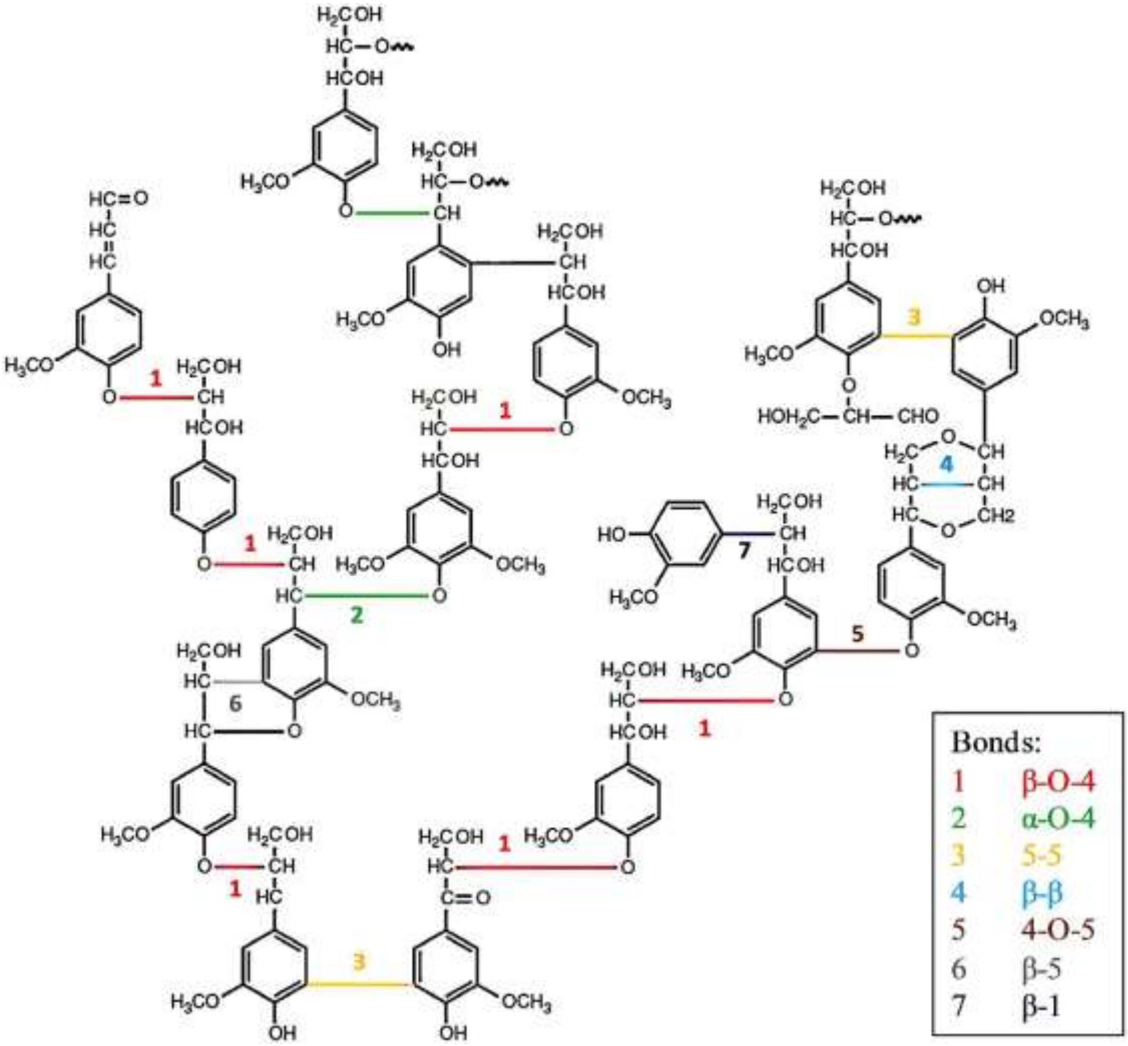

Scheme. 1.4. Main linkage in softwood lignin (Laurichesse and Avérous, 2014)

1.3.3. Lignin extraction processes

Lignin is extracted from the different lignocellulosic parts by physical and/or chemical and biochemical treatments. Technical lignin is classified based on different chemical nature (Table 1.1). Common pulping processes are based on the splitting of ether and ester linkages. As consequence, resulted technical lignin differ significantly from the plant lignin. In this part, major commercially available extraction processes are discussed, which are used to recover technical lignins. Based on the chemical processes they are classified into two main categories such as sulphur-bearing and sulphur-free processes, as shown in Figure 1.8.

Table 1.1. Classification of technical lignins.

Lignin Type	**Scale**	**Purity**	**Chemistry**	**Sulphur content**
Kraft	Industrial	High	Alkaline	Low
Lignosulfonate	Industrial	Low	Acidic	High
Organosolv	Industrial/Pilot	High	Acidic	Free
Soda	Industrial/Pilot	Moderate	Alkaline	Free

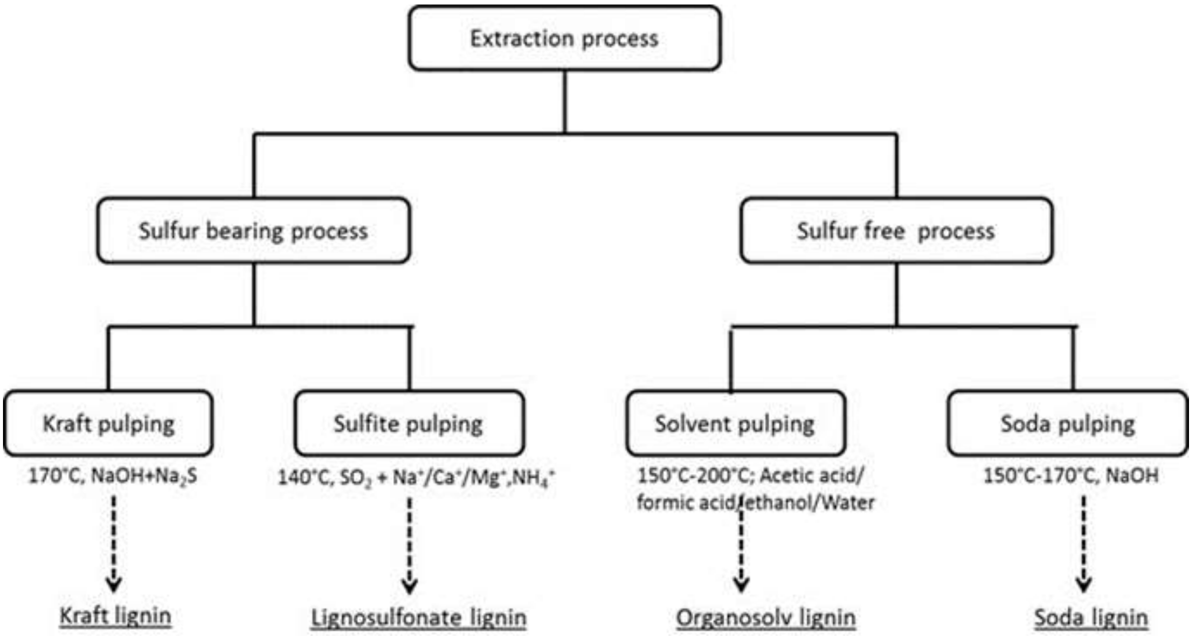

Figure 1.8. Different extraction processes to separate lignin from lignocellulosic biomass and the corresponding technical lignins.

1.3.3.1. Sulphur-bearing process

Sulphur lignin includes Kraft and lignosulfonates lignin, which are primarily produced by pulp and paper industries and mainly correspond to the lignin extraction from the cellulose.

- **Kraft Process**

The Kraft process uses a mixture of chemicals including sodium sulphide (Na_2S) and sodium hydroxide (NaOH), known as white liquor, which breakdowns the lignin and cellulose linkages. It mostly converts wood or non-wood material into pulp; the converted black liquor is then acidified to recover lignin. Considering the high sulphur environment used for kraft lignin extraction, it is quite surprising that the residual sulphur content is very low, typically below 2–3 % of dry weight. Moreover, it contains a high amount of condensed structures and a high level of phenolic hydroxyl groups (Laurichesse and Avérous, 2014), due to extensive cleavage of β-aryl bonds during cooking. The number-average molar mass (M_n) of kraft lignin is generally low, between 1000 and 3000 g mol^{-1} (Marton and Marton, 1964).

- **Sulphite process**

Sulphite lignin is the most abundant type of commercial lignin available because traditionally this was the most used type of pulping process. It is based on the cooking of pulp with an aqueous sulphur dioxide (SO_2) and a calcium, sodium, magnesium or ammonium salt. Lignosulphonates contain a significant amount of sulphur in the form of sulfonate groups linked on the aliphatic side chains. They have a broad polydispersity index, around 6-8 with a higher number-average molar mass than kraft lignin (Vishtal and Kraslawski, 2011). However, they are generally contaminated by the cations used during pulp production and recovery. Lignosulphonate are water soluble, and their reactivity also depends on the cation species. Calcium and ammonium-based products exhibit the lowest and the highest reactivity, respectively, while sodium and magnesium-based lignosulphonates show a medium reactivity (El Mansouri et al., 2007).

1.3.3.2. Sulphur-free process

Sulphur-free lignin is an emerging class of lignin products which has a low macromolecular weight (M_n), after fractionation steps. The structure of these lignins is considered to be close to those of the native lignins. They exhibit interesting properties that can make them an attractive source of low-molecular-mass phenol or aromatic compounds. Based on the chemicals used, this process can be divided into solvent pulping (Organosolv lignin) and alkaline pulping (soda lignin), respectively.

▪ Organosolv process

Organosolv lignins are generally considered the purest ones, with the highest quality (Sannigrahi et al., 2010). They are practically insoluble in water since they are highly hydrophobic but exhibit high solubility in common organic solvents. This lignin is obtained from the solvent by precipitation, which typically includes fine-tuning of different parameters, such as temperature, concentration, and pH. The most common organosolv processes are based on ethanol/water pulping (e.g., Alcell) and pulping with acetic acid, holding a small amount of mineral acid such as hydrochloric or sulfuric acid (Shukry et al., 2008). Another extraction technology based on a mixture of formic acid, acetic acid and water, was developed by CIMV Company (France). The lignin produced was called Bio-lignin©, is supposed to be linear and have low molecular weight according to some previous reports (Delmas, 2008; Kham et al., 2005). Nevertheless, some of these isolation concepts, such as the Alcell process, using aqueous ethanol, are now being commercialized as a biorefinery technology whereby the cellulose fraction is being used for ethanol production (Berlin et al., 2011).

▪ Soda process

This process is primarily used for annual plants such as bagasse, flax, straw and to some extent in hardwoods (Rodríguez et al., 2010; Saake et al., 2007). In this process, the extraction carried out by hydrolytic cleavage of the native lignin, but it results in relatively chemically unmodified lignin compared to the other lignin types. A technology developed by Granit SA, Switzerland (Granit process) with a particular methodology for the precipitation of lignin in the black liquor of soda process, where typically a mineral acid is employed to adjust the pH value of the liquor.

This process is specially adapted from paper factories in the production of cellulose from annual plants or agricultural residual substances, The recovery of spent cooking liquor from pulping of non-woods is not without problem, because of the high content of silica which may co-precipitate with the lignin which gives a lower quality (Gellerstedt and Henriksson, 2008; Lora, 2008). In the meantime, industries have claimed to solve this problem in order to obtained soda lignins with low ash and silica content (R J A Gosselink et al., 2004).

Various alternative pulping processes such as ionic liquids (ILs), steam explosion, hydrothermal, and enzymatic have been developed but still far from industrial or large-scale implementation due to several reasons. There are many efforts and new approaches searching for new technologies and enhancing the value of lignin and lignin products (Adorjan et al., 2006).

1.3.3.3. Influence of extraction processes

The successful introduction of lignin in the production of new biobased materials is highly dependent on its structure and purity. Extraction processes represent the key point to use lignin in industrial applications. However, despite these limitations, the large amount of available lignin has driven numerous efforts and researches to develop its uses for industrial applications. The difference among organosolv (OL), ionic liquid (IL) and Klason (KL) processes were studied by Kim et al. (2013) for extracting lignin from the same botanical source, e.g., poplar wood. Milled lignin (ML) was used as reference (Björkman, 1956). First, each process yielded to a different amount of lignins that are 5.5 wt% for ML, 3.9 wt% for OL, 5.8 wt% for IL and 19.5 wt% for KL. Therefore, the amount of recovered lignin is mainly dependent on the extraction process. Organosolv and soda processes were also compared by FTIR spectroscopy (Bykov, 2008), it was established that the lignin produced by the soda cooking is more oxidized than that from organosolv cooking. Indeed, a higher amount of carbonyl and carboxylic acid groups were detected.

In this context, when speaking about lignin material, its botanical source and extraction process should be known. Numerous lignin should be considered, and in the frame of this work, the study focused on lignin available at high volume.

1.3.4. Lignin incorporation in polymer materials

At present, only 2 % of the lignin production from the pulp industry is used for value-added products. Lignin can lead to high-value products thanks to the fragmentation (oxidation or pyrolysis). However, the production of high-value chemicals from lignin is complex to industrialize. Another promising domain of applications is to use lignin from its initial state in the polymer system, as additive, filler, reinforcement agents, etc. Moreover, according to its structure, chemical functionalization can be undertaken to tune its properties. Crosslinking with other polymers is also possible via its hydroxyl groups to give rise to novel materials. Lignin is known for enhancing the biodegradability of polymers where it has been incorporated. The current and potential applications of technical lignin are shown in Figure 1.9.

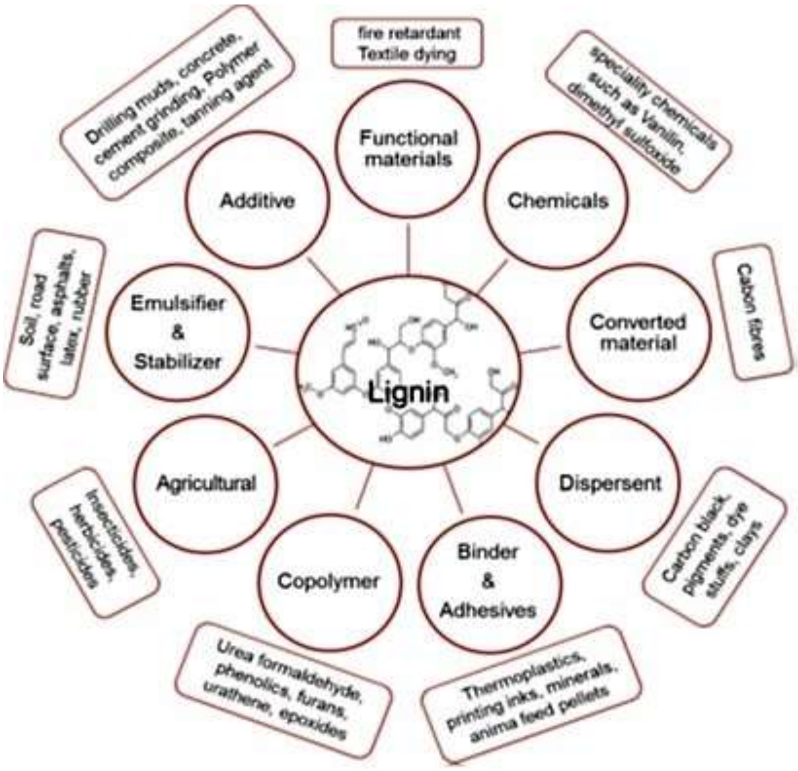

Figure 1.9. Current and the potential applications of the lignin.

The lignin-based composite material has been developed in the form of thermoplastically processed products, consists of unmodified technical lignin and natural fibres for car interior design, furniture, toys, shoes, electrical boards, and musical instruments. One of the prominent examples of such material is known under the trade name Arborform® (Tecnaro GmbH company), the material developed at the Fraunhofer-Institut für Chemische Technologie (H. Nagele et al., 2000; Nägele et al., 2002; Ziegler et al., 2014). Arborform® is made of natural renewable raw constituents and processed by injection molding-like thermoplastics. It can be constituted of lignin matrix up to 60 wt%. Lignin is used as a additive, filler, coupling agent, or compatibilizer in thermoplastic blends or composites. All technical lignins are suitable for these applications. Lignin is mixed to different thermoplastics like polyethylene, polypropylene, or polystyrene. Recently, Mamun et al. tested lignin as filler in bioplastic matrix, the biopolymers PLA, poly(3- hydroxybutyrate) (PHB), and polyamide 10,10 were used (Al Mamun et al., 2016). Lignin incorporation increased the stiffness of the material because tensile and flexural moduli improved, but the flexural strength was observed to be much lesser than that of neat polymers. Besides, Sahoo et al. developed biodegradable polymer matrix-based hybrid composites using polybutylene succinate (PBS) as the biodegradable polymer matrix and lignin, loading content varying from 30−65 wt% (Sahoo et al., 2011). Furthermore, the introduction of 1% PMDI (polymeric dimethylene diphenyl diisocyanate) compatibilizer in 50 wt% lignin filled composites improved the mechanical properties and led to better interfacial adhesion between the lignin and the polymer matrix and the same was confirmed by the SEM images of the polymer composites with different concentration of lignin.

1.4. Lignin as fire retardant additive

1.4.1. Process of thermal decomposition

The thermal stability and decomposition of lignin are studied in several ways, pyrolysis, i.e., the thermal degradation in the absence of oxygen is a common analytical technique for lignin characterization. Pyrolysis generates decomposition products which are related to structural parts of the initial lignin. Another efficient technique is a pyrolizer followed by a gas chromatography column coupled with a mass spectrometer (Py-GCMS). The degradation products are separated in the column and analyzed by the MS (Brebu et al., 2013; Zhao et al., 2014). Generally, pyrolysis is divided into two different approaches; the conventional “slow” pyrolysis in which the heating rate, as well as the maximum temperature, are relatively low compared to “flash” pyrolysis, which involves extremely high heating rates. Depending on the pyrolysis conditions (Figure 1.10), the degraded lignin generates liquids (oils), solids (char) and gaseous products (methane, carbon dioxide, phenolic compounds) in different ratios depending on the pyrolysis conditions (Amen-Chen et al., 2001; McKendry, 2002).

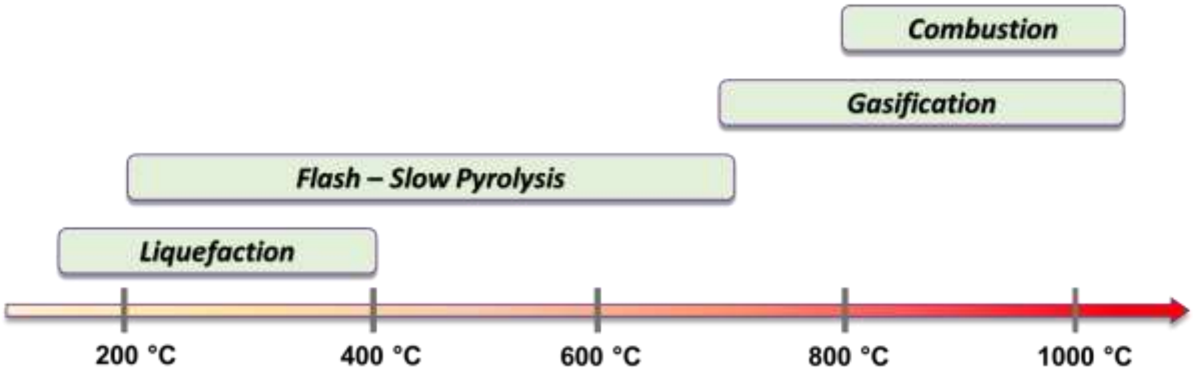

Figure 1.10. Temperature ranges for lignin fragmentation (Prieur et al., 2016).

1.4.2. Temperature ranges and kinetics of thermal decomposition

Temperature ranges of the different degradation steps depend on the lignin type, as well as kinetic models of thermal degradation (Faravelli et al., 2010). Once again, due to its complex structure, the thermal degradation behavior of lignin is highly affected by its botanical origin and extraction process. Moreover, the heating rate, as well as the atmosphere, strongly influence the thermal behavior of lignin. Therefore, a general conclusion about degradation temperature range, conversion, and product yield have to be assumed carefully. Typical behavior in TGA is shown in Figure 1.11, which compares the thermal stability of different lignins. Lignin decomposes from 200 to 500 °C depending on the type. Prior to lignin decomposition, moisture release occurred below 150 °C. The dTG curves of lignin decomposition show one or many broad peaks which reveal a complex and numerous reactions taking place. Heated up at 10 °C/min under inert atmosphere, lignin degrades slowly, and decomposition rates rarely exceed 0.3 wt%/°C and weight loss ranges between 44 and 54 wt% at 600 °C. Several studies reported the kinetic analysis of lignin (Caballero et al., 1996, 1993; Faravelli et al., 2010).

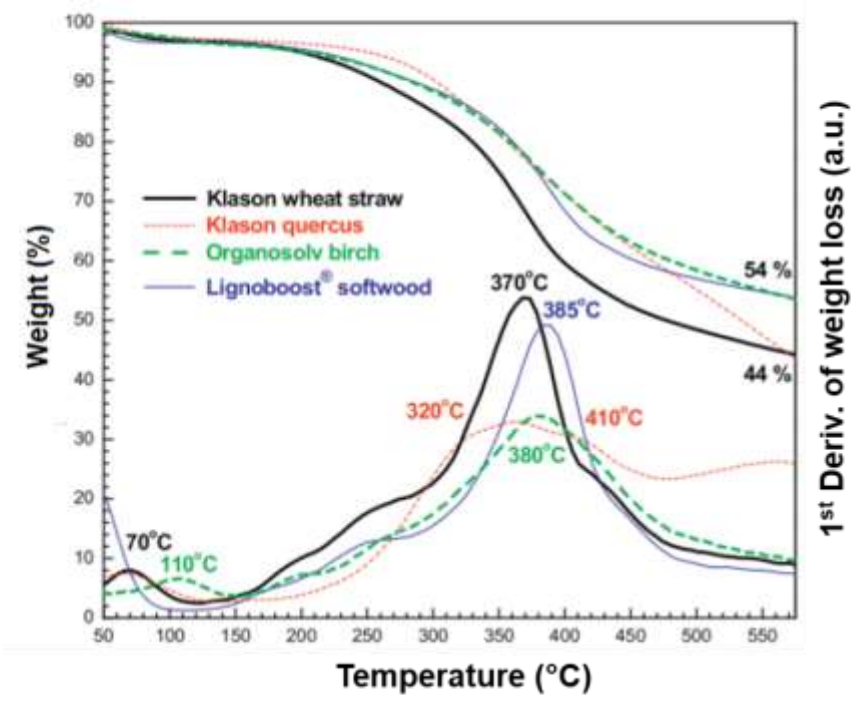

Figure 1.11. Thermal degradation of various lignins followed by TGA (10 °C/min, Helium gas flow) (Brebu et al., 2013).

Usually, lignin decomposition in inert atmosphere is assumed to occur in a unique reaction of the first order. The conventional kinetic parameters were determined, such as the activation energy, which lies between 54 and 79 kJ/mol in the range of 244 to 309 °C, and increases to 81 kJ/mol over 327 to 1167 °C. It was also demonstrated that heat and mass transfer processes influence the thermal degradation significantly by affecting the activation energy and the pre-exponential factor (Adam et al., 2013).

1.4.3. Mechanism and evolved product of thermal decomposition

Lignin thermally decomposes over a wide temperature range, because different functional groups from its structure have different thermal stabilities, their splitting occurs at different temperatures. The scission of the functional groups evolves low molecular weight products, while the complete rearrangement of the backbone at higher temperatures leads to 30 – 50 wt% char residue formation. The cleavage of the aryl–ether linkages results in the formation of highly reactive and unstable free radicals that might further react through rearrangement, electron abstraction or radical–radical interactions, to form products with increased stability. Figure 1.12 summarizes the decomposition products generated when lignin is thermally degraded.

The degradation starts slowly between 200 and 275 °C. Dehydration occurs first from 200 °C. Starting from 230 to 260 °C, the degradation of the propanoid side chain leads to the formation of methyl-ethyl and vinyl guaiacol. At higher temperatures (275 – 350 °C), several reactions occur. C–O bonds such as the aryl–ether linkages (β-0-4, α-0-5…) cleave, and so do the C–C and β-β inter-monomeric linkages. It results from these rearrangements the production of guaiacyl and syringyl compounds and the separation of the aliphatic side chains form aromatic rings. When the temperature increases up to 350 – 450 °C, the demethylation of the dimethoxy groups involves the conversion of phenols into pyrocatechols. Eventually, rearrangement of the backbone occurs between 500 and 700 °C, producing an aromatic structure like char and may explain a higher amount of residue (30 – 50 wt%)

Despite the main decomposition products from lignin degradation, acetic acid, and non-condensable gases also evolve during the pyrolysis (Brebu and Vasile, 2010). CO is formed the first from 230 °C. It is followed by CH_4, both gradually increasing up to 500 °C. Evolution of CO at low temperature is attributed to the cleavage of aryl-ether linkages and increases at a higher temperature since diaryl ether bonds also break. Methane is originated from the weakly bonded methoxy group (– OCH_3–). In conclusion, decomposition of the substitution group and aliphatic structure induces the release of CO_2, H_2O from the hydroxyl groups CO from the weakly bonded oxygen groups, and finally H_2 from the rearrangement and condensation of the aromatic rings (Avni et al., 1985).

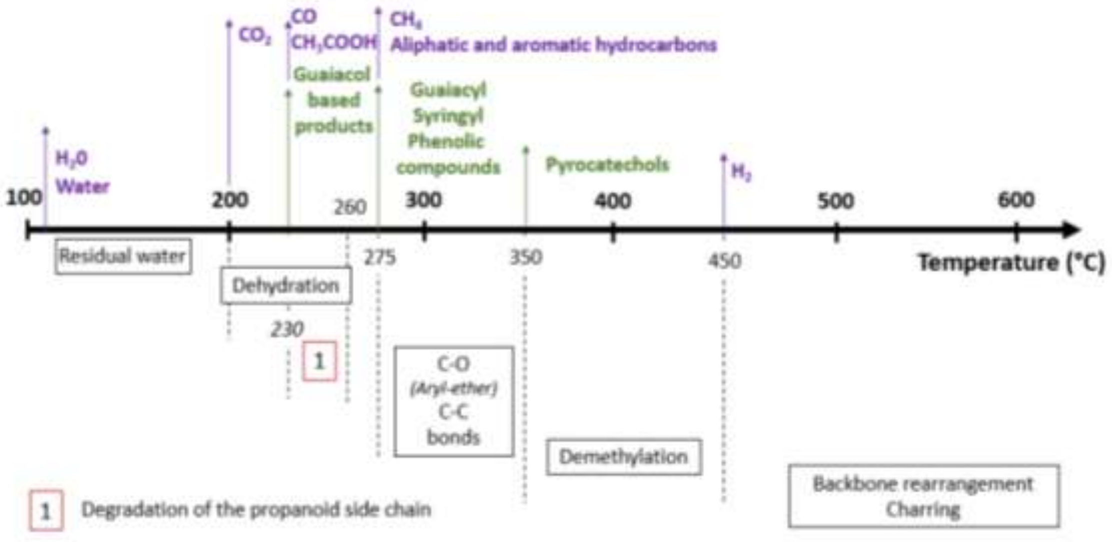

Figure 1.12. Overview of the decomposition product evolving during lignin's thermal decomposition (Prieur, 2016).

1.4.4. Lignin as Char former

In general, char is a highly cross-linked carbonaceous structure and looks like a porous solid which act as a heat insulator. The char formation takes place when a charring material is exposed to an external heat source. Chemical decomposition, cross-linking as well as bubble formation and mass transport are phenomena occurring during char formation. During the combustion of a charring system, the carbonaceous structure evolves from disordered polycyclic aromatic hydrocarbons to a more ordered structure, meaning a lower amount of amorphous phase, higher aromaticity, and more compact structure. Usually, made from phenolic resins, such heat shields do burn, forming a residual char which insulates the interior of the material from further heating.

Lignin is made of phenylpropanoid units, the amount of the three monolignols strongly affects lignin thermal degradation, and subsequently the amount of char formed. The phenylpropanoid units mainly linked via ether (C–O–C) and carbon-carbon (C–C) linkages. Li et al. (2002) investigated the thermal degradation and char formation of manchurian ash lignins. Through FTIR analysis (Figure 1.13), it was found that the relative absorbance of ether C–O–C (1120 cm^{-1}), phenolic and aliphatic –OH (1327 and 1033 cm^{-1}) and vibration of aliphatic carbon C–H (2940 cm^{-1}) decreased when the temperature increases. This evolution indicates that the cleavage of ether bonds took place first during heating. It was also noticed that the relative absorbance of aromatic ring vibration at around 1596 cm^{-1} increased while heating. Such degradation leads to a reorganization of the carbonaceous structure into more conjugated groups via crosslinking reactions. The thermal decomposition of lignins occurs in a wide temperature range and can be divided into three major steps: (i) moisture release below 200 °C, (ii) from 200 to 500 °C (continuous main mass loss through devolatilization), and (iii) beyond 500 °C (devolatilization with charring), where 40−60 wt% of all lignin still remain unvolatized due to the formation of condensed aromatic structures (Brebu and Vasile, 2010; Yang et al., 2007). During the first degradation step, the water release, related to the loss of free and bound water molecules, varies in the presence of oxygen-containing groups.

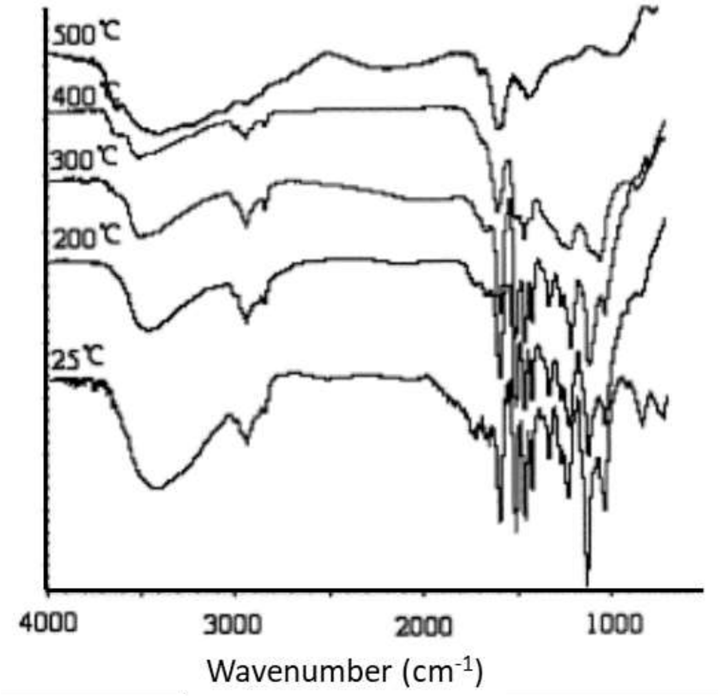

Figure 1.13. FTIR spectra of the manchurian ash lignin treated at different temperatures (Li et al., 2001).

Furthermore, it was also noticed by Ház et al. that during this first stage, a plasticization phenomenon occurs, which is observed by the reduction in glass transition temperature (Ház et al., 2013; Kun and Pukánszky, 2017). Consequently, the broad range temperature degradation is associated to the chemical structure of the lignins, and more specifically to the presence of various oxygen functional groups, the scissions of which occur at different temperatures. Accordingly, in the earlier stages, there are the scissions of weak ether, aryl−alkyl, and phenyl glycoside bonds, and unstable C−C bonds. The mass loss observed is mainly ascribed to the degradation of components of carbohydrates converted to volatile gases such as CO, CO_2, and CH_4. At the end of the second step, above 400 °C, the polyaromatic compound formed further decomposes to volatile species such as phenolic, alcohols, or aldehyde, and more condensed char is resulted due to the formation of stronger bonds.

1.4.5. Lignin as FR additive in the polymer system

The presence of lignin gives peculiar properties to the composite. Lignin can act as a stabilizer preventing polymer aging due to its antioxidant activity (Gregorová et al., 2006; Pouteau et al., 2003; Wood et al., 2011). In many cases, the thermal stability at a high temperature of the composites with lignin is improved in comparison to neat polymer. Moreover, lignin exhibits an interesting thermal degradation behaviour and naturally produce remarkable char residue at high temperature. Since char formation is one of the solutions to confer flame retardancy to the polymers, it has been considered as a potential charring agent for thermoplastic polymers. Furthermore, the addition of classical FR additive in can also improve the FR properties of the polymer.

1.4.5.1. Synthetic polymers

- **Polyolefin**

Polypropylene (PP) is one of the most versatile polymers used in a variety of applications, both as a plastic and as a fibre. Its low cost, low density, and easy processability make it suitable for applications in packaging, automobiles and textile industries. However, PP has some drawbacks such as low thermal stability, thermal oxidation, and high flammability. Gallina et al. presented the first study dealing with lignin as flame retardant in PP. in the late 90s. The fire behaviour was characterized by using mass loss cone calorimeter, and the tests were performed on thick sheet samples (6 mm), which influence significantly the cone results (changes of heat and mass transfer). With 20 wt% loading of steam exploded lignin in PP, the peak of heat release rate (PHRR) is remarkably decreased by 66 %, but the combustion time was much longer. The author concluded that such FR performance was achieved due to char formed during the combustion test (Gallina et al., 1998). Few years later, A. De Chirico et al. utilized lignin in the PP matrix to study thermal stability and fire performance of PP composite, blends containing 5, 10, 15 and 20 wt% of lignin were prepared. TG analysis showed the interactions between the PP and the lignin led to the formation of a protective surface shield, which was able to reduce the oxygen diffusion towards the polymer bulk (De Chirico et al., 2003). The same research group used lignin as charring agent with other traditional phosphorus

FR for improving the flame retardancy of PP. TGA and cone calorimetry study showed that a combination of lignin in intumescent formulation delayed the combustion time, enhanced the char residue and reduced the heat release rate during burning (Canetti et al., 2006).

Another study proposed by Yu et al. wherein alkali lignin was modified by chemical grafting of FR phosphorous and nitrogen-containing macromolecules, modified lignin (PN-lignin) was blended with the PP matrix to enhance fire retardant properties. Cone calorimetry study showed PN-lignin reduces the peak heat release rate (– 45 %) and slows the combustion process, modified lignin (PN-lignin) also exhibits a much higher char-forming ability with a char of 61.4 wt% as compared to 40.7 wt% for lignin at 600 °C in N_2 (Yu et al., 2012). A similar strategy was used by Liu et al. to fabricate flame retardant wood plastic (WP) PP composite. Lignin was chemically modified by grafting of P-N macromolecule and then coordinated with metal ions. Flammability of samples was tested using UL94: the obtained results reported that adding 15 wt% of modified lignin resulted in a self-extinction (V-1 rating), showing better FR properties than PP/WP composite. Cone tests showed that optimum loading of modified lignin in PP/WP was 15 wt%, which gave the best FR result by reducing PHRR, THR, and MARHE. Moreover, smoke production was also reduced by 30 wt% (Liu et al., 2016b).

▪ Acrylonitrile Butadiene-Styrene polymers

In a different study, Song et al. studied the influence of lignin addition in the acrylonitrile-butadiene-styrene copolymer (ABS). Cone calorimetry results showed the introduction of 20 wt% lignin resulting in 32 % reduction in peak heat release rate. The addition of styrene ethylene-co-butadiene styrene-grafted maleic anhydride (SEBS-g-MA) as in situ reactive compatibilizer for ABS/lignin composite further reduces peak heat release rate (PHRR), indicating enhanced flame retardancy due to the improved interfacial adhesion. The in situ reactive compatibilization with SEBS-g-MA also contributes to a protective char layer formation (Song et al., 2011).

▪ Polyethylene terephthalate

Polyethylene terephthalate (PET) is highly flammable and extensively used in a variety of applications. Using lignin as FR additive was considered by Canetti and Bertini. They investigated the thermal degradation and melting behaviour of PET and lignin blends. Thermal decomposition, melting behaviour, and crystallinity of the resulting blends were studied by thermogravimetry, differential scanning calorimetry, and X-ray diffraction, respectively. TG analyses results show that the introduction of lignin leads to char formation and effective char layer (~27 wt.%) formed with 20 wt% lignin content. It was observed by DSC analysis that the presence of lignin in blends promotes the crystallization process and induces a faster crystalline reorganization than that of the pure PET (Canetti and Bertini, 2009b).

▪ Polyurethane

Several studies have reported the use of neat or modified lignin as macromolecule in the preparation of biobased polyurethane (PU) (Jeong et al., 2013; Lu et al., 2018). A research group from China investigated lignin-modified PU foam as a single component with excellent flame retardancy (Zhu et al., 2014). To this, the corn straw lignin was first grafted with phosphate-melamine containing group to prepare a compound named as LPMC and then different wt% ratio (5, 10, 15 and 20 wt%) of LPMC were copolymerized with isocyanate to produce lignin-modified PU foam. The presence of LPMC promotes the generation of nonflammable gases during PU degradation, inhibiting the flame propagation and dehydration of PU to form compact char layer. Further, the char formation dramatically increases with increasing LPMC content. Flame retardancy assessed by limiting oxygen index (LOI) and UL-94 flame spread test revealed self-extinguishment (V-1 rating) and inhibition from melt dripping was achieved with 15 wt% LPMC in PU foam.

1.4.5.2. Biobased Polymers

- **Polylactic acid**

In this regard, Zhang et al. reported a novel intumescent flame retardant (IFR) consisting of microencapsulated ammonium polyphosphate (MCAPP) and lignin to confer fire retardancy to PLA (Zhang et al., 2013). The IFRs formulation was made up of MCAPP, lignin and organically modified montmorillonite (OMMT). PLA composite containing 21 wt% MCAPP/lignin and 2 wt% OMMT showed the best LOI value of 35.3 and UL-94 V-0 rating and exhibited a remarkable enhancement of the flame retardancy. For the same blend, the reduction of PHRR was 79%, and THR was 60% as assessed by cone calorimetry test. In addition, the char residue analysis clearly showed that the incorporation of OMMT can improve the char quality with a much more compact and continuous morphology. Alternatively, Reti et al. studied lignin-based intumescent to provide flame retardant PLA. 10 wt% kraft lignin and 30 wt% APP were blended with PLA and compared with the PLA/APP/starch and PLA/APP/PER systems containing the same formulation (Réti et al., 2008). The blends containing lignin exhibited LOI value as high as 32 vol.%, slightly lower than starch containing blends (40 vol.%) but acceptable to achieve self-extinction. However, UL-94 test revealed that the presence of lignin and starch leads to superior fire properties and V-0 rating was achieved. Cone calorimeter results showed that lignin-based formulation under test condition form an efficient intumescent protective char layer structure, which reduced the PHRR to 47%, was higher than that of the starch containing (PHRR, −41%) blend. However, the best cone test results were obtained for pentaerythritol blends (PHRR, - 64%).

- **Polyhydroxy butyrate (PHB)**

In another study, Bertini et al. exploited rice husk lignin, isolated by means of acidolytic (AL) and alkaline enzymatic (AEL) extraction methods (Bertini et al., 2012). The isolation methods provide lignin samples with significant differences among their molecular, thermal and chemical features. Bio-composites of poly(3-hydroxybutyrate) (PHB) with AL and AEL lignin were prepared. The morphological, structural and thermal characteristics of the bio-composites were intensively studied. TG analysis of the PHB-AL bio-composites showed an enhancement of the thermal resistance, thermal degradation shifted to higher temperature region. The increase of thermal stability was observed as a function of the lignin amount in PHB-AL bio-composites (Bertini et al., 2012).

- **Polybutylene succinate**

Further, Ferry et al. (2015) used lignins (alkali and organosolv) as flame retardant to improve the fire behaviour of polybutylene succinate (PBS). Lignin was modified by grafting of macromolecular phosphonate compounds. The blends were prepared with unmodified and modified lignin in PBS. When unmodified lignin introduced in PBS the HRR reduced but the cracks were found on the char surface. The introduction of modified lignin not only reduced the heat release rate but also promotes thick charring behaviour. Alkali modified lignin exhibited higher FR result than organosolv lignin. In the same context, Liu et al. study the modification of alkali lignin by grafting of phosphorus-nitrogen-zinc-containing macromolecule and blending of modified lignin (PNZn-lignin) with PBS. Incorporation of PNZn-lignin effectively increases to some extent the thermal stability of PBS composites by shifting T_{max}. With the addition of 10 wt% of PNZn-lignin, PHRR and THR are reduced by 51 and 68%, respectively. Meanwhile, the TSR is also decreased up to 55% as compared to pure PBS. Interestingly, the char residue is enhanced from 9 wt% for pure PBS to 55 wt% with 10 wt% of PNZn-lignin content. The presence of Zn (II) ions leads to a compact, thick and robust char layer and reduced flammability and low smoke release (Liu et al., 2016a).

1.4.6. Polyamide 11: Preparation and flame retardancy

Polyamide 11(PA), $[C_{11}H_{21}ON]_n$, one of the promising engineering plastics is a semicrystalline polymer that can also be produced from renewable resources, such as castor oil or canola oil.

PA has attracted much attention due to its high mechanical strength, good resistance to chemicals (particularly hydrocarbons), abrasion resistance, high dimensional stability, and low density. Because of the excellent properties, PA has been exploited in various industries such as transport, automotive, electronics, oil and gas, wire & cables, aerospace, sports applications, and textile industries (Arkema Inc., 2012; Griffiths, 2007; Holbery and Houston, 2006; Kuciel et al., 2012). In Textile industries, PA is another fibre grade polyamide put on the market in much lower quantities than PA6 and PA66 fibres (Wesołowski and Płachta, 2016).

PA (Rilsan®), is continuously produced by Arkema for more than fifty years from castor oil. PA is synthesized by the condensation polymerization of the monomer 11-aminoundecanoic acid, which in turn is a product from chemical conversion of ricinoleic acid, the major fatty acid component of castor oil (Ogunniyi, 2006). In this process, castor oil is hydrolyzed to give ricinoleic acid and glycerol, which are separated. High-temperature treatment of the methyl ester of ricinoleic acid produces 11-undecanelic acid and heptanal. Bromination of the double bond of 11-undecalenic acid followed by reaction with ammonia gives 11-aminoundecanoic acid (Gotro, 2013). All the steps involved in the process are shown in Scheme 1.5. Besides, the synthesis of PA monomer from an alternative renewable feedstock, namely canola oil is also reported (Spiccia et al., 2013).

Processing of PA is relatively easier due to the low melting point (around 200 °C) when compared with other polyamides. It can be processed using most processing technologies (extrusion, extrusion-blow molding, injection molding, and rotomolding). Furthermore, the PA matrix accommodates several additives and filling agents, for example, stabilizers, plasticizers, lubricants, colorants, impact modifiers, glass fiber, carbon fiber, etc.

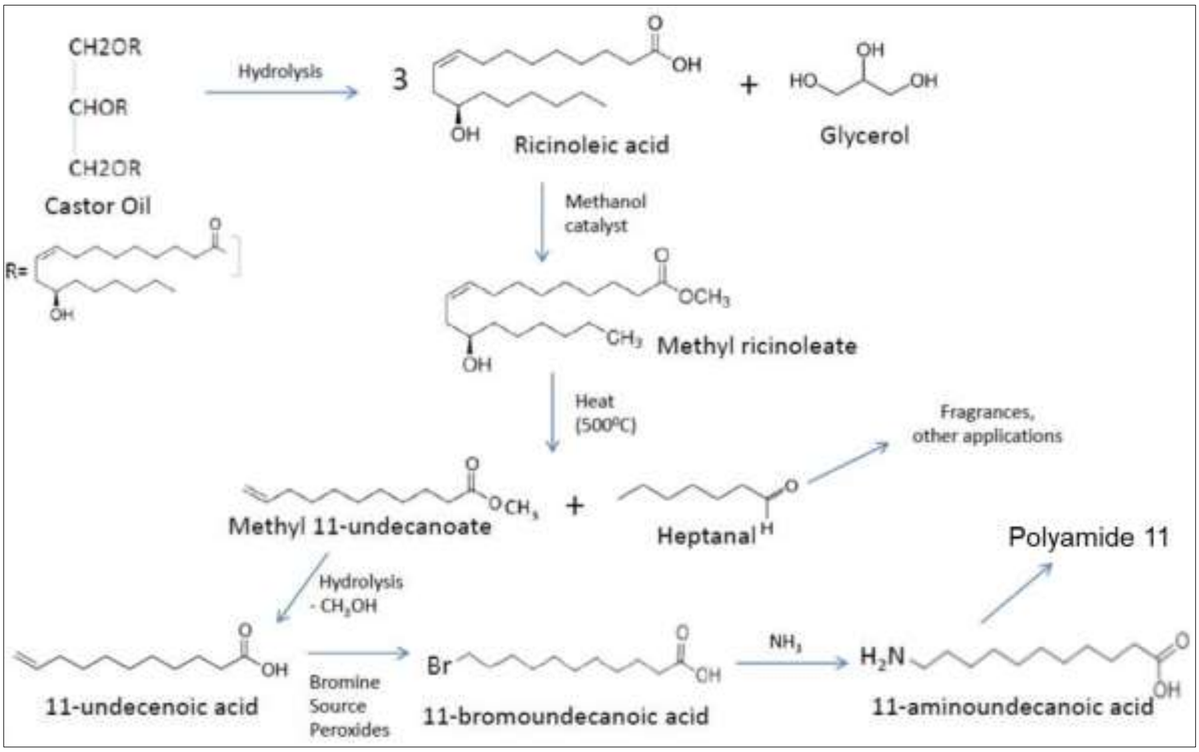

Scheme 1.5. Polyamide 11 production steps from castor oil, (Adopted from Polymer Innovation Blog, http://polymerinnovationblog.com/bio-polyamides-where-do-they-come-from/)

Because of the environmental challenges, Rilsan® PA is gaining more attention as an alternative to their petroleum-based counterparts. Nevertheless, to achieve specifications bound to applications, some of the polymer properties must be modified. Thermal stability and flammability are crucial in many areas, such as automotive, transportation, building, electrical devices, and high-performance textiles. In those sectors, a certain level of FR properties are required, and thus polyamide fibre faces strong competition from polyester fibre, for which acceptable FR solutions already exist. Indeed, one of the classical solutions to flame retardant polyester is to incorporate a comonomeric phosphinic acid unit into the PET polymeric chain (trade name Trevira® CS).

In order to improve the fire performance of PA, considerable works have been carried out. Mailhos-Lefievre et al. (1989) used a mixture of decabromodiphenyl-antimony trioxide in highlighting a bromine–nitrogen synergism for improving the flame retardancy of PA11. A few years later, the effect of APP on the thermal decomposition of PA11 and PA12 was investigated (Levchik et al., 1992). The interaction of APP with PA11 suggests the formation of intermediate phosphate ester bonds which further decompose to favor the formation of an intumescent char. Recently, Cayla et al. studied the optimal ratio between APP and kraft lignin to be used in PA for optimization of FR properties. It was found that the presence of 20 wt% lignin in PA showed a charring effect and reduced PHRR to 66 % in PCFC test. However, when lignin combined with APP, PHRR was reduced only up to 30% for the prepared blends, which indicates that interaction between APP and lignin is not effective in PA (Cayla et al., 2019). In the same context, PA11/nanocomposites based on nanoparticles such as organic clay and carbon nanofiber (CNF) have been widely used to improve the fire resistance of PA. The introduction of nanofillers (OMMT and CNF), combined with conventional intumescent FR (Clariant® OP) has resulted in the enhancement of flame retardancy. Flame spread test (UL94) showed that at least 5 wt% loading of nanofiller and 20 wt% of FR additive were required to achieve V-0 rating. It was found that CNF exhibited a better synergistic effect with all FR formulations. (Lao et al., 2008). The same research group worked on various types of nanoparticles, e.g., nanoclays (NCs), carbon nanofibers (CNFs), and nanosilicas (NSs) to improve the fire behavior of PA11 (Lao et al., 2011, 2010, 2009). PA11 and PA12 were melt-blended with low concentrations (i.e., 2.5, 5 and 7.5 wt%) of all nanoparticles, an intumescent FR additive (Clariant® OP) was added to the mechanically superior NC and CNF PA11 formulations. Their study showed that nanoparticles improve the thermal stability of the polymer. For the PA11/FR/NCs blends, only the 20% FR/7.5% NC sample passed the UL94 V-0 test; for the PA11/FR/CNF blends, all three formulations passed UL94 V-0 test.

Although, there has been a considerable amount of research work going on in the area of polymer nanocomposites, there has been limited success in developing fibre and textile structure with them.

1.5. The strategy of FR treatment for textile

Textiles are an integral part of human life whether they are textiles of clothing, furnishings or decorative. However, their combustible nature makes them potentially hazardous materials with considerable risk to users. Therefore, it is necessary that solutions must be developed for materials in fibre or fabric form. In order to confer flame retardant properties to materials in fabric form, several methods are adopted. These methods are closely depended on the nature of the textile material used. various processes carried out in the literature are reviewed, which deal with the improvement of the FR properties of fibrous materials.

1.5.1. High-performance fibres

High-performance fibers are those that are engineered for specific uses that require exceptional strength, chemical and heat resistance, and flame resistance. Developing textiles from high-performance fibres is a reliable way to achieve excellent fire resistance. Several communications have reviewed the marketed fibres whose fire properties are far superior to conventional thermoplastic fibres (Bourbigot and Flambard, 2002; Smith, 1999).

Few examples of these fibres listed in Table 1.2 are used in aerospace, biomedical, civil engineering, construction, protective apparel, geotextiles or electronic areas. Fabrics employed from these materials would significantly limit the propagation of the flame which is crucial when combustion occurs. In fibrous form, Bourbigot et al. studied the thermal degradations (Bourbigot et al., 2001a) and fire reactions (Bourbigot et al., 2001b) of knitted structures based on Zylon® and Kevlar® fibres. The textiles in Zylon® showed better thermal stability and reaction to fire than those in Kevlar® with lower PHRR (150 against 430 kW/m² under a heat flux of 75 kW/m²). The smoke release was also lower for textiles in Zylon®. Very recently, Ramgobin et al. studied several aspects of polymeric materials that have a significant role in the thermal stability and fire behavior of a high-performance polymeric material (Ramgobin et al., 2019). Despite the efficiency of these fire-resistant fibres, the technical (production complexity) or economical (high price) aspect restrict their utilization in wide-spread areas. Also, some of them are very sensitive to ultraviolet radiation. One of the most common solutions for such hindrance is the combination of fibres, the mixture of materials allows to combine their physical characteristics and, in some cases, lower the cost of the final product.

Table 1.2. List of heat and flame resistance high-performance polymer fibres (Didane, 2012).

Chemical name	Generic	Trade name	LOI
Poly (p-phenylene-terephtal-amide)	para-aramide	Kevlar, Twaron,	25-28
Poly (m-phenylene-isophtal-amide)	meta-aramide	Nomex, Teijinconex	30
Poly (amide-imide)	PAI	Kermel, Torlon	30-32
Polyimides	PI	P-84	38
Poly (ether-ether-ketone)	PEEK	Zyex	35
Poly (phenylene sulfide)	PPS	Ryton, Procon,	34
Aromatic polyester	-	Vectran	37
Poly (melamine-co-formaldehyde)	-	Basofil	32
Poly (phenylene-benzobis-oxazole)	PBO	Zylon	68
Poly (benzimidazole)	PBI	PBI	41
Poly(tetra-fluoro-ethylene)	PTFE	Teflon, Toyoflon	95
Polyetherimide	PEI	Ultem	45

1.5.2. Flame retardant finishing

FR finishing technique is also used to bring flame retardancy to fibre or textiles. The major advantage of this process is that it preserves the mechanical properties of the material and that its implementation is relatively simple with low cost compared to other FR methods. This method can be applied to synthetic and natural fibres. However, treatments are sometimes not resistant to friction and washes, in some cases, deteriorate the sensory properties of the fabric.

Thus, the use of FR finishing is one of the solutions to enhance the fire behaviour of textiles. For polyamide, semi-durable finishes based on thiourea derivatives are often used but usually only on industrial nylon textiles where washability is not an issue (Horrocks, 1996). Durable but stiff flame retardant finishes based on methylated urea-formaldehyde with thiourea-formaldehyde have been applied to nylon, which is heat cured with an acid catalyst (Horrocks, 2001). It is commercially available as Flamegard® 908 (Syborn chemicals) (Weil and Levchik, 2008a). Few durable compounds initially designed for polyester are reported to be also effective for polyamide such as Antiblaze® CU/CT, which is a cyclic oligomeric phosphonate (Horrocks, 2001). Besides, Durable flame retardant for polyamides is developed by Thor chemicals, AFLAMMIT® NY is a system of two compounds, comprising NY1 and NY2, the first being an organic nitrogen/sulphur FR, and the second methylated urea used as a reactive crosslinking component (Thor Chemicals, 2011).

Chemical grafting of materials to the surfaces of fibres has also been tried. For example, PA6 fibres have been surface grafted with poly(2-methyl-5-vinyl pyridine) and then further treated with various halogenated flame retardants to give LOIs of up to 31 vol.% (Efros et al., 1983) and with o-chlorophenol to similar effect (Mukherjee et al., 1981).

1.5.3. Flame retarding fibres with additives

The direct incorporation of flame retardants in the molten polymer during extrusion seems to be the simplest way to produce the fire retardant fibre with an advantage to vary the types of FR additive and their concentration in polymer bulk. Once the additive is introduced into the polymer matrix by extrusion, it is processed by melt-spinning. However, problems of compatibility with several FR additives occur at the high temperatures used during melt-spinning of polymers like polyamide, polyester, and polypropylene (Horrocks, 2001). The presence of quite high FR concentrations (> 20 wt%) necessary to confer FR properties, not only creates spinning fluid compatibility problem but also causes a reduction in fibre tensile strength and other essential textile properties. This may prevent the successful incorporation of

FR during the process; as consequence, only a few fire retarded fibres are commercially available.

Trevira® CS (Trevira GmbH, formerly Hoechst) is one of the most successful commercially available FR polyester fibres. The flame retardancy has been achieved in commercial PET fibre by direct incorporation of reactive comonomeric organophosphorus units in the main chain (Bourbigot, 2008; Weil and Levchik, 2004). Another commercially utilized P-containing comonomer is the 9,10-dihydro-9-oxa-10-phosphaphenanthrenyl-10-oxide (DOPO). PET fibres containing this FR comonomer are commercially available from Toyobo under the trade name, HEIM® and have LOI ranging up to 28 vol.% (Weil and Levchik, 2004).

For polyamides, Bourbigot et al. developed multifilament based on PA6 and Cloisite® 30B at a loading of 5 wt% (Bourbigot et al., 2002). The fabrics produced from the loaded multifilament showed, a reduction of 40% in the PHRR under a heat flux of 50 kW/m^2 compared to the fabric from unfilled PA6. The same additives were studied by Solarski et al. in a polylactide matrix. With 4 wt% of Cloisite® 30B, the authors observed improved fire retardancy for knitted structure (Solarski et al., 2007). Vargas et al. reported a small amount of 0.75 wt% of sepiolite improved the fire performance of polypropylene multifilament. Textiles structure showed decreases in PHRR and THR in comparison with the pure PP textile (Vargas et al., 2010). In addition, the FR additives for PP and their potential suitability for use in fibre application has been extensively reviewed (Zhang and Horrocks, 2003).

The same nanocomposite approach was adopted by Shanmuganathan et al. for developing the melt-spun FR fibres of PA6/OMMT system (Shanmuganathan et al., 2008). Nanocomposites with 8 wt% OMMT offered better spinnability and the fibres have satisfactory physical properties to be knitted into fabrics. It was found that the FR effect depends on fabric geometry as well as the test conditions. Char forming kinetics was relatively slow to protect the material from flame spread in horizontal flame spread test and hence, the nanocomposite fabric does not show a significant difference in flame spread behavior compared to nylon 6 fabrics. However, under radiant heat conditions, the fibres melt and enable the formation of a continuous charred surface at very early stages of burning resulting in improved flame retardancy properties. Fabric tightness factor plays a crucial role in favouring the formation of char, and with higher tightness factor, enhanced flame retardancy was achieved.

1.6. Conclusion and strategy

The flame retardancy of polymers and the main additives used to flame retard polyamides were reviewed in the first part. Halogenated FR additives are very effective but have a negative impact on the environment and human health. Thus, the research trend moved toward the development of non-halogenated alternatives. It was found that char promoting FR additives appeared to be a reliable and effective substance with regards to design the environmentally friendly FR system. Phosphinate FR developed since the 1990s appeared to an effective compound in polyamides. Various studies on their FR effect and mode of action in polyester and polyamide have been reviewed. The next part detailed the lignin as a biobased compound and its extraction processes. Due to the global sustainability demands, more interest is given towards the valorization of lignin to find the emerging application of this biobased material, which presents interesting properties as additive in polymers, and hence lignin can be used in many applications. Furthermore, thermal decomposition of lignin in inert atmosphere offers a significant amount of char formation. Char formation under fire condition is one of the basic requirements in intumescent action. Indeed, char acts as a protective and insulating barrier. Thus, a literature study has been presented to reveal the use of lignin as FR additive alone or in combination with FRs in numerous.

Polyamide 11 (PA) produced from renewable resources is an alternative to petroleum-based counterparts. Due to its biobased nature, PA has attracted much attention in various industrial applications including textile applications. However, low FR properties limit its potential applications in high performance textiles. Existing solutions for flame retarding PA are detailed through literature study. Some of the fire retardants used in the bulk are not suitable to be used in fibre applications due to compatibility issue during melt spinning and to the high loading content (> 20 wt%) of FR additive. Thus, flame retarding solution for PA in fibre form still remain a significant challenge.

In this context, the purpose of this study is to utilize low-cost industrial lignin as FR additive in the fibre forming PA. Char promoting phosphinate FR will be used in combination with lignin at low loadings. The study of optimal ratio between lignin and FR will be studied to optimize fire retardant properties.

The purpose of this study will be achieved in the following sub objectives:

- Consider lignin which is commercially available in large quantities
- Develop a FR formulation which contains a higher amount of lignin
- Optimize the FR and lignin ratio in terms of fire performance
- Demonstrate the mode of action of lignin in FR system

To fulfill these objectives; the multi-step approach is adopted. In a first step, different lignin with PA will be mixed and thermal stability and fire retardancy properties will be studied. Then, laboratory grade lignin with ZnP will be used as a primary study for the proof-of-concept in order to optimize the ratio and to understand interaction as well as the fire retardant behaviour. In the next step, low-cost industrial lignin will be used in combination with phosphinate FR for scale-up and production of multifilaments. Ternary blend pellets will be characterized by various techniques. fire retardant properties on plate samples will be investigated. Finally, the selected formulation will be used for the production of multifilament by melt spinning. Mechanical properties, fineness, and distribution of additives in fibre will be evaluated. Fire performance in fabric form will be studied on knitted fabric samples.

References

Adam, M., Ocone, R., Mohammad, J., Berruti, F., Briens, C., 2013. Kinetic Investigations of Kraft Lignin Pyrolysis. Ind. Eng. Chem. Res. 52, 8645–8654. https://doi.org/10.1021/ie400979x

Adorjan, I., Zhou, Z., Jaaskelainen, A.S., 2006. European workshop on lignocellulosics and Pulp.

Agrawal, A., Kaushik, N., Biswas, S., 2014. Derivatives and Applications of Lignin – An Insight.

Al Mamun, A., Nikousaleh, M.A., Feldmann, M., Rüppel, A., Sauer, V., Kleinhans, S., Heim, H.-P., 2016. Lignin Reinforcement in Bioplastic Composites, in: Lignin in Polymer Composites. Elsevier, pp. 153–165. https://doi.org/10.1016/B978-0-323-35565-0.00008-4

Alongi, J., Han, Z., Bourbigot, S., 2015. Intumescence: Tradition versus novelty. A comprehensive review. Prog. Polym. Sci. 51, 28–73. https://doi.org/10.1016/j.progpolymsci.2015.04.010

Amen-Chen, C., Pakdel, H., Roy, C., 2001. Production of monomeric phenols by thermochemical conversion of biomass: a review. Bioresour. Technol. 79, 277–299. https://doi.org/10.1016/S0960-8524(00)00180-2

Aoyama, T., Morikawa, M., Kato, N., Hashiba, I., Nagano, M., Aramaki, K., 1976. Fire resistance polyester and polyamide composition. JP51088549.

Arias, P., 2001. Borominated flame retardants - An overview, in: Proc. 2nd Int. Workshop on Brominated Flame Retardants, Stockholm, Sweden. pp. 17–19.

Arkema Inc., 2012. Rilsan® PA11 : Technical report.

Avni, E., Coughlin, R.W., Solomon, P.R., King, H.H., 1985. Mathematical modelling of lignin pyrolysis. Fuel 64, 1495–1501. https://doi.org/10.1016/0016-2361(85)90362-X

Berlin, A., Balakshin, M.Y., Raymond, M., Maximenko, G., ORTIZ, D., 2011. Organosolv Process. WO/2011/097720.

Bertini, F., Canetti, M., Cacciamani, A., Elegir, G., Orlandi, M., Zoia, L., 2012. Effect of ligno-derivatives on thermal properties and degradation behavior of poly(3-hydroxybutyrate)-based biocomposites. Polym. Degrad. Stab. 97, 1979–1987.

https://doi.org/10.1016/j.polymdegradstab.2012.03.009

Birnbaum, L.S., Staskal, D.F., 2004. Brominated flame retardants: cause for concern? Environ. Health Perspect. 112, 9–17.

Björkman, A., 1956. Studies on finely divided wood. Part 1. Extraction of lignin with neutral solvents. Sven. papperstidning 59, 477–485.

Boerjan, W., Ralph, J., Baucher, M., 2003. Lignin Biosynthesis. Annu. Rev. Plant Biol. 54, 519–546. https://doi.org/10.1146/annurev.arplant.54.031902.134938

Bourbigot, S., 2008. Flame retardancy of textiles: new approaches, in: Advances in Fire Retardant Materials. Woodhead Publishing, pp. 9–40. https://doi.org/10.1533/9781845694701.1.9

Bourbigot, S., Bras, M. Le, Duquesne, S., Rochery, M., 2004. Recent Advances for Intumescent Polymers 499–511. https://doi.org/10.1002/mame.200400007

Bourbigot, S., Bras, M. Le, Leeuwendal, R., Shen, K.K., Schubert, D., 1999. Recent advances in the use of zinc borates in fame retardancy of EVA 64.

Bourbigot, S., Devaux, E., Flambard, X., 2002. Flammability of polyamide-6/clay hybrid nanocomposite textiles. Polym. Degrad. Stab. 75, 397–402. https://doi.org/10.1016/S0141-3910(01)00245-2

Bourbigot, S., Flambard, X., 2002. Heat Resistance and Flammability of High Performance Fibres: A Review. FIRE Mater. Fire Mater 26, 155–168. https://doi.org/10.1002/fam.799

Bourbigot, S., Flambard, X., Poutch, F., 2001a. Study of the thermal degradation of high performance fibres-application to polybenzazole and p-aramid fibres. Polym. Degrad. Stab. 74, 283–290. https://doi.org/10.1016/S0141-3910(01)00159-8

Bourbigot, S., Flambard, X., Poutch, F., Duquesne, S., 2001b. Cone calorimeter study of high performance fibres-application to polybenzazole and p-aramid fibres. Polym. Degrad. Stab. 74, 481–486. https://doi.org/10.1016/S0141-3910(01)00175-6

Braun, U., Bahr, H., Schartel, B., 2010. Fire retardancy effect of aluminium phosphinate and melamine polyphosphate in glass fibre reinforced polyamide 6. e-Polymers.

Braun, U., Bahr, H., Sturm, H., Schartel, B., 2008. Flame retardancy mechanisms of metal phosphinates in combination with melamine cyanurate in glass-fiber reinforced poly (1 , 4-butylene terephthalate): the influence of metal cation. Polym. Adv. Technol. 19, 680–

692. https://doi.org/10.1002/pat.1147

Braun, U., Schartel, B., 2008. Flame Retardancy Mechanisms of Aluminium Phosphinate in Combination with Melamine Cyanurate in Glass-Fibre-Reinforced. Macromol. Mater. Eng. 293, 206–217. https://doi.org/10.1002/mame.200700330

Braun, U., Schartel, B., Fichera, M.A., Jäger, C., 2007. Flame retardancy mechanisms of aluminium phosphinate in combination with melamine polyphosphate and zinc borate in glass-fibre reinforced polyamide 6,6. Polym. Degrad. Stab. 92, 1528–1545. https://doi.org/10.1016/j.polymdegradstab.2007.05.007

Brebu, M., Tamminen, T., Spiridon, I., 2013. Thermal degradation of various lignins by TG-MS/FTIR and Py-GC-MS. J. Anal. Appl. Pyrolysis 104, 531–539. https://doi.org/10.1016/j.jaap.2013.05.016

Brebu, M., Vasile, C., 2010. Thermal Degradation of Lignin - A Review. Cellul. Chem. Technol. 44, 353–363.

Bykov, I., 2008. Characterization of Natural and Technical Lignins using FTIR Spectroscopy. Lulea University of Technology.

Caballero, J.A., Font, R., Marcilla, A., 1996. Study of the primary pyrolysis of Kraft lignin at high heating rates: yields and kinetics. J. Anal. Appl. Pyrolysis 36, 159–178. https://doi.org/10.1016/0165-2370(96)00929-1

Caballero, J.A., Font, R., Marcilla, A., García, A.N., 1993. Flash pyrolysis of Klason lignin in a Pyroprobe 1000. J. Anal. Appl. Pyrolysis 27, 221–244. https://doi.org/10.1016/0165-2370(93)80011-N

Camino, G., Costa, L., Trossarelli, L., 1984a. Study of the mechanism of intumescence in fire retardant polymers: Part III—Effect of urea on the ammonium polyphosphate-pentaerythritol system. Polym. Degrad. Stab. 7, 221–229. https://doi.org/10.1016/0141-3910(84)90098-3

Camino, G., Costa, L., Trossarelli, L., 1984b. Study of the mechanism of intumescence in fire retardant polymers: Part II—Mechanism of action in polypropylene-ammonium polyphosphate-pentaerythritol mixtures. Polym. Degrad. Stab. 7, 25–31. https://doi.org/10.1016/0141-3910(84)90027-2

Canetti, M., Bertini, F., 2009. Influence of the lignin on thermal degradation and melting behaviour of Poly(ethylene terephthalate) based composites. E-Polymers 1–10.

https://doi.org/ 10.1515/epoly.2009.9.1.596

Canetti, M., Bertini, F., Chirico, A. De, Audisio, G., 2006. Thermal degradation behaviour of isotactic polypropylene blended with lignin 91, 494–498. https://doi.org/10.1016/j.polymdegradstab.2005.01.052

Cayla, A., Rault, F., Giraud, S., Salaün, F., Sonnier, R., Dumazert, L., 2019. Influence of Ammonium Polyphosphate/Lignin Ratio on Thermal and Fire Behavior of Biobased Thermoplastic: The Case of Polyamide 11. Materials (Basel). 12, 1146. https://doi.org/10.3390/ma12071146

Clarke, F.B., 1999. The effects of brominated flame retardants on the elements of fire hazard: a re-examination of earlier results. Fire Mater. 23, 109–116.

Cullis, C.F., Hirschler, M.M., Taot, Q.M., 1991. Studies of the Effects of Phosphorus-Nitrogen-Bromine System on the Combustion of some Thermoplastic Polymers. Eur. Polym. J 27, 281–289.

Cusack, P.A., Heer, M.S., Monk, A.W., 1997. Zinc hydroxystannate as an alternative synergist to antimony trioxide in polyester resins containing halogenated flame retardants. Polym. Degrad. Stab. 58, 229–237. https://doi.org/10.1016/S0141-3910(97)00055-4

Darnerud, P.O., 2003. Toxic effects of brominated flame retardants in man and in wildlife. Environ. Int. 29, 841–853. https://doi.org/10.1016/S0160-4120(03)00107-7

De Chirico, A., Armanini, M., Chini, P., Cioccolo, G., Provasoli, F., Audisio, G., 2003. Flame retardants for pp based on lignin. Polym. Degrad. Stab. 79, 139–145.

de Wit, C.A., 2002. An overview of brominated flame retardants in the environment. Chemosphere 46, 583–624.

Delmas, M., 2008. Vegetal Refining and Agrichemistry. Chem. Eng. Technol. 3, 792–797. https://doi.org/10.1002/ceat.200800052

Didane, N., 2012. Elaboration et caractérisation fonctionnelle de matériaux polymères intumescents - Application aux textiles de recouvrement. University of Lille.

Didane, N., Giraud, S., Devaux, E., 2012a. Fire performances comparison of back coating and melt spinning approaches for PET covering textiles. Polym. Degrad. Stab. 97, 1083–1089. https://doi.org/10.1016/j.polymdegradstab.2012.04.010

Didane, N., Giraud, S., Devaux, E., Lemort, G., 2012b. A comparative study of POSS as synergists with zinc phosphinates for PET fire retardancy. Polym. Degrad. Stab. 97, 383–391. https://doi.org/10.1016/j.polymdegradstab.2011.12.004

Didane, N., Giraud, S., Devaux, E., Lemort, G., 2012c. Development of fire resistant PET fibrous structures based on phosphinate-POSS blends. Polym. Degrad. Stab. 97, 879–885. https://doi.org/10.1016/j.polymdegradstab.2012.03.038

Doherty, W.O.S., Mousavioun, P., Fellows, C.M., 2011. Value-adding to cellulosic ethanol: Lignin polymers. Ind. Crops Prod. 33, 259–276. https://doi.org/10.1016/j.indcrop.2010.10.022

Dorrestijn, E., Laarhoven, L.J.J., Arends, I.W.C.E., Mulder, P., 2000. The occurrence and reactivity of phenoxyl linkages in lignin and low rank coal. J. Anal. Appl. Pyrolysis 54, 153–192. https://doi.org/10.1016/S0165-2370(99)00082-0

Duquesne, S., Fontaine, G., Cérin-Delaval, O., Gardelle, B., Tricot, G., Bourbigot, S., 2013. Study of the thermal degradation of an aluminium phosphinate–aluminium trihydrate combination. Thermochim. Acta 551, 175–183. https://doi.org/10.1016/J.TCA.2012.10.025

Efros, V.A., Tyuganova, M.A., Galbraikh, L.S., 1983. Preparation of a fire-resistant nonmelting polycaprolactam fiber. Khim. Volokna 6, 31–32.

El Mansouri, N., Pizzi, A., Salvadó, J., 2007. Lignin-based wood panel adhesives without formaldehyde. Holz als Roh- und Werkst. 65, 65–70. https://doi.org/10.1007/s00107-006-0130-z

Faravelli, T., Frassoldati, A., Migliavacca, G., Ranzi, E., 2010. Detailed kinetic modeling of the thermal degradation of lignins. Biomass and Bioenergy 34, 290–301. https://doi.org/10.1016/j.biombioe.2009.10.018

Feng, C.-M., Zhang, Y., Dong, L., Liu, S.-W., Zhen-Guo, C., Xu, J.-R., 2013. Flame Retardant Mechanism of a Novel Intumescent Flame Retardant Polypropylene. Procedia Eng. 52, 97–104. https://doi.org/10.1016/j.proeng.2013.02.112

Ferry, L., Dorez, G., Taguet, A., Otazaghine, B., Lopez-Cuesta, J.M., 2015. Chemical modification of lignin by phosphorus molecules to improve the fire behavior of polybutylene succinate. Polym. Degrad. Stab. 113, 135–143. https://doi.org/10.1016/j.polymdegradstab.2014.12.015

Gallina, G., Bravin, E., Badalucco, C., Audisio, G., Armanini, M., De Chirico, A., Provasoli, F., 1998. Application of cone calorimeter for the assessment of class of flame retardants for polypropylene. Fire Mater. 22, 15–18.

Gellerstedt, G., Henriksson, G., 2008. Lignins: Major Sources, Structure and Properties, in: Monomers, Polymers and Composites from Renewable Resources. Elsevier, pp. 201–224. https://doi.org/10.1016/B978-0-08-045316-3.00009-0

Global Lignin Market - Industry Analysis, Size, Growth, Trends, Statistics, Segment and Forecast 2014-2020 [WWW Document], 2015. URL http://www.marketresearchstore.com/report/lignin-market-for-z36379

Gosselink, R J A, Abächerli, A., Semke, H., Malherbe, R., Käuper, P., Nadif, A., Van Dam, J.E.G., 2004. Analytical protocols for characterisation of sulphur-free lignin. Ind. Crops Prod. 19, 271–281. https://doi.org/10.1016/j.indcrop.2003.10.008

Gosselink, R.J.A., de Jong, E., Guran, B., Abächerli, A., 2004. Co-ordination network for lignin—standardisation, production and applications adapted to market requirements (EUROLIGNIN). Ind. Crops Prod. 20, 121–129. https://doi.org/10.1016/j.indcrop.2004.04.015

Gotro, J., 2013. Bio-Polyamides: Where Do They Come From? - Polymer Innovation Blog. https://polymerinnovationblog.com/bio-polyamides-where-do-they-come-from/

Green, J., 1996. Phosphorus-bromine flame retardant synergy in polycarbonate/ABS blends. Polym. Degrad. Stab. 54, 189–193. https://doi.org/10.1016/S0141-3910(96)00043-2

Gregorová, A., Košíková, B., Moravčík, R., 2006. Stabilization effect of lignin in natural rubber. Polym. Degrad. Stab. 91, 229–233. https://doi.org/10.1016/j.polymdegradstab.2005.05.009

Griffiths, K., 2007. Polyamides in aerospace industry. Trans. IMF 85, 235–236. https://doi.org/10.1179/174591907X229536

H. Nagele, J. Pfitzer, P. Eyerer, N. Eisenreich, P. Elsner, W. Eckl, 2000. Methods for producing a fibre-reinforced plastic substance. WO 00/27925.

Hastie, J.W., 1973. Molecular Basis of Flame Inhibition. J. Res. Notional Bur. Stand. Phys. Chem. 77.

Hastie, J.W., Bonnell, D.W., 1980. Molecular Chemistry of Inhibited Combustion Systems. https://doi.org/10.6028/NBS.IR.80-2169

Ház, A., Jablonský, M., Orságová, A., 2013. Determination of Temperature Regions. 4nd Int. Conf. Renew. Energy Sources 2013 200280301, 1–6.

Holbery, J., Houston, D., 2006. Natural-fiber-reinforced polymer composites in automotive applications. JOM 58, 80–86. https://doi.org/10.1007/s11837-006-0234-2

Hörold, S., 2014. Phosphorus-based and Intumescent Flame Retardants, in: Polymer Green Flame Retardants. Elsevier, pp. 221–254. https://doi.org/10.1016/B978-0-444-53808-6.00006-8

Horrocks, A.R., 2011. Flame retardant challenges for textiles and fibres: New chemistry versus innovatory solutions. Polym. Degrad. Stab. 96, 377–392. https://doi.org/10.1016/j.polymdegradstab.2010.03.036

Horrocks, A.R., 2001. Textiles, in: Fire Retardant Materials. Woodhead Publishing, pp. 128–181. https://doi.org/10.1533/9781855737464.128

Horrocks, A.R., 1996. Developments in flame retardants for heat and fire resistant textiles—the role of char formation and intumescence. Polym. Degrad. Stab. 54, 143–154. https://doi.org/10.1016/S0141-3910(96)00038-9

Jenewein, E., Kleiner, H., Wanzke, W., Budzinsky, W., 2002. Synergistic flame protection agent combination for thermoplastic polymers. US6365071B1.

Jenewein, E., Kleiner, W., Budzinsky, W., 2002. Synergistic flame protection agent combination for thermoplastic polymers. US6365071.

Jeong, H., Park, J., Kim, S., Lee, J., Ahn, N., Roh, H. gyoo, 2013. Preparation and characterization of thermoplastic polyurethanes using partially acetylated kraft lignin. Fibers Polym. 14, 1082–1093. https://doi.org/10.1007/s12221-013-1082-7

Joseph Louis Gay-Lussac, 1821. Annales de Chimie et de Physique 18, 221.

Kashiwagi, T., Harris, R.H., Zhang, X., Briber, R.M., Cipriano, B.H., Raghavan, S.R., Awad, W.H., Shields, J.R., 2004. Flame retardant mechanism of polyamide 6–clay nanocomposites. Polymer (Guildf). 45, 881–891. https://doi.org/10.1016/J.POLYMER.2003.11.036

Kham, L., Le Bigot, Y., Delmas, M., Avignon, G., 2005. Delignification of wheat straw using a mixture of carboxylic acids and peroxoacids. Ind. Crops Prod. 21, 9–15. https://doi.org/10.1016/j.indcrop.2003.12.002

Kim, J.-Y., Oh, S., Hwang, H., Kim, U.-J., Choi, J.W., 2013. Structural features and thermal degradation properties of various lignin macromolecules obtained from poplar wood. Polym. Degrad. Stab. 98, 1671–1678. https://doi.org/10.1016/J.polymdegradstab.2013.06.008

Klein, J., Dorge, S., Trouvé, G., Venditti, D., Durécu, S., 2009. Behaviour of antimony during thermal treatment of Sb-rich halogenated waste. J. Hazard. Mater. 166, 585–593. https://doi.org/10.1016/J.JHAZMAT.2008.12.006

Kleiner, H.-J., Budzinsky, W., Kirsch G, 1996. flame retardant polyester molding composition. EP0699708A2.

Kleiner, H.-J., Budzinsky, W., Kirsch G, 1997. Fire proofing polyamide molding composition containing calcium and aluminium phosphinate salt. EP0792912A2.

Kleiner, H.J., Budzinsky, W., Kirsch, G., 1998. Low-flammability polyamide molding materials. US5773556.

Kuciel, S., Kuzniar, P., Liber-Kneć, A., 2012. Polyamides from renewable sources as matrices of short fiber reinforced biocomposites. Polimery 57, 627–634. https://doi.org/10.14314/polimery.2012.627

Kun, D., Pukánszky, B., 2017. Polymer/lignin blends: Interactions, properties, applications. Eur. Polym. J. 93, 618–641. https://doi.org/10.1016/J.EURPOLYMJ.2017.04.035

Kvalnes, D.E., Grove, P., Brace, N.O., Du, E.I., 1954. Organic phosphorus compounds for increasing the flame resistance of textiles and method of applying the same. Application. US2691466.

Laachachi, A., Cochez, M., Leroy, E., Ferriol, M., Lopez-cuesta, J.M., Verlaine-metz, P., Demange, V., Cedex, S., 2007. Fire retardant systems in poly (methyl methacrylate): Interactions between metal oxide nanoparticles and phosphinates 92, 61–69. https://doi.org/10.1016/j.polymdegradstab.2006.09.011

Langan, P., Naskar, A.K., Chen, F., Biddy, M.J., Wyman, C.E., Gilna, P., Davison, B.H., Saddler, J.N., Dixon, R.A., Tschaplinski, T.J., Davis, M.F., Keller, M., Tuskan, G.A., Chandra, R., Beckham, G.T., Ragauskas, A.J., 2014. Lignin Valorization: Improving Lignin Processing in the Biorefinery. Science (80-.). 344, 1246843–1246843. https://doi.org/10.1126/science.1246843

Lao, S.C., Koo, J.H., Moon, T.J., Londa, M., Ibeh, C.C., Wissler, G.E., Pilato, L.A., 2011.

Flame-retardant polyamide 11 nanocomposites: further thermal and flammability studies. J. Fire Sci. 29, 479–498. https://doi.org/10.1177/0734904111404658

Lao, S.C., Koo, J.H., Moon, T.J., Londa, M., Ibeh, C.C., Wissler, G.E., Pilato, L.A., 2009. Flame-retardant Polyamide 11 and 12 nanocomposites: Thermal and Flammability Properties. J. Compos. Mater. 43, 1803–1818. https://doi.org/10.1177/0734904111404658

Lao, S.C., Koo, J.H., Moon, T.J., Yong, W., Lam, C., Zhou, J., Hadisujoto, B., Wissler, G., Pilato, L., Luo, Z.P., 2008. Flame Retardant Intumescent PA11 Nanocomposites - Further Study, in: SFF Symposium. pp. 55–66.

Lao, S.C., Yong, W., Nguyen, K., Moon, T.J., Koo, J.H., Pilato, L., Wissler, G., 2010. Flame-retardant polyamide 11 and 12 nanocomposites: Processing, morphology, and mechanical properties. J. Compos. Mater. 44, 2933–2951. https://doi.org/10.1177/0021998310369580

Laurichesse, S., Avérous, L., 2014. Chemical modification of lignins: Towards biobased polymers. Prog. Polym. Sci. 39, 1266–1290. https://doi.org/10.1016/j.progpolymsci.2013.11.004

Levchik, S. V., Costa, L., Camino, G., 1992. Effect of the fire-retardant ammonium polyphosphate on the thermal decomposition of aliphatic polyamides. I. PA11 and PA12. Polym. Degrad. Stab. 36, 31–41. https://doi.org/10.1016/0141-3910(94)90224-0

Levchik, S. V, 2007. Introduction to Flame Retardancy and Polymer Flammability, in: Flame Retardant Polymer Nanocomposites.

Levchik, S. V, Weil, E.D., 2000. Combustion and fire retardancy of aliphatic nylons. Polym. Int. 49, 1033–1073. https://doi.org/10.1002/1097-0126(200010)49:10<1033::AID-PI518>3.0.CO;2-I

Li, B., Zhang, X., Su, R., 2002. An investigation of thermal degradation and charring of larch lignin in the condensed phase: The effects of boric acid, guanyl urea phosphate, ammonium dihydrogen phosphate and ammonium polyphosphate. Polym. Degrad. Stab. 75, 35–44. https://doi.org/10.1016/S0141-3910(01)00202-6

Li, J., Li, B., Zhang, X., Su, R., 2001. The study of flame retardants on thermal degradation and charring process of manchurian ash lignin in the condensed phase. Polym. Degrad. Stab. 72, 493–498. https://doi.org/10.1016/S0141-3910(01)00049-0

Li, M., Zhong, Y., Wang, Z., Fischer, A., Ranft, F., Drummer, D., Wu, W., 2016. Flame retarding mechanism of Polyamide 6 with phosphorus-nitrogen flame retardant and DOPO derivatives. J. Appl. Polym. Sci. 133, n/a-n/a. https://doi.org/10.1002/app.42932

Lin, S.Y., Dence, C.W., 1992. Methods in lignin chemistry. Springer-Verlag.

Liu, L., Huang, G., Song, P., Yu, Y., Fu, S., 2016a. Converting industrial alkali lignin to biobased functional additives for improving fire behavior and smoke suppression of polybutylene succinate. ACS Sustain. Chem. Eng. 4, 4732–4742. https://doi.org/10.1021/acssuschemeng.6b00955

Liu, L., Qian, M., Song, P., Huang, G., Yu, Y., Fu, S., 2016b. Fabrication of Green Lignin-based Flame Retardants for Enhancing the Thermal and Fire Retardancy Properties of Polypropylene/Wood Composites. ACS Sustain. Chem. Eng. 4, 2422–2431. https://doi.org/10.1021/acssuschemeng.6b00112

Liu, P., Liu, M., Gao, C., Wang, F., Ding, Y., Wen, B., Zhang, S., Yang, M., 2013. Preparation, characterization and properties of a halogen-free phosphorous flame-retarded poly(butylene terephthalate) composite based on a DOPO derivative. J. Appl. Polym. Sci. 130, 1301–1307. https://doi.org/10.1002/app.39318

Lora, J., 2008. Industrial Commercial Lignins: Sources, Properties and Applications, in: Monomers, Polymers and Composites from Renewable Resources. Elsevier, pp. 225–241. https://doi.org/10.1016/B978-0-08-045316-3.00010-7

Lorenzetti, A., Modesti, M., Gallo, E., Schartel, B., Besco, S., Roso, M., 2012. Synthesis of phosphinated polyurethane foams with improved fi re behaviour. Polym. Degrad. Stab. 97, 2364–2369. https://doi.org/10.1016/j.polymdegradstab.2012.07.026

Lu, W., Li, Q., Zhang, Y., Yu, H., Hirose, S., Hatakeyama, H., Matsumoto, Y., 2018. Lignosulfonate / APP IFR and its flame retardancy in lignosulfonate- based rigid polyurethane foams. J. Wood Sci. 64, 287–293. https://doi.org/10.1007/s10086-018-1701-4

Mailhos-Lefievre, V., Sallet, D., Martel, B., 1989. Thermal Degradation of Pure and Flame-retarded. Polym. Degrad. Stab. 23, 327–336. https://doi.org/10.1016/0141-3910(89)90055-4

Marton, J., Marton, T., 1964. Molecular weight of kraft lignin. Tappi J. 47, 471–476.

McKendry, P., 2002. Energy production from biomass (part 2): conversion technologies.

Bioresour. Technol. 83, 47–54. https://doi.org/10.1016/S0960-8524(01)00119-5

Morgan, A.B., Gilman, J.W., 2012. An overview of flame retardancy of polymeric materials: application, technology, and future directions. Fire Mater. https://doi.org/10.1002/fam

Mukherjee, A.K., Duraiswamy, R., Sengupta, A.K., 1981. Modification of nylon 6 by o-chlorophenol. Man-Made Text. India 24, 310–316.

Naegele, H., Pfitzer, J., Ziegler, L., Inone-Kauffmann, E.R., Eisenreich, N., 2016. Applications of Lignin Materials and Their Composites (Lignin Applications in Various Industrial Sectors, Future Trends of Lignin and Their Composites), Lignin in Polymer Composites. Elsevier Inc. https://doi.org/10.1016/B978-0-323-35565-0.00013-8

Nägele, H., Pfitzer, J., Nägele, E., Inone, E.R., Eisenreich, N., Eckl, W., Eyerer, P., 2002. Arboform® - A Thermoplastic, Processable Material from Lignin and Natural Fibers, in: Chemical Modification, Properties, and Usage of Lignin. Springer US, Boston, MA, pp. 101–119. https://doi.org/10.1007/978-1-4615-0643-0_6

Nass Bernd, Wanzke Wolfgang, 2001. Synergistic flame proofing combination for polymers. US6207736B1.

Negrell, C., Frénéhard, O., Sonnier, R., Dumazert, L., Briffaud, T., Flat, J.J., 2016. Self-extinguishing bio-based polyamides. Polym. Degrad. Stab. 134, 10–18. https://doi.org/10.1016/j.polymdegradstab.2016.09.022

Nicolas Smolarski, 2012. High-Value Opportunities for Lignin: Unlocking its Potential Lignin potential. Paris.

Noetzel S, Herwig W, 1974. Flame retardant polyamide molding compounds. DE2447727.

Obadjah Wyld, 1735. British Patent. BP551.

Ogunniyi, D., 2006. Castor oil: A vital industrial raw material. Bioresour. Technol. 97, 1086–1091. https://doi.org/10.1016/j.biortech.2005.03.028

Pouteau, C., Dole, P., Cathala, B., Averous, L., Boquillon, N., 2003. Antioxidant properties of lignin in polypropylene. Polym. Degrad. Stab. 81, 9–18. https://doi.org/10.1016/S0141-3910(03)00057-0

Price, D., Anthony, G., Carty, P., 2001. Introduction: polymer combustion, condensed phase pyrolysis and smoke formation, in: Fire Retardant Materials. Elsevier, pp. 1–30. https://doi.org/10.1533/9781855737464.1

Prieur, B., 2016. Modified lignin as flame retardant for polymeric materials. Doctoral thesis, University of Lille.

Racky, W., Kleiner, H.-J., Herwig, W., 1972. Flame retardant thermoplastic polyester. DE2252258.

Ralph, J., Lundquist, K., Brunow, G., Lu, F., Kim, H., Schatz, P.F., Marita, J.M., Hatfield, R.D., Ralph, S.A., Christensen, J.H., Boerjan, W., 2004. Lignins: Natural polymers from oxidative coupling of 4-hydroxyphenyl- propanoids. Phytochem. Rev. 3, 29–60. https://doi.org/10.1023/B:PHYT.0000047809.65444.a4

Ramgobin, A., Fontaine, G., Bourbigot, S., 2019. Thermal Degradation and Fire Behavior of High Performance Polymers. Polym. Rev. 0, 1–69. https://doi.org/10.1080/15583724.2018.1546736

Réti, C., Casetta, M., Duquesne, S., Bourbigot, S., Delobel, R., 2008. Flammability properties of intumescent PLA including starch and lignin. Polym. Adv. Technol. 19, 628–635. https://doi.org/10.1002/pat.1130

Rodríguez, A., Sánchez, R., Requejo, A., Ferrer, A., 2010. Feasibility of rice straw as a raw material for the production of soda cellulose pulp. J. Clean. Prod. 18, 1084–1091. https://doi.org/10.1016/j.jclepro.2010.03.011

Roy Choudhury, A.K., 2017. Flame- and fire-retardant finishes, in: Principles of Textile Finishing. Woodhead Publishing, pp. 195–244. https://doi.org/10.1016/b978-0-08-100646-7.00008-4

Saake, B., Lehnen, R., 2007. Lignin, in: Ullmann’s Encyclopedia of Industrial Chemistry. Wiley-VCH Verlag GmbH & Co. KGaA, Weinheim, Germany. https://doi.org/10.1002/14356007.a15_305.pub3

Sahoo, S., Misra, M., Mohanty, A.K., 2011. Enhanced properties of lignin-based biodegradable polymer composites using injection moulding process. Composite 42, 1710–1718. https://doi.org/10.1016/j.compositesa.2011.07.025

Sakharov, A.M., Sakharov, P.A., Lomakin, S.M., Zaikov, G.E., 2014. Novel Class of Eco-Flame Retardants Based on the Renewable Raw Materials, in: Polymer Green Flame Retardants. Elsevier B.V., pp. 255–266. https://doi.org/10.1016/B978-0-444-53808-6.00007-X

Salmeia, K.A., Gaan, S., Malucelli, G., 2016. Recent advances for flame retardancy of textiles based on phosphorus chemistry, Polymers. https://doi.org/10.3390/polym8090319

Samyn, F., Bourbigot, S., 2012. Thermal decomposition of flame retarded formulations PA6/aluminum phosphinate/melamine polyphosphate/organomodified clay: Interactions between the constituents? Polym. Degrad. Stab. 97, 2217–2230. https://doi.org/10.1016/j.polymdegradstab.2012.08.0

Sannigrahi, P., Ragauskas, A.J., Miller, S.J., 2010. Lignin structural modifications resulting from ethanol organosolv treatment of Loblolly pine. Energy and Fuels 24, 683–689. https://doi.org/10.1021/ef900845t

Schlosser, E., Nass, N., Wanzke, W., 2003. Flame retardant combination for thermoplastic polymers. US6547992B1.

Schwarzer, M., Korwitz, A., Komber, H., Häußler, L., Dittrich, B., Schartel, B., Pospiech, D., 2018. Phosphorus-Containing Polymer Flame Retardants for Aliphatic Polyesters. Macromol. Mater. Eng. 303, 1–16. https://doi.org/10.1002/mame.201700512

Shanmuganathan, K., Deodhar, S., Dembsey, N., Fan, Q., Calvert, P.D., Warner, S.B., Patra, P.K., 2007. Flame retardancy and char microstructure of nylon-6/layered silicate nanocomposites. J. Appl. Polym. Sci. 104, 1540–1550. https://doi.org/10.1002/app.25542

Shanmuganathan, K., Deodhar, S., Dembsey, N.A., Fan, Q., Patra, P.K., 2008. Condensed-phase flame retardation in nylon 6-layered silicate nanocomposites: Films, fibers, and fabrics. Polym. Eng. Sci. 48, 662–675. https://doi.org/10.1002/pen.20993

Shukry, N., Fadel, S.M., Agblevor, F.A., El-Kalyoubi, S.F., 2008. Some physical properties of acetosolv lignins from bagasse. J. Appl. Polym. Sci. 109, 434–444. https://doi.org/10.1002/app.28059

Sjöström Eero, 1993. Wood chemistry: Fundamentals and applications, 2nd Editio. ed. Elsevier Inc. https://doi.org/https://doi.org/10.1016/C2009-0-03289-9

Smith, W.C., 1999. High Performance And High Temperature Resistant Fibers-Emphasis on Protective Clothing.

Solarski, S., Mahjoubi, F., Ferreira, M., Devaux, E., Bachelet, P., Bourbigot, S., Delobel, R., Coszach, P., Murariu, M., Da silva Ferreira, A., Alexandre, M., Degee, P., Dubois, P., 2007. (Plasticized) Polylactide/clay nanocomposite textile: thermal, mechanical, shrinkage and fire properties. J. Mater. Sci. 42, 5105–5117. https://doi.org/10.1007/s10853-006-0911-0

Song, P., Cao, Z., Fu, S., Fang, Z., Wu, Q., Ye, J., 2011. Thermal degradation and flame retardancy properties of ABS/lignin: Effects of lignin content and reactive compatibilization. Thermochim. Acta 518, 59–65. https://doi.org/10.1016/j.tca.2011.02.007

Spiccia, N., Border, E., Illesinghe, J., Jackson, W., Robinson, A., 2013. Preparation of a Nylon-11 Precursor from Renewable Canola Oil. Synthesis (Stuttg). 45, 1683–1688. https://doi.org/10.1055/s-0033-1338478

Thor Chemicals, 2011. Durable Textiles Flame Retardants [WWW Document]. URL https://www.acti-chem.co.za/flameretardantstextilesdurable.html (accessed 5.9.19).

Thunga, M., Chen, K., Grewell, D., Kessler, M.R., 2014. Bio-renewable precursor fibers from lignin/polylactide blends for conversion to carbon fibers. Carbon N. Y. 68, 159–166. https://doi.org/10.1016/j.carbon.2013.10.075

Tribot, A., Amer, G., Abdou Alio, M., de Baynast, H., Delattre, C., Pons, A., Mathias, J.D., Callois, J.M., Vial, C., Michaud, P., Dussap, C.G., 2019. Wood-lignin: Supply, extraction processes and use as bio-based material. Eur. Polym. J. 112, 228–240. https://doi.org/10.1016/j.eurpolymj.2019.01.007

Vannier, A., Duquesne, S., Bourbigot, S., Alongi, J., Camino, G., Delobel, R., 2009. Investigation of the thermal degradation of PET , zinc phosphinate , OMPOSS and their blends - Identification of the formed species. Thermochim. Acta 495, 155–166. https://doi.org/10.1016/j.tca.2009.06.013

Vannier, A., Duquesne, S., Bourbigot, S., Castrovinci, A., Camino, G., Delobel, R., 2008. The use of POSS as synergist in intumescent recycled poly (ethylene terephthalate) 93, 818–826. https://doi.org/10.1016/j.polymdegradstab.2008.01.016

Vargas, A.F., Orozco, V.H., Rault, F., Giraud, S., Devaux, E., López, B.L., 2010. Influence of fiber-like nanofillers on the rheological, mechanical, thermal and fire properties of polypropylene: An application to multifilament yarn. Compos. Part A Appl. Sci. Manuf. 41, 1797–1806. https://doi.org/10.1016/J.COMPOSITESA.2010.08.018

Vishtal, A., Kraslawski, A., 2011. Challenges in industrial applications of technical lignins. BioResources 6, 3547–3568.

Weil, E.D., Levchik, S. V., 2008a. Flame retardants in commercial use or development for textiles. J. Fire Sci. 26, 243–281. https://doi.org/10.1177/0734904108089485

Weil, E.D., Levchik, S. V., 2008b. Flame Retardants in Commercial Use or Development for Textiles. J. Fire Sci. 26, 243–281. https://doi.org/10.1177/0734904108089485

Weil, E.D., Levchik, S. V., 2004. Commercial Flame Retardancy of Thermoplastic Polyesters – A Review. J. Fire Sci. 22, 339–350. https://doi.org/10.1177/0734904104042188

Wesołowski, J., Płachta, K., 2016. The Polyamide Market. Fibres Text. East. Eur. 24, 125–131. https://doi.org/10.5604/12303666.1215537

Whetten Ross, MacKay John, Sederoff Ronald, 1998. Recent Advances in understanding lignin biosynthesis. Annu. Rev. Plant Physiol. Plant Mol. Biol. 49, 585–609. https://doi.org/10.1146/annurev.arplant.49.1.585

Wilkie, C.A., Morgan, A.B., 2010. Fire retardancy of polymeric materials. CRC Press.

Windeisen, E., Wegener, G., 2012. Lignin as Building Unit for Polymers, Polymer Science: A Comprehensive Reference, 10 Volume Set. Elsevier B.V. https://doi.org/10.1016/B978-0-444-53349-4.00263-6

Wood, B.M., Coles, S.R., Maggs, S., Meredith, J., Kirwan, K., 2011. Use of lignin as a compatibiliser in hemp/epoxy composites. Compos. Sci. Technol. 71, 1804–1810. https://doi.org/10.1016/j.compscitech.2011.06.005

Yang, H., Yan, R., Chen, H., Lee, D.H., Zheng, C., 2007. Characteristics of hemicellulose, cellulose and lignin pyrolysis. Fuel 86, 1781–1788. https://doi.org/10.1016/j.fuel.2006.12.013

Yu, Y., Fu, S., Song, P., Luo, X., Jin, Y., Lu, F., Wu, Q., Ye, J., 2012. Functionalized lignin by grafting phosphorus-nitrogen improves the thermal stability and flame retardancy of polypropylene. Polym. Degrad. Stab. 97, 541–546. https://doi.org/10.1016/j.polymdegradstab.2012.01.020

Zhang, R., Xiao, X., Tai, Q., Huang, H., Yang, J., Hu, Y., 2013. The effect of different organic modified montmorillonites (OMMTs) on the thermal properties and flammability of PLA/MCAPP/lignin systems. J. Appl. Polym. Sci. 127, 4967–4973. https://doi.org/10.1002/app.38095

Zhang, S., Horrocks, A.R., 2003. A review of flame retardant polypropylene fibres. Prog. Polym. Sci. 28, 1517–1538. https://doi.org/10.1016/J.PROGPOLYMSCI.2003.09.001

Zhao, J., Xiuwen, W., Hu, J., Liu, Q., Shen, D., Xiao, R., 2014. Thermal degradation of softwood lignin and hardwood lignin by TG- FTIR and Py-GC / MS. Polym. Degrad. Stab. 108, 133–138. https://doi.org/10.1016/j.polymdegradstab.2014.06.006

Zhu, H., Peng, Z., Chen, Y., Li, G., Wang, L., Tang, Y., Pang, R., Khan, Z.U.H., Wan, P., 2014. Preparation and characterization of flame retardant polyurethane foams containing phosphorus–nitrogen-functionalized lignin. RSC Adv. 4, 55271–55279. https://doi.org/10.1039/C4RA08429B

Ziegler, L., Regina, E., Eckl, W., Eisenreich, N., 2014. Lignin Matrix Composites from Natural Resources – ARBOFORM, in: Bio-Based Plastics: Materials and Applications. John Wiley & Sons, Ltd.

2. MATERIALS AND METHODS

2.1. Materials

2.1.1. Polymer matrix

The polymer matrix used in this study is Polyamide 11 (PA), is another thermoplastic fibre-grade polyamide commercially available in the market. It is worth mentioning that PA is made of fully renewable resources. It has been produced for nearly half a century under the trade name of Rilsan® by the French company Arkema Inc. Rilsan® PA11 is easy to process, using most processing technologies (extrusion, extrusion-blow molding, injection molding) and compatible with various additives and fillers. Rilsan® BMNO-TLD a natural grade, Mn=17,000 g/mol, Melt flow index (MFI) = 36.5 g/10 min at 235 °C, kindly supplied for this study, was chosen as a polymer matrix for the production of multifilaments. Characteristics of polyamide 11 are collected in Table 2.1.

Table 2.1. Characteristics of polyamide 11 polymer (Source: MatWeb material property data, http://www.matweb.com/search/datasheet.aspx?matguid=d41cf1f35ec4447e86816e786bf6c246&ckck=1)

Properties	Nominal	Units	Test method
Density	1.03	g/cc	ISO 1183
Water absorption	1.9	% (w/w)	ISO 62
Melt flow index (235 °C, 2.16 kg)	36.5	g/10 min	ISO1133
Melting point	189	°C	DSC, 10 °C/ min
Flammability	V-2	NA	IEC 60695-11-10
Oxygen index	25	%	ISO 4589-1/-2
Tensile strength, yield	41	MPa	ISO 527-1/-2
Elongation at break	>50	%	ISO 527-1/-2
Tensile Modulus	1.32	GPa	ISO 527-1/-2

TGA of neat PA carried out in nitrogen atmosphere with heating rate 10 °C/min. TGA profile of PA shows a characteristic single degradation step, taking place between 370 and 500 °C with a maximum of mass loss rate (MMLR) at 423 °C (T_{max}) without leaving the char residue at the end of the degradation process.

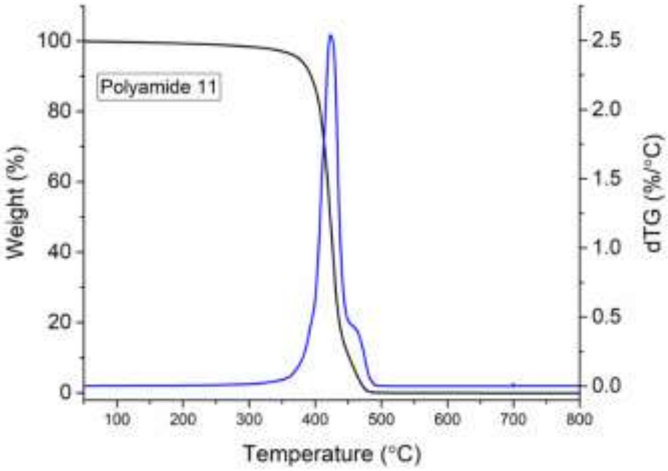

Figure 2.1. TG (black line) and dTG (blue line) curves for polyamide11 (PA) in N_2 and 10 °C/min.

2.1.2. Lignin

lignosulphonate and kraft lignin, which are the most produced industrial lignins in the world are used in this study. Lignin used as FR additive (charring agent), differing as far as the plant resource, chemical nature, and purity are concerned: lignosulfonate lignin was provided from Domsjö Fabriker AB, Sweden (herein after coded as LL) and an alkali kraft lignin was obtained from UPM Biochemicals, Finland (European distributor of Domtar BioChoice® lignin) and coded as DL. LL contains mainly Na-lignosulfonate (about 70 %) and small amounts of Mg and Ca lignosulfonates, and some impurities such as ash and carbohydrates (about 20 %). DL comprises mostly alkali kraft with 90 % purity level. Purity of all four lignins collected in Table 2.2. In order to compare the effectiveness of industrial lignin in polymer matrix two pure grade lignin with the same chemical nature were used: the first one is alkali kraft low sulfonate (4 wt% sulfur) lignin (hereinafter coded as LS) and the second one is kraft lignin (hereinafter coded as KL) was purchased from Sigma-Aldrich, France, respectively. Physical appearance of all four types of lignins is shown in Figure 2.2. The purpose of using these four types of lignin was to assess their effect on the thermal stability and fire retardancy of PA.

Table 2.2. The purity of different lignin used in this study.

Grade	Product name	Chemical nature	Purity
Pure lignin	Kraft	Kraft	>99%
	Alkali kraft low	4 % sulphonate	> 99%
Industrial lignin	BioChoice™	Kraft	>90%
	Domsjo lignin	Lignosulphonate	>60%

Figure 2.2. The physical appearance of lignins used in this study.

2.1.3. Flame retardant additives

Metal phosphinates are considered very efficient and have several advantages like mostly non-hygroscopic, non-toxic, thermally stable (>350 °C) and resistant to hydrolysis. They can act both in the gas phase as radical scavengers and flame inhibitors or in the condensed phase and promote residue formation. Most of the times both mechanisms are present. They are commercialized by Clariant, under the trade name of Exolit® OP: Exolit® OP950 (ZnP) and Exolit® OP1230 (AlP), are the most widely used to enhance the flame retardancy of thermoplastic engineering polymers. In this thesis aluminium diethylphosphinate (AlP) and zinc bis-diethyl phosphinate (ZnP) were used as FR additives (Figure 2.3) with lignin as charring agent for developing flame retardant system for textile applications. Characteristics of both the phosphinate salts are listed in Table 2.3. ZnP used in this thesis was supplied from two different suppliers, the first one Pekoflam SMAp^{TM}, was supplied by Archroma, France and the second one Exolit OP950 was provided from Clariant, Switzerland. Pekoflam SMAp^{TM} ZnP is used with laboratory grade LS in the primary study to investigate the morphology, thermal stability and fire behaviour of ternary blends. In the next step, to scale up the production of flame retarding blends for melt spinning and fabric manufacturing and industrial practicability more widely used Exolit® OP950 is used. The latter is combined with low-cost industrial grade lignin (LL and DL) in PA to study the fire behaviour and spinnability of flame retarded blends.

It has a melting point of above 200 °C that melts during the polymer processing which makes it more suitable for the production of textile fibres. The concentration of phosphorus in the ZnP ranges between 19.5 and 20.5 %; its fusible character makes it a perfect candidate for the implementation in the molten process. Consequently, its insertion into the polymer matrix would generate less rheological and mechanical changes. Utilizing a zinc salt promotes good fire retardancy properties known from zinc borate in combination with phosphorus derivatives due to the formation of an effective zinc phosphate layer (Braun et al., 2007). Therefore, the different morphological, thermal and FR properties of the introduction of ZnP were studied in PA and specifically in ternary blends.

AlP (Exolit® OP1230) was supplied from Clariant, Switzerland, is considered as potential non-halogen FR for polyamide matrix. AlP is widely used with various polymer system and has proven to be effective FR due to the concentration of phosphorus (23.3 to 24 %) in the AlP is higher than the ZnP, which possess better flame retardancy compared to the ZnP. However, its infuse character and the large size of its particles are limiting parameters for the implementation in the molten process. Its insertion into the polymer matrix could generate more rheological and mechanical changes in comparison with the ZnP, which is fusible.

Therefore, the different thermal and morphological properties of the two phosphinates appeared interesting for us to study when implementing in fire retarded PA and specifically during molten spinning.

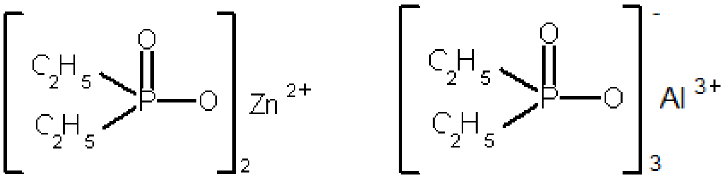

Figure 2.3. Structure of ZnP and AlP used in this study.

Table 2.3. Characteristics of metal phosphinate used in this study.

Properties	Unit	ZnP	AlP
Chemical formula		$[(C_2H_5)_2POO]_2^- Zn^{2+}$	$[(C_2H_5)_2POO]_3^- Al^{3+}$
Amount	% (w/w)	19.5 – 20.5	23.3 - 24
Water/Moisture	% (w/w)	≤ 0.25	≤ 0.20
Particle size	µm	-	20 - 40
Density at 20 °C	g/cm^3	1.3	1.35
Melting temperature	°C	200	-
Decomposition	°C	> 350	> 300

2.2. Material processing

2.2.1. Extrusion

Different flame retarded formulations based on PA and lignin for binary blends or PA in a combination with lignin and phosphinate for ternary blends were prepared by extrusion. The extruder (Thermo Haake PTW-16) has two corotating screw of lengths L = 400 mm and diameter D = 16 mm, or L/D = 25. The extruder has five heating zones and for this work the temperature profiles of the five heating zones set as follows, 170, 190, 210, 210 and 220 °C. The rotation speed of the screws was set at 100 rpm for all the blends preparation. Polymer and all the additives were dried overnight (12 h) at 80 °C before compounding. The polymer in the form of granules and additives as powder form were introduced into extruder at feeding zone. The polymer was melted and mixed homogeneously with the additives by shearing, extruder output was then obtained in the form of a rod. In all cases, the extruded rods were pelletized. Pellets were dried overnight at 80 °C before use for any analysis. The schematic representation of the extrusion process assembly is shown in Figure 2.4.

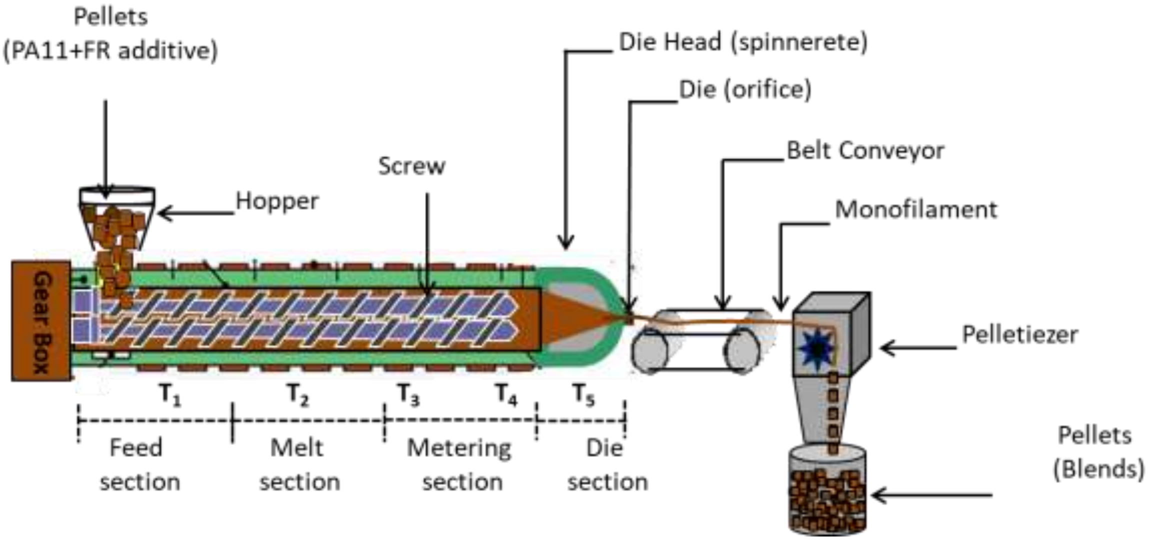

Figure 2.4. Schematic of the extrusion process and palletization.

2.2.2. Preparation of blends

2.2.2.1. Binary blends

In the first step, the influence of the direct addition using different types of lignin on thermal stability and FR properties of PA were investigated. For this purpose, the various formulations based on lignins and PA were prepared. The maximum additive loading of 20 wt% was used in blend formulation; lignin concentration was varied from 5, 10, 15 and 20 wt%. LS and KL belong to laboratory grade lignin whereas LL and DL are industrial grades. LS and LL contain sulphonated functionality in their structure; however, KL and DL are alkali kraft lignins by chemical nature. Prepared formulations are listed in Table 2.4.

2.2.2.2. Ternary blends

In the second step, ternary blends of selected lignins combined with phosphinate flame retardants (i.e., AlP and ZnP) and three different types of formulations were prepared. A total flame retardant and lignin loading of 20 wt% was used in all cases; Phosphinate, being the major constituent, was varied from 10 to 15 wt% and lignin from 5 to 10 wt%.

The primary study was done using ZnP flame retardant combined with laboratory grade LS, three different formulations were prepared (Table 2.5). ZnP (Pekoflam SMAp™) used in this study, was kindly supplied from Archroma, France.

Table 2.4. PA/lignin-based blends formulations.

Samples	PA	LS	LL	KL	DL
PA	100	–	–	–	–
PA$_{95}$-LS$_{5}$	95	5	–	–	–
PA$_{90}$-LS$_{10}$	90	10	–	–	–
PA$_{85}$-LS$_{15}$	85	15	–	–	–
PA$_{80}$-LS$_{20}$	80	20	–	–	–
PA$_{95}$-LL$_{5}$	95	–	5	–	–
PA$_{90}$-LL$_{10}$	90	–	10	–	–
PA$_{85}$-LL$_{15}$	85	–	15	–	–
PA$_{80}$-LL$_{20}$	80	–	20	–	–
PA$_{95}$-KL$_{5}$	95	–	–	5	–
PA$_{90}$-KL$_{10}$	90	–	–	10	–
PA$_{85}$-KL$_{15}$	85	–	–	15	–
PA$_{80}$-KL$_{20}$	80	–	–	20	–
PA$_{95}$-DL$_{5}$	95	–	–	–	5
PA$_{90}$-DL$_{10}$	90	–	–	–	10
PA$_{85}$-DL$_{15}$	85	–	–	–	15
PA$_{80}$-DL$_{20}$	80	–	–	–	20

Table 2.5. PA blend formulations with LS and ZnP.

sample	Polyamide 11 (wt%)	Lignin (DL in wt%)	Phosphinate (ZnP in wt%)
PA	100	-	-
PA$_{80}$-LS$_{5}$-ZnP$_{15}$	80	5	15
PA$_{80}$-LS$_{7}$-ZnP$_{13}$	80	7	13
PA$_{80}$-LS$_{10}$-	80	10	10

Table 2.6. PA blend formulations with different lignin and phosphinate.

sample	Polyamide 11 (wt%)	Lignin (DL in wt%)	Lignin (LS in wt%)	Lignin (LL in wt%)	Phosphinate (ZnP in wt%)
PA	100	-	-	-	-
PA$_{80}$-LS$_{5}$-ZnP$_{15}$	80	5	-	-	15
PA$_{80}$-LS$_{7}$-ZnP$_{13}$	80	7	-	-	13
PA$_{80}$-LS$_{10}$-ZnP$_{10}$	80	10	-	-	10
PA$_{80}$-DL$_{5}$-ZnP$_{15}$	80	-	5	-	15
PA$_{80}$-DL$_{7}$-ZnP$_{13}$	80	-	7	-	13
PA$_{80}$-DL$_{10}$-ZnP$_{10}$	80	-	10	-	10
PA$_{80}$-LL$_{5}$-ZnP$_{15}$	80	-	-	5	15
PA$_{80}$-LL$_{7}$-ZnP$_{13}$	80	-	-	7	13
PA$_{80}$-LL$_{10}$-ZnP$_{10}$	80	-	-	10	10
PA$_{80}$-DL$_{5}$-AlP$_{15}$	80	5	-	15	-
PA$_{80}$-DL$_{7}$-AlP$_{13}$	80	7	-	13	-
PA$_{80}$-DL$_{10}$-AlP$_{10}$	80	10	-	10	-
PA$_{80}$-LL$_{5}$-AlP$_{15}$	80	-	5	15	-
PA$_{80}$-LL$_{7}$-AlP$_{13}$	80	-	7	13	-
PA$_{80}$-LL$_{10}$-AlP$_{10}$	80	-	10	10	-

In order to scale up the production of flame retarding blends for melt spinning and fabric manufacturing. Industrial grade low-cost lignins and widely used Exolit® OP FRs were used.

Two different types of industrial lignins, varying in chemical nature: the first one LL, provided from Domsjö Fabriker AB, Sweden and the second one DL supplied from UPM Biochemicals, Finland (European distributor of Domtar BioChoice® lignin). Two different types of phosphinate FR, ZnP (Exolit® OP950) and AlP (Exolit® OP1230) were supplied by Clariant. Prepared formulations and identification of samples are shown in Table 2.6.

2.2.2.3. Preparation of testing samples

Pellets were transformed into a plate or sheet form to characterize the fire properties of the material. For this purpose, a Dolouets hydraulic press (hot press) was used in ENSAIT-GEMTEX laboratory. However, a Collins Teach Line 200 hydraulic press (hot press) was used in Politecnico di Torino laboratory. Specimens size in accordance with cone calorimeter (100 × 100 mm) and UL 94 (125 × 13 mm) tests were elaborated, the thickness of Plates was 3 mm. The operation condition was the same for both instruments. The hot press preheated at a set temperature of 220 °C, sample mold with pellets was placed on the lower plate and heated for 2 minutes without pressure and then the pressure increased to 20 bar for 2 minutes and finally 60 bar applied with stay time of 2 minutes.

2.2.3. Fibrous material preparation

2.2.3.1. Multifilaments development via melt spinning

The implementation of polymers in fibrous form was carried out by using the melt spinning device (SPINBOY I, Busschaert Engineering, Belgium), schematic of the spinning machine is shown in Figure 2.5. The pellets were fed into the hopper, which passes through the single screw extruder. This extruder has a L/D ratio of 30 and is broken down into two main parts: the first with L/D 27.5 and a second called the output head with L/D of 2.5. The first part divides itself into three zones; feeding (L/D = 12), the compression (L/D = 8) and the pumping zone (L/D = 7.5). The spinning device has six heating zones (five at the extruder and one at the spinning level) whose temperature ranged 180, 200, 210, 215 and 220 °C and spinning level at

230 °C, were chosen according to the material to be transformed. Under thermal and mechanical stresses, pellets melt and are transported to the volumetric pump (chamber volume = 3.5 cm^3) whose rotational speed is set beforehand to ensure a constant flow of material to the spinneret (80 holes, 1.2 mm diameter). Then the consistent monofilament bundles which are coming out of spinneret are cooled and finished with spin-oil to limit electrostatic effects and ensure inter-filament cohesion. They are then drawn to the winder, passing through two different rollers that apply a stretching on the multifilament. Finally, the multifilaments are winded on a bobbin. The flow of the pump and the rate of stretching, affect the quality of the developed multifilament and their mechanical properties.

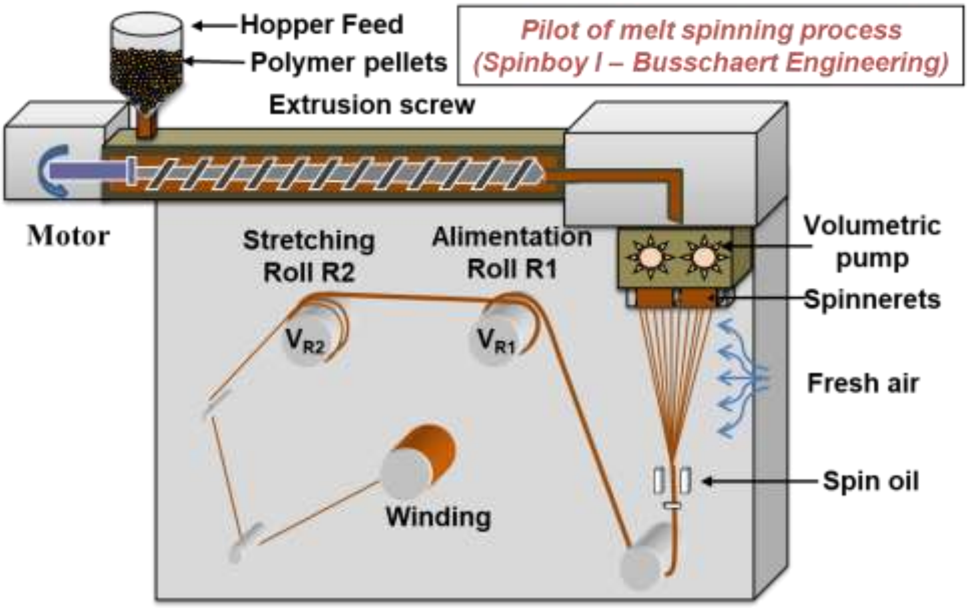

Figure 2.5. Schematic of melt spinning machine.

2.2.3.2. Knitted fabrics development

Due to their structural properties (thickness, drape, density, etc.) and easy processability, knitted textile structures have been preferred over woven and nonwovens fabrics. The knitting structures were produced on automatic flat knitting machine of brand Shima Seiki model SES122 FF. First, the knitting structure was built upon the computer program APEX. For the fire testing (e.g., cone calorimeter and UL94 test) specimen, the fabric structure that has low air permeability is preferred, so that the interlock structure created on the program, with a pattern repeat of 2 rows (Figure 2.6). All the knitted fabrics had a grammage of about 1400 ± 50 gm^{-2} and same thicknesses of 3 mm.

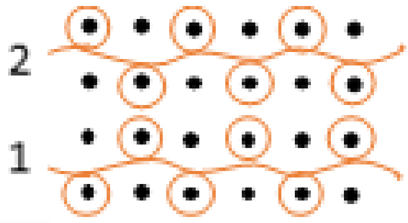

Figure 2.6. Interlock yarn pathway pattern.

2.3. Characterization methods

2.3.1. Melt Flow Index

Thermo Scientific Haake Melt Flow HT indexer complies with the standard ASTM D1238 has been used for MFI measurement to analyze spinning feasibility and to determine the spinning temperature condition (Figure 2.7). Beforehand, the piston was preheated at 220 °C for 2 min, and then the barrel was filled with dried material (7 g per measurement) and preheated for 4 minutes, and then measurements were carried out under a load of 2.16 kg. This procedure was repeated three times for each sample and the result was averaged.

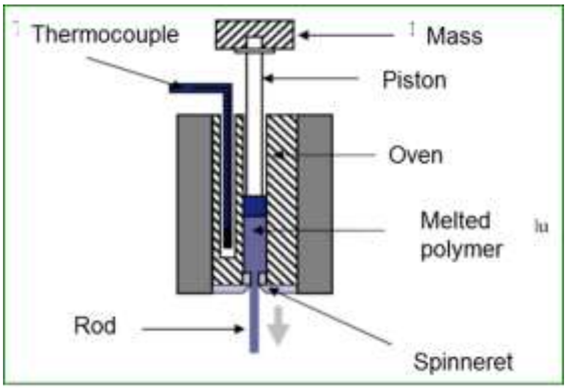

Figure 2.7. Melt flow indexer.

2.3.2. Mechanical properties

In order to evaluate the performance of flame retarded blends and appropriateness for the melt spinning, it is necessary to achieve a sufficient level of mechanical performance to anticipate the commercial application of FR material. The tensile strength, elongation at break and modulus were investigated by a tensile test. The test was carried out with dumbbell shaped specimen dimensions 75 mm × 5 mm × 2 mm as shown in Figure 2.8, according to ASTM D638 standard, using INSTRON testing machine, model 5967 available at University of Soochow Laboratory. Distance between two jaws was 20 mm and a crosshead speed of 20 mm/min, the load sensor was 10 kN. Tensile strength and elongation at break were evaluated from the load-displacement curve. Samples were conditioned under a standard condition, temperature 23 ± 2 °C and relative humidity of 60 ± 5%, five samples of each formulation were tested and the result was averaged.

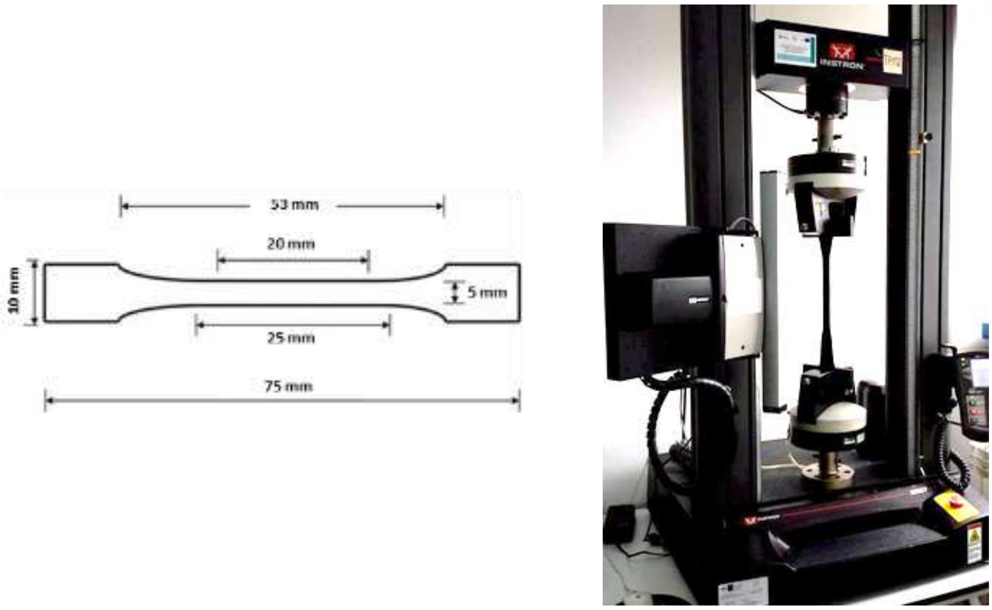

Figure 2.8. Tensile testing tests specimen dimension and apparatus used.

Mechanical properties of developed fibres with monofilament or multifilament form were studies by tensile tests. The section (diameter) of each monofilament was measured using a Zweigle vibroscope (according to ISO 1973) which allows measuring the fineness of the monofilament in tex (g/km). The section is calculated as follows:

$$S_{mono} = (D^2 \times \pi) / 4$$

$$S_{multi} = S_{mono} \times n$$

S_{mono} : section of a monofilament

D : diameter of a monofilament

n : number of monofilament

S_{multi} : section of multifilament

Measurement of the mechanical properties of monofilament was carried out on a tensile testing machine ZWICK 1456 available at ENSAIT- GEMTEX. The force sensor used was 10N. the length between jaws was 20 mm and the crosshead speed was 20 mm/min. Multiple tests, set of 10 was conducted using a standard conditioned sample at a confined temperature of 23 ± 2 °C and relative humidity of 65 ± 5%. Obtained results were then averaged and analyzed.

2.3.3. Microscopic analysis

Low range microscopic observations were first performed by using a microscope (Axiolab, Carl Zeiss, Germany), equipped with a uEYE camera (IDS, Obersulm, Germany). Various lignin particles were observed at 10x magnification in order to analyze the mean diameter. Further, images were processed in ImageJ online available particle analysis software to measure the mean particle diameter. In the case of multifilament, longitudinal and cross-section views were observed at 20x magnification to analyze the surface aspects and regularity

High range microscopic observation of blend samples was carried out using LEO-1450VP (Carl Zeiss, Germany) SEM apparatus, equipped with a X-ray probe (INCAEnergy Oxford, Cu Kα X-ray source, k =1.540 562 Å) under the voltage of 20 kV. Pellets of different blends were fractured in liquid nitrogen and then gold metalized. The SEM is used to characterize the dispersion status of additives in the polymer matrix. Energy dispersive X-rays (EDX) helps to detect the chemical elements presents in the samples.

2.3.4. Differential scanning calorimetry

Thermal behavior of PA/lignin blends was investigated using a TAQ20 analyzer (differential scanning calorimetry, DSC) equipped with TA Advantage control software. Indium was used as a standard for temperature calibration, and the analysis was made under a constant nitrogen flux (50 mL/min). Samples were placed in aluminum pans, which were hermetically sealed before testing and subjected to the following thermal cycle: heating cycle starting from 0 to 250 °C, at ramp rate of 10 °C/min, followed by 5 min isothermal treatment at 250 °C, cooling from 250 to 0 °C at 10 °C/min, and final heating from 0 to 250 °C at 10 °C/ min. The crystallization exotherm recorded from the cooling cycle and the second heating cycle was evaluated to determine the melting endotherm. The degree of crystallinity (X_c) was calculated according to the following equation:

$$X_c = \frac{\Delta H_m}{\Delta H_m^{\circ}(1-W_m)} \times 100 \tag{1}$$

Where ΔH_m is the enthalpy of fusion registered in the heating, ΔH_m° is the theoretical enthalpy of fusion of 100% crystalline polyamide 11 (189.05 J/g) (Frübing et al., 2006; Ricou et al., 2005) and W_m is the weight fraction of lignin.

2.3.5. FTIR analysis

Functional group characterization of each lignin was carried out by FITR using a Nicolet Nexus spectrophotometer (available at ENSAIT – GEMTEX). Lignin samples were ground and mixed with KBr to prepare pellets and spectra were recorded from 4000 to 500 cm^{-1}, using 64 scans and with 4 cm^{-1} resolution.

In a similar way, functional groups of char residue of PA blends was characterized using a Thermo Avatar 370 spectrophotometer (available at Politecnico di Torino). The residue sample was collected at the end of TG analysis (800 °C) carried out in nitrogen, ground and mixed with KBr. Spectra were recorded at room temperature from 4000 to 500 cm^{-1}, using 32 scans and with 4 cm^{-1} resolution.

2.3.6. Thermogravimetric analysis

Thermogravimetric (TG) analyses were carried out with a TA instruments thermal analyzer Q500 (USA), either under air or nitrogen atmosphere at a purge rate of 60 ml/min, with a heating rate of 10 °C/min from 50 to 800 °C, using alumina crucible and sample weight of 10±0.2 mg. TG curves were recorded from experiments, and dTG (derivative) curves were obtained from TA universal data analysis software for all the samples. The decomposition parameters, such as initial decomposition temperature at 5 % weight loss ($T_{5\%}$), and residue at 700°C were obtained from the TG curve. Furthermore, the maximum mass loss rate (MMLR) and the corresponding temperature (T_{max}) were obtained from dTG curves. During TG analyses in the air, the main decomposition step (T_{max1}) and the second thermo-oxidative degradation step (T_{max2}) were evaluated. Each sample was tested two times to ensure repeatability.

The weight loss difference curves were calculated (eq. 2) in order to determine potential increase or decrease in the thermal stability of the blends. This represents the difference between the experimental TGA curves for blends and the linear combination of TGA curves for the neat materials.

$$\Delta(M(T)) = M_{\exp}(T) - M_{theo}(T) \qquad (2)$$

Where, $\Delta(M(T))$ is a residual weight loss difference, $M_{\exp}(T)$ is the experimental residual weight of blends (variation with temperature T), $M_{theo}(T)$ is the theoretical residual weight of the same composition computed by a linear combination between the experimental weights of PA and additives. The main purpose of this method is to point out if the addition of the additives will stabilize or destabilize the system.

Analysis of evolved gas was carried out by TG-FTIR experiments, using a TGA 4000 thermo balance (Perkin Elmer, USA) coupled with an infrared spectrometer FTIR Spectrum Two (Perkin Elmer, USA). TG experiments were performed both in air (flow 25 ml/min) and nitrogen (flow 35 ml/min) atmosphere with a heating rate of 10 °C from 50 to 800 °C, using alumina crucibles with samples (10±0.2 mg). In order to evaluate the gaseous decomposition products in real time (Figure 2.9). A transfer tube connecting the TG and the infrared cell was heated to 280 °C, in order to avoid the condensation of the evolved gaseous products. All these TG-FTIR analyses were carried out in an inert atmosphere (nitrogen). The infrared spectrometer, equipped with DTGS KBr detector, was operated at 4 cm^{-1} optical resolution. The identification was based on the characteristic absorption peak indicating the chemical compound.

Figure 2.9. Picture of TGA coupled with FTIR apparatus.

2.3.6.1. Cone calorimeter tests by oxygen consumption

Cone calorimeter is a well-known bench-scale instrument for testing of fire behaviour which provides a combustion scenario that is typical of investigating a developing or developed fire. This device function based on the principle of oxygen consumption during combustion. It has been shown that the combustible materials, natural or synthetic generate approximately 13.1 MJ of energy per kg of oxygen consumed. Hence, heat release rate (HRR) is based on the fact that the oxygen consumed during combustion is proportional to the heat released. The HRR is the most important parameter for determining the propensity of the material to contribute to the development of a fire. The lower the value of the HRR, the better the fire retarding properties. The material surface can be radiated with different heat fluxes (e.g. 25, 35, 50 and 75) by this instrument, which represents different fire scenarios. The combustion is initiated by electrical sparking igniter and when sample ignites and burns in excess of the gaseous mixture, cone calorimeter represents a well-defined flaming condition. Then, various fire response parameters for fire performance analysis can be recorded, such as time to ignition (TTI), mass loss rate, effective heat of combustion, heat release parameters, smoke release parameters along with toxic gases, and other parameters related to burning.

In this study, cone calorimeter tests for all blend materials were performed at a heat flux of 35 kW/m^2 to assess the forced combustion behavior of sheets (100 x 100 x 3 mm^3) in accordance with ISO 5660 standard (ISO 5660, 2002). The schematic representation of the device is shown in Figure 2.10. The distance between the sample and the heating cone was 25 or 60 mm based on the material behaviour during the test. Before performing the tests, all specimens were conditioned at 23 °C and 50% RH for 72 h. Three tests were carried out on each formulation, and the results averaged. According to this analytical method, the parameters that were taken into account are:

- Time to ignition (TTI) in seconds.
- Heat release rate (HRR) and its peak of heat release rate (PHRR) in kW/m^2.
- Total heat release (THR) in MJ/m^2 during combustion.
- Effective heat of combustion (EHC) in MJ/kg that relates to the ratio of THR to consumed mass.
- Average rate of heat emission (ARHE) in kW/m^2 that corresponds to cumulative heat emission divided by the time, and its maximum value (MAHRE) is a good measure of the propensity of fire development.
- Total smoke release (TSR) in m^2/m^2 that reflects the amount of smoke produced in m^2 per m^2 of sample area.
- Average specific extinction area (ASEA) in m^2/kg.
- CO and CO_2 yield in kg/kg and its ratio, which indicates the CO and CO_2 yield in kg per kg of sample combustion.
- Char residue mass after combustion test in %

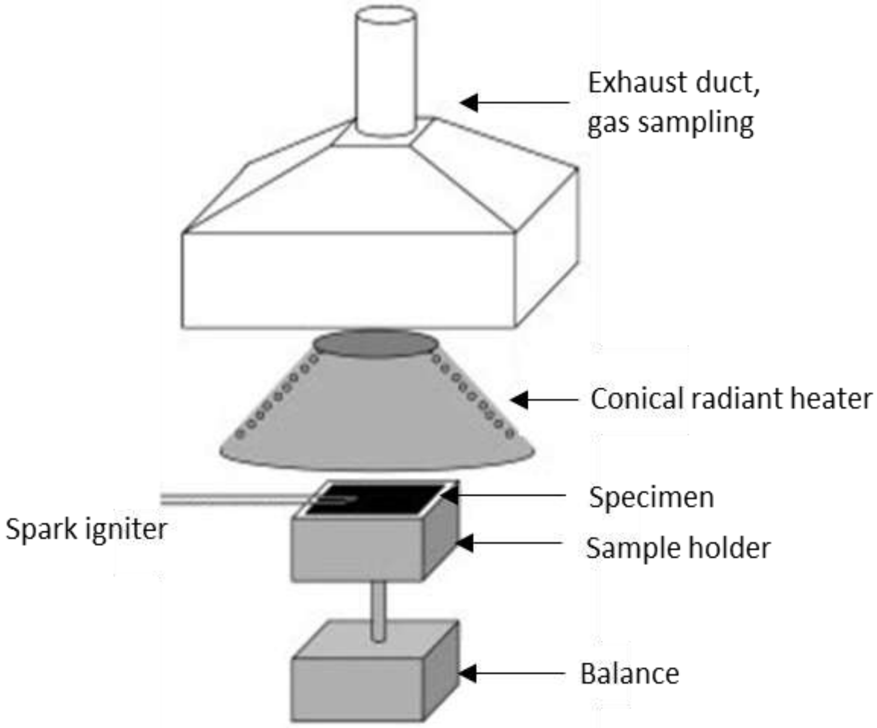

Figure 2.10. Schematic of cone calorimeter.

2.3.6.2. Mass loss cone calorimeter

Mass Loss Calorimeter (Fire Testing Technology) was used to carry out measurements on knitted fabric samples following the procedure defined in ASTM E 906. Tests were performed at UMET laboratory, University of Lille. The equipment is identical to that used in oxygen consumption cone calorimetry (ASTM E-1354-90), except that a thermopile in the chimney is used to obtain heat release rate (HRR) rather than employing the oxygen consumption principle. Our procedure involved exposing specimens measuring 100 mm × 100 mm × 3 mm in a horizontal orientation. External heat flux of 35 kW/m^2 was used for running the experiments. This flux corresponds to common heat flux in a mild fire scenario. The mass loss calorimeter was used to determine heat release parameters. The data reported in this work are the average of three replicated experiments.

2.3.7. UL94 vertical flame spread test

The UL94 is used to characterize the behaviour of different plastic and fabric samples when exposed to flame. The test was carried out on sheet specimens (125 x 12.5 x 3 mm^3) by placing vertically in stand according to test method IEC 60695-11-10 (Troitzsch, 2004). A controlled flame (20 mm, blue Bunsen flame) is applied from the bottom for 10 seconds (t_1) and removed. The specimen's flaming combustion and dripping are observed and recorded. When the sample extinguishes, controlled flame reapplied for another 10 seconds (t_2) and removed. Again, the flaming combustion is observed. This test is aimed at assessing a material capability to extinguish a flame. It classifies specimens from NC (Not classified), V-2, V-1, and V-0, whereas V-0 is the best rating. Materials were classified on the basis of burning rate, time to flame extinction and burning drips. The different criteria for the classifications are presented in Table 2.7. The experimental set-up for the UL94 test is shown in Figure 2.11.

Table 2.7. Classification of material according to UL94 vertical flame test.

Criteria	V-0	V-1	V-2
Afterflame time for each individual flaming	≤ 10s	≤ 30s	≤ 30s
Afterflame + afterglow time for each individual specimen, after second flaming	≤ 30s	≤ 60s	≤ 60s
Total afterflame time for any condition set (5 flaming)	≤ 50s	≤ 250s	≤ 250s
Cotton indicator ignition by flaming drops	NO	NO	Yes
Afterflame or afterglow for any specimen up to the holding clamp	NO	NO	NO

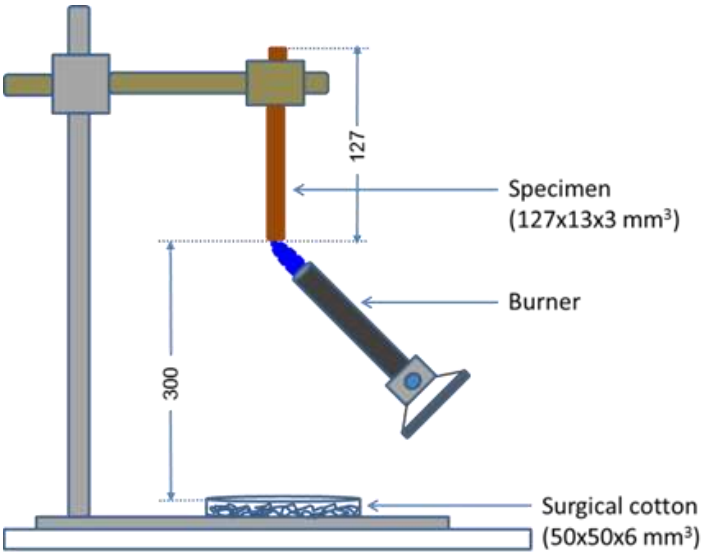

Figure 2.11. Schematic of UL94 vertical flame test.

2.4. Characterization of raw material

2.4.1. Characterization of Lignin

2.4.1.1. FTIR analysis

FTIR spectra of various lignins are shown in Figure 2.12, and the peak positions of the typical absorption bands are summarized in Table 2.8, identification of peaks is based on assignments given by Faix, (1991). Identifications of the recorded spectra of the lignin samples are in agreement with those reported in the scientific literature (Boeriu et al., 2004; Hu et al., 2013; Poletto and Zattera, 2013). A broad absorption around 3411cm^{-1} was observed for all spectra, assigned to the hydroxyl stretching in aliphatic and phenolic structures. Alkyl C–H are found in the range of 2929 to 2840 cm^{-1}, besides the C=O stretching of unconjugated and conjugated was shown at 1760 and/or 1695 cm^{-1}, respectively. The shifting of the band near higher wavelength is attributed to the presence of the sulphonate group in sulphonated lignins sample. The absorption peak at 1591 cm^{-1} originated due to the presence of carbonyl group, which showed that the C=O bonds are in conjugation with the aromatic ring.

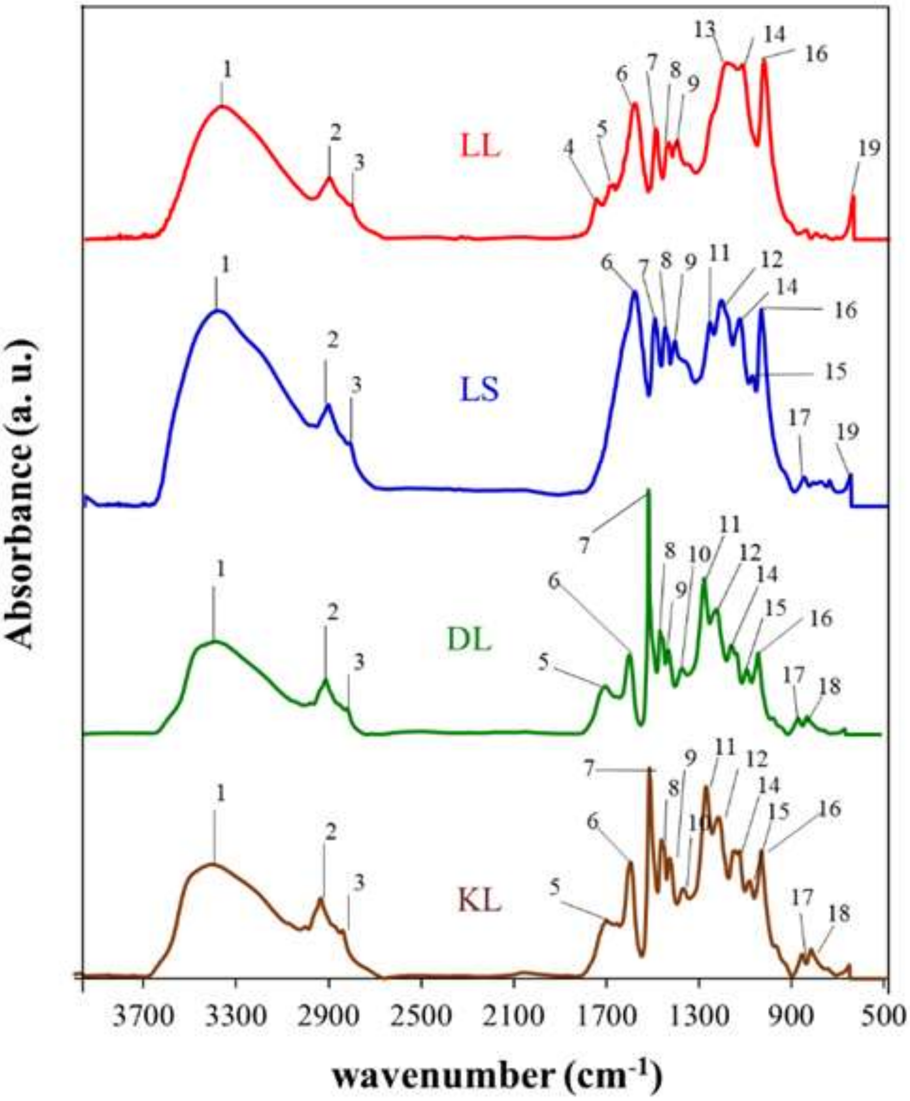

Figure 2.12. FTIR spectra of the four kinds of lignins used in this study.

Furthermore, the absorption peaks at 1510, 1450, and 848, 810 cm^{-1} is assigned to C=C stretching and C–H out-of-plane vibrations in position 2, 5 and 6 of guaiacyl units in the aromatic groups, respectively. In LS, DL and KL spectra, the peak at 1261 cm^{-1} assigned to C–O stretching of the guaiacyl ring, and the band at 1130-1138 cm^{-1} is related to aromatic C-H in-plane deformation in the guaiacyl ring, C-O deformations of secondary alcohols and aliphatic ethers are found at 1076 cm^{-1}. Moreover, in the LL and LS spectra, the peak at around 652 cm^{-1} (from S–O structure) and two other bands at 1178 and 1130 cm^{-1} representing asymmetric and symmetric –SO_2 vibrations are typical of sulphonate structures. In conclusion, the absence of characteristic absorption band at 1325 and 1108 cm^{-1}, which is related to C–O stretching and aromatic C–H deformation of the syringyl ring confirms the absence of Hardwood lignin: thus, all lignins have softwood characteristics. In addition, DL and KL have more Guaiacyl ring (G unit) characteristic.

Table 2.8. FTIR spectra of different lignin used in this study.

Peak label	LL Peak (cm^{-1})	LS Peak (cm^{-1})	KL Peak (cm^{-1})	DL Peak (cm^{-1})	Peak assignment
1	3397	3415	3398	3411	O−H stretching vibration
2	2929	2929	2929	2931	C−H stretching vibration of methyl and methylene group
3	2835	2835	2835	2835	C−H stretching vibration of methyl and methylene group
4	1760	-	-	-	C=O stretching vibration of aliphatic carbonyl and ester groups
5	1695	-	1693	1693	C=O stretching vibration of conjugated carbonyl (aromatic ring)
6	1591	1591	1591	1593	Aromatic skeletal vibration and C=O stretching
7	1508	1504	1512	1512	Aromatic skeletal vibration
8	1450	1459	1452	1459	C−H deformation in methyl and methylene group
9	1416	1416	1421	1423	Aromatic skeletal vibrations combined with C−H in-plane deform.
10	-	-	1356	1356	Aliphatic C−H Stretching vibration of CH_3, not in $O-CH_3$
11	-	1261	1265	1267	C−O of the guaiacyl ring (G unit)
12	-	1209	1209	1209	C−C plus C−O Stretching, typical of G units
13	1178	-	-	-	asymmetric and symmetric $–SO_2$ vibrations
14	1130	1130	1132	1138	aromatic C−H in-plane deformation; typical of G units
15	-	1076	1076	1074	C-O deformations of secondary alcohols and aliphatic ethers
16	1039	1039	1029	1029	Aromatic C−H in plane deformation (G>S)
17	-	848	848	848	C−H out-of-plane in Position 2, 5 and 6 of G units
18	-	-	810	810	C−H out-of-plane in Position 2, 5 and 6 of G units
19	657	659	-	-	sulphonic groups (S−O stretching vibration) Typical in sulphonate containing lignin

2.4.1.2. Structure morphology

Before the implementation of lignin in PA, the mean diameter and morphology of lignin particles were evaluated by optical microscopy and SEM analysis. The particle size distribution and the mean diameter of lignin mainly depend on their chemical structure, botanical source, extraction process and their molecular weight (Tolbert et al., 2012; Wörmeyer et al., 2011). Mean diameters and particle size distributions of various lignins were first observed by using an optical microscope. Further, images were processed in ImageJ online available particle analysis software to measure the mean particle diameter. Table 2.9 reports the lignin mean particle diameter obtain from optical microscopic images. Consequently, LL and LS samples (sulphonate products) have a mean diameter (63±13 and 71±18 µm, respectively) higher than the two other samples 31±9 µm for DL and 39 ± 10 µm for KL (Figure 2.13). Furthermore, LS sample shows a broader range of mean diameter than the other samples, which is indicated by the higher value of standard deviation. In various medium lignins tend to form some aggregates, which influences the compounding and the preparation of lignin-based advanced materials. The SEM images of lignin samples (Figure 2.14) confirm the OM pictures: In particular, the lignin samples show noteworthy changes according to their origin. In this way, high pure lignins from Sigma Aldrich (LS and KL samples) have a smooth spherical shape, and a porous inner core, whereas the two industrial samples demonstrate a rough and irregular polygonal shape, with the presence of impurities on the particle surface.

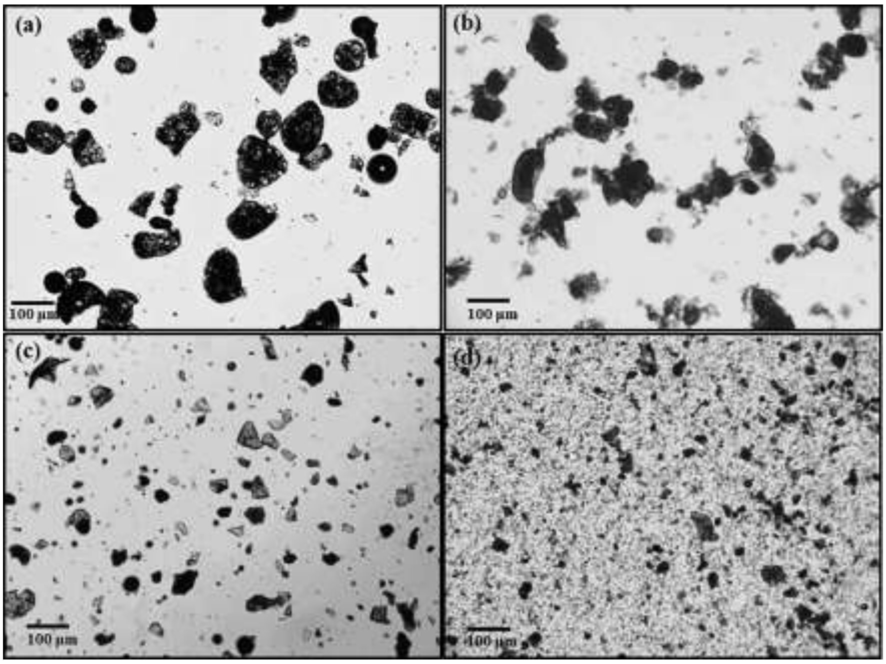

Figure 2.13. Optical microscopy images of different lignin powders at 10x magnification for (a) LS, (b) LL, (c) KL and (d) DL samples.

Table 2.9. Lignin mean particle diameter obtained from optical microscopic images.

Lignin type	Chemical nature	Mean particle diameter (µm)
LS	Alkali low sulphonate lignin	71 ± 18
LL	Lignosulphonate	63 ± 13
KL	Alkali kraft	39 ± 10
DL	Alkali kraft	31 ± 9

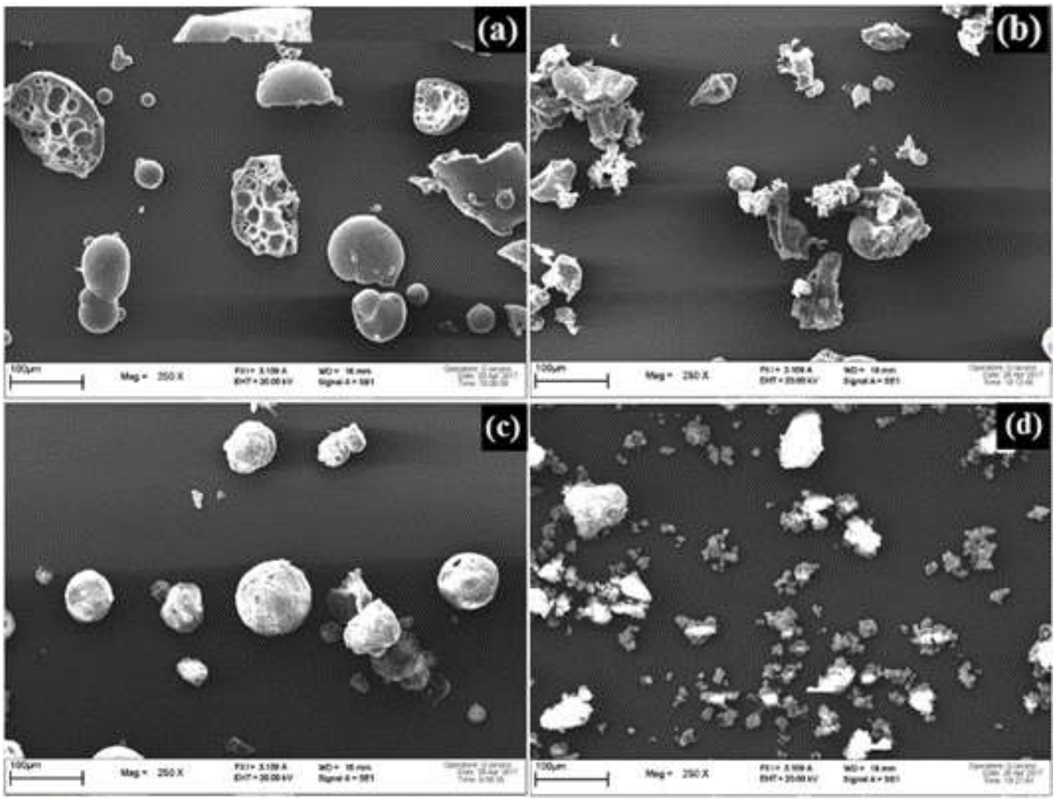

Figure 2.14. SEM micrographs of different lignins (a) LS, (b) LL, (c) KL, and (d) DL samples.

2.4.1.3. Thermogravimetric analysis

The thermal stability of all four types of lignins was assessed by TG analyses carried out in nitrogen at a heating rate of 10 °C/min. Weight loss (TG) and derivative of weight loss (dTG) curves are plotted in Figure 2.15. The thermal decomposition phenomenon of lignin samples can be divided into three main steps: (i) from 60 to 150 °C (moisture release), (ii) from 150 to 500 °C (Mass loss through devolatilization), and (iii) beyond 500 °C (devolatilization with charring), whereas 40−60 wt % of all lignin samples still remain unvolatized due to the development of condensed aromatic structures (Brebu and Vasile, 2010; Yang et al., 2007). From a general perspective, in the first degradation step, the moisture release or mass loss, associated with the loss of bound and free water, varies in the presence of sulfonate groups. Moreover, it was reported by Ház et al. (2013) that, a plasticization phenomenon occurs during this first decomposition step. The broad range of thermal degradation is related to the chemical composition of the lignins, and more specifically to the presence of various oxygen functional groups, the scissions of which occur at different temperatures. Subsequently, in the prior stages, there is the scission of weak ether, aryl−alkyl, and phenyl glycoside bonds, and unstable C−C bonds. The mass loss observed is mainly caused by the degradation of subunits of carbohydrates converted to volatile gases such as CO, CO_2, and CH_4. Toward the end of the second stage, over 400 °C, the polyaromatic compound are formed, which further decomposes into volatile species such as, alcohols, or aldehyde, phenolic, and eventually transformed into char layer in the condensed phase due to the formation of stronger bonds.

Overall, LS has the highest thermal stability and the most noteworthy char yield (58%), followed by LL (55%), KL (48%), and DL (41%). The lesser production of char residue from kraft lignin degradation can be attributed to its higher methoxy content than sulfonated lignins (Hosoya et al., 2009). As shown in the dTG curves, the main degradation steps of LL sample occur at a lower temperature than the other samples with a T_{max} at 250 °C. The maximum devolatilization rate temperatures of the three other lignins can be found at 318 °C for LS, 358 °C for KL, and 385 °C for DL. These results also confirmed that all lignins have some differences in their structures and chemical natures. The decomposition of LL and LS mainly takes place by dehydration and decarboxylation reaction whereas decomposition of KL and DL release higher organic volatiles resulting less amount of char residue (Jakab et al., 1991).

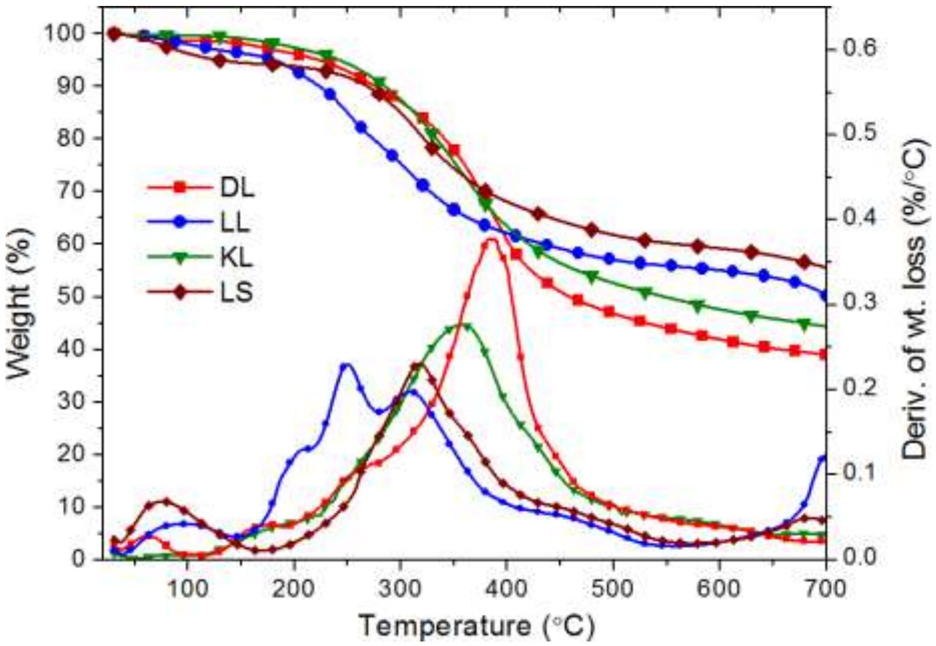

Figure 2.15. TG and dTG curves of lignin samples in N_2 (heating rate 10 °C/min).

2.4.2. Thermogravimetric analysis of phosphinates

TG analyses of phosphinate flame retardants used in this thesis were carried out in nitrogen (60 ml/min) at a heating rate 10 °C/min. All three phosphinates are characterized by a single decomposition peak with maximum weight loss between 460 and 490 °C and a considerable amount of residue at the end of the experiment remained unvolatilized. TG and dTG profile of all three phosphinates are shown in Figure 2.16 and data thermogravimetric are collected in Table 2.10.

Table 2.10. Thermal stability of different phosphinates FR studied.

Phosphinate FR	Trade name, Supplier	$T_{5\%}$ (°C)	T_{max} (°C)	MMLR (%/°C)	Residue at 700 (°C)
ZnP	Pekoflam SMAp, Archroma	472	430	2.4	18
ZnP	Exolit OP950, Clariant	485	437	1.8	19
AlP	Exolit OP1230, Clariant	485	442	2.6	16

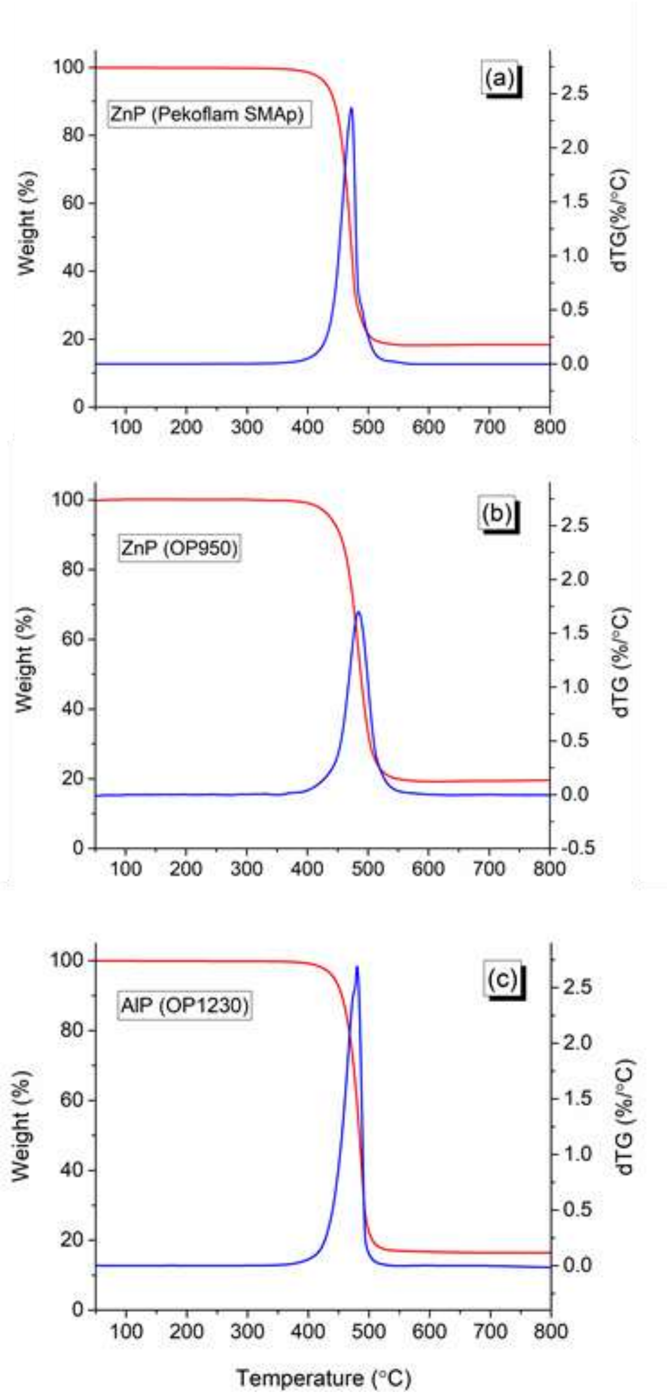

Figure 2.16. TG (red line) and dTG (blue line) curves of neat ZnP and AlP in N_2 (heating rate 10 °C/min).

References

Boeriu, C.G., Bravo, D., Gosselink, R.J.A., Van Dam, J.E.G., 2004. Characterisation of structure-dependent functional properties of lignin with infrared spectroscopy. Ind. Crops Prod. 20, 205–218. https://doi.org/10.1016/j.indcrop.2004.04.022

Braun, U., Schartel, B., Fichera, M.A., Jäger, C., 2007. Flame retardancy mechanisms of aluminium phosphinate in combination with melamine polyphosphate and zinc borate in glass-fibre reinforced polyamide 6,6. Polym. Degrad. Stab. 92, 1528–1545. https://doi.org/10.1016/j.polymdegradstab.2007.05.007

Brebu, M., Vasile, C., 2010. Thermal Degradation of Lignin - A Review. Cellul. Chem. Technol. 44, 353–363.

Faix, B.O., 1991. Classification of Lignins from Different Botanical Origins by FT-IR Spectroscopy. Holzforschung 45, 21–28.

Frübing, P., Kremmer, A., Gerhard-Multhaupt, R., Spanoudaki, A., Pissis, P., 2006. Relaxation processes at the glass transition in polyamide 11: From rigidity to viscoelasticity. J. Chem. Phys. 125, 1–8. https://doi.org/10.1063/1.2360266

Ház, A., Jablonský, M., Orságová, A., 2013. Determination of Temperature Regions. 4nd Int. Conf. Renew. Energy Sources 2013 200280301, 1–6.

Hosoya, T., Kawamoto, H., Saka, S., 2009. Role of methoxyl group in char formation from lignin-related compounds. J. Anal. Appl. Pyrolysis 84, 79–83. https://doi.org/10.1016/j.jaap.2008.10.024

Hu, J., Xiao, R., Shen, D., Zhang, H., 2013. Structural analysis of lignin residue from black liquor and its thermal performance in thermogravimetric-Fourier transform infrared spectroscopy. Bioresour. Technol. 128, 633–639. https://doi.org/10.1016/j.biortech.2012.10.148

ISO 5660, 2002. Fire Test, Reaction to Fire, Rate of Heat Release (Cone Calorimeter Method), International Organization for Standardization, Geneva, Switzerland 2002.

Jakab, E., Till, F., Szeekely, T., Faix, O., 1991. Thermogravimetry/mass spectrometry of various lignosulfonates as well as of a kraft and acetosolv lignin. Holzforschung 45, 355–360. https://doi.org/10.1515/hfsg.1991.45.5.355

Poletto, M., Zattera, A.J., 2013. Materials produced from plant biomass: part III: degradation kinetics and hydrogen bonding in lignin. Mater. Res. 16, 1065–1070. https://doi.org/10.1590/S1516-14392013005000112

Ricou, P., Pinel, E., Juhasz, N., 2005. Temperature experiments for improved accuracy in the calculation of polyamide-11 crystallinity by x-ray diffraction, in: Denver X-Ray Conference on Applications of X-Ray Analysis. pp. 170–175. https://doi.org/10.4028/www.scientific.net/MSF.278-281.151

Tolbert, A., Akinosho, H., Khunsupat, R., Naskar, A.K., Ragauskas, A.J., 2012. Characterization and analysis of the molecular weight of lignin for biorefi ning studies Allison. Biofuels, Bioprod. Biorefining 6, 246–256. https://doi.org/10.1002/bbb

Troitzsch, J., 2004. Plastics flammability handbook : principles, regulations, testing, and approval. Hanser.

Wörmeyer, K., Ingram, T., Saake, B., Brunner, G., Smirnova, I., 2011. Comparison of different pretreatment methods for lignocellulosic materials. Part II: Influence of pretreatment on the properties of rye straw lignin. Bioresour. Technol. 102, 4157–4164. https://doi.org/10.1016/j.biortech.2010.11.063

Yang, H., Yan, R., Chen, H., Lee, D.H., Zheng, C., 2007. Characteristics of hemicellulose, cellulose and lignin pyrolysis. Fuel 86, 1781–1788. https://doi.org/10.1016/j.fuel.2006.12.013

3. DEVELOPMENT OF BINARY BLENDS

3.1. Introduction

This chapter is focused on the thermal stability, charring efficiency and fire-retardant properties brought by the direct addition of lignin. The major concern in the context of lignin valorization regards the different grades of available lignin. The extraction processes contribute to change the structure of the original lignin. various lignins show different thermal decomposition behaviour hence varied charring behaviour which requires to be elucidated before being considered for further studies. Charring ability of lignin in PA blends is advantageous in the context of the valorization of lignin. Selection of lignins, blend formulation and processing are discussed first in this chapter and the performance of prepared blends detailed. Finally, thermal decomposition and fire properties of lignin and PA blends are discussed.

Industrial production of lignins indicates that kraft lignin and lignosulphonate lignin are the most used industrial lignin to date. The primary concern in the context of lignin valorization regards the different grades of available lignin. For this reason, kraft lignin and lignosulphonate lignin are used in this study. In order to compare the fire-retardant properties resulted in the addition of industrial grade lignin, two types of laboratory grade lignins were also used. Chemical nature of laboratory grade lignins was similar to the industrial grade lignins, except the difference in their purity. Four types of lignins, i.e., two laboratory grade (LS and KL) two Industrial grades (LL and DL) were used in this study.

The binary blends are prepared using twin screw extruder with varying lignin content from 5, 10, 15 and 20 wt% as described in Chapter 2. Morphology of blends is characterized by SEM analysis. Thermal stability is analyzed by TG analyses and fire behaviour by UL94 vertical flame and cone calorimeter tests.

3.2. Morphology of binary blends

The influence of lignin dispersion in resulting blends was studied by SEM analysis. The cross-section images of fractured surfaces are shown in Figure 3.1 (a-f). It was noticed that, during the preparation of blends, lignin particles are reduced in size and mixed homogeneously in the PA matrix. SEM images of DL containing blends show a homogeneous dispersion and DL particles are well mixed in the polymer matrix up to 15 wt%. Beyond this loading content, the morphology of the following blends changes and larger size (up to 10 μm) lignin particles are visible in the polymer matrix (Figure 3.1 (c)). However, DL particles are distributed in entire surface and fused with the polymer matrix. KL blends also show a similar morphology owing to the similarity in their chemical nature and particle size.

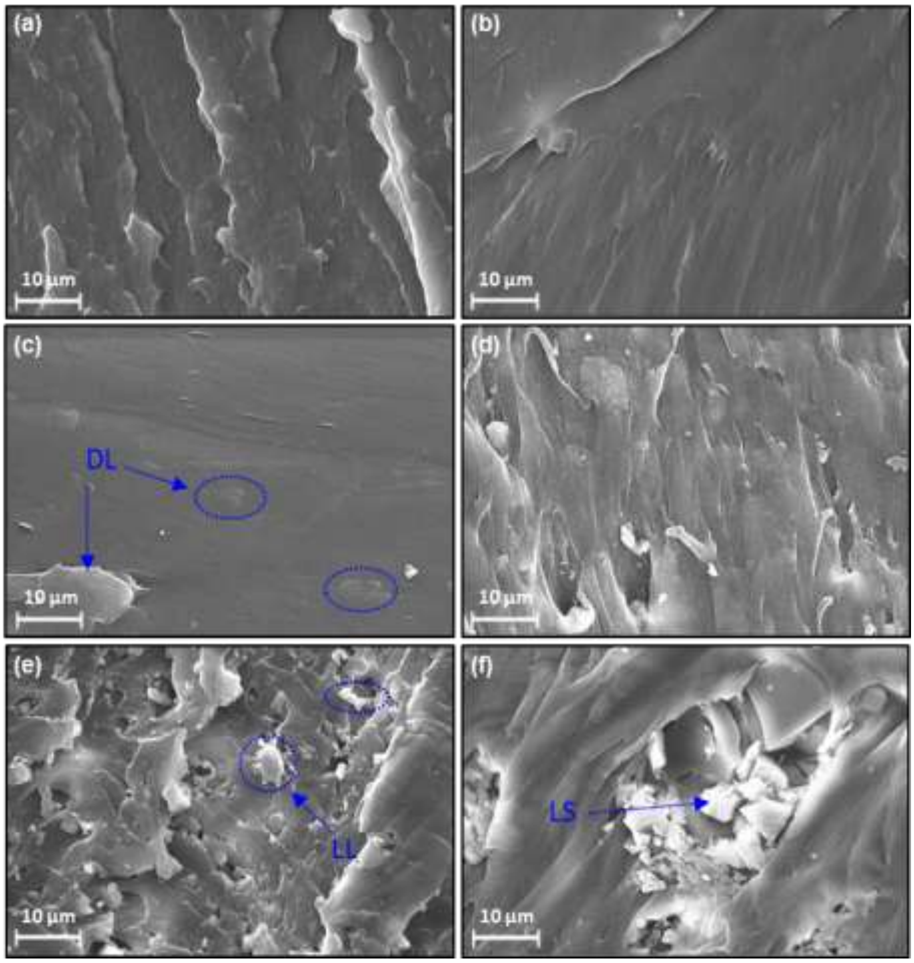

Figure 3.1. SEM micrographs of binary blends of PA and lignin, (a) unfilled PA, (b) PA_{85}-DL_{15}, (c) PA_{80}-DL_{20}, (d) PA_{85}-LL_{15}, (e) PA_{80}-LL_{20}, (f) aggregation in PA_{80}-LS_{20} blend.

On the other hand, the blends with LL (Figure 3.1 (d-e)) show rough surface morphology because LL particles are not fused in polymer matrix. However, particles are uniformly dispersed in polymer phase and no aggregation is observed, except PA_{80}-LL_{20} blend shows more rougher surface due to increasing the LL content to 20 wt%. Similar morphology was revealed by LS lignin up to 15 wt%. However, increasing LS loading to 20 wt%, LS particles tend to form aggregates (Figure 3.1 (f)) in the polymer matrix. In conclusion, different morphology from kraft lignin and sulphonated lignin blends can influence the thermal stability and charring effect of lignin.

3.3. Thermal stability and decomposition study

3.3.1. Thermal properties by DSC

Melting and crystallization properties of PA and its blends with different lignins were studied through DSC measurements; specifically, melting temperature (T_m), enthalpy of fusion (ΔH_m), crystallization temperature (T_c) and enthalpy of crystallization (ΔH_c) were assessed, results are collected in Table 3.1. For unfilled PA, the peak of melting temperature and crystallization temperature was occurred at around 187 °C and 157 °C, respectively. The microstructure and therefore the thermal properties of the blends can be governed by the nucleation process. The addition of lignin in certain polymers act as a nucleating agent, for example, PET and PHB matrices (Canetti and Bertini, 2007; Weihua et al., 2004). It can be noticed that the crystallization temperature marginally rises by 1 to 3 °C at low lignin content, but it declines with the introduction of higher amounts. Moreover, from the T_c onset results, it can be concluded that lignin is not acting as a nucleating agent in PA/lignin blends. Furthermore, whatever the source of lignin, it does not influence the melting of the blends since the T_m onset and T_m peak values are practically similar to those of unfilled PA. For all the systems, the presence of lignin impacts the X_c; in particular, X_c value decreases with increasing lignin content in PA. It is assumed at lower lignin content PA molecular chains are entangled with lignin and arranged in order without any free volume. Hence, the maximum X_c is noticed at low lignin content for all the PA/lignin blends. However, increasing lignin content incorporate disorder in polymer phase, and hence, X_c is increased.

Table 3.1. Thermal properties of PA/lignin blends.

Samples	**T_m onset (°C)**	**T_m Peak (°C)**	**ΔH_m (J/g)**	**T_c onset (°C)**	**T_c Peak (°C)**	**ΔH_c (J/g)**	**X_c (%)**
PA_{100}	179.0	187.1	52.8	161.8	157.4	47.7	27.9
PA_{95}-LS_5	178.8	187.1	57.6	163.3	160.4	47.0	32.0
PA_{90}-LS_{10}	179.9	187.0	52.6	162.3	158.1	43.4	30.9
PA_{85}-LS_{15}	179.2	186.8	48.3	162.4	158.4	39.9	30.1
PA_{80}-LS_{20}	178.5	186.7	46.0	162.5	158.8	40.8	30.4
PA_{95}-LL_5	180.7	187.2	58.3	163.4	159.6	47.1	32.5
PA_{90}-LL_{10}	180.5	187.0	56.5	163.5	159.7	45.9	33.2
PA_{85}-LL_{15}	180.3	186.4	48.6	162.3	158.4	40.4	30.3
PA_{80}-LL_{20}	179.0	185.1	44.3	160.1	155.2	38.0	29.3
PA_{95}-KL_5	179.2	187.0	57.6	162.6	159.1	48.6	32.1
PA_{90}-KL_{10}	179.2	186.7	53.6	161.0	156.1	45.6	31.5
PA_{85}-KL_{15}	178.0	185.2	52.1	160.5	154.7	44.9	32.4
PA_{85}-KL_{20}	177.8	184.8	46.7	159.2	154.2	41.7	30.9
PA_{95}-DL_5	179.2	186.6	61.0	162.1	158.0	51.9	34.0
PA_{90}-DL_{10}	179.4	185.9	57.7	161.9	157.8	49.5	33.9
PA_{85}-DL_{15}	178.0	185.4	54.3	160.4	156.6	48.0	33.8
PA_{80}-DL_{20}	177.4	184.4	41.5	157.7	152.8	44.9	27.5

3.3.2. Effect of lignins on the thermal stability of PA blends

The thermal stability of PA and lignin blends was assessed through thermogravimetric analyses carried out in nitrogen with heating rate 10 °C/min. In particular, the effect of lignins on the thermal stability of PA was studied by selecting the different lignin blends with same lignin concentration; blends with 20 wt% loading content are chosen. Table 3.2 collects the data regarding initial 5 wt% weight loss temperature ($T_{5\%}$), the temperature at a maximum rate of weight loss (T_{max}) and the corresponding mass loss rate (MMLR), and char residue at 600 °C.

The TG and dTG curves of unfilled PA and its blends are shown in Figure 3.2, PA display a typical single degradation step, taking place between 390 and 440 °C with sharp dTG peak, and a quick mass loss rate, without generating any char residue at the end (Lao et al., 2011). The presence of LS leads to increase of T_{max}; at the same time, $T_{5\%}$ decreases. Comparable behavior appears in PA−LL blends. In this case, $T_{5\%}$ significantly reduces up to 278 °C: this outcome can be attributed to a rapid weight loss occurring due to the degradation of subunits of lignin and evolution of hydrocarbons and CO_2 at lower temperature (inset image Figure 3.2). Furthermore, as a result of the slow degradation rates of LS and LL, their blends produce a significant amount of char residue (reported at 600 °C). It is assumed that the presence of the sulphonate group (HSO_3^-) also support in the attainment of stable char residue because during degradation SO_2 is released and Na_2SO_4 is formed by cationic moiety, hence providing increased thermal stability (Jakab et al., 1991).

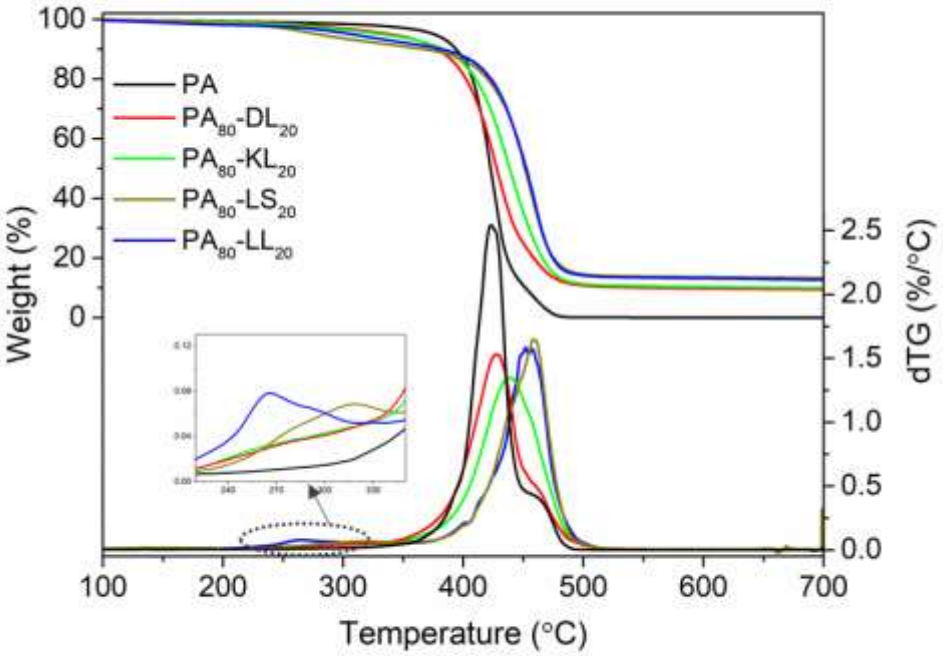

Figure 3.2. TG and dTG curves of PA/lignin blends containing 20 wt% lignin (10 °C/min in N_2).

Conversely, the introduction of KL and DL in PA reduces $T_{5\%}$ up to 40 °C, which is less than what is observed in LS and/or LL blends. In contrast to LS and LL, kraft lignin blends show a very limited or even no change in T_{max} as compared to unfilled PA. This leads to a substantial weight loss for these blends and lower char residue at the end of the test. This behavior can be elucidated by the maximum mass loss of KL and DL in the range of 350 to 450 °C (Chapter 2, Figure 2.15), due to the devolatilization of lignin with the evolution of alcoholic, carbonyls and phenolic compounds, which cannot be detected by TGA. It is also reported that lower molecular weight of kraft lignin leading to the evolution of a higher amount of volatile products during thermal degradation (Sameni et al., 2014).

Table 3.2. Thermogravimetric results for neat PA and blends of PA/lignin.

Samples	$T_{5\%}$ (°C)	T_{max} (°C)	MMLR (%/°C)	Residue at 600 °C (%)
PA_{100}	375	423	2.5	0.4
PA_{95}-LS_5	383	473	2.0	2.7
PA_{90}-LS_{10}	355	468	2.0	6.2
PA_{85}-LS_{15}	328	462	1.8	8.9
PA_{80}-LS_{20}	307	461	1.6	13.2
PA_{95}-LL_5	367	463	2.1	3.7
PA_{90}-LL_{10}	310	461	1.9	8.3
PA_{85}-LL_{15}	297	456	1.8	9.9
PA_{80}-LL_{20}	278	452	1.6	13.7
PA_{95}-KL_5	362	425	2.6	3.0
PA_{90}-KL_{10}	351	427	1.8	6.3
PA_{85}-KL_{15}	338	431	1.6	8.5
PA_{80}-KL_{20}	331	440	1.4	10.3
PA_{95}-DL_5	364	423	2.2	2.5
PA_{90}-DL_{10}	361	415	2.2	4.5
PA_{85}-DL_{15}	345	420	1.8	8.1
PA_{80}-DL_{20}	338	428	1.5	9.8

3.3.3. Influence of lignin content on the thermal stability of PA blends

The lignin loading in the blends also affects their thermal stability and charring phenomena. In order to systematic understanding the effect of lignin content on thermal stability and charring ability of blends, Figure 3.3 (a-d) shows thermogram profile of PA and its blends with different lignin with loading content ranging from 5 to 20 wt%. PA and its blends show a one-step decomposition. The major difference between them is the char residue at 600 °C. Figure 3.3 (a-b) shows increasing lignin (LS/LL) loading in PA gradually reduces both the $T_{5\%}$ and T_{max} temperature, e.g., PA_{80}-LL_{20} blends decreases $T_{5\%}$ and T_{max} temperature up to 278 °C and 452 °C, respectively. While the char residue progressively increases up to 13.2 wt%. In addition, the maximum weight loss rate (MMLR) gradually decreases with increasing lignin content, which indicates that lignin allows PA to degrade slowly, and it is because of the stronger bond formation in the condensed phase due to devolatilization of lignin. As a consequence, thermal stability of these blends increases by shifting T_{max} temperature to higher region (about 40 – 50 °C). Moreover, increasing lignin content from 5 to 20 wt% decelerates the MMLR, hence resulting in a higher amount of char residue at the end of the experiment.

Conversely, Figure 3.3 (c-d) shows the effect of increasing kraft lignin (DL/KL) loading content in PA. It was noticed that reduction in $T_{5\%}$ temperature is less influenced as compared to sulphonated lignin blends (Table 3.2), this finding can be attributed to a slow rate of degradation of lignin in lower temperature region. As a result, increasing kraft lignin content up to 20 wt%, $T_{5\%}$ only reduces up to 40 °C than that of PA. Unlike sulphonated lignin blends, increasing KL/DL content has little influence on thermal stability of these blends (Figure 3.3 (c-d)), T_{max} slightly shift to higher temperature up to 17 °C for PA-KL blends. This is ascribed to the maximum decomposition of lignin with release of more organic volatiles taking place in this temperature region; as a consequence, low amount of char residue is reported compared to LL/LS blends (Table 3.2). The lesser production of char residue from kraft lignin blends degradation can be attributed to a higher methoxy content in kraft lignin than sulfonated lignins (Hosoya et al., 2009).

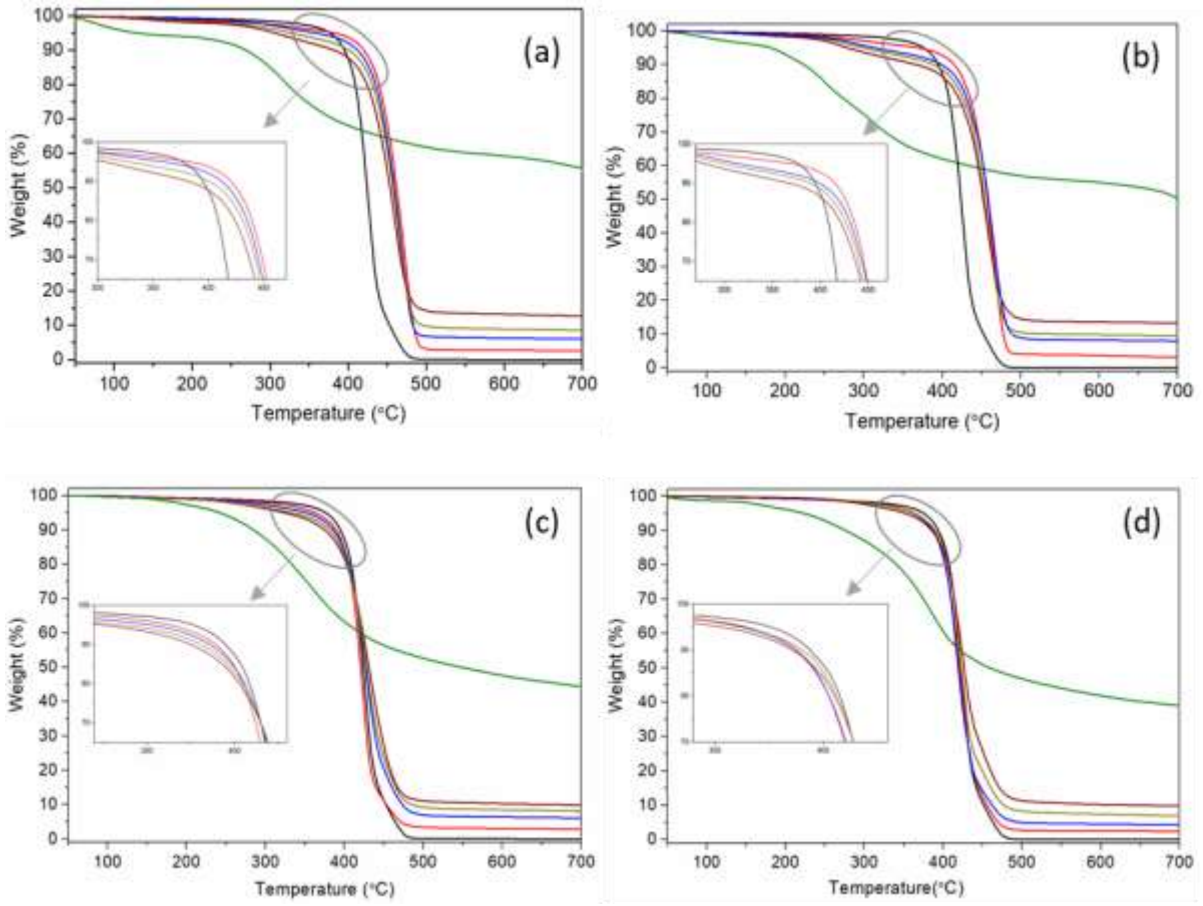

Figure 3.3. TG analysis curves of PA/lignin blends, (a) PA-LS, (b) PA-LL, (c) PA-KL, (d) PA-DL, (—) PA, (—) L, (—), PA_{95}-L_5, (—) PA_{90}-L_{10}, (—) PA_{85}-L_{15}, (—) PA_{80}-L_{20}, L= lignin, containing 5, 10, 15 and 20 wt% (heating rate 10 °C/min in nitrogen) .

Conclusion about TGA analysis

TGA analysis of different industrial and laboratory grade lignin blends revealed that the thermal decomposition behaviour and the amount of charred residue obtained was practically similar for LL and LS. The thermal decomposition of kraft lignins was distinctively different from sulphonated lignins. Both, the DL and KL also showed comparable thermal decomposition. However, the amount of char residue in sulphonated lignins was higher than that of kraft lignins. Sulphonated lignin blends showed much reduced $T_{5\%}$ temperature than kraft lignin counter part due to the decomposition of LL or LS which start at lower temperature mainly by dehydration and decarboxylation reactions. Moreover, the presence of sulphonate groups also help in getting higher amount of residue due to the formation of thermally stable bonds in the condensed phase. Conversely, the KL and DL blends have little influence on $T_{5\%}$ and T_{max} temperature and lead to maximum mass loss due to the evolution of more organic volatile and generate lower amount of char residue than LL and/or LS blends. As described in state of the art, the char forming ability of polymer can effectively reduce the heat release rate and increases the fire retardant properties.

3.4. Analysis of fire properties

3.4.1. UL94 vertical flame spread test

UL94 is broadly used for assessing relative flammability phenomenon and melt dripping of plastics and polymeric materials. The data collected in Table 3.3, include combustion time (t_1 and t_2) after 1st and 2nd flame application, total combustion time, cotton ignition and UL94 rating for the developed formulations. The addition of LS lignin to PA rises the total combustion time, which further increases in line with the lignin loading. This finding is attributed to the initial decomposition of blends ($T_{5\%}$) that occurs at a lower temperature as compared to unfilled PA; therefore, high flammability is noticed, and the samples cannot be classified according to UL94 test rating. On the other hand, LL limits the flammability by decreasing combustion time; likewise, the FR properties improved with increasing the LL content. In particular, the blend comprising 15 wt% LL shows a remarkable reduction of total combustion time and achieve V-1 rating. It was noticed that during the test protective char layer is formed, which acts as a barrier for heat and mass transfer. It is expected, the presence of sulphonate functionality and different impurities in LL facilitates to the formation of the thermally stable compound in the condensed phase which additionally contributes in the construction of effective char layer that leads to self-extinction to PA_{85}-LL_{15} blend, hence improving the rating.

Table 3.3. Results from UL 94 vertical flame spread tests.

samples	1st Combustion t_1 (s)	2nd Combustion t_2 (s)	Total combustion t_1+t_2 (s)	Cotton ignition	Rating
PA_{100}	13 ± 1	11 ± 2	24 ± 1	Yes	V-2
PA_{95}-LS_5	26 ± 3	17 ± 4	42 ± 5	Yes	V-2
PA_{90}-LS_{10}	25 ± 12	43 ± 22	68± 23	Yes	NC
PA_{85}-LS_{15}	37 ± 4	45 ± 8	82 ± 4	Yes	NC
PA_{80}-LS_{20}	27 ± 5	58 ± 18	85 ± 16	Yes	NC
PA_{95}-LL_5	25 ± 1	22 ± 6	47 ± 5	Yes	NC
PA_{90}-LL_{10}	10 ± 2	8 ± 2	18 ± 2	Yes	V-2
PA_{85}-LL_{15}	2 ± 1	4 ± 1	6 ± 2	Yes	V-1
PA_{80}-LL_{20}	5 ± 1	5 ± 1	10 ± 2	Yes	V-2
PA_{95}-KL_5	17 ± 1	5 ± 1	22 ± 1	Yes	V-2
PA_{90}-KL_{10}	16 ± 3	8 ± 2	24 ± 1	Yes	V-2
PA_{85}-KL_{15}	16 ± 1	18 ± 3	34 ± 4	Yes	NC
PA_{80}-KL_{20}	28 ± 7	23 ± 6	51 ± 11	Yes	NC
PA_{95}-DL_5	12 ± 1	18 ± 5	29 ± 5	Yes	NC
PA_{90}-DL_{10}	9 ± 4	10 ± 1	20 ± 4	Yes	V-2
PA_{85}-DL_{15}	4 ± 1	6 ± 1	10 ± 2	Yes	V-2
PA_{80}-DL_{20}	9 ± 4	9 ± 3	18 ± 7	Yes	V-2

Conversely, the addition of KL to PA has a detrimental effect; at high lignin contents (15 – 20 wt%): the samples cannot be classified. Besides, the blends containing KL (at low loading, i.e., 5 and 10 wt%) show strong dripping phenomena, responsible for V-2 rating. Unlike KL, increasing DL amount in PA provides a reduced total combustion time. It is interesting to note that 15 wt% loading of LL and DL shows most reduced combustion time: lignin loading seems better for enhancing the flame-retardant properties of PA.

3.4.2. Forced combustion test

Cone calorimetry tests were carried out at 35 kW/m^2 for evaluating the combustion behaviour of PA and its blends. Cone calorimetry has been widely used to simulate a developed fire behaviour of the material in a real fire condition. In this test, Heat release parameters, i.e., heat release rate (HRR) and total heat release (THR) are the key parameters in order to evaluate the combustion behaviour of a material exposed to specific heat flux. Therefore, in this study, HRR, THR and char residue of the prepared blends were compared with unfilled PA; the data for all four types of lignin are reported in Table 3.4. Figure 3.4 (a – d) and Figure 3.5 (a – d) show the effect of lignin and its content on HRR and THR. It is worth to note that Figure 3.4 represents curves for sulphonated lignins, i.e., LS and LL and Figure 3.5 refers to kraft lignins, i.e., KL and DL. Unfilled PA shows a peak of HRR of about 862 kW/m^2 with total heat released (THR) of about 98 MJ/m^2. It is worth noticing that all PA/lignin blends provoke the ignitability: this finding can be attributed to lignin degradation that begins at lower temperature, i.e., below that of PA. Moreover, the blends containing sulphonated lignins effectively reduce the PHRR and THR (Figure 3.4 (a–d)), due to the formation of a higher char residue (Table 3.4). It is assumed that the sulphonate containing lignins generate higher char residue due to the condensed aromatic structure. It is also expected the presence of sulphonate functionality also contribute to bringing down HRR, as reported during degradation SO_2 is released hence limiting the heat release and thermally stable Na_2SO_4 is formed in the condensed phase (Ferry et al., 2015), ensuring in the diminution of PHRR and other fire parameters. Conversely, kraft lignins containing blends show the detrimental effect as the PHRR and THR values increases in comparison with unfilled PA (Figure 3.5 (a–d)). This finding can be explained by their high mass loss during TG experiments and the higher average mass loss rate (AMLR) values in forced combustion test than that of unfilled PA (Table 3.4). It was observed from the TGA of KL and DL that more organic volatiles are release during their decomposition, these organic products are combustible which can feed to the flame: as consequence, HRR and PHRR increases.

Table 3.4. Cone calorimetry data for PA/lignin blends.

Samples	TTI (s)	Peak HRR (kW/m^2)	Δ (%)	THR (MJ/m^2)	Δ (%)	AMLR (g/s)	Residual mass (%)
PA	79 ± 11.2	862 ± 140	-	98 ± 8.5	-	0.101	0.6 ± 0.8
PA$_{95}$-LS$_5$	56 ± 1.7	1040 ± 61	+17.1	106 ± 2.4	+7.8	0.111	2.1 ± 0.1
PA$_{90}$-LS$_{10}$	45 ± 2.6	688 ± 44	-20.2	99 ± 1.4	+1.1	0.099	3.4 ± 0.2
PA$_{85}$-LS$_{15}$	42 ± 4.7	558 ± 19	-35.3	92 ± 2.2	-5.9	0.079	5.6 ± 0.2
PA$_{80}$-LS$_{20}$	36 ± 3.6	451 ± 53	-47.7	75 ± 14.3	-23.1	0.074	8.7 ± 0.2
PA$_{95}$-LL$_5$	60 ± 3.2	886 ± 8	+2.7	88 ± 5.4	-9.7	0.181	2.3 ± 0.3
PA$_{90}$-LL$_{10}$	58 ± 6.0	715 ± 70	-17.1	83 ± 8.2	-15.5	0.091	3.8 ± 0.1
PA$_{85}$-LL$_{15}$	51 ± 1.7	468 ± 36	-45.8	82 ± 0.6	-16.5	0.072	5.9 ± 0.3
PA$_{80}$-LL$_{20}$	58 ± 6.1	425 ± 12	-50.8	76 ± 2.0	-22.2	0.052	8.4 ± 0.2
PA$_{95}$-KL$_5$	55 ± 7.6	1374 ± 22	+37.3	103 ± 3.7	+5.0	0.150	2.0 ± 0.1
PA$_{90}$-KL$_{10}$	42 ± 0.6	1166 ± 137	+26.1	98 ± 3.5	-0.1	0.174	4.5 ± 1.1
PA$_{85}$-KL$_{15}$	47 ± 6.2	1138 ± 134	+24.2	97 ± 3.8	-0.7	0.137	5.3 ± 1.1
PA$_{80}$-KL$_{20}$	50 ± 3.5	851 ± 35	-1.3	90 ± 7.4	-8.5	0.164	7.3 ± 0.3
PA$_{95}$-DL$_5$	55 ± 1.0	971 ± 73	+11.2	97 ± 0.3	-0.4	0.107	1.8 ± 0.1
PA$_{90}$-DL$_{10}$	50 ± 3.0	936 ± 48	+7.8	96 ± 0.9	-1.6	0.138	3.2 ± 0.1
PA$_{85}$-DL$_{15}$	53 ± 9.2	1030 ± 42	+16.3	90 ± 1.6	-8.0	0.125	5.5 ± 0.2
PA$_{80}$-DL$_{20}$	43 ± 5.7	917 ± 76	+5.9	84 ± 0.8	-14.1	0.089	8.3 ± 1.1

Besides, increasing the lignin content in PA-LS blends decreases PHRR and THR. The presence of 5 wt% lignin increases PHRR (1040 kW/m^2) and THR (106 MJ/m^2) with respect to unfilled PA: this detrimental effect might be attributed to low lignin content, which is not sufficient for triggering the formation of a stable char layer. Moreover, the blends containing 10 wt% LS displays a two-step combustion process: the initial step can be associated with the char formation; then a steady state region is observed, that undergoes cracking or damage, giving rise to the second HRR peak. However, with increasing lignin content, a higher char amount is observed: as a consequence, the shape of curve changes from non-charring to thick charring behaviour (Schartel and Hull, 2007).

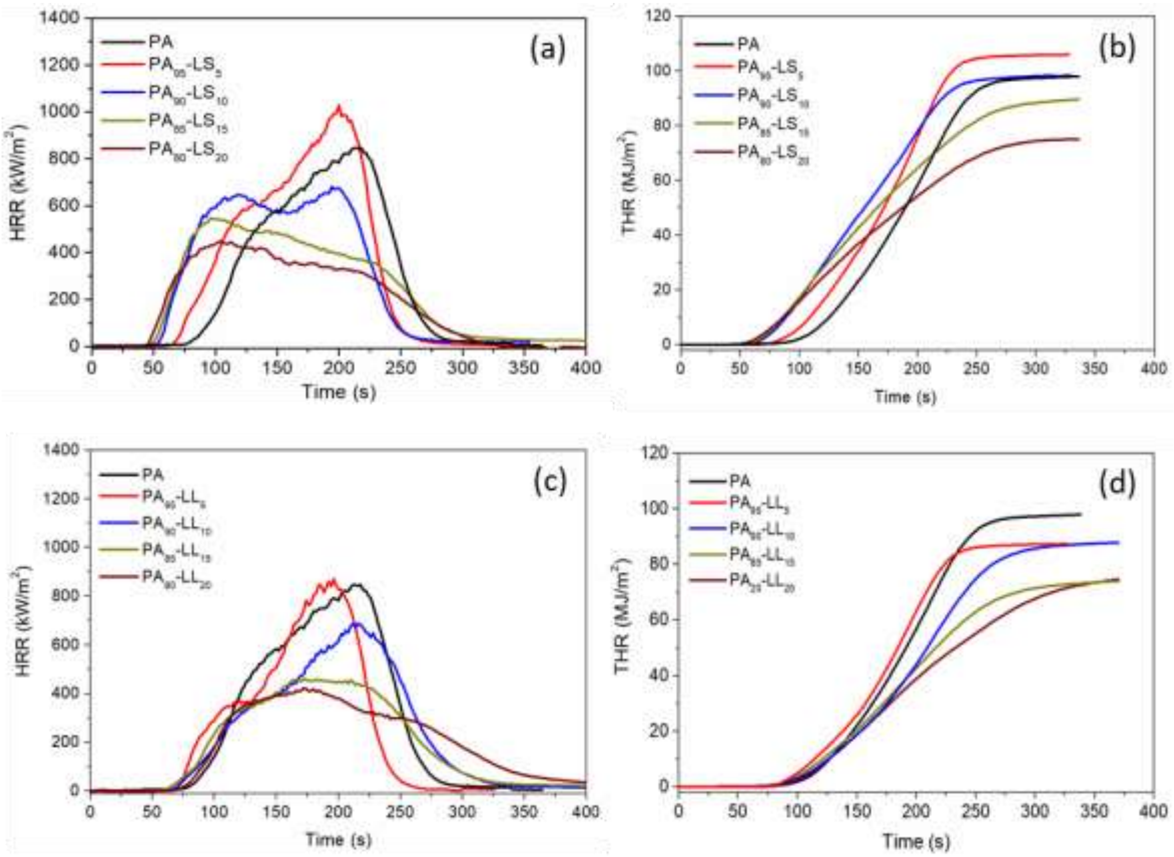

Figure 3.4. HRR and THR curves for PA/lignin blends, (a-b) for PA-LS, (c-d) for PA-LL blends

Further increasing the LS content to 20 wt% considerably reduces both PHRR (- 48%) and THR (-23%). With some enhancements in PHRR value, a comparable trend is found with increasing LL loading in PA. On the other hand, the increase of kraft lignins (KL and DL) content up to 15 wt% does not show any significant improvement in fire retardant properties. Finally, the presence of 20 wt% of DL is responsible for THR reduction (-14%).

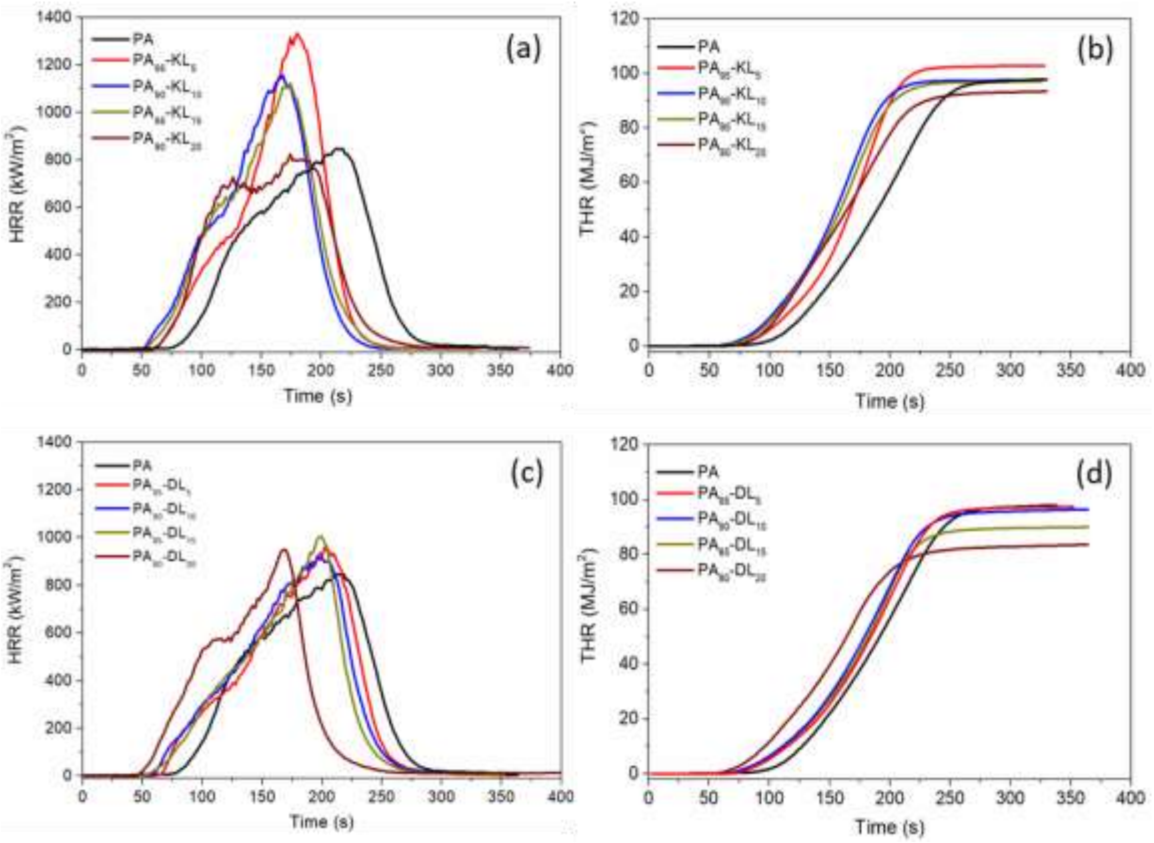

Figure 3.5. HRR and THR curves for PA/lignin blends, (a-b) for PA-KL, (c-d) for PA-DL blends.

3.4.3. Morphology of char residue

Figure 3.6 shows the digital pictures of residue obtained after forced combustion tests. It is noticed that the residue from PA is very thin and practically negligible. However, the introduction of lignin in PA steadily increased the char residue with an increasing lignin amount, which can also be seen from the residual mass (reported in Table 3.4) after forced combustion tests. Moreover, char residue amount and the morphology strongly depend on the type of lignin and its chemical nature. It can be seen that sulphonate containing lignin blends generates a higher amount of residue than kraft containing counterpart. Infect, higher loading of LS and/or LL (PA_{80}-LS_{20} / PA_{80}-LL_{20}) show coherent and compact char formation, which is capable of reducing the release of flammable and non-flammable gases throughout the polymer. However, lowering the LS content gives rise to a mechanically thin char layer with several cracks on the surface. The presence of cracks and insufficient residue leads to the formation of a weak protective layer, as consequence, performance of blends deteriorates. Besides, the char residue of kraft lignin blends shows a loose and porous structure with several cracks, which easily allow the transfer of oxygen and heat flux and increases the heat release and flammability of the underlying polymer.

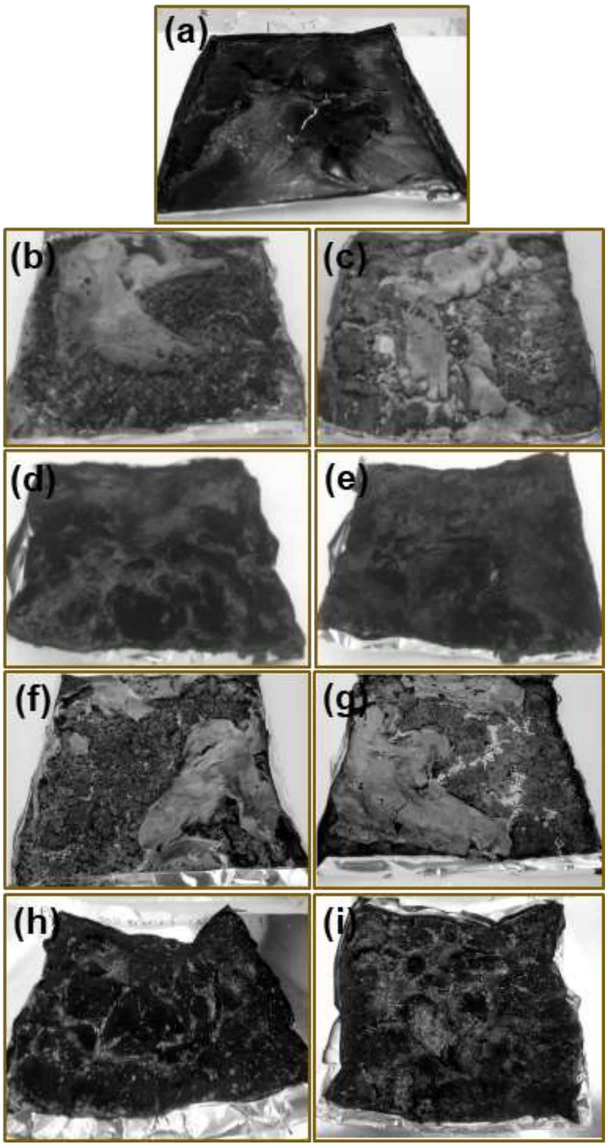

Figure 3.6. Pictures of char residues collected at the end of cone calorimetry test: (a) unfilled PA, (b) PA_{80}-LS_{20}, (c) PA_{90}-LS_{10}, (d) PA_{80}-KL_{20}, (e) PA_{90}-KL_{10}, (f) PA_{80}-LL_{20}, (g) PA_{90}-LL_{10}, (h) PA_{80}-DL_{20}, (i) PA_{90}-DL_{10} blends.

3.5. Conclusion

Different industrial and laboratory grade lignin blends with PA have been studied in this chapter. More attention was focused on thermal decomposition and fire behaviour analysis. The binary blends were prepared by varying lignin content from 5, 10, 15 and 20. SEM analyses of the blends revealed that kraft lignin (DL/KL) particles were mixed with the matrix and homogenously dispersed in the polymer phase up to 15 wt% loading content. With increasing the loading content, lignin particles up to 10 µm were observed. Besides, LS and LL also show similar morphology up to 15 wt%, except lignin particles were not fused in the polymer matrix, which makes surface rougher. Increasing LS loading to 20 wt%, agglomeration phenomena was observed. DSC analyses showed that the presence of lignins exhibit no practical change in melting and crystallization temperatures. However, with 5 wt. lignin content maximum increases of X_c was observed. Further increasing the lignin loading promotes the decrease of X_c as compared to unfilled PA.

TG analyses revealed that the slow degradation and evolution of less organic products form sulphonated lignins as well as the presence of sulfonate groups in LL and LS was responsible for the formation of a high quantity of char residue. The lower char residue obtained from kraft lignins (KL and DL) was attributed to the higher mass loss rate due to the presence of less thermally stable subunits that produce increasingly volatile products during degradation. Flammability behaviour was assessed by UL94 vertical flame spread tests, only PA−LL revealed improvements in flame retardant properties, and self-extinction (V-1 rating) was achieved with 15 wt% lignin loading, thus indicating that this loading is optimum for flame retardant purposes. Cone calorimetry tests clearly showed that the introduction of sulfonated lignins (LS and LL) considerably reduced PHRR and THR; the addition of 20 wt% LL was able to drop PHRR by 51% and THR by 22%, respectively. Furthermore, char residue improved with increasing lignin content, approaching 8.7% in the blends containing 20 wt%

of LS. Conversely, the presence of kraft lignins (KL and DL) showed a detrimental effect on both HRR and THR. In conclusion, from a general perspective, the use of lignin in PA appears to be very encouraging, also bearing in mind the “green” character of both the polymer matrix and the proposed FR additive.

All the studies carried out in this chapter allowed us to improve our understanding on charring properties and thermal decomposition behaviour of PA and lignin blends that is necessary for exploring lignin as additive in developing fire retardant systems, which will be studied in the following chapters.

References

Braaten, S.M., Christensen, B.E., Fredheim, G.E., 2003. Comparison of Molecular Weight and Molecular Weight Distributions of Softwood and Hardwood Lignosulfonates. J. Wood Chem. Technol. 23, 197–215. https://doi.org/10.1081/WCT-120021925

Canetti, M., Bertini, F., 2007. Supermolecular structure and thermal properties of poly(ethylene terephthalate)/lignin composites. Compos. Sci. Technol. 67, 3151–3157. https://doi.org/10.1016/j.compscitech.2007.04.013

Ferry, L., Dorez, G., Taguet, A., Otazaghine, B., Lopez-Cuesta, J.M., 2015. Chemical modification of lignin by phosphorus molecules to improve the fire behavior of polybutylene succinate. Polym. Degrad. Stab. 113, 135–143. https://doi.org/10.1016/j.polymdegradstab.2014.12.015

Glasser, W.G., Davé, V., Frazier, C.E., 1993. Molecular Weight Distribution of (Semi-) Commercial Lignin Derivatives. J. Wood Chem. Technol. 13, 545–559. https://doi.org/10.1080/02773819308020533

Jakab, E., Till, F., Szeekely, T., Faix, O., 1991. Thermogravimetry/mass spectrometry of various lignosulfonates as well as of a kraft and acetosolv lignin. Holzforschung 45, 355–360. https://doi.org/10.1515/hfsg.1991.45.5.355

Kun, D., Pukánszky, B., 2017. Polymer/lignin blends: Interactions, properties, applications. Eur. Polym. J. 93, 618–641. https://doi.org/10.1016/J.EURPOLYMJ.2017.04.035

Lao, S.C., Koo, J.H., Moon, T.J., Londa, M., Ibeh, C.C., Wissler, G.E., Pilato, L.A., 2011. Flame-retardant polyamide 11 nanocomposites: further thermal and flammability studies. J. Fire Sci. 29, 479–498. https://doi.org/10.1177/0734904111404658

Mousavioun, P., Doherty, W.O.S., George, G., 2010. Thermal stability and miscibility of poly(hydroxybutyrate) and soda lignin blends. Ind. Crops Prod. 32, 656–661. https://doi.org/10.1016/j.indcrop.2010.08.001

Ricou, P., Pinel, E., Juhasz, N., 2005. Temperature experiments for improved accuracy in the calculation of polyamide-11 crystallinity by x-ray diffraction, in: Denver X-Ray Conference on Applications of X-Ray Analysis. pp. 170–175. https://doi.org/10.4028/www.scientific.net/MSF.278-281.151

Sallem-Idrissi, N., Sclavons, M., Debecker, D.P., Devaux, J., 2016. Miscible raw lignin/nylon

6 blends: Thermal and mechanical performances. J. Appl. Polym. Sci. 133, n/a-n/a. https://doi.org/10.1002/app.42963

Sameni, J., Krigstin, S., Rosa, D. dos S., Leao, A., Sain, M., 2014. Thermal Characteristics of Lignin Residue from Industrial Processes. BioResources 9, 725–737.

Schartel, B., Hull, T.R., 2007. Development of fire-retarded materials—Interpretation of cone calorimeter data. Fire Mater. 31, 327–354. https://doi.org/10.1002/fam.949

Song, P., Cao, Z., Fu, S., Fang, Z., Wu, Q., Ye, J., 2011. Thermal degradation and flame retardancy properties of ABS/lignin: Effects of lignin content and reactive compatibilization. Thermochim. Acta 518, 59–65. https://doi.org/10.1016/j.tca.2011.02.007

Weihua, K., He, Y., Asakawa, N., Inoue, Y., 2004. Effect of lignin particles as a nucleating agent on crystallization of poly(3-hydroxybutyrate). J. Appl. Polym. Sci. 94, 2466–2474. https://doi.org/10.1002/app.21204

4. DEVELOPMENT OF TERNARY BLENDS

Introduction

This chapter discusses, the development of flame retarded ternary blends based on lignin and phosphinate salt. In this regards, primary study is carried out using more pure laboratory grade lignin combined with ZnP to investigate the influence of the blends on thermal stability and fire properties. Different formulations based on lignins and ZnP were prepared using twin screw extruder (described in chapter 2) and thoroughly investigated. Analyses were carried out in order to understand possible interaction between ZnP and lignin, also with polymer, and their influence on fire-retardant properties. This study provides an insight into the thermal decomposition and fire behaviour.

In the next stage, industrial lignins were used with commercial phosphinate FRs. Purpose of this work to study the influence of industrial lignin in fire retardant system. Lignin is formulated with phosphinate salt without any pretreatment. These formulations were exploited to scale-up the production of flame retarded blends as well as to reduce the cost to facilitate the practical application of blends in the melt spinning process. Industrial lignins, i.e., Domsjo lignosulphonate lignin (LL) and Domtar kraft lignin (DL) studied in Chapter 3 were mixed with ZnP or AlP to develop flame retarded blends. For the systematic understanding, various FR formulations by varying the FR loading are prepared and investigated. Thermogravimetric (TG) experiments were carried in order to investigate thoroughly the influence on the thermal stability and char-forming ability of these blends. Furthermore, Fire behaviour of prepared blends was assessed by the vertical flame spread and cone calorimetry tests. In addition to this, the morphology of char residues after cone calorimetry experiments was also observed by SEM.

4.1. Combination of laboratory grade lignin and ZnP

The following study discusses the development of flame retarded PA blends using LS and ZnP. All the materials were dried at 80 °C for 12 h before extrusion. Three different formulations were prepared with a total loading content of 20 wt%, ZnP being the major constituent, was varied from 10 to 15 and lignin from 5 to 10 wt%. Extrusion was performed according to temperature profile 170, 190, 200, 220 and 220 °C as described in Chapter 2. Dispersion of both fillers was evaluated by SEM analysis. Thermal decomposition, as well as evolved gases, were studied to understand the mechanism of FR. Flaming combustion and dripping behaviour were evaluated by the UL94 test. Cone calorimeter tests on plate samples were carried out to investigate heat release and smoke release parameters.

4.1.1. Dispersion analysis by SEM

After extrusion, the blends are fractured in liquid nitrogen and cross-section view observed to analyze the dispersion of additives as shown in Figure 4.1. SEM images of the ternary blends show the dispersion and distribution of lignin and ZnP into the PA matrix. It was observed that up to 20 wt% loading, LS and ZnP particles are homogeneously dispersed in the polymer matrix. Furthermore, SEM images show no aggregation. In addition, EDX spectra were recorded and identification of elements Phosphorus (P), Zinc (Zn), Sulphur (S) also confirms the dispersion of ZnP and LS particles in a polymer matrix (e.g., EDS spectrum of PA_{80}-LS_{10}-ZnP_{10} blend in Figure 4.2). The ZnP particles are distributed in the matrix. As far as lignin distribution is concerned, it was noticed from binary blends morphology that extrusion process not only makes uniform mixing but also reduces the particle size (up to 8 µm) from their original size (about 70 µm). It is anticipated that a homogeneous dispersion of LS and ZnP in the polymer matrix would improve the combustion behavior.

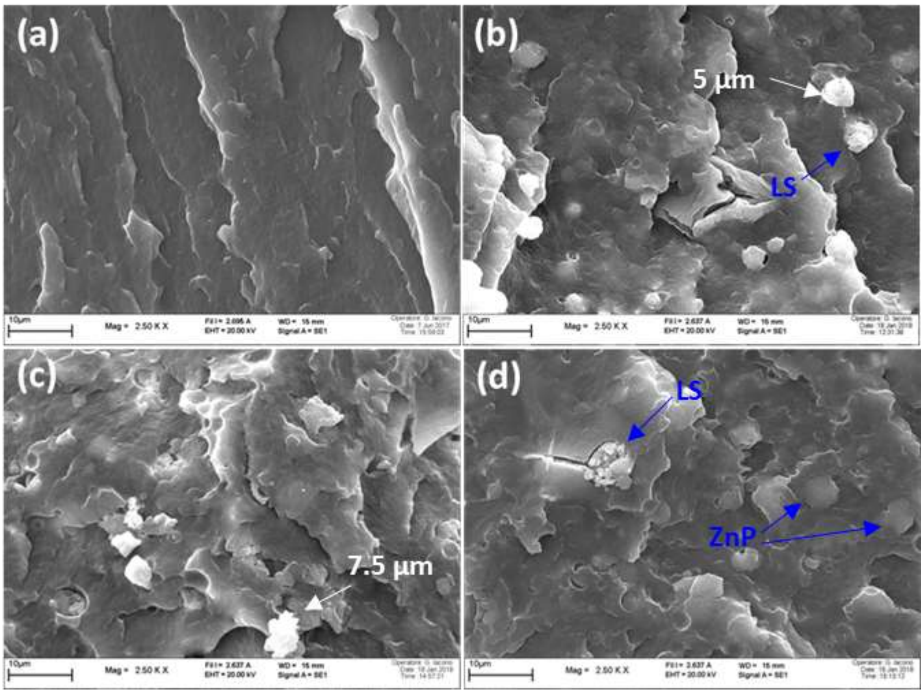

Figure 4.1. SEM morphology for PA, LL and ZnP combination (a) PA, (b) PA_{80}-LS_{10}-ZnP_{10}, (b) PA_{80}-LS_{7}-ZnP_{13}, (c) PA_{80}-LS_{5}-ZnP_{15} blends at 2500x magnifications.

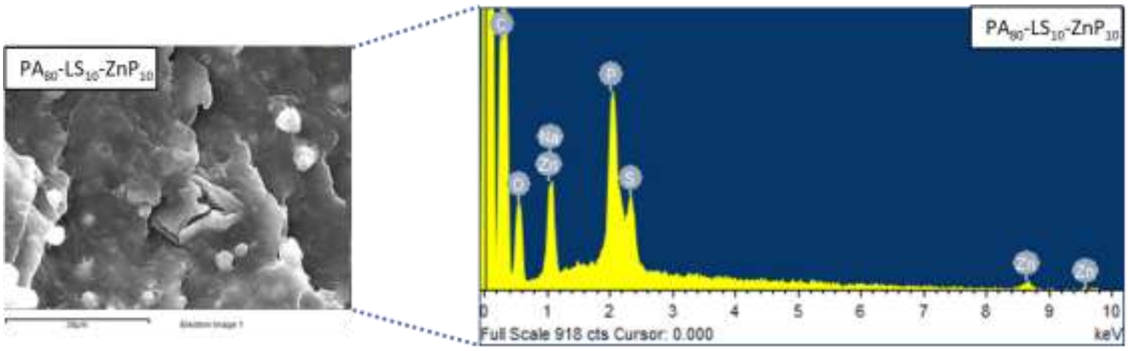

Figure 4.2. Identification of elements in EDS spectrum for PA_{80}-LS_{10}-ZnP_{10} blend.

4.1.2. Thermal decomposition analysis

TG and dTG curves of unfilled PA, its blends with ZnP and LS in nitrogen and air atmosphere, are shown in Figure 4.3. Under N_2 atmosphere, PA shows a single step with a maximum of mass loss rate (MMLR) and corresponding temperature at around 430 °C (T_{max}) without leaving the char residue at the end of the test. However, in air, PA decomposes in two steps; the first step is at around 452 °C (T_{max1}), leading to the formation of volatile compounds. The second step, at around 567 °C (T_{max2}), can be attributed to the further oxidation of hydrocarbon species with the evolution of CO and CO_2, giving rise to a continuous weight loss until 800 °C.

It is observed, as compared to unfilled PA, the binary blend of ZnP shows an increment in thermal stability ($T_{5\%,}$ and T_{max}). The char-forming ability in the PA_{80}-ZnP_{20} was practically negligible. This behavior indicates that as far as charring property is concerned, ZnP and PA interaction is not effective, which destabilizes the char residue. On the other hand, the LS introduction, increases the char formation in PA_{80}-LS_{20} blend, indicating the charring effect of lignin in the blend.

Conversely, the combination of LS and ZnP changes the degradation profile, for example, increasing the LS loading (5, 7 and 10 wt%, respectively) increases the T_{max} temperature; at the same time, the $T_{5\%}$ and MMLR values are decreased, thus favoring the development of an improved residue at the end of the test. Furthermore, the ternary blend containing 10 wt% of both filler LS (10 wt%) showed an increased experimental residue compared to the calculated one (9.3 wt%); the experimental residue is slightly higher (10.2 wt%), hence indicating the positive interaction with polymer matrix and within the additives, which stabilizes the char residue. Conversely, the lower residue value was noticed for the increasing loadings (13 and 15 wt%) of ZnP in the ternary blends: this finding is attributed to the non-charring characteristic of ZnP with PA.

As far as thermo-oxidative stability is concerned, the ternary blends show a comparable trend, with two decomposition steps: the first one is occurred due to the main degradation at around 480 °C (T_{max1}), with the evolution of volatile products. The second step at around 610 °C (T_{max2}) is attributed to further oxidation with the formation of CO and CO_2 (Herrera et al., 2001; Karstens and Rossbach, 1989). In conclusion, compared to the binary blends, the highest residue is reported for the ternary blends. It is expected, the presence of LS and ZnP favors the formation of a thermally stable char as compared to unfilled PA. The formation of a stable char residue is an indication of the interaction of LS and ZnP with PA.

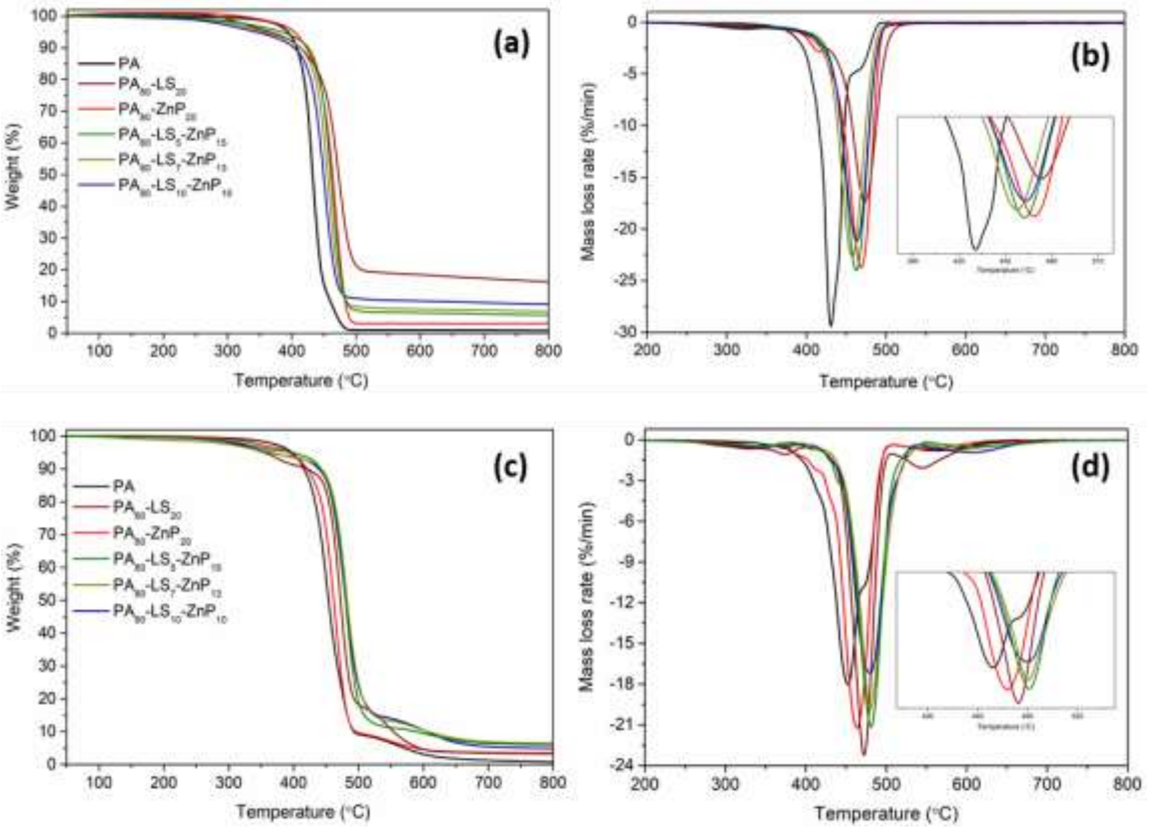

Figure 4.3. TG and dTG curves for PA and its blends in nitrogen and air atmosphere (10 °C/min).

4.1.3. Analysis of evolved gas

The identification of the decomposition gases, released during thermal decomposition, was studied using TGA coupled with FTIR (TG-FTIR). This technique allows to evaluate the chemical functional groups of evolving gas. The spectra of the whole decomposition process showing initial, main and final degradation stages presented in Figure 4.4. The identification of release products in FTIR spectra are reported in Table 4.1, which is related to the published scientific publications (Brebu and Vasile, 2010; Levchik et al., 1992; Naik et al., 2014; Socrates, 2001; Zhao et al., 2014). Unfilled PA starts a noticeable evolution of gaseous species after 390 °C, which corresponds to initial degradation ($T_{5\%}$) step; a gradual evolution of hydrocarbon species (2928, 2856, 1480 cm^{-1}), a weak peak of vinyl (1440, 990, 910 cm^{-1}) and

C=O (1704 cm^{-1}) are noticed. The evolution of vinyl group might be related to the scission of an amide bond. The main degradation occurs at 430 °C, with the evolution of nitrile (weak peak at 2233 cm^{-1}), $–CH_2–$ (2930, 2855, 1480 cm^{-1}), vinyl group (1440, 990, 910 cm^{-1}), and $–CO–NH_2–$ (1636 cm^{-1}) groups (Levchik et al., 1992). From this point, at around 490 °C, carbonyl and amide start to decrease, and only hydrocarbon peaks are detected.

Concerning pure ZnP, the progressive weight reduction begins after 420 °C, with the formation of phosphinate anion (765, 1058, 1145 cm^{-1}) and ethane (945 cm^{-1}) as primary decomposition products. At around 480 °C, through the main degradation step hydrocarbon (2930, 2855 cm^{-1}), phosphinic salt and phosphinic acid (low signals located at 3650, 1055, 1140 cm^{-1}) are detected. At around 520 °C, the generation of phosphinic acid reduced. Regarding pure LS, decomposition starts beyond 200 °C with the formation of volatiles assigned to the characteristic bands of CO_2 (2390, 2255, 666 cm^{-1}) and the weak peak of CH_4 around 3000 cm^{-1}. The production of CO_2 at the initial stage could be linked to the decarboxylation reaction and the cleavage of carboxyl, carbonyl, and carbonyl ester functionality present in the side chains of the phenylpropane units of lignin, whereas CH_4 release, might be because of demethylation of the methoxy groups. Then, during the main degradation at around 320 °C, showing the peaks of hydrocarbons and CO_2 along with other peaks such as phenolic (1496 cm^{-1}), carbonyl (1740 cm^{-1}), and CO (2125, 2000 cm^{-1}); thereafter, toward the end of T_{max}, at about 400 ºC, unlike that of CO_2, CO and hydrocarbon species, the formation of phenolic and carbonyl compounds reduces.

The binary blend of ZnP reveals the formation of the gaseous products analogous to that of ZnP: the only difference identifies with the lower peak intensity as a result of the low concentration of ZnP compared to the gases evolved from pure ZnP. Besides, the spectra of the released gases (PA_{80}-ZnP_{20}) do not show the presence (or not detectable) of signals attributable to phosphinic acid; as a consequence of the low ZnP content in the polymer, similar findings were also reported by Vannier et al. in PET matrix (Vannier et al., 2009). This remark may rationalize a partial decomposition of ZnP into the hydrocarbon, phosphinate salt and phosphinic acid (very small amounts). Similarly, the decomposition of PA_{80}-LS_{20} blend releases the gaseous products comparable to that of LS, though with a lower intensity.

The ternary blend PA_{80}-LS_{10}-ZnP_{10} exhibits initial degradation at around 330 °C (corresponding to $T_{5\%}$), with the generation of phosphinate anions at the starting (1145, 1058, 765 cm^{-1}); then, a weak presence of hydrocarbon species (2930 cm^{-1}) was also detected. When the temperature reaches at about 390 °C, hydrocarbon species release increases, and some other characteristic peaks are identified, attributed to carbonyl (1691 cm^{-1}), and CO_2 (2340, 2240 cm^{-1}). The formation of these compounds increases at the main decomposition temperature (corresponding to 470 °C) and above (at 530 °C); only the CO_2 peak decreases. Phenolic compounds peaks were not detected in ternary blends as it was identified in LS spectrum.

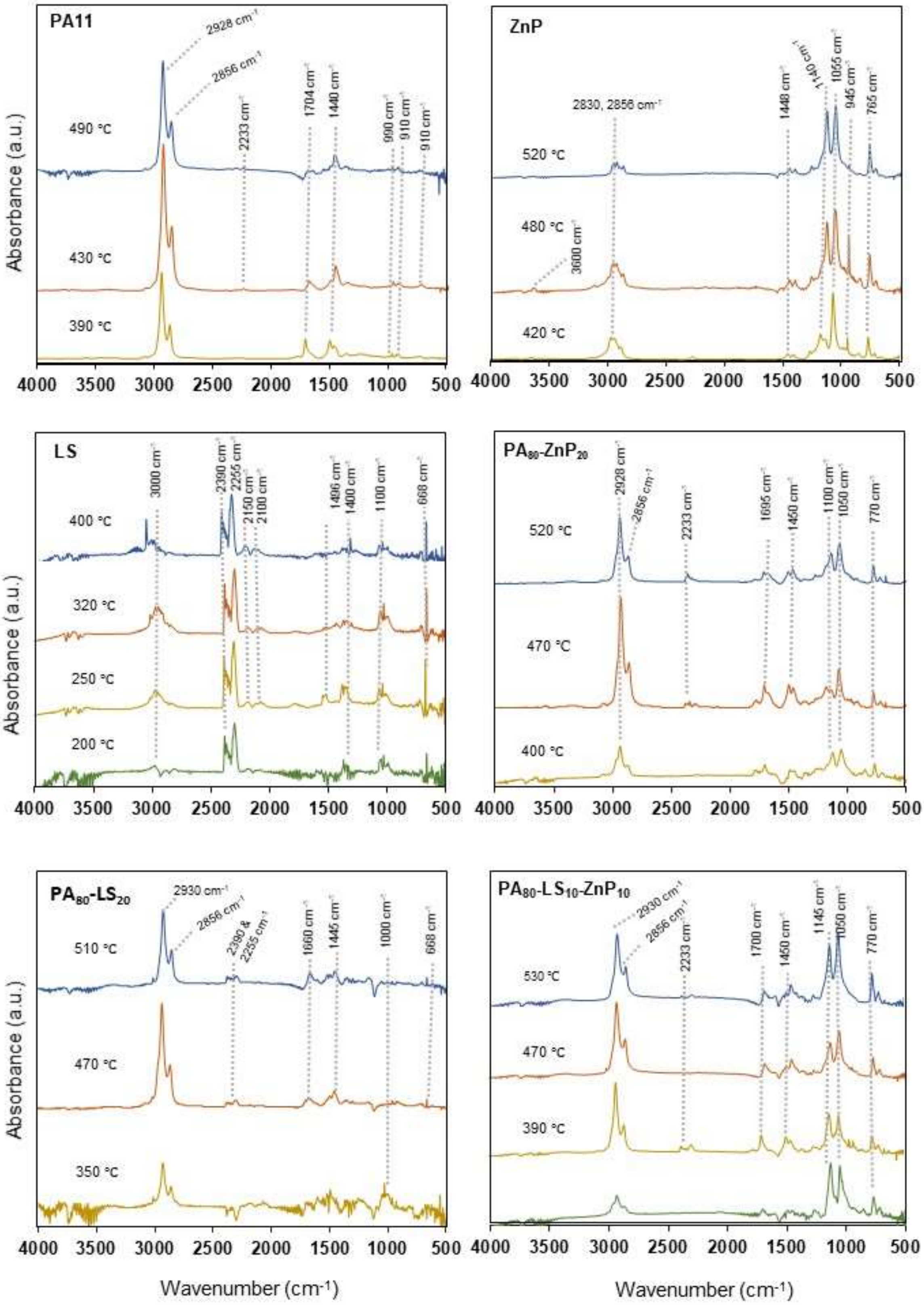

Figure 4.4. Characteristic spectra of evolved gaseous products during thermal decomposition of the neat products and PA blends (heating rate 10 °C/min in nitrogen).

Table 4.1. Main decomposition products and characteristic peak position observed during analysis.

Decomposition product	**Functional group**	**Characteristic band (cm^{-1})**
Polyamide 11		
Hydrocarbon species ($R-CH_2-CH_3$)	C–H	2928. 2856, 1480
Carbonyl compound	C=O	1704
Alkyl vinyl ($R-CH=CH_2$)	Vinyl cis-substitution	1440, 990, 910
Alkyl nitrile	–C≡N	2233
Amide compound	($–CO-NH_2–$)	1636
Neat ZnP & PA_{80}-ZnP_{20}		
Phosphinate compound	P=O, P–O	765, 1058, 1145
Phosphinic acid from neat ZnP	P–OH, P=O, P–O	3650, 1055, 1140
Ethane	C–H, C–C	2958, 2856, 945
Neat LS & PA_{80}-LS_{20}		
Methane	C–H	3000
Carbon dioxide	O=C=O	2390, 2255, 668
Carbon monoxide	CO	2125, 2000
Phenolic from neat LS	OH, C=C, C–O	3600, 1496, 1100
Methoxyl	C–H, C–O	3000, 1100
PA_{80}-LS_{10}-ZnP_{10}		
Phosphinate compound	P=O, P–O	1145, 1058, 765
Hydrocarbon species	C–H	2930, 2850
Carbonyl compound	C=O	1690
Carbon dioxide	O=C=O	2390, 2255

Evolved gas analysis of ternary blend reveals the decomposition of PA-LS-ZnP blends is mainly governed by the formation of hydrocarbons, carbonyls and phenolic compounds (small amount) along with phosphinate and CO_2. Organic compounds are combustible and could contribute to feed the flame. This finding can be confirmed by flaming combustion behaviour during flammability test. In ternary blends, ZnP mainly release phosphinate ions and hydrocarbons in the gas phase and transformed into thermally stable phosphate compound in the condensed phase.

Conclusion about thermal decomposition analysis

TG analysis revealed that the combination of LS and ZnP increased the thermal stability by shifting T_{max} to higher temperature region. The presence of LS allowed to decrease $T_{5\%}$ temperature by 55 °C due to the LS degradation occurring at lower temperature region, and a considerable amount of char residue was obtained at the end of the test. Amount of char residue increases with increasing lignin content in the blend. Furthermore, evolved gas analysis of ternary blend showed the decomposition of PA-LS-ZnP blends is mainly governed by the formation of hydrocarbon, carbonyls along with phosphinate compounds and CO_2. Phenolic compounds were also identified in neat material; however, they were not detectable in ternary blends. Meanwhile, in the condensed phase an aromatic charred layer is formed because of the presence of LS and phosphate compounds are formed due to the presence of ZnP. Evolution of organic compounds in the gas phase may affect the flaming combustion; at the same time, aromatic char layer formation in the condensed phase can contribute to improve fire retardant properties.

4.1.4. UL94 vertical flame spread test

Flammability behaviour of blends was investigated by UL94 vertical flame test, and the results for PA and its blends are collected in

Table 4.2. It was found that the PA_{80}-LS_{20} blend increases the total burning time due to the fact that the LS decomposition that occurs at a lower temperature as compared to PA determines high flammability thus the sample cannot be classified by the UL94 test. Conversely, as compared to PA, the binary blend of ZnP (i.e., PA_{80}-ZnP_{20}) shows a slight improvement in total combustion time but no improvement in flammability rating. As far as dripping is concerned, it was noticed that PA_{80}-ZnP_{20} specimens show slightly lower dripping compared to that of unfilled PA. However, the most enhanced results were obtained with the ternary blends, explicitly referring to PA_{80}-LS_{10}-ZnP_{10} blend, which achieves self-extinction

(V-1 rating). It is noteworthy that this blend shows the minimum ZnP loading. In fact, high ZnP loadings in blends deteriorate the flammability performances of the systems, as ZnP endorses the melt dripping phenomena, burning the cotton located beneath the specimen. Based on visual observation, it was noted that in the second flame application dripping is progressively dominant because of the softening of ZnP during combustion of the material that leads to higher dripping. Concerning the flame-retardant action, gas release analysis in the above section revealed that ZnP decomposition generates phosphinate compounds in the gas phase that can release $P-O^{\bullet}$ radicals: this latter can act as radical scavengers and lead to flame inhibition, hence improving the flame retardancy of blends. These results demonstrate that the proposed LS/ZnP combinations are effective.

Table 4.2. UL94 vertical flame test for PA and its blends with LS and ZnP.

Sample	1st Combustion t_1 (s)	2nd Combustion t_2 (s)	Total Combustion t_1+t_2 (s)	Cotton ignition	Dripping	Rating
PA	13 ± 1	11 ± 2	24 ± 1	Yes	Yes	V-2
PA_{80}-LS_{20}	27 ± 5	57 ± 18	85 ± 15	Yes	Yes	NC
PA_{80}-ZnP_{20}	7 ± 1	4 ± 1	11 ± 1	Yes	Yes	V-2
PA_{80}-LS_{10}-ZnP_{10}	5 ± 1	4 ± 1	9 ± 1	No	Yes	V-1
PA_{80}-LS_7-ZnP_{13}	8 ± 1	3 ± 1	11 ± 1	Yes	Yes	V-2
PA_{80}-LS_5-ZnP_{15}	11 ± 1	5 ± 1	16 ± 1	Yes	Yes	V-2

4.1.5. Analysis of fire properties

Cone calorimeter tests (forced combustion) at 35 kW/m^2 were carried out on plate samples in order to analyse the fire-retardant properties. The heat release rate (HRR) and total heat release (THR) are key parameters to assess the fire behavior of material applied to certain heat flux (Mouritz et al., 2006; Schartel and Hull, 2007). Besides heat release parameters, the smoke released in the course of the combustion of material is also important; total smoke release

(TSR) is one of the key parameters for investigating the smoke formation during a fire. Mostly, carbon monoxide (CO) is a common toxicant resulting from the combustion of any organic substance; hence, the formation of CO and CO_2 was also investigated to understand the combustion behaviour of flame retarded blends.

4.1.5.1. Forced combustion test: Heat release parameter

The cone calorimetry data are collected in Table 4.3. Figure 4.5 (a-b) shows the influence of LS and ZnP on HRR and THR. The binary blend (PA_{80}-LS_{20}) significantly decreases both HRR and PHRR (-49%) and facilitate the high char formation at the end of the experiment. It was noticed that the charring ability of LS significantly reduces both HRR and THR. Conversely, in the binary blend (PA_{80}-ZnP_{20}), the ZnP introduction does not show any significant reduction in the forced combustion behavior; besides, the HRR curve shows non-charring appearance. Compared to PA, the addition of ZnP produce higher smoke (TSR, 1430 m^2/m^2) indicated in Table 4.4.The ternary blends containing LS and ZnP showed lower ignition time as compared to PA: this finding might be attributed to the presence of LS. When the lignin content is higher (10 wt%), PHRR and THR values of ternary blend (PA_{80}-LS_{10}-ZnP_{10}) significantly dropped about – 50% and – 15%, respectively, and a noticeable amount of residue is collected after the test. It is expected, the formation of phosphate compounds from ZnP also provide stability to char residue. However, when the LS content reduced to 7 and 5 wt%, the PHRR and other fire parameters decreased (Table 4.3). This behaviour indicates the main mode of action of these blends is based on the formation of char in the condensed phase. The HRR curves of ternary blends reveal a single peak of HRR, hence representing the formation of an effective protective char layer.

The average rate of heat emission (AHRE) curves are shown in Figure 4.5 (c). This parameter is defined as the cumulative heat emission divided by the time, and its maximum (MAHRE) value is considered as a good measure of the propensity for fire development in a real scenario (Duggan et al., 2004). The ternary blends show a noticeable reduction (of about 65%) in MARHE values as compared to unfilled PA, while, a small reduction (within 20 and 24%) is noticed with the binary blends. Furthermore, effective heat of combustion (EHC) is another parameter, which can verify the FR action of blends with respect to neat PA. A higher value of EHC of PA proves more complete combustion of volatiles. However, EHC values of blends containing ZnP are lower, hence evidencing that the flame inhibition occurs with the incomplete combustion, thus increasing the smoke and the CO release (Table 4.4) in the gas phase.

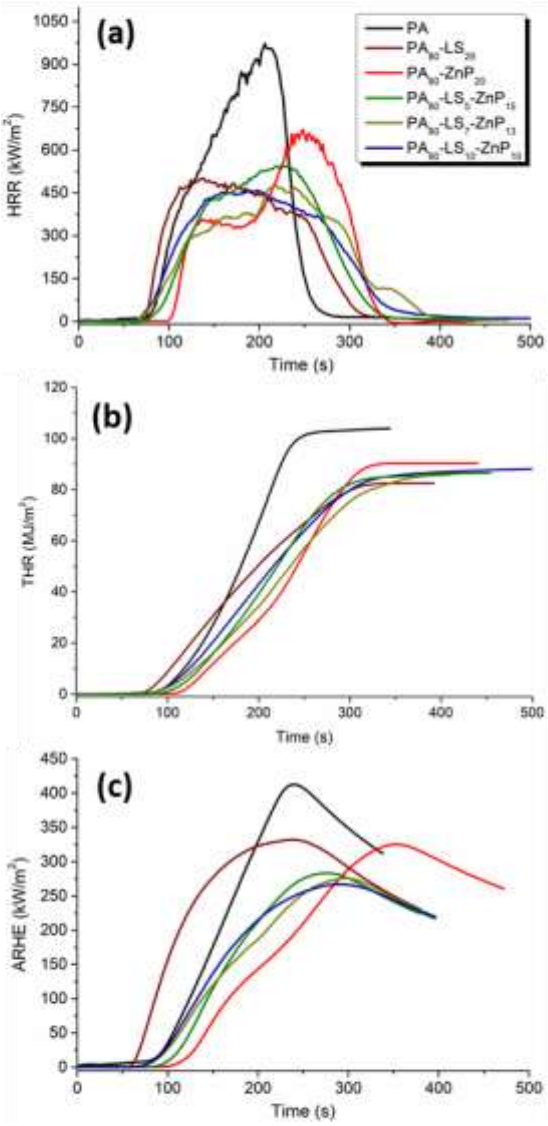

Figure 4.5. Different heat release curves for PA and its blends during cone calorimeter tests at a heat flux of 35 kW/m^2: (a) heat release rate, (b) total heat release, (c) average rate of heat emission.

In order to compare the char residue developed during combustion test the mass loss curves of PA blends are shown in Figure 4.6, and the residue amount at the end of the test is collected in Table 4.3. It is accepted from the scientific community that combustion is likely to occur mostly in the anaerobic environment between ignition and flame out stages. Consequently, the residue at the end of combustion is comparable with that obtained from TGA in nitrogen at that temperature (Verdolotti et al., 2016). The amounts of final residues obtained from cone calorimetry tests for binary and ternary blends indicate a similar trend with respect to those obtained from TGA in the nitrogen (Figure 4.3). The char residue in ternary blends subject to the LS loading in the blends; as a consequence, PA_{80}-LS_{10}-Zn_{10} shows the highest char formation among the ternary blends. Furthermore, the low HRR and PHRR values indicate that PA_{80}-LS_{10}-Zn_{10} can reduce the release of flammable and non-flammable gases through the polymer: thus, flame retardant properties are enhanced.

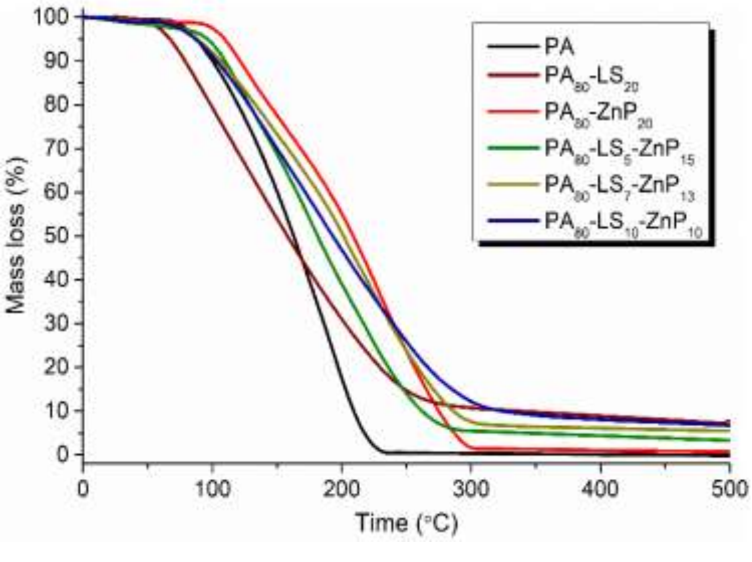

Figure 4.6. Mass loss curves from the combustion test.

Table 4.3. Cone calorimetry data for PA and its blends.

Sample	TTI (s)	PHRR (kW/m^2)	Δ (%)	MARHE (kW/m^2)	Δ (%)	THR (MJ/m^2)	EHC (MJ/kg)	Residue (%)
PA	70 ± 6	980 ± 1	–	413 ± 10	–	105 ± 2	36.4 ± 0.1	0.5 ± 0.1
PA$_{80}$-LS$_{20}$	52 ± 3	502 ± 34	– 49	308 ± 14	– 25	83 ± 1	31.2 ± 0.5	8.8 ± 0.3
PA$_{80}$-ZnP$_{20}$	94 ± 4	671 ± 8	– 31	337 ± 18	– 18	90 ± 3	29.9 ± 0.8	1.4 ± 0.8
PA$_{80}$-LS$_{10}$-ZnP$_{10}$	58 ± 4	486 ± 38	– 50	267 ± 3	– 35	89 ± 3	30.8 ± 0.2	7.0 ± 0.3
PA$_{80}$-LS$_{7}$-ZnP$_{13}$	57 ± 6	554 ± 54	– 43	277 ± 3	– 33	87 ± 3	29.3 ± 1.1	6.0 ± 0.9
PA$_{80}$-LS$_{5}$-ZnP$_{15}$	65 ± 2	587 ± 36	– 40	275 ± 7	– 33	86 ± 1	29.1 ± 0.6	4.8 ± 0.4

4.1.5.2. Forced combustion test: Smoke release parameters

The smoke production during the combustion of material is also considered a very critical parameter during a fire; average specific extinction area (ASEA) and total smoke production (TSR) are discussed in this section. The evolution of CO and CO$_2$ was also investigated (Figure 4.7) to understand the combustion behavior of PA blends, and the corresponding data are collected in Table 4.4. In binary blends, ASEA and TSR values increase with the addition of 20 wt% ZnP as compared with those of pure PA, while, no practical difference is noticed with the same loading of LS. Consequently, the introduction of ZnP reduces the CO$_2$ release and its peak; at the same time, the CO release increases in comparison with unfilled PA (Figure 4.7 (b-c)), referring the incomplete oxidation of gaseous species: causing the formation of more CO gas. Conversely, in the PA$_{80}$-LS$_{20}$ blend, the low peak value of CO refers to the lower CO evolution during the combustion, also confirming the extended oxidation of the evolved gaseous products.

On the other hand, ternary blends of LS and ZnP show a significant increase in ASEA and TSR: this finding can be attributed to the lower amount of ZnP in the blends, which is inadequate to exert a fuel dilution effect, and hence, ZnP is not capable of generating sufficient phosphinic acid. Another reason could be that more gaseous products with incomplete oxidation are released. Furthermore, the evolution peak of CO increases with increasing the loading of ZnP in the ternary blends. The maximum CO release is found for PA_{80}-LS_5-ZnP_{15}, due to the higher ZnP loading. Interestingly, the PA_{80}-LS_{10}-ZnP_{10} shows the lowest CO yield with respect to other ternary blends: this finding may be attributed to the interactions taking place between LS and ZnP in the ternary blend containing 10 wt% of both fillers, which lead to extended oxidation of the evolved gaseous products. Based on results, it can be concluded that a higher loading of ZnP generates a higher amount of CO and promotes smoke toxicity to some extent.

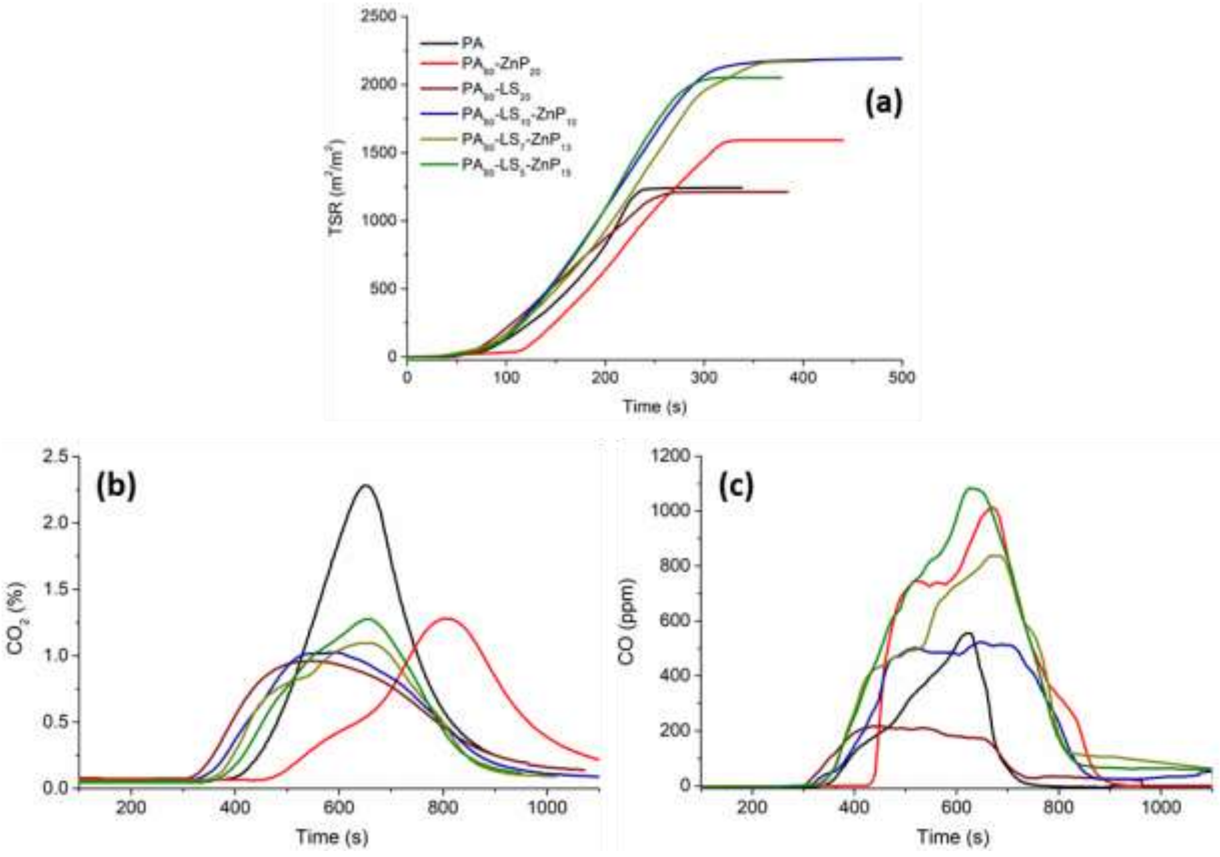

Figure 4.7. TSR (a), CO (b), and CO_2 (c) evolution during combustion for PA and its blends.

Table 4.4. Smoke parameters data during combustion for PA and its blends.

Sample	TSR (m^2/m^2)	Δ (%)	ASEA (m^2/kg)	Δ (%)	CO yield (g/kg)	CO_2 yield (kg/kg)
PA	1192 ± 23	–	411 ± 3	–	33 ± 1	2.6 ± 0.1
PA_{80}-LS_{20}	1201 ± 3	+ 1	444 ± 1	+ 7	30 ± 1	2.3 ± 0.1
PA_{80}-ZnP_{20}	1430 ± 20	+ 17	517 ± 2	+ 21	91 ± 2	1.8 ± 0.1
PA_{80}-LS_{10}-ZnP_{10}	2239 ± 45	+ 47	770 ± 1	+ 47	80 ± 1	2.1 ±0.1
PA_{80}-LS_7-ZnP_{13}	2178 ± 59	+ 45	734 ± 9	+ 44	88 ± 2	1.9 ±0.1
PA_{80}-LS_5-ZnP_{15}	2036 ± 12	+ 42	681 ± 9	+ 40	105 ± 4	1.9 ± 0.1

4.1.6. Char Residue analysis

4.1.6.1. Residue morphology

Digital pictures of the residues obtained after combustion test are shown in Figure 4.8. In particular, PA alone and ZnP with PA did not show any noticeable char formation. However, the PA_{80}-LS_{20} blend shows a significant amount of char formation but the surface was fragile. Besides, in the ternary blend, a compact char is observed for PA_{80}-LS_{10}-Zn_{10}, which effectively reduced the PHRR and other fire parameters. In addition to this, the pictures of PA_{80}-LS_7-Zn_{13} and PA_{80}-LS_5-Zn_{15} samples exhibit a loose and porous structure with some cracks on the surface. The formation of unstable char layer from these blends decreased the fire performance parameters than PA_{80}-LS_{10}-Zn_{10} blend. Hence, it is assumed that the formation of char layer is primarily responsible for improving the fire-retardant properties. Furthermore, the cross-section view of char residue SEM images (Figure 4.9) shows the formation of a complex sandwich-type structure, which is not comparable to the classical intumescent structure. The outer layer of the sandwich structure shows a rough and irregular surface; the middle layer is compact and thick, acting like a protective layer, providing a flame barrier for the underlying polymeric material, while the bottom layer is quite furry. To elucidate this behaviour and the formation of different layers further analyses are required.

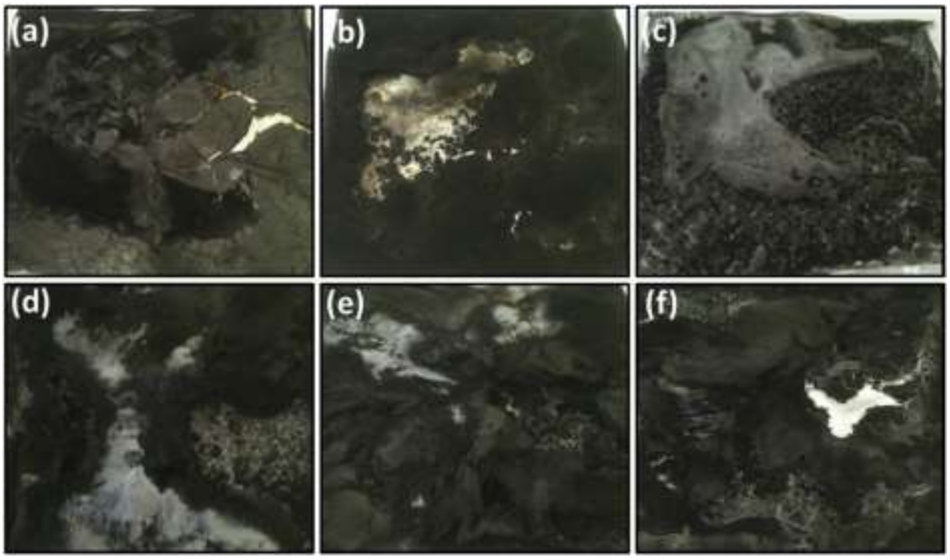

Figure 4.8. Pictures of char residues collected at the end of cone calorimetry test: (a) unfilled PA, (b) PA_{80}-ZnP_{20}, (c) PA_{80}-LS_{20}, (d) PA_{80}-LS_{10}-ZnP_{10}, (e) PA_{80}-LS_{7}-ZnP_{13} and (f) PA_{80}-LS_{5}-ZnP_{15}.

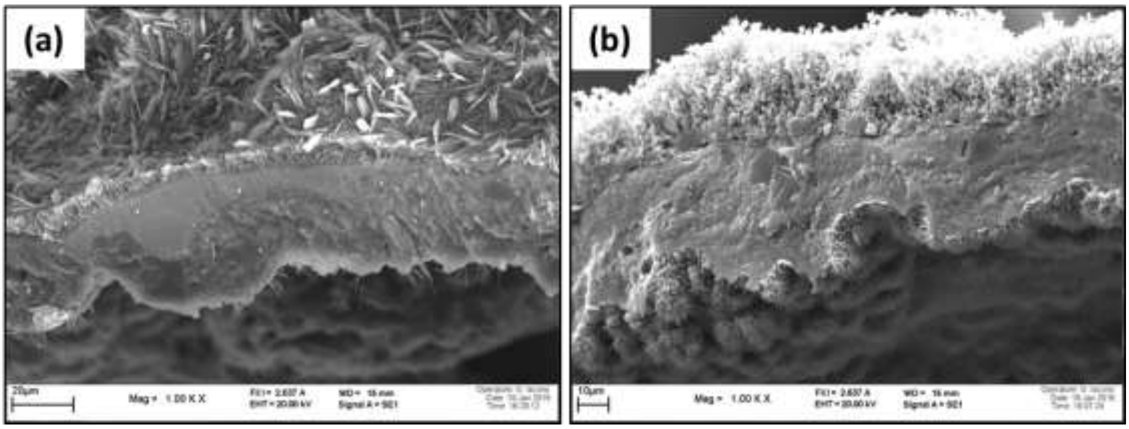

Figure 4.9. Cross-section SEM images of residue blends: (a) PA_{80}-LS_{10}-ZnP_{10}, (b) PA_{80}-LS_{20}.

4.1.6.2. Residue FTIR

The residue obtained from TG analysis in nitrogen was collected for chemical identification by FTIR analysis. Therefore, it was conceivable to comprehend the condensed phase action mechanism of LS and ZnP in PA. Figure 4.10 shows the FTIR spectra of residue from binary and ternary blends. The spectrum of the PA_{80}-LS_{20} blend residue displays the band identified at 3700 – 3400 cm^{-1} assigned to stretching vibration of -OH, along with an absorption band at 1610 cm^{-1} indicating the formation of conjugated unsaturated carbon structure of polyaromatic carbonaceous species; besides, the weak absorption band at 2950-2850 cm^{-1} and the hydrocarbon (C-H) peak at 1450 cm^{-1} also confirm the presence of -CH_2- group representing aliphatic char structure. The two peaks at around 1100 and 860 cm^{-1} are owing to out-plane and in-plane bending vibration of phenolic hydrogen; it is reasonable to assume that, the C-O stretching at 1100 cm^{-1} overlaps with C-H out of plane stretching. In fact, the absorptions peaks revealed that the PA_{80}-LS_{20} blend provides either aromatic or aliphatic char structure. The spectrum of PA_{80}-ZnP_{20} blend residue indicates hydrocarbon peaks (2950, 2830, 1440 cm^{-1}). The absorption peaks in the range of types of phosphoryl groups (1370-1050 cm^{-1}) show P–O and P=O bonds, which indicate the phosphate group formation; in addition, the signal situated at 778 cm^{-1} might be ascribed to zinc phosphate ester bond [8,29].

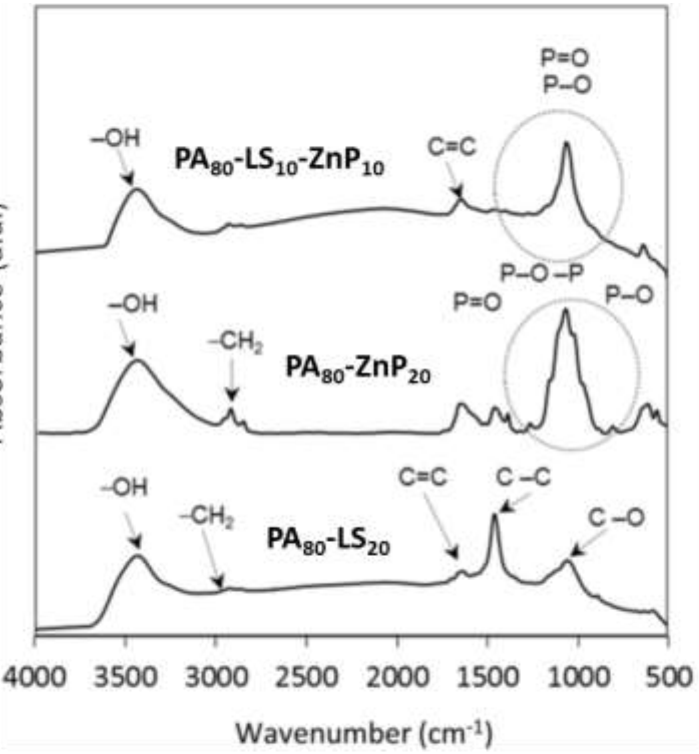

Figure 4.10. FTIR spectra with characteristic peaks from the residue of PA blends.

On the other hand, the ternary blend with 10 wt% concentration of both additives shows a spectrum including the signals associated with the PA_{80}-ZnP_{20} and PA_{80}-LS_{20} blends. In the same line, the peak located at 1610 cm^{-1} is comparable to that of PA_{80}-LS_{20} blend. Hence, it can be attributed to aromatic char structure. Similarly, the absorption peaks between 1370 and

1050 cm^{-1} can be ascribed to the presence of ZnP, and their intensities are correlated to the lower ZnP content in the ternary blend. This finding indicates that the condensed phase of the ternary blend contains polyaromatic char layer and phosphate moieties.

4.1.7. Conclusion

In order to explore the valorization of lignin, a primary study of flame retarded blend development with laboratory grade lignin and FR was important to have an understanding of lignin and FR synergy and optimal ratio to achieve high fire retardant properties. For this study, LS was combined with ZnP, and various FR formulations by varying the contents of the additive were prepared and investigated. SEM analyses of the blends showed that the addition of lignin and phosphinates up to 20 wt% showed homogenous dispersion of fillers in the polymer phase. TG analyses showed the incorporation of lignin in the ternary blends increased the thermal stability of PA, promoting the obtainment of a stable char residue at the end of the experiments. Furthermore, the study of evolved gas performed on PA_{80}-LS_{10}-ZnP_{10} blend showed that the ternary blends mainly produces phosphinate ion and hydrocarbons along with the small amount of phosphinic acid during the main degradation stage; though, phosphinic acid was not detectable in the blends. While hydrocarbons and phenolic compounds along with CO and CO_2 are released in the gas phase. In the meantime, the condensed phase developed an aromatic char layer owing to the presence of LS; phosphate compounds are formed because of the presence of ZnP. Flammability test (UL 94 vertical flame spread) showed the combination of LS and ZnP reducing the combustion time: the most desirable flammability properties were achieved with 10 wt% loading of both the additives in the ternary blends. Furthermore, cone calorimetry tests showed the interactions between LS and ZnP promoted a significant reduction of PHRR (around –50%), THR (about –13%) and MARHE (about –35%). This finding was attributed to the formation of a protective char layer. Regarding the smoke parameters, TSR and SEA values were very high for all the ternary blends due to the presence of ZnP. However, increasing the lignin loading effectively reduced the CO and CO_2/CO yield compared to PA. The morphology of char residue showed that the formation of compact char layer is primarily responsible for the improved flame-retardant properties.

4.2. Combination of industrial lignins and phosphinates FR

The study conducted in the previous part showed the presence of lignin with ZnP significantly improve fire retardant properties of PA blends due to the formation of stable char layer in the condensed phase. The following study conducted to develop flame retarded blends using industrial lignin with phosphinate FR. Industrial lignins (i.e., LL and DL) studied in Chapter 3 were combined with ZnP or AlP to develop flame retarded blends. For the systematic understanding, various FR formulations by varying the FR loading are prepared and investigated. Dispersion of additives in the polymer phase was analyzed by SEM analysis. Thermogravimetric (TG) experiments were carried in order to thoroughly study the influence on the thermal stability and char-forming ability of these blends. Furthermore, Fire behaviour of prepared blends was assessed by the vertical flame spread and cone calorimetry tests.

4.2.1. Dispersion analysis by SEM

The final properties of blends, such as the mechanical and FR performance, depend on the quality of dispersion of fillers in the polymer matrix (Song et al., 2011). SEM micrographs of unfilled PA, binary blends and the ternary blends containing 10 wt% loading of both additives are shown in Figure 4.11 (a-f). In order to further assess the dispersion, EDX spectra are recorded (Figure 4.12) for the ternary blends. As mentioned in Chapter 3, the dispersion of LL and DL was homogenous without any aggregation phenomenon, except LL shows more rougher surface due to a larger particle size than DL. Though, small particles (< 10 µm) of lignin are observed on the surface attributed to a higher concentration of lignin in the blend. As far as dispersion of FR in the binary and ternary blends is concerned, the ZnP blends show a homogenous dispersion where ZnP is evenly distributed in the entire polymer phase. Besides, the ZnP particles (about 5-6 µm) are embedded in the matrix: this morphology was observed due to the broad range of size distribution in the pristine ZnP (30 – 200 µm). It is observed that blends containing ZnP show circular cavity, which can be ascribed to a fusible characteristic of ZnP (Sicken et al., 2004). EDX spectra of ternary blends also confirm the identification of Carbon (C), Oxygen (O), Zinc (Zn) and Phosphorus in blends. This technique gives the qualitative evidence of dispersion and distribution level of elements. Conversely, AlP dispersion in the blends shows that the distribution of particles is not homogenous, as micro agglomeration (about 10 µm) are observed in the polymer matrix (Figure 4.11 (i)). This behaviour may affect the mechanical properties and the mobility of molecular chains of polymer. EDX analysis confirms the dispersion of AlP in the polymer matrix. Carbon (C), Oxygen (O), Aluminium (Al) and Phosphorus (P) elements were mainly detected and confirmed the presence of AlP within the polymer matrix.

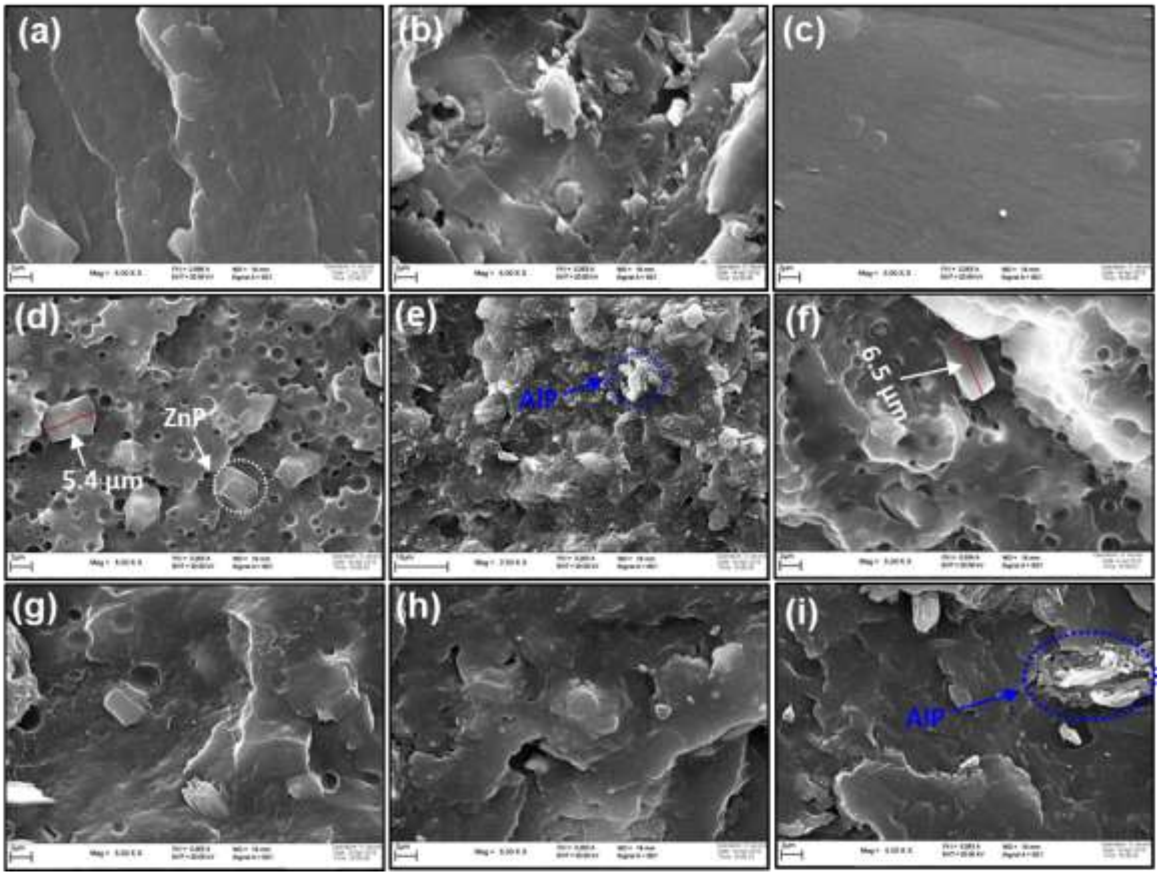

Figure 4.11. SEM morphology for PA in combination with lignin and ZnP (a) PA, (b) PA_{80}-LL_{20}, (c) PA_{80}-DL_{20}, (d) PA_{80}-ZnP_{20} (e) PA_{80}-AlP_{20} (f) PA_{80}-DL_{10}-ZnP_{10} (g) PA_{80}-LL_{10}-ZnP_{10} (h) PA_{80}-DL_{10}-AlP_{10} (i) PA_{80}-LL_{10}-AlP_{10} blends at 5000x magnifications.

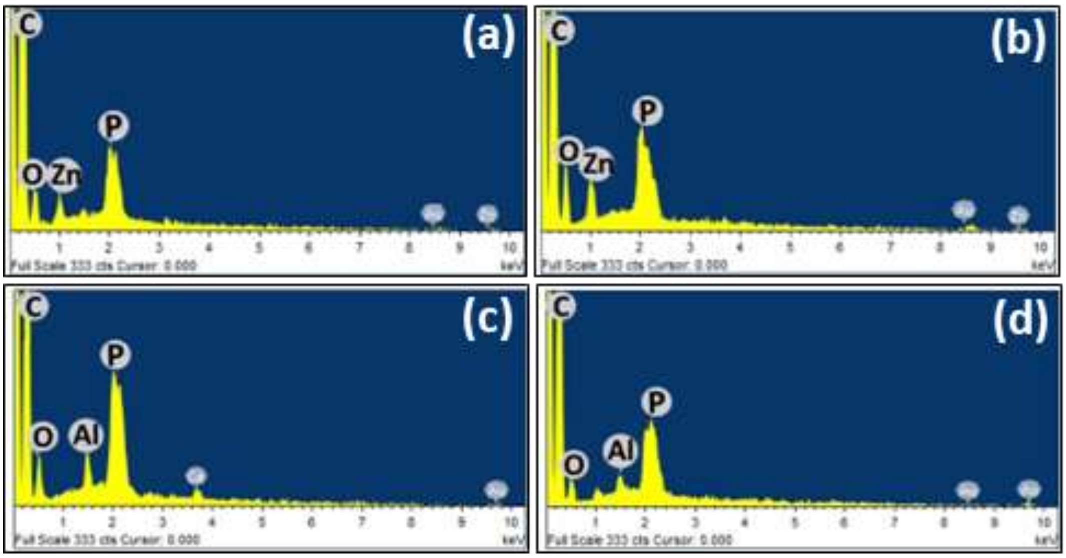

Figure 4.12. EDX spectra for ternary blends containing 10 wt% loading of both fillers, (a) PA_{80}-DL_{10}-ZnP_{10}, (b) PA_{80}-DL_{10}-AlP_{10}, (c) PA_{80}-LL_{10}-ZnP_{10}, (d) PA_{80}-LL_{10}-AlP_{10}

4.2.2. Mechanical properties

The influence of the incorporation of lignin and FR on mechanical properties was studied by tensile tests. Experiments were carried out with dumbbell-shaped plate specimens using INSTRON tensile testing machine (model 5967) as described in Chapter 2. Tensile properties, i.e., tensile strength, modulus and elongation at break were determined for PA and its blends, results are collected in Table 4.5. As observed before the nature of different FR and their particle size affect the dispersion and distribution in the polymer matrix. Tensile strength and modulus measured for PA was 61.5 and 470 MPa, respectively, with high elongation around 566 MPa. Concerning the tensile properties of binary blends, the addition of LL resulted in a decrease in the elongation and tensile strength with respect to unfilled PA. This reduction in tensile properties is attributed to the infusibility of LL in polymer matrix; hence, a higher modulus is observed. The PA_{80}-DL_{20} blend improves the tensile strength due to the uniform distribution of DL in PA matrix that provided better stress transfer from the matrix to DL, but the elongation was very low about 15 % compared to PA. Unlike PA_{80}-DL_{20} blend, the introduction of ZnP considerably increases the elongation; at the same time lower the modulus, which is attributed to the interaction between fusible ZnP and polymer matrix. Besides, the addition of AlP reduces the tensile strength and elongation due to poor stress transferred between FR and polymer. This behaviour is attributed to the uneven distribution and agglomeration of AlP and its infusible characteristic.

Table 4.5. Tensile properties of PA and its blends.

sample	Tensile strength at break (MPa)	Elongation at break (%)	Modulus
PA	61.5 ± 1	566 ± 51	470 ± 2
PA$_{80}$-DL$_{20}$	59.7 ± 2	15 ± 2	554 ± 11
PA$_{80}$-LL$_{20}$	56.2 ± 4	14 ± 2	609 ± 10
PA$_{80}$-ZnP$_{20}$	54.3 ± 4	498 ± 109	419 ± 7
PA$_{80}$-AlP$_{20}$	45.6 ± 1	286 ± 5	459 ± 65
PA$_{80}$-LL$_{5}$-ZnP$_{15}$	51.9 ± 1	450 ± 22	411 ± 18
PA$_{80}$-LL$_{7}$-ZnP$_{13}$	53.9 ± 4	403 ± 84	380 ± 13
PA$_{80}$-LL$_{10}$-ZnP$_{10}$	54.3 ± 4	370 ± 106	441 ± 27
PA$_{80}$-DL$_{5}$-ZnP$_{15}$	69.9 ± 7	678 ± 65	435 ± 26
PA$_{80}$-DL$_{7}$-ZnP$_{13}$	60.5 ± 4	543 ± 129	412 ± 25
PA$_{80}$-DL$_{10}$-ZnP$_{10}$	59.7 ± 3	467 ± 82	468 ± 20
PA$_{80}$-LL$_{5}$-AlP$_{15}$	48.5 ± 1	34 ± 4	481 ± 56
PA$_{80}$-LL$_{7}$-AlP$_{13}$	48.1 ± 1	16 ± 7	519 ± 36
PA$_{80}$-LL$_{10}$-AlP$_{10}$	47.1 ± 4	14 ± 1	607 ± 46
PA$_{80}$-DL$_{5}$-AlP$_{15}$	50.3 ± 1	266 ± 39	543 ± 57
PA$_{80}$-DL$_{7}$-AlP$_{13}$	50.9 ± 1	15 ± 1	463 ± 31
PA$_{80}$-DL$_{10}$-AlP$_{10}$	55.5 ± 1	14 ±1	600 ± 15

Regarding the tensile properties of ternary blends, the combination of DL and ZnP significantly increases the elongation at break, the increment was proportional to the ZnP content in the blends. However, increasing the DL content reduces elongation but still high compared to other ternary blends. Presence of DL also provides better stress transfer between additive and polymer; as a consequence, tensile strength of ternary blends increases. Besides, ZnP and LL containing ternary blends show lower tensile strength and elongation compared to PA-DL-ZnP blends. This can be attributed to the dispersion of LL in PA matrix, stemming to a larger particle size of LL (67 µm) than DL (39 µm) in the original material. As a result, increasing LL content decreases the tensile strength and elongation at break. The lower elastic region is also indicated by low values of modulus.

On the other hand, a combination of AlP with lignin (DL/LL) significantly reduces the tensile strength and the elongation at break, decrease in the tensile properties was proportionate to the AlP content in the blend. This finding was ascribed to the nonhomogeneous distribution of AlP particle in PA matrix. Furthermore, the combination of AlP and LL worsen the tensile properties. Moreover, higher modulus observed for these blends showing stiffness of the blends.

In conclusion, blends showing the high tensile strength and elongation, increase the ductility of the blends. Conversely, the lower value of elongation and tensile strength increases the stiffness of blends which is also indicated by a higher elastic region with a high value of modulus. These behaviours may strongly influence the melt spinning process.

4.2.3. Thermal decomposition analysis

The thermal and thermo-oxidative stability of the ternary blends was assessed by TG analyses in N_2 and air atmosphere with a heating rate of 10 °C/min from 50 to 800 °C. Thermal degradation behaviour and various parameters are discussed.

4.2.3.1. Thermal decomposition of ZnP and lignin blends

Thermo-oxidative degradation profiles of blends containing industrial lignin and ZnP are shown in Figure 4.13 and Figure 4.14. In nitrogen, the presence of LL or DL in binary blends initiate the degradation (i.e., lowering 5 wt% loss) at 285 and 341 °C, respectively. As compare to PA, significant reduction of $T_{5\%}$ temparature in LL blends was attributed to the decomposition of LL subunits and evolution of less thermal stable compounds, e.g., hydrocarbons and CO_2, which results the formation of stronger bonds in condensed phase and leads to the thermal stability shifts to a higher temperature: consequently, its blend generates a higher amount of char residue (13.5 wt% at 700 °C) as compared to the theoretical one (12.5 wt%). Besides, in inert atmosphere, the thermal stability of binary blends of ZnP increases, and the decomposition step occurs around 460 °C. However, no residue is left from the PA_{80}-ZnP_{20} blend (Braun et al., 2008).

In air, the blends containing lignins generate a lower amount of char residue because of the destabilization of the resulting char. However, ZnP blend generates a considerable amount of residue, which is attributed to the phosphate compounds formation in the condensed phase.

When ZnP and lignins (LL/DL) were combined with PA, the decomposition behaviour changed (Figure 4.13 and Figure 4.14). In all ternary blends, the presence of DL/LL reduces the initial decomposition temperature ($T_{5\%}$); at the same time, T_{max} increases. This behavior is ascribed to lignin degradation, which starts at a lower temperature and due to scission of weak ether, aryl−alkyl, and unstable C−C bonds and the maximum decomposition products evolved between 400 and 500 °C. In the meantime, thermally stable bonds are formed in the condensed phase; as a consequence, a noticeable amount of char residue is collected at the end of the tests. It was observed in the previous study that decomposition of ZnP evolves phosphinate anion in gas phase and transformed into zinc phosphate, which also contribute to the obtainment of thermally stable char residue. It is noteworthy that, increasing the LL loading content in PA-LL-ZnP blends strongly reduces the $T_{5\%}$ between 375 to 326 °C and slows down the MMLR; as a consequence, the recorded experimental char residue is higher with respect to the theoretical one, hence indicating the positive interaction within the additives and with the polymer matrix. It is assumed that, during the decomposition of LL, the sulfonate compounds release SO_2 and transform into thermally stable Na_2SO_4, hence giving rise to the stable char (Jakab et al., 1991). Unlike PA-LL-ZnP blends, increasing DL content in its ternary blends, slightly decrease $T_{5\%}$ between 360 and 340 °C, and a higher mass loss rate occurs between 400 and 500 °C due to the evolution of more organic products from DL and a lower char residue at the end of the experiment is observed.

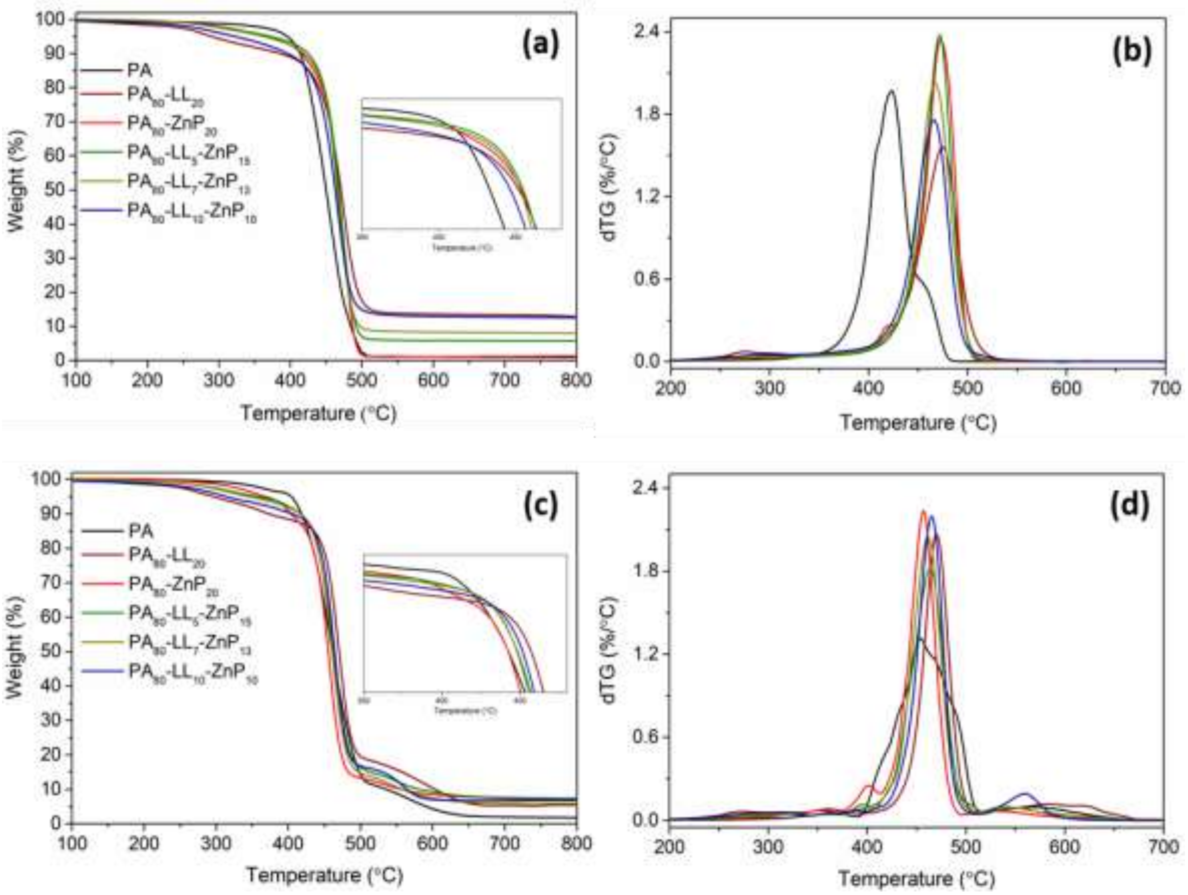

Figure 4.13. TG curves of PA ternary blends of LL in combination with ZnP in N_2 and air atmosphere (heating rate 10 °C/min).

As far as the thermo-oxidative stability is concerned, similar to binary blends, the ternary blends show two decomposition steps: the first one is ascribed to the main degradation step taking place between 450 and 470 °C (T_{max1}), giving rise to the generation of volatile species such as phosphinate compound and phosphinic acid. The second step, occurring at around 550 to 610 °C (T_{max}) due to the oxidation of decomposition products with the evolution of CO and

CO_2, and formation of thermally stable phosphate compounds in the condensed phase. It was observed the residue obtained in oxidative condition was much lower compared to intert condition. This finding is ascribed to the oxidative decomposition of lignin, which catalyzes further oxidation with the formation of CO and CO_2 and continuous weight loss untill 800 °C.

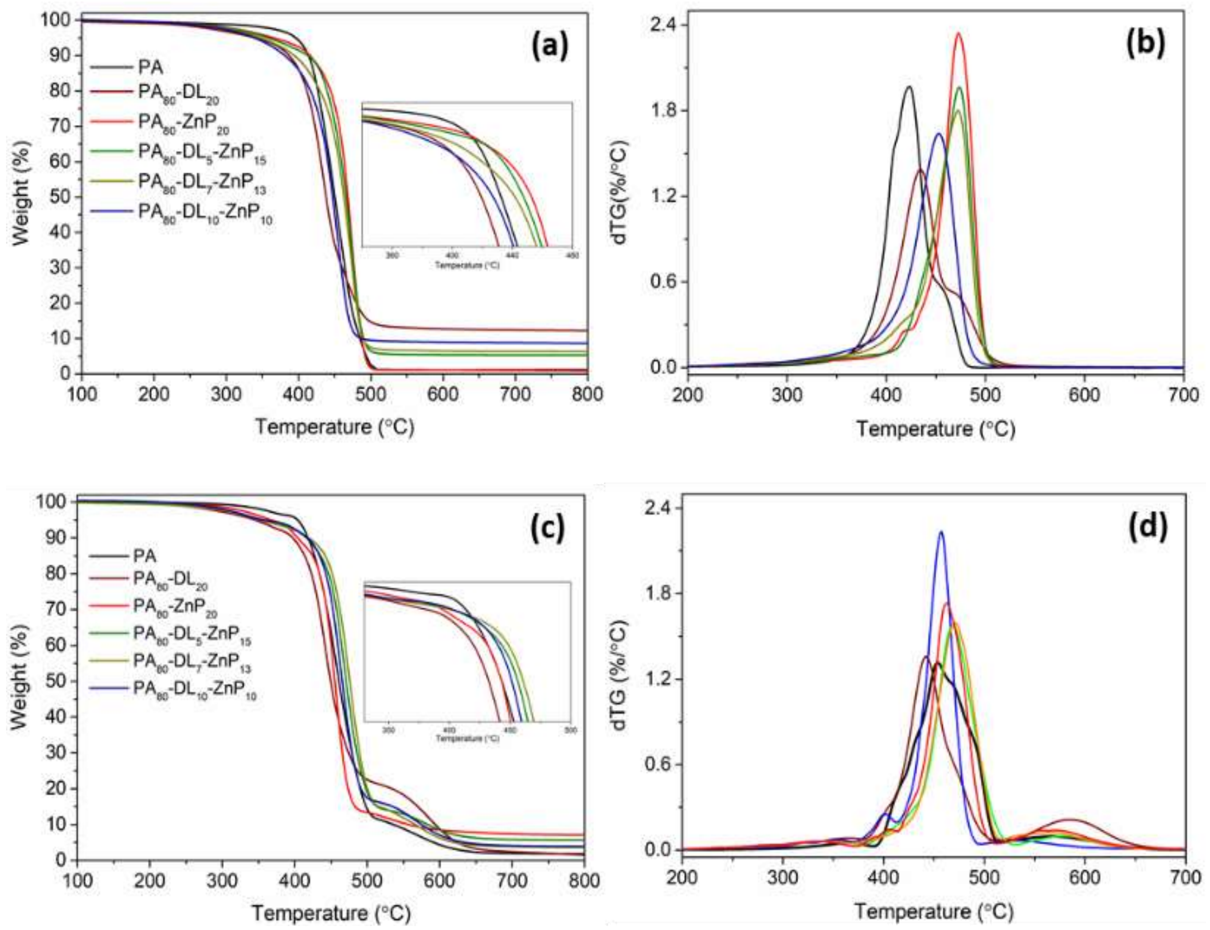

Figure 4.14. TG curves of PA ternary blends of DL in combination with ZnP in N_2 and air atmosphere (heating rate 10 °C/min).

4.2.3.2. Thermal decomposition of AlP and lignin blends

Thermo-oxidative degradation profile of blends containing lignin and AlP is shown in Figure 4.15 and Figure 4.16. In inert atmosphere, the thermal stability of the binary blend of AlP increases, and a single decomposition step occurs within 460 to 470 °C. In addition, a slightly higher residue for PA_{80}-AlP_{20} blend reveals that the interaction between AlP and polymer matrix, resulting in a thermally stable residue. Conversely, the blend containing a higher amount of AlP generates a higher residue, due to the formation of a stable phosphate compounds in the condensed phase (Braun et al., 2010, 2008).

The ternary blends of AlP and DL strongly reduces the initial decomposition temperature ($T_{5\%}$) between (334 and 315 °C) comparing to that of AlP and LL blends (around 363 to 330 °C), but increases the maximum decomposition temperature (T_{max}) between 445 and 470 °C than that of PA (423 °C). However, the amount of residue collected at the end of the experiment was slightly lower than the residue collected from the ZnP and lignin combination. It is expected that the presence of AlP catalyzes the evolution of decomposition products and residue amount is lowered with respect to ZnP and lignin blends. Unlike PA-LL-AlP blends, increasing DL content in its ternary blends, evolution of more decomposition product reduces the thermal stability of char residue; as consequence, lower production of the char residue from DL blends is reported with respect to LL counterpart. DL contains a higher number of less thermally stable methoxy groups that give rise to the formation of more volatile products during decomposition (Hosoya et al., 2009).

As far as the thermo-oxidative stability is concerned, it was noticed that the ternary blends containing AlP show a second decomposition step between 600 and 610°C (T_{max2}) as compared to ZnP containing ternary blends, which give T_{max2} at lower temperatures (i.e., within 550 and 580 °C). This finding confirms that the phosphate compound formation from AlP is more favored than that from ZnP. Furthermore, the residue obtained in oxidative condition was lower than that of inert atmosphere, which is attributed to the oxidative decomposition of lignin, giving rise to the geneation of more CO and CO_2 and continuous weight loss untill 800 °C.

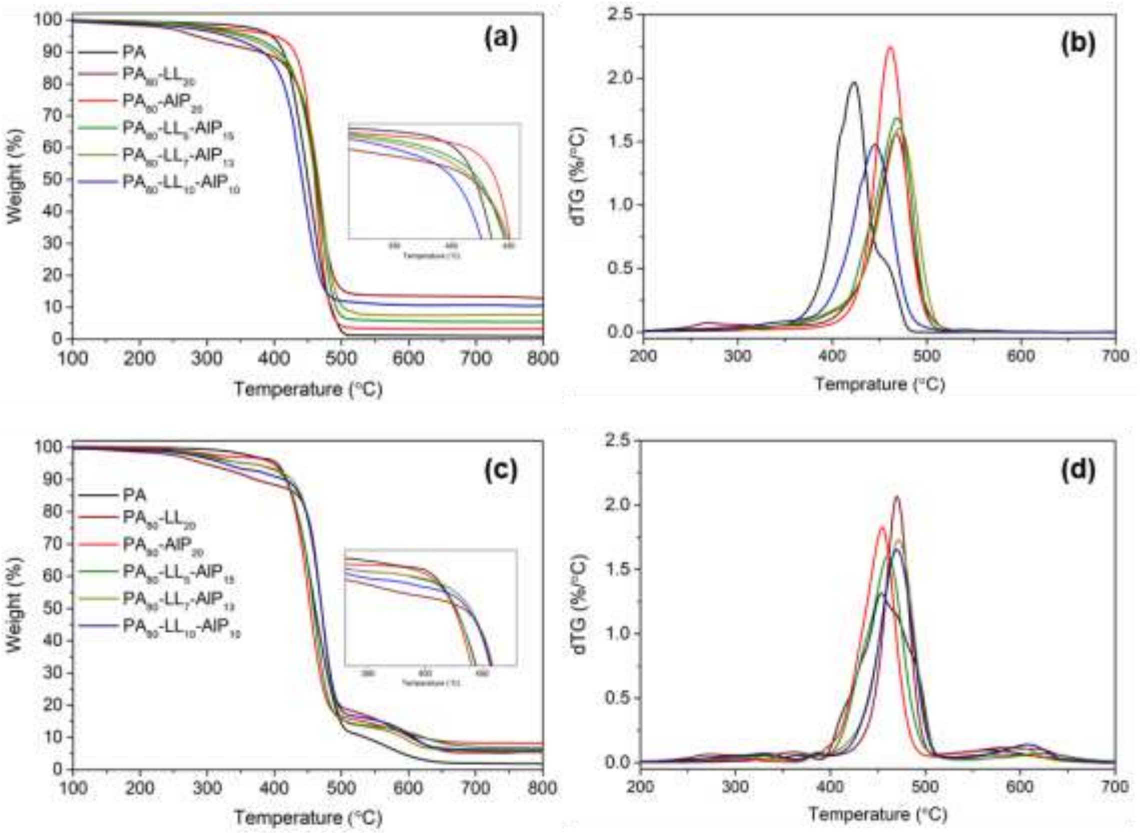

Figure 4.15. TG and dTG curves of PA and its blends with LL and AlP in nitrogen and air (10 °C/min).

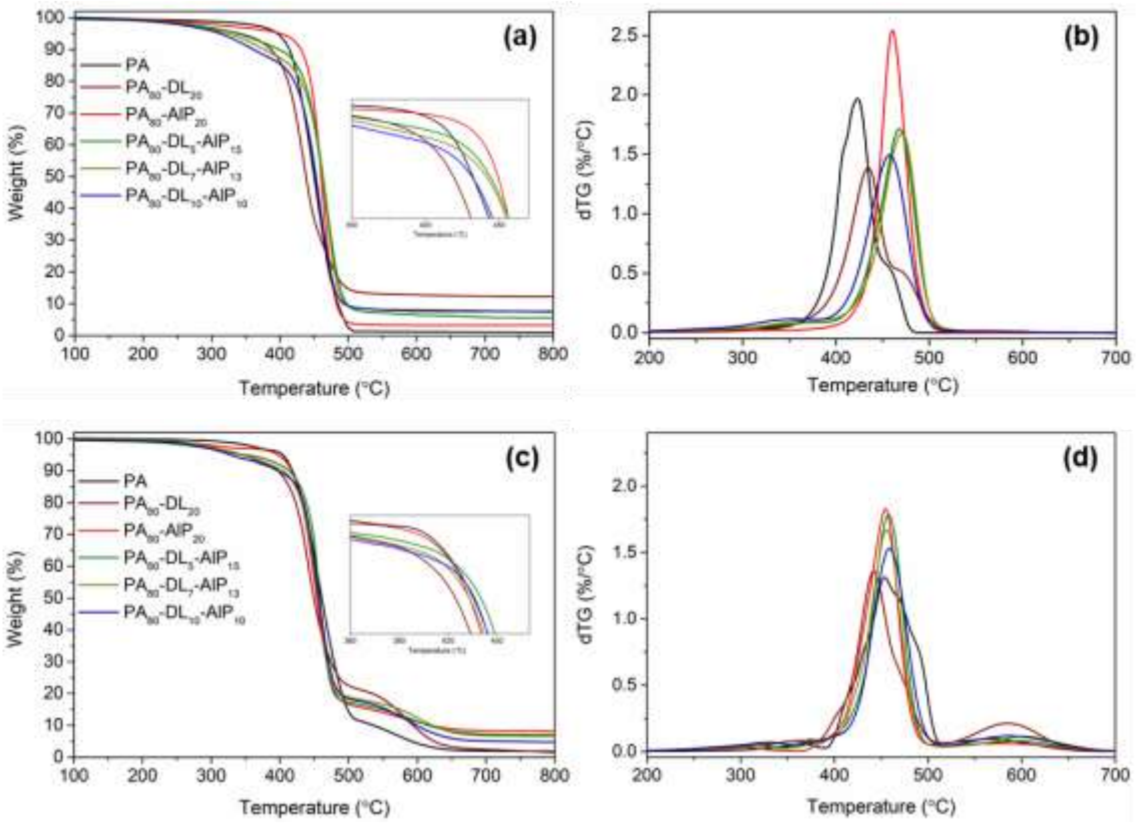

Figure 4.16. TG and dTG curves of PA and its blends with DL and AlP in nitrogen and air (10 °C/min).

4.2.3.3. Mass loss difference curves

TG analysis showed the thermo-oxidative stability of lignin and AlP ternary blends was higher as compared to ZnP containing blends. Therefore, the interaction between AlP and lignin was assessed through weight loss difference curves ΔM (%) as shown in Figure 4.17. The ternary blends of LL and AlP show slightly destabilisation region (ΔM below – 2 %) between 280 and 400 °C and then stabilisation from 400 to 500 °C; afterward, the destabilisation region continues until 800 °C. In addition, an increase of ΔM and thermal stability was observed with increasing LL loading in blends, hence confirming the positive interaction of LL with fire retardant additives. For example, PA_{80}-LL_{10}-AlP_{10} blend shows stabilisation between 400 and 500 °C, and then destabilisation of transient char continues up to 800 °C.

On the other hand, the presence of DL with AlP decreases the thermal stability, as indicated by the destabilization region at a lower temperature between 250 and 400 °C (ΔM upto – 4 %). Further, PA-DL-AlP blends show small stabilisation region (ΔM is below 5%) between 400 and 450 °C and large destabilisation (ΔM below -16%) between 450 and 520 °C due to the evolution of more volatile compounds. Finally, stabilisation of transient char continues until 800 °C due to the formation of a stable phosphate layer in the solid phase. Interestingly, increasing the DL content has no positive significant influence on mass difference and stabilisation region, hence indicating a weak interaction of DL with AlP additive.

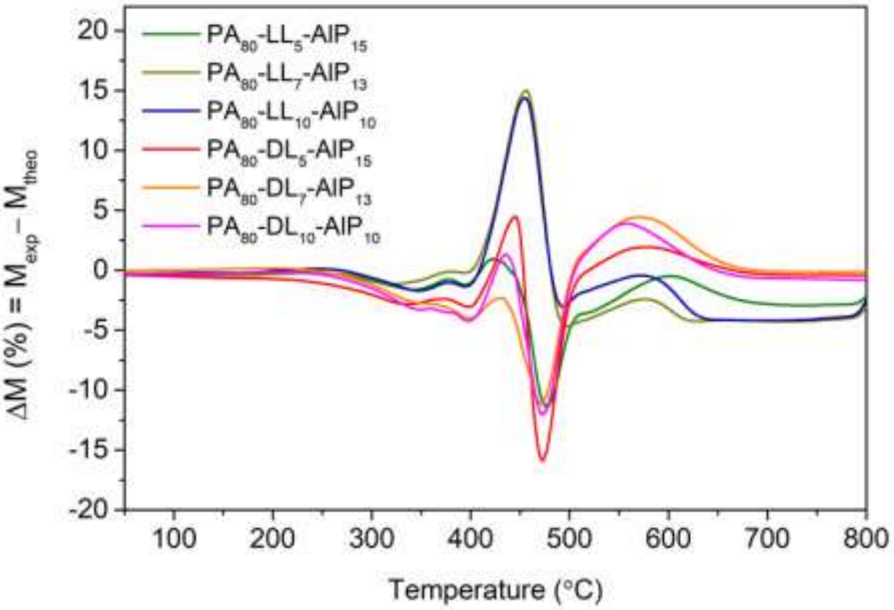

Figure 4.17. Curves of residual mass loss difference for AlP and lignin blends in air atmosphere (10 °C/min).

Conclusion about TG analysis

Thermal decomposition analysis showed the presence of lignin reduced the initial decomposition temperature, at the same time, increases the maximum decomposition temperature owing to the decomposition of lignin which occurs in wide temperature range. In inert atmosphere, the addition of LL with ZnP or AlP generates higher amount of char residue compared to the char residue obtained from DL and ZnP or AlP blends. Furthermore, the decomposition of ZnP/AlP provide stability to the char residue due to the formation of phosphate compounds in the condensed phase. Besides, in oxidative condition, the lower amount of residue obtained due to the oxidative decomposition of lignin, giving rise to further oxidation with the formation of CO and CO_2 and continuous weight loss untill 800 °C observed. The formation properties of these blends can effectively reduce heat release rate and other fire parameters due to the charring effect.

4.2.4. UL94 vertical flame spread test

The results of the UL94 tests are summarized in Table 4.6, and the typical pictures of the specimens left after the tests are shown in Figure 4.18. Dripping was observed in all the blends. the binary blend of LL and PA limits the flammability by reducing the total combustion time. It is expected that the presence of sulfonate functionality in LL may lead to the formation of a thermally stable compound. Besides, the addition of DL lignin to PA has a detrimental effect; the binary blend shows high melt dripping and a higher combustion time as compared to PA_{80}-LL_{20}. The binary blend of AlP and PA improved the flame-retardant performance, which achieves self-extinction (V-0 rating); further, no melt dripping is observed. These finding can be ascribed to the release of phosphinic acid and phosphinate compounds in the gas phase, which dilutes the fuel. On the other hand, the addition 20 wt% ZnP loading is not sufficient to improve flame retardancy and UL94 rating: in fact, PA_{80}-ZnP_{20} specimens lead to high flammability and dripping.

The presence of LL in ternary blends decreases the total combustion time. However, the best flame-retardant results were obtained with PA-LL-ZnP blends, specifically the PA_{80}-LL_7-ZnP_{13} and PA_{80}-LL_{10}-ZnP_{10} blend achieve self-extinction and V-1 classification. It was noticed that increasing ZnP loadings deteriorate the performances, as ZnP promotes melt dripping phenomena (Didane et al., 2012a). As regards to the flame-retardant action, it was assumed that ZnP decomposition release phosphinate compounds in the gas phase that can form $P-O^{\bullet}$ radicals: this latter may act as radical scavengers and lead to flame inhibition through radical trapping, hence improving the flame retardancy of blends (Braun and Schartel, 2004; Lewin and Weil, 2001). Conversely, the presence of DL in ternary blends do not show significant improvement under UL94 tests, as all these ternary blends have a V-2 classification. This behavior was attributed to the rapid decomposition of DL in air; further, DL decomposed mainly (T_{max1}) during the decomposition of PA.

Table 4.6. UL94 test data for PA and its blends.

Samples	**1st combustion t_1 (s)**	**2nd combustion t_2 (s)**	**Total Combustion t_1+t_2 (s)**	**Cotton ignition**	**Dripping**	**Rating**
PA	11 ± 1	7 ± 1	18 ± 1	Yes	Yes	V-2
PA_{80}-LL_{20}	5 ± 1	5 ± 1	10 ± 1	Yes	Yes	V-2
PA_{80}-DL_{20}	9 ± 4	9 ± 3	18 ± 7	Yes	Yes	V-2
PA_{80}-ZnP_{20}	21 ± 1	3 ± 1	24 ± 1	Yes	Yes	V-2
PA_{80}-AlP_{20}	0	2 ± 1	2 ± 1	No	No	V-0
PA_{80}-LL_5-ZnP_{15}	11 ± 1	3 ± 1	14 ± 1	Yes	Yes	V-2
PA_{80}-LL_7-ZnP_{13}	4 ± 1	3 ± 1	7 ± 1	No	Yes	V-1
PA_{80}-LL_{10}-ZnP_{10}	6 ± 1	3 ± 1	9 ± 1	No	Yes	V-1
PA_{80}-DL_5-ZnP_{15}	10 ± 1	4 ± 1	14 ± 2	Yes	Yes	V-2
PA_{80}-DL_7-ZnP_{13}	11 ± 1	4 ± 1	15 ± 2	yes	Yes	V-2
PA_{80}-DL_{10}-ZnP_{10}	7 ± 1	3 ± 1	10 ± 1	yes	Yes	V-2
PA_{80}-LL_5-AlP_{15}	16 ± 1	6 ± 2	22 ± 1	Yes	Yes	V-2
PA_{80}-LL_7-AlP_{13}	24 ± 2	4 ± 1	28 ± 2	Yes	Yes	V-2
PA_{80}-LL_{10}-AlP_{10}	8 ± 1	4 ± 1	12 ± 2	Yes	Yes	V-2
PA_{80}-DL_5-AlP_{15}	22 ± 2	5 ± 1	27 ± 2	Yes	Yes	V-2
PA_{80}-DL_7-AlP_{13}	19 ± 1	4 ± 1	23 ± 2	Yes	Yes	V-2
PA_{80}-DL_{10}-AlP_{10}	18 ± 1	3 ± 1	20 ± 1	Yes	Yes	V-2

The combination of lignin (DL/LL) and AlP did not allow to improve the flammability behaviour and UL94 rating. During the combustion, the majority of polymers drips, and ignites the cotton. Small flaming drips fall on applying the flame first time (t_1) while strong dripping was observed on applying the flame second time (t_2), the dripping leads the extinction of the flame. It was noticed, the sample extinguishes immediately when a big flaming part of the sample falls on the cotton pad. Therefore, it decreases the t_2 combustion time and total combustion time. As a result, the presence of DL in ternary blends do not show significant improvement under UL94 tests, as all these ternary blends have a V-2 classification. Increasing the amount of lignin reduces the total combustion time, but not enough to extinguish the sample.

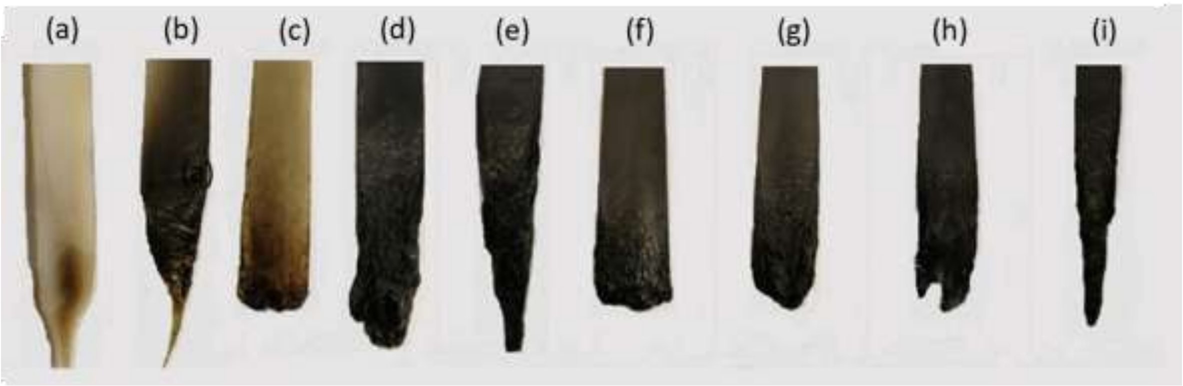

Figure 4.18. Pictures of PA11 blends specimen left after UL 94 vertical flame test. (a) PA, (b) PA_{80}-ZnP_{20}, (c) PA_{80}-AlP_{20}, (d) PA_{80}-LL_{20}, (e) PA_{80}-DL_{20}, (f) PA_{80}-LL_{10}-ZnP_{10}, (g) PA_{80}-DL_{10}-ZnP_{10}, (h) PA_{80}-LL_{10}-AlP_{10}, (f) PA_{80}-DL_{10}-AlP_{10} blends.

4.2.5. Analysis of fire properties

4.2.5.1. Forced combustion test: Heat release parameters

Cone calorimeter tests (forced combustion) at 35 kW/m^2 were carried out on plate samples in order to analyse the fire-retardant properties. The HRR and THR curves are shown in Figure 4.19 (a-d) and Figure 4.20 (a-d), the cone calorimetry data for all blends are collected in Table 4.7. Figure 4.19 (a-b) shows the influence of LL/DL and ZnP on HRR and THR. As mentioned addition of LL decreases TTI due to the rapid mass loss of LL taking place before the decomposition of PA, which substantially decrease PHRR and THR from 884 to 454 kW/m^2 and from 92 to 78 kW/m^2, respectively; in addition, the samples show a noticeable char residue after the forced combustion tests (Table 4.7). Conversely, the addition of ZnP up to 20 wt% in PA does not show any significant reduction in fire parameters.

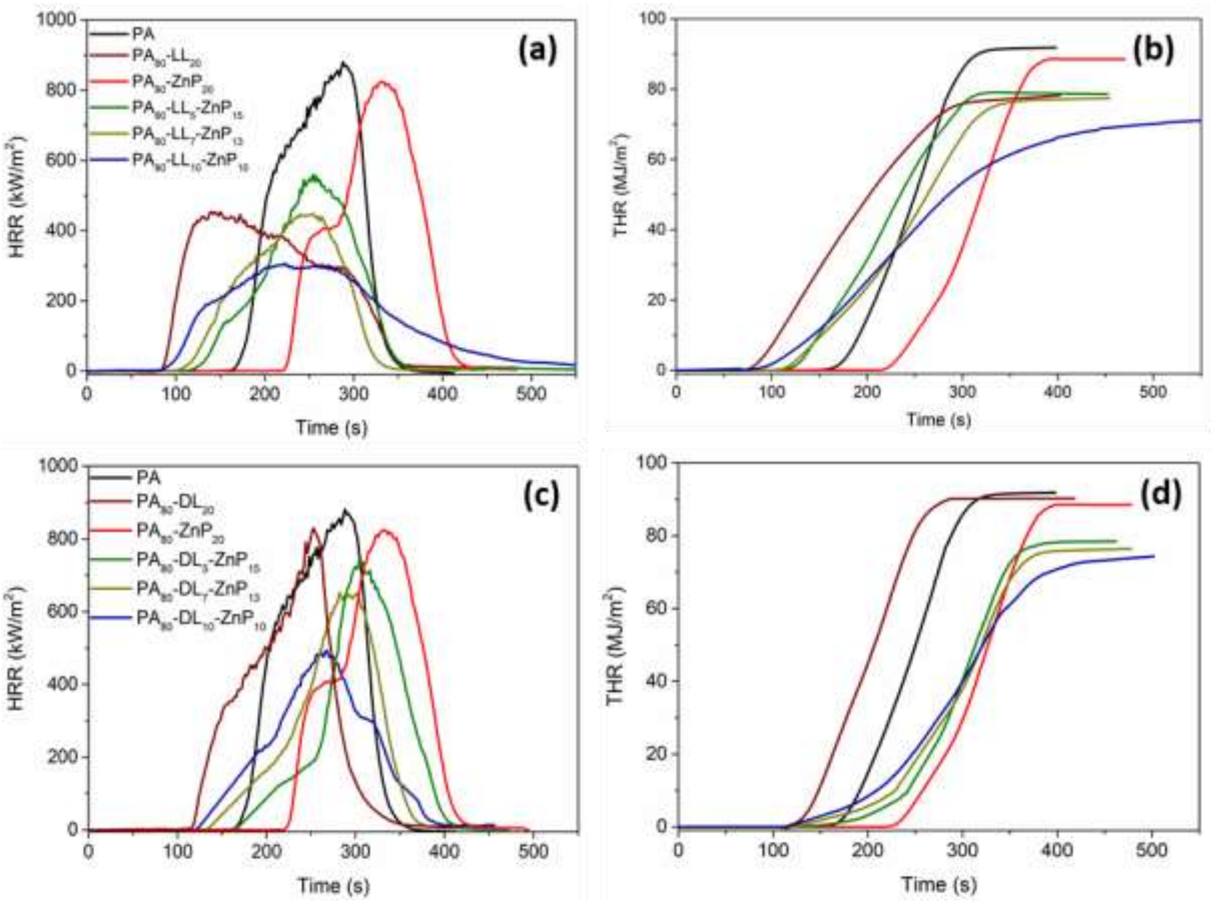

Figure 4.19. HRR and THR curves of PA blends, for PA-LL-ZnP blends ((a) and (b)), and for PA-DL-ZnP blends ((c) and (d)), heat flux 35 kW/m^2.

Besides, the ternary blends containing LL and ZnP exhibit lower TTI as compared to unfilled PA, as anticipated by TG analyses in air: in fact, the adding of 5 to 10 wt% LL strongly reduces its $T_{5\%}$, at the same time, promoting the formation of a thermally stable char residue. A similar trend was observed during combustion tests: TTI value decreases with increasing LL content from 5 to 10 wt% with respect to unfilled PA. Besides, PHRR and THR values substantially drop (by -64% and -22%, respectively) for PA_{80}-LL_{10}-ZnP_{10} blend, due to the formation of a protective char layer in the condensed phase. In addition, Figure 4.19 (c-d) shows the influence of DL and ZnP on HRR and THR. It is worthy to note that, unlike LL lignin, the addition of DL with ZnP does not show a significant reduction in PHRR and THR. However, a certain reduction in PHRR (-43%) is seen when DL content achieves 10 wt%.

Table 4.7. Heat release data from cone calorimetry for PA and its blends.

Samples	TTI (s)	PHRR (kW/m^2)	Reduction (%)	THR (MJ/m^2)	Residue (%)
PA	154 ± 3	884 ± 4	-	92 ± 4	0.6 ± 0.1
PA$_{80}$-LL$_{20}$	72 ± 12	454 ± 30	49	78 ± 6	8.7 ± 0.3
PA$_{80}$-DL$_{20}$	112 ± 10	821 ± 27	7	90 ± 2	7.6 ± 0.1
PA$_{80}$-ZnP$_{20}$	223 ± 14	825 ± 29	7	88 ± 6	1.4 ± 0.2
PA$_{80}$-AlP$_{20}$	114 ± 4	700 ± 33	21	86 ± 2	4.2 ± 0.1
PA$_{80}$-LL$_{5}$-ZnP$_{15}$	112 ± 12	560 ± 40	37	79 ± 2	5.9 ± 0.2
PA$_{80}$-LL$_{7}$-ZnP$_{13}$	92 ± 9	443 ± 21	50	77 ± 4	6.2 ± 0.2
PA$_{80}$-LL$_{10}$-ZnP$_{10}$	86 ± 9	315 ± 11	64	73 ± 2	8.5 ± 0.3
PA$_{80}$-DL$_{5}$-ZnP$_{15}$	150 ± 18	740 ± 23	16	79 ± 2	3.8 ± 0.2
PA$_{80}$-DL$_{7}$-ZnP$_{13}$	128 ± 14	678 ± 36	23	77 ± 3	5.2 ± 1.5
PA$_{80}$-DL$_{10}$-ZnP$_{10}$	116 ± 13	500 ± 48	43	75 ± 7	8.2 ± 0.5
PA$_{80}$-LL$_{5}$-AlP$_{15}$	142 ± 11	554 ± 33	37	78 ± 6	5.8 ± 0.3
PA$_{80}$-LL$_{7}$-AlP$_{13}$	124 ± 10	420 ± 27	52	77 ± 3	7.1 ± 0.3
PA$_{80}$-LL$_{10}$-AlP$_{10}$	108 ± 12	230 ± 14	74	72 ± 4	11.5 ±
PA$_{80}$-DL$_{5}$-AlP$_{15}$	174 ± 14	424 ± 39	42	76 ± 4	7.7± 0.5
PA$_{80}$-DL$_{7}$-AlP$_{13}$	140 ± 12	406 ± 34	54	74 ± 5	8.6 ± 0.5
PA$_{80}$-DL$_{10}$-AlP$_{10}$	95 ±7	320 ± 10	64	72 ± 1	10.4± 0.5

Figure 4.19 (a-b) shows the influence of LL/DL and ZnP on HRR and THR. The ternary blends containing LL and AlP showed lower TTI as compared to unfilled PA, TTI value decreases with increasing LL content from 5 to 10 wt.% in blends: this finding is attributed to the rapid mass loss of LL taking place before the decomposition of PA. Besides, PHRR and THR values remarkably decrease up to 230 kW/m^2 and 72 MJ/m^2 (PHRR, -74% and 22%, respectively) for PA$_{80}$-LL$_{10}$-AlP$_{10}$. In addition, the HRR curve reveals a broad and single peak of HRR, hence indicating the formation of an effective protective char layer. It is noteworthy that the LL and AlP formulation used in this study showed the enhanced fire performance under forced combustion test as compared to the lignin and ZnP combination. This superior fire-retardant

property in forced combustion tests is due to the presence of an efficient aluminium phosphate layer, able to confer stability to the char residue. The increased char residue at the end of the test (Table 4.7) further confirms the formation of the protective layer, the addition of DL with AlP shows a reduction of PHRR (-64%) and THR (-22%) for PA_{80}-DL_{10}-AlP_{10}. This is attributed to the presence of AlP, which promotes the formation of a stable char layer acting as a protective barrier, limiting the heat and mass transfer from and to the underlying polymer.

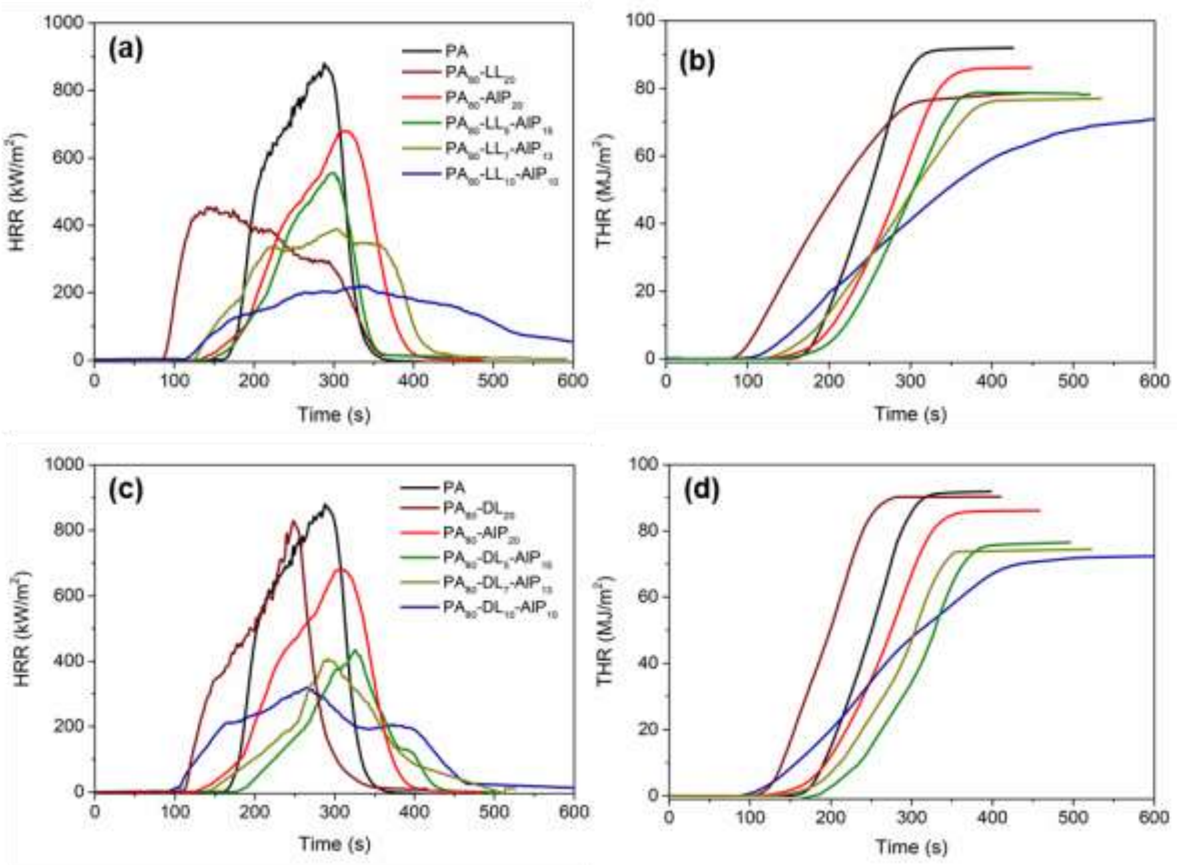

Figure 4.20. HRR and THR curves of PA blends, (a) and (b) for PA-DL-ZnP blends, (c) and (d) for PA-DL-AlP blends.

4.2.5.2. Forced combustion test: Smoke release parameters

The release of smoke and CO during combustion is not only a key fire hazard but also is an indication of the FR mechanism. For instance, a significant increase in the smoke release and CO amount is originated by the incomplete oxidation of gaseous products, which indicates a flame inhibition action by radical trapping reactions taking place in the gas phase. Alternatively, a decrease in smoke release indicates a better-ventilated combustion process, in which the flame retardancy is dominated by fuel dilution and/or thermal barrier (Braun and Schartel, 2005, 2004). Therefore, total smoke release (TSR), CO and CO_2 total yield and CO_2/CO yield were assessed; the corresponding data are collected in Table 4.8. Figure 4.21 shows CO and CO_2 yield; first of all, the CO_2 yield is practically similar for all the blends. As compared to PA, binary blends with ZnP increase the smoke release and CO yield and lower the CO_2/CO yield, hence indicating the incomplete oxidation of gaseous products. Conversely, the incorporation of LL and DL lowers TSR and CO yield and increase CO_2/CO yield, also confirming the extended oxidation of the evolved gaseous products. The binary blends with AlP increase the smoke release and CO yield and lower the CO_2/CO yield, hence indicating the incomplete oxidation of gaseous products.

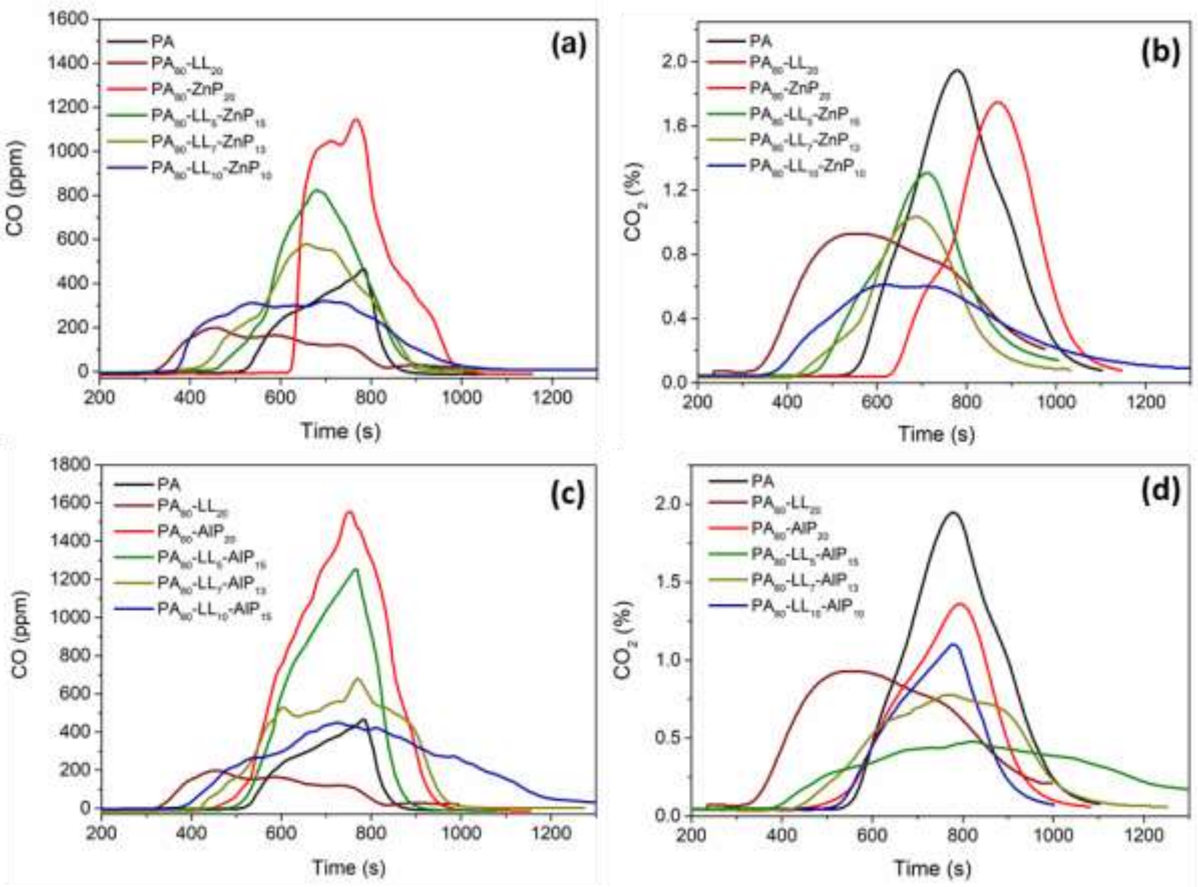

Figure 4.21. CO and CO_2 evolution during combustion for PA-LL-ZnP blend blends.

Table 4.8. Smoke parameters data during combustion test for PA and its blends.

Samples	TSR (m^2/m^2)	CO yield (g/kg)	CO_2 yield (kg/kg)	CO_2/CO
PA	1033 ± 1	33 ± 1	2.6 ± 0.1	78.8
PA_{80}-LL_{20}	1198 ± 20	29 ± 1	2.1 ± 0.2	72.4
PA_{80}-DL_{20}	1290 ± 25	23 ± 1	1.6 ± 0.1	69.6
PA_{80}-ZnP_{20}	1640 ± 62	94 ± 2	2.3 ± 0.1	24.5
PA_{80}-AlP_{20}	2118 ± 41	164 ± 2	2.1 ± 0.1	12.8
PA_{80}-LL_5-ZnP_{15}	1799 ± 48	88 ± 1	1.9 ± 0.1	21.6
PA_{80}-LL_7-ZnP_{13}	1652 ± 151	92 ± 1	2.1 ± 0.1	22.8
PA_{80}-LL_{10}-ZnP_{10}	1691 ± 26	72 ± 2	2.0 ± 0.1	27.8
PA_{80}-DL_5-ZnP_{15}	1720 ± 36	71 ± 3	2.2 ± 0.1	31.0
PA_{80}-DL_7-ZnP_{13}	1800 ± 88	73 ± 4	2.1 ± 0.1	28.8
PA_{80}-DL_{10}-ZnP_{10}	1745 ± 62	61 ± 6	2.1 ± 0.1	34.4
PA_{80}-LL_5-AlP_{15}	1959 ± 28	98 ± 3	1.9 ± 0.1	19.4
PA_{80}-LL_7-AlP_{13}	2034 ± 37	85 ± 3	2.0 ± 0.1	23.5
PA_{80}-LL_{10}-AlP_{10}	1995 ± 18	71 ± 6	2.1 ± 4	29.6
PA_{80}-DL_5-AlP_{15}	1819 ± 40	99 ± 2	2.0 ± 0.1	20.2
PA_{80}-DL_7-AlP_{13}	1929 ± 45	90 ± 3	2.0 ± 0.1	22.2
PA_{80}-DL_{10}-AlP_{10}	1967 ± 68	86 ± 5	2.1 ± 0.1	24.4

On the other hand, the combination of lignin and phosphinate worsens the smoke parameters, confirming the occurrence of incomplete combustion. However, increasing the lignin content reduces the CO evolution, which is attributed to the further complete oxidation of evolved gaseous products. Figure 4.21 shows the influence of LL combined with flame retardants on CO and CO_2 evolution. Interestingly, the blends containing 10 wt% of both fillers show the lowest CO release with respect to other ternary blends: more specifically, PA_{80}-LL_{10}-ZnP_{10} blend remarkably lowers the peak of CO release up to 300 ppm without compromising the other FR properties. Similarly, PA_{80}-LL_{10}-AlP_{10} blend significantly lowers the peak of CO yield up to 450 ppm. This finding can be ascribed to the interactions taking place between LL and ZnP in the ternary blend, which leads to extended oxidation of the released gaseous products as well as to the formation of a protective char in the condensed phase. Based on results, it can be concluded that the combination of lignin and phosphinate promotes the smoke and CO release; however, high lignin loading significantly reduces CO release, hence minimize the smoke toxicity.

4.2.6. Char residue morphology

Pictures of char residues obtained after forced combustion tests are shown in Figure 4.22. It is clearly observed that the residue from PA is very thin and practically negligible. Similarly, PA_{80}-ZnP_{20} (Figure 4.22 (b)) shows a mechanically thin and non-charring characteristic. However, PA_{80}-AlP_{20} slightly increases the residue (Figure 4.22 (c)), Besides, the binary blends of lignin (LL and DL) display a higher char residue formation: in particular, PA_{80}-LL_{20} (Figure 4.22 (d)) gives rise to a coherent and compact char layer formation. However, the presence of cracks deteriorates the performance. Conversely, the char residue of PA_{80}-DL_{20} shows a loose and porous surface with many cracks (Figure 4.22 (e)). although the presence of cracks and insufficient residue leads to the formation of a weak protective layer. Besides, the combination of lignin and phosphinate not only increases the char residue but also leads to the formation of a stable char layer with barrier features against heat flux and release of combustible gases. For example, the combination of LL with AlP or ZnP (Figure 4.22 (f-g)) shows a compact and protective layer due to sufficient char formation. Conversely, ternary blends of DL with AlP/ZnP show a thin char layer and relatively loose structure with many cracks; more specifically, PA_{80}-DL_{10}-ZnP_{10} and PA_{80}-DL_{10}-AlP_{10} (Figure 4.22 (h-i)) give a fragile and mechanically weak char layer.

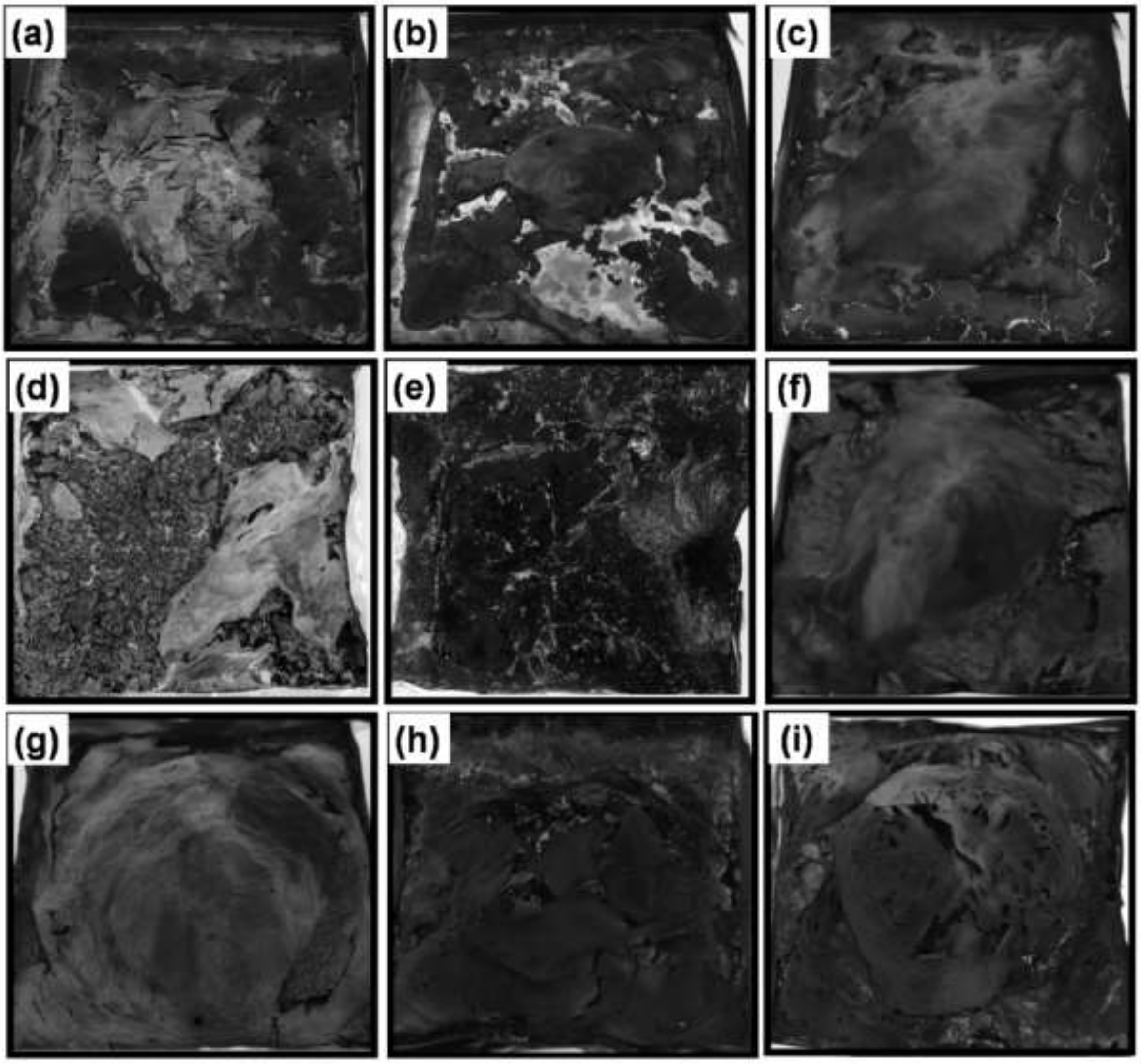

Figure 4.22. Pictures of char residues collected at the end of cone calorimetry test: (a) unfilled PA, (b) PA_{80}-AlP_{20}, (c) PA_{80}-LL_{20}, (d) PA_{80}-DL_{20}, (e) PA_{80}-LL_{10}-AlP_{10}, (g) PA_{80}-LL_{10}-ZnP_{10} (h) PA_{80}-DL_{10}-AlP_{10} and (i) PA_{80}-DL_{10}-ZnP_{10} blends.

In order to further investigate the surface morphology and structure of the charred layer, the top surface of ternary blends containing 10 wt% loading of both the fillers was also observed by SEM (Figure 4.23 (a-d)). It can be observed that the surface morphology of char residue from PA_{80}-LL_{10}-AlP_{10} (Figure 4.23 (a)) presents a relatively more compact structure in comparison with PA_{80}-LL_{10}-ZnP_{10}, due to the higher char formation and interaction between LL and AlP providing a stable protective char layer, which contributes to enhanced fire retardancy. Similar char residue morphology with AlP was observed by other researchers

(Huang et al., 2018; Zhan et al., 2015). The PA_{80}-LL_{10}-ZnP_{10} blend (Figure 4.23 (b)) presents a less compact structure than the PA_{80}-LL_{10}-ZnP_{10}, although compact char layer is present with some holes on the surface. On contrary, the surface morphology of residue from DL and (AlP or ZnP) containing blends (Figure 4.23 (c-d)) does not form an intact char layer due to insufficient char formation during combustion; as a consequence, a loose and porous structure is formed.

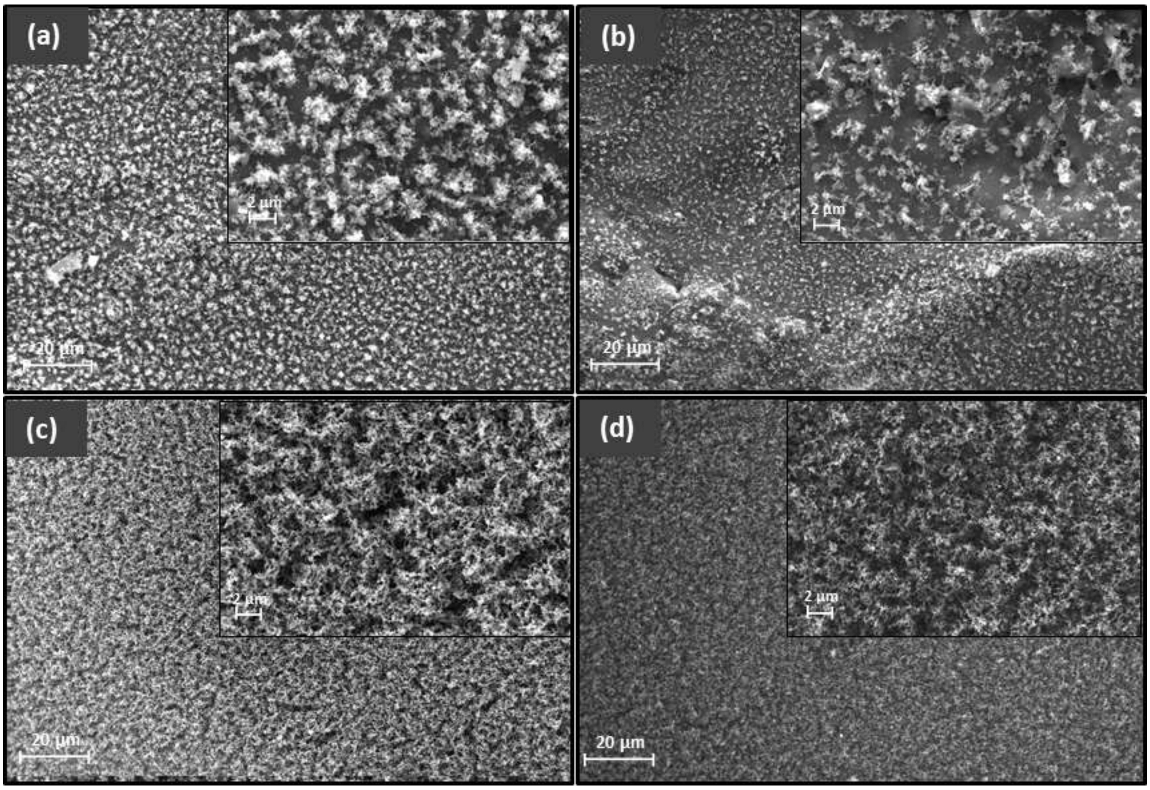

Figure 4.23. SEM micrographs of char residue surface after forced combustion for (a) PA_{80}-LL_{10}-AlP_{10} (b) PA_{80}-LL_{10}-ZnP_{10} and (c) PA_{80}-DL_{10}-AlP_{10} (d) PA_{80}-DL_{10}-ZnP_{10} blends at 1000x and 5000x magnification.

4.2.7. Conclusions

In order to enhance the use of industrial lignin, in this work, different lignins, i.e., LL and DL were combined with two phosphinate FR (i.e., ZnP and AlP). The influence of the presence of lignin and phosphinate FR on the thermal and fire retardancy was thoroughly assessed by TGA, UL94 vertical flame and cone calorimetry tests. SEM analysis of ternary blends showed that lignin (DL or LL) and ZnP blends have homogeneous dispersion of fillers in PA matrix. ZnP particles were fused in PA matrix. However, lignin (DL or LL) and AlP blends (in particular, PA_{80}-LL_{10}-AlP_{10}) showed that small size (< 10 µm) aggregates of AlP were found on the surface. Distribution of lignin and AlP has influence on mechanical properties, which significantly reduced the tensile strength and percent elongation. TG analyses showed that the incorporation of lignin in the ternary blends increased the thermal stability of PA, promoting the stable char formation at the end of the tests. However, the char residue obtained from AlP blends was lower than that of ZnP blends. Flaming combustion assessed by UL 94 vertical flame spread tests showed the most desirable flammability properties were achieved with LL and ZnP combination when 10 wt% loading of both additives. PA_{80}-LL_{7}-ZnP_{13} and PA_{80}-LL_{10}-ZnP_{10} blends achieved self-extinction and V-1 rating. On the other hand, a combination of lignin with AlP did not improve the FR properties, all blends showed V-2 rating. Furthermore, in forced combustion test the interactions between lignin and phosphinate promoted a remarkable reduction of PHRR and THR. In particular, the best fire-retardant performance was found by combining LL with AlP (i.e., PA_{80}-LL_{10}-AlP_{10}), resulting in a strong reduction of PHRR (-74%) and THR (-22%) values. On the other hand, smoke parameters, namely TSR and CO yield, increased in ternary blends; however, increasing the lignin loading effectively reduced the CO and CO_2/CO yield as compared to PA.

In conclusion, from an overall point of view, the use of industrial lignin with phosphinate in PA seems to be quite promising as far as fire retardancy is concerned, also considering the “biobased” character of both the polymer matrix and lignin. It is also important, within the framework of this project to study the feasibility of developing multifilament yarns and textile structure from these formulations. The following study is carried out in the next chapter.

References

Braun, U., Bahr, H., Schartel, B., 2010. Fire retardancy effect of aluminium phosphinate and melamine polyphosphate in glass fibre reinforced polyamide 6. e-Polymers.

Braun, U., Bahr, H., Sturm, H., Schartel, B., 2008. Flame retardancy mechanisms of metal phosphinates in combination with melamine cyanurate in glass-fiber reinforced poly (1 , 4-butylene terephthalate): the influence of metal cation. Polym. Adv. Technol. 19, 680–692. https://doi.org/10.1002/pat.1147

Braun, U., Schartel, B., 2005. Effect of red phosphorus and melamine polyphosphate on the fire behavior of HIPS. J. Fire Sci. 23, 5–30. https://doi.org/10.1177/0734904105043451

Braun, U., Schartel, B., 2004. Flame retardant mechanisms of red phosphorus and magnesium hydroxide in high impact polystyrene. Macromol. Chem. Phys. 205, 2185–2196. https://doi.org/10.1002/macp.200400255

Brebu, M., Vasile, C., 2010. Thermal Degradation of Lignin - A Review. Cellul. Chem. Technol. 44, 353–363.

Didane, N., Giraud, S., Devaux, E., 2012. Fire performances comparison of back coating and melt spinning approaches for PET covering textiles. Polym. Degrad. Stab. 97, 1083–1089. https://doi.org/10.1016/j.polymdegradstab.2012.04.010

Duggan, G.J., Grayson, S.J., Kumar, S., 2004. New fire classifications and fire test methods for the European railway industry, Flame retardants 2004, in: Fire and Material. Interscience Communications, Londan.

Herrera, M., Matuschek, G., Kettrup, A., 2001. Main products and kinetics of the thermal degradation of polyamides. Chemosphere 42, 601–607. https://doi.org/10.1016/S0045-6535(00)00233-2

Hosoya, T., Kawamoto, H., Saka, S., 2009. Role of methoxyl group in char formation from lignin-related compounds. J. Anal. Appl. Pyrolysis 84, 79–83. https://doi.org/10.1016/j.jaap.2008.10.024

Huang, W., He, W., Long, L., Yan, W., He, M., Qin, S., Yu, J., 2018. Highly efficient flame-retardant glass-fiber-reinforced polyamide 6T system based on a novel DOPO-based derivative: Flame retardancy, thermal decomposition, and pyrolysis behavior. Polym. Degrad. Stab. 148, 26–41. https://doi.org/10.1016/j.polymdegradstab.2018.01.008

Jakab, E., Till, F., Szeekely, T., Faix, O., 1991. Thermogravimetry/mass spectrometry of various lignosulfonates as well as of a kraft and acetosolv lignin. Holzforschung 45, 355–360. https://doi.org/10.1515/hfsg.1991.45.5.355

Karstens, T., Rossbach, V., 1989. Thermo-oxidative degradation of polyamide 6 and 6,6. Kinetics of the formation and inhibition of UV/VIS-active chromophores. Die Makromol. Chemie 190, 3033–3053. https://doi.org/10.1002/macp.1989.021901201

Levchik, S. V., Costa, L., Camino, G., 1992. Effect of the fire-retardant ammonium polyphosphate on the thermal decomposition of aliphatic polyamides. I. PA11 and PA12. Polym. Degrad. Stab. 36, 31–41. https://doi.org/10.1016/0141-3910(94)90224-0

Lewin, M., Weil, E., 2001. Mechanisms and modes of action in flame retardancy of polymers. Woodhead Publishing Ltd., Cambridge UK, pp. 31–68.

Mouritz, A.P., Mathys, Z., Gibson, A.G., 2006. Heat release of polymer composites in fire. Compos. Part A Appl. Sci. Manuf. 37, 1040–1054. https://doi.org/10.1016/j.compositesa.2005.01.030

Naik, A.D., Fontaine, G., Samyn, F., Delva, X., Louisy, J., Bellayer, S., Bourgeois, Y., Bourbigot, S., 2014. Outlining the mechanism of flame retardancy in polyamide 66 blended with melamine-poly (zinc phosphate). Fire Saf. J. 70, 46–60. https://doi.org/10.1016/j.firesaf.2014.08.019

Schartel, B., Hull, T.R., 2007. Development of fire-retarded materials – Interpretation of cone calorimeter data. Fire Mater. 31, 327–354. https://doi.org/10.1002/fam.949

Sicken, M., Schlosser, E., Wanzke, W., Burghardt, D., 2004. Fusible zinc phosphinate. US 2004/0176506. https://doi.org/10.1037/t24245-000

Socrates, G., 2001. Infrared and Raman Characteristic Group Frequencies Contents, Third. ed. John Wiley & Sons, Ltd.

Song, P., Cao, Z., Fu, S., Fang, Z., Wu, Q., Ye, J., 2011. Thermal degradation and flame retardancy properties of ABS/lignin: Effects of lignin content and reactive compatibilization. Thermochim. Acta 518, 59–65. https://doi.org/10.1016/j.tca.2011.02.007

Vannier, A., Duquesne, S., Bourbigot, S., Alongi, J., Camino, G., Delobel, R., 2009. Investigation of the thermal degradation of PET , zinc phosphinate , OMPOSS and their blends – Identification of the formed species. Thermochim. Acta 495, 155–166.

https://doi.org/10.1016/j.tca.2009.06.013

Verdolotti, L., Oliviero, M., Lavorgna, M., Iannace, S., Camino, G., Vollaro, P., Frache, A., 2016. On revealing the effect of alkaline lignin and ammonium polyphosphate additives on fire retardant properties of sustainable zein-based composites. Polym. Degrad. Stab. 134, 115–125. https://doi.org/10.1016/j.polymdegradstab.2016.10.001

Zhan, Z., Xu, M., Li, B., 2015. Synergistic effects of sepiolite on the flame retardant properties and thermal degradation behaviors of polyamide 66 / aluminum diethylphosphinate composites. Polym. Degrad. Stab. 117, 66–74.

Zhao, J., Xiuwen, W., Hu, J., Liu, Q., Shen, D., Xiao, R., 2014. Thermal degradation of softwood lignin and hardwood lignin by TG- FTIR and Py-GC / MS. Polym. Degrad. Stab. 108, 133–138. https://doi.org/10.1016/j.polymdegradstab.2014.06.006

5. DEVELOPMENT AND STUDY OF FIRE RETARDANT FABRICS

Introduction

The previous chapter analyzed the thermal degradation and fire-retardant properties of PA blends developed by industrial lignin and phosphinate FR. This chapter discusses the study and development of multifilament and fibrous textile structures in view of the final application of the project. A large scale of blends based on industrial lignin and phosphinates FR prepared using twin screw extruder and studied in Chapter 4, are utilized in this chapter. In the first part, multifilaments are developed using pilot scale melt spinning set-up. The mechanical properties of the filaments are evaluated by tensile tests. The surface morphology is characterized by microscopic analysis. In the second part, textile structure development and fire-retardant properties are discussed.

5.1. Melt fluidity

The melt flow index (MFI) is inversely proportional to the viscosity of the melt at the test conditions. However, the MFI for any such material relies on the applied load and temperature, which has a viable influence on determining the ease of flowability during melt spinning under a prescribed condition. MFI tests for PA loaded with lignin and ZnP up to 20 wt% were carried at 220 °C with 2.16 kg of the applied load. Various binary and ternary blends based on industrial lignin and phosphinates FR were studied. Ideal values of MFI ranged between 15 and 30 g/10 min for melt spinning facility used in this study.

5.1.1. Melt fluidity of lignin and ZnP blends

The influence of lignin (DL or LL) and ZnP combination on MFI is shown in Figure 5.1. The addition of LL up to 20 wt% decreases the fluidity of the blend with respect PA. This behaviour might be attributed to the higher molecular weight of sulphonated lignin and molecular weight distribution (Kun and Pukánszky, 2017). SEM analysis of this blend (Chapter 3) showed the presence of LL particles (about 10 µm) in PA matrix, which may create resistance to flow during MFI tests. Besides, the introduction of DL increases the MFI value due to a homogenous dispersion and distribution of KL. This is attributed to the lower molecular weight of kraft lignin, decreasing entanglement density, and weaker intermolecular interaction (Kun and Pukánszky, 2017). However, miscibility of lignin in polyamides is reported (Sallem-Idrissi et al., 2018, 2016). The binary blend of ZnP (PA_{80}-ZnP_{20}) also slightly reduces the MFI value to 23.7 g/10 min but still remain in the spinning zone.

The ternary blends exhibit different behaviour than binary blends. The PA-DL-ZnP blends show the combination of DL and ZnP decreases the MFI of ternary blends compared to the binary blends of them. Increasing the DL content improves the fluidity (Figure 5.1). Conversely, the MFI of PA-LL-ZnP blends shows the combination of LL and ZnP slightly increases the fluidity of ternary blends compared to the binary blends. In all cases, the MFI value of the ternary blends remains compatible to melt spinning process.

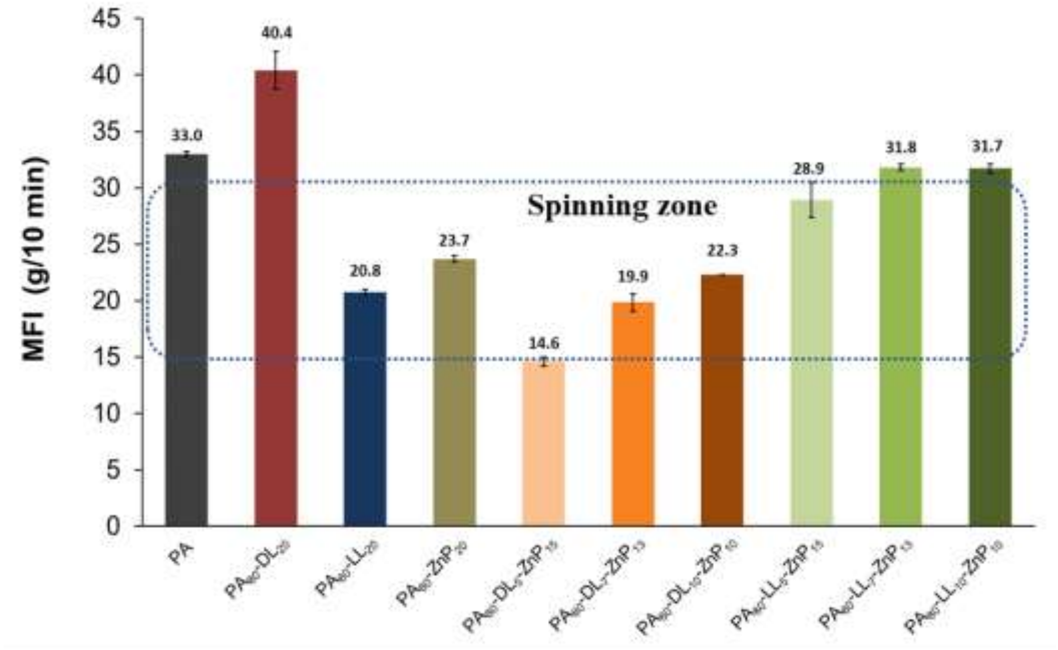

Figure 5.1. MFI for PA and its blends with lignin and ZnP blends, (220 °C, 2.16 kg load).

5.1.2. Melt fluidity of lignin and AlP blends

The influence of lignin (DL or LL) and AlP combination on MFI is shown in Figure 5.2. It was found that the addition of AlP (PA_{80}-AlP_{20} blend) significantly reduces the MFI value as compared to PA, reduction in mobility of molecular chain of PA is attributed to the presence of infusible AlP compared to the ZnP. The ternary blends of PA-DL-AlP show the improvement in the MFI value is related to the amount of DL in the blends. DL contributes to decreasing entanglement between AlP and polymer and weaker the intermolecular interaction. As a result, PA_{80}-DL_5-AlP_{15} shows MFI very low (10.8 g/10 min) and PA_{80}-DL_{10}-AlP_{10} has higher MFI of 21.4 g/10 min. On the other hand, the combination of LL and AlP does not alter the fluidity significantly and MFI value varies between 15.7 and 22.3 g/10 min. increasing the LL content slightly increases the MFI.

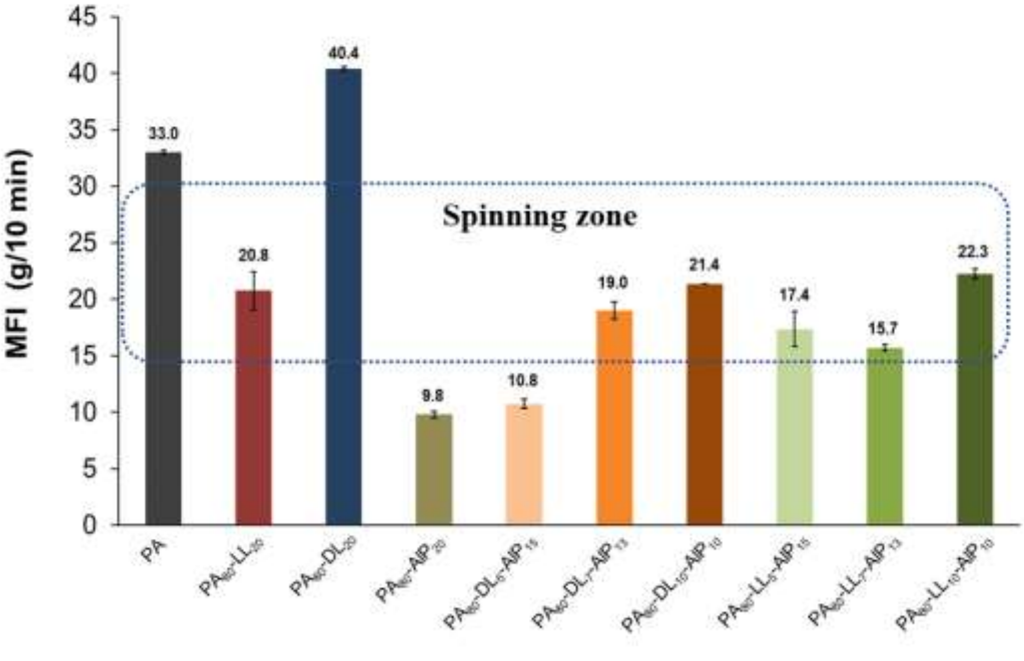

Figure 5.2. MFI for PA and its blends with lignin and AlP blends, (220 °C, 2.16 kg load).

5.2. Melt spinning and development of multifilaments

The comparative studies conducted in this thesis showed that thermal, mechanical and fire retardant properties of the polymer are considerably governed by incorporated fillers. For the following work, various formulations comprising industrial lignin (DL and LL) and phosphinate (ZnP and AlP) were selected for transformation into multifilaments by melt spinning process (Figure 5.3). All the formulations were extruded into pellets according to the temperature profile: 170, 190, 210, 210 and 220 °C. The pelletss were then transformed into multifilaments by molten-channel spinning (Rault et al., 2015). The spinning device has six heating zones (five at the extruder and one at the spinning level) whose temperatures ranged 180, 200, 210, 215 and 220 °C and spinning level at 230 °C, were chosen according to the material to be transformed. Under thermal and mechanical stresses, pellets melt and are transported to the volumetric pump (chamber volume = 3.5 cm^3) whose rotational speed is set beforehand to ensure a constant flow (70 cm^3/min) of material to the spinneret (80 holes (40x2), 1.2 mm diameter). The multifilament yarns obtained consisted of 80 circular continuous filaments are collected on the winder, passed through two different rollers that apply a stretching on the multifilaments. The multifilament properties are proportional to the pump flow rate and stretching rate. The unfilled PA multifilaments were spun first according to profile A. Table 5.1 detailed the different profiles selected to allow the development of multifilaments.

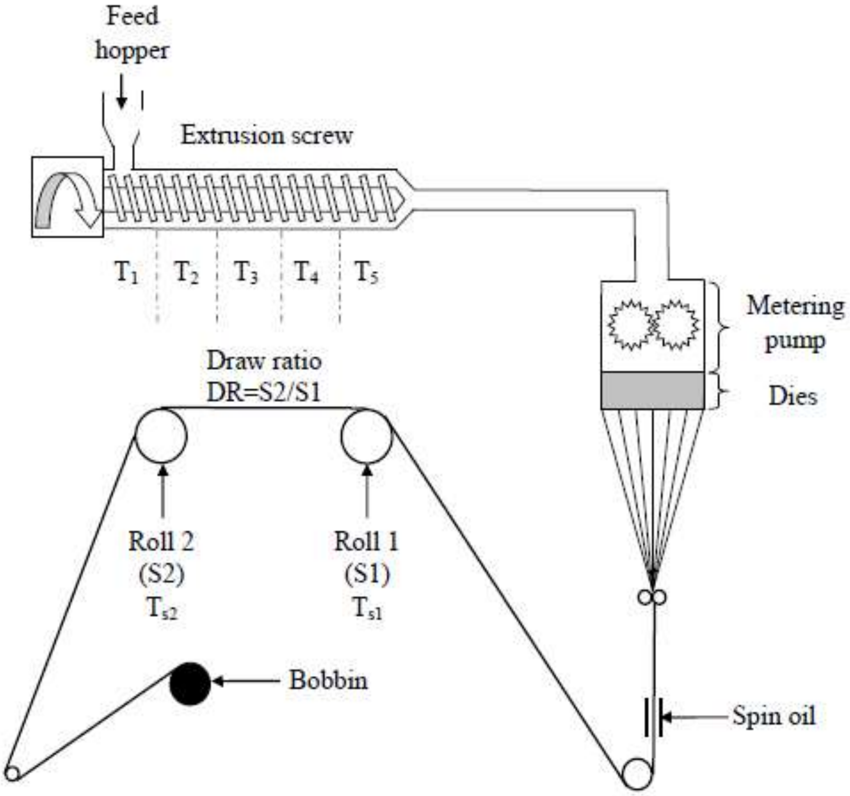

Figure 5.3. Schematic of melt spinning machine (Rault et al., 2015).

5.2.1. Spinning trials of ZnP and lignin-containing blends

All the ZnP and lignin (DL or LL) based blends were successfully transformed into filaments form. Feasibility of spinning for these formulations also indicated by fluidity test wherein MFI values for the binary and ternary blends are compatible with spinning condition. Different spinning parameters and temperature profile are collected in Table 5.1, ZnP and DL blends were melt spun according to profile A. The multifilaments generated from spinneret were continuous and have acceptable fluidity. This behaviour led to the continuous production of multifilament without much difficulty (Figure 5.4). It was observed that DL and ZnP blends achieve the stretching speed (R_2) up to 200 m/min. However, the LL and ZnP blend found its drawing limit with a stretching speed (R_2) up to 130 m/min (profile B), increasing this speed cause the disturbance and breakage in multifilament production. Thus, LL and ZnP multifilament produced according to profile B.

Table 5.1. Spinning parameters

	Temperature of Spinneret	**The volumetric flow rate**	**Roller 1**		**Roller 2**	
	(°C)	(cm^3/min)	(°C)	(m/min)	(°C)	(m/min)
Profile A	230	70	75	100	90	200
Profile B	230	70	75	100	90	130

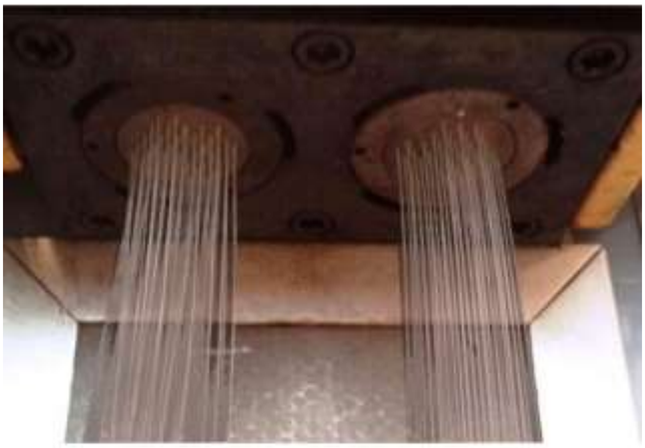

Figure 5.4. The continuous flow of multifilament during melt spinning.

5.2.2. Spinning trials of AlP and lignin-containing blends

The incorporation of AlP and lignin blends complicates the spinning stages as can be seen from Figure 5.5. Spinning trials with PA-LL-AlP and PA-DL-AlP blends resulted in failure. Irrespective of the selected spinning parameters, the non-spinnable blends show an irregular flow with a regular breakage of the multifilament with all temperature profile. This behavior makes it impossible to continue the filaments on the rollers side. This behaviour is attributed to the low ductility of blends, which was indicated during tensile testing.

Figure 5.5. Discontinuity in the spinning (non-spinnable).

5.3. Analysis of multifilaments

The multifilaments based on PA-DL-ZnP and PA-LL-ZnP blends were spun successfully and characterized by optical microscopic analysis to evaluate the surface morphology of the fibres and the surface regularity. In addition, the mechanical properties of the multifilaments are also determined. Finally, fire behaviour is investigated by mass loss calorimetry tests.

Figure 5.6. Picture of multifilaments after melt spinning step.

5.3.1. Microscopic analysis

Microscopic images of monofilament of PA and its blends filled with ZnP and lignin are shown in Figure 5.7. As discussed above, blends from AlP and lignin blends were not spinnable; hence, multifilaments were not obtained for this formulation. Microscopic images provide the qualitative observation of the surface smoothness and regularity in monofilament. In addition to this, the monofilament diameter was also measured on at least 10 samples and the averaged value is reported (Figure 5.8). It can be observed that PA has a smooth and regular surface with an average diameter of 60 ± 5 µm, fibre diameters have no significant deviation (Figure 5.7 (a). The ternary blends of PA-DL-ZnP show that DL and ZnP loading show less effect on surface regularity of monofilament because the surface of the filament stays regular (Figure 5.7 (b-d)). It can be observed that DL and ZnP well mixed and evenly dispersed in the polymer matrix, there was no visible agglomeration observed. These observations explain to reach the required stretching of multifilament and continuous spinning without breaking of filaments. Conversely, the blends, which contain LL and ZnP tend to have an irregular surface and a high variation in the diameter values. This irregularity is related to the agglomeration (up to 10 µm) of particles on the surface. This behaviour affects the spinnability of multifilament, due to this, the stretching speed of roller (R_2) was limited to 130 m/min instead of 200 m/min (Table 5.1).

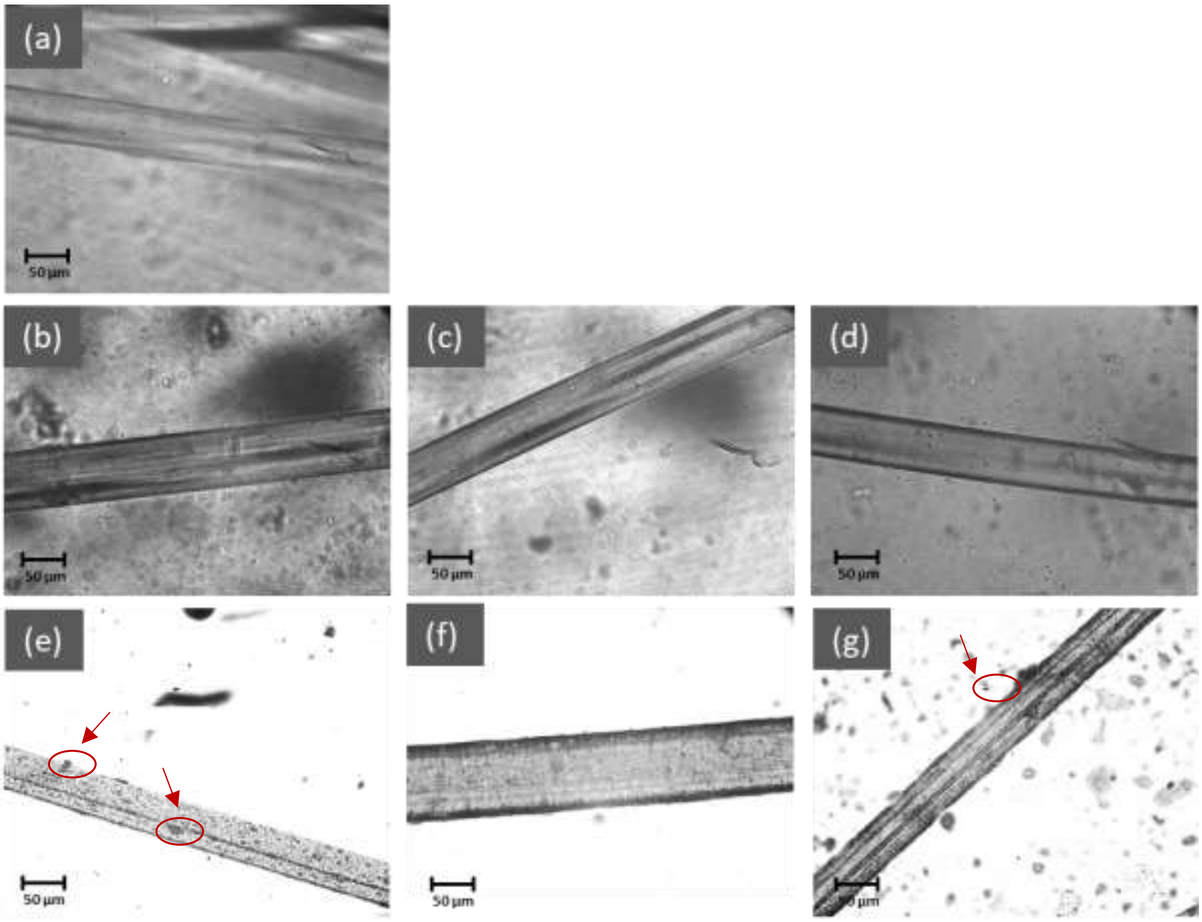

Figure 5.7. Microscopic images of monofilaments, (a) PA, (b) PA_{80}-DL_5-ZnP_{15}, (c) PA_{80}-DL_7-ZnP_{13}, (d) PA_{80}-DL_{10}-ZnP_{10}, (e) PA_{80}-LL_5-ZnP_{15}, (f) PA_{80}-LL_7-ZnP_{13}, (g) PA_{80}-LL_{10}-ZnP_{10}, longitudinal view at 20x magnification.

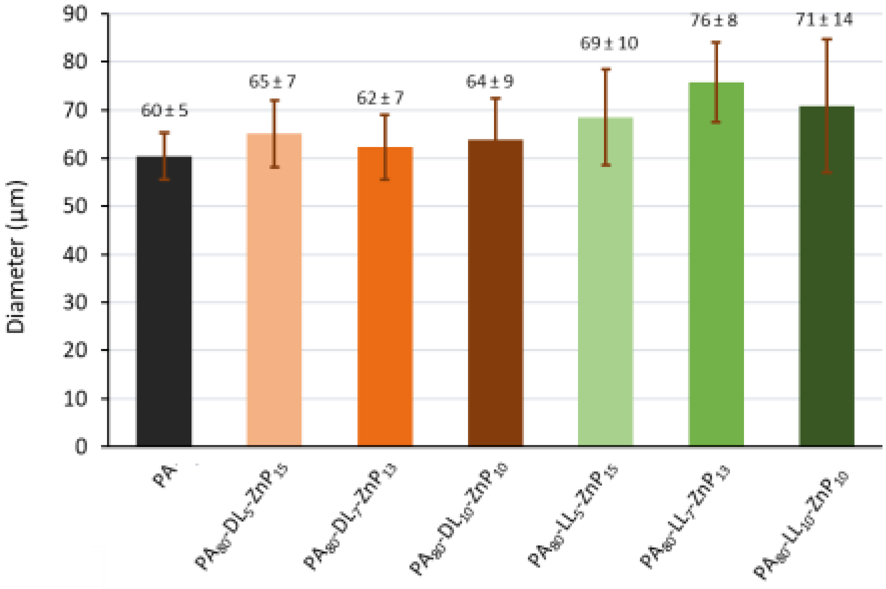

Figure 5.8. Average diameters of monofilaments extracted from multifilaments.

5.3.2. Analysis of mechanical properties

Measurement of the tensile properties of monofilament was carried out on Zwick 1456 device. The force sensor used was 10N. the length between jaws was 20 mm and the crosshead speed was 20 mm/min. At first, the maximum force at the breaking point was measured (Figure 5.9) and then the % elongation of monofilament before breaking was also measured by tensile tests (Figure 5.10). PA shows the force at breaking point around 75 cN and elongation about 195 %. These properties affected with the addition of lignin and FR in PA. The incorporation of DL and ZnP mixture (20 wt%) in PA slightly reduces force at the rupture. This reduction takes place from 75 cN for PA to 57 cN for PA_{80}-DL_7-ZnP_{13}, which is equivalent to a reduction of about -24%. However, the substitution of DL by LL has a significant impact on the force at the rupture of the monofilaments. With respect to PA, these blends (PA-LL-ZnP) show the reduction of force at rupture up to 48%. As far as the elongation at break is concerned, the blends containing DL and ZnP lowers the elongation as compared to unfilled PA. The elongation reduces with increasing loading content of DL in blends. On the other hand, LL and ZnP blends show higher elongation than that of PA, at the same time, higher standard deviation also noticed that reflect the uneven dispersion of additives and the irregularity of monofilaments.

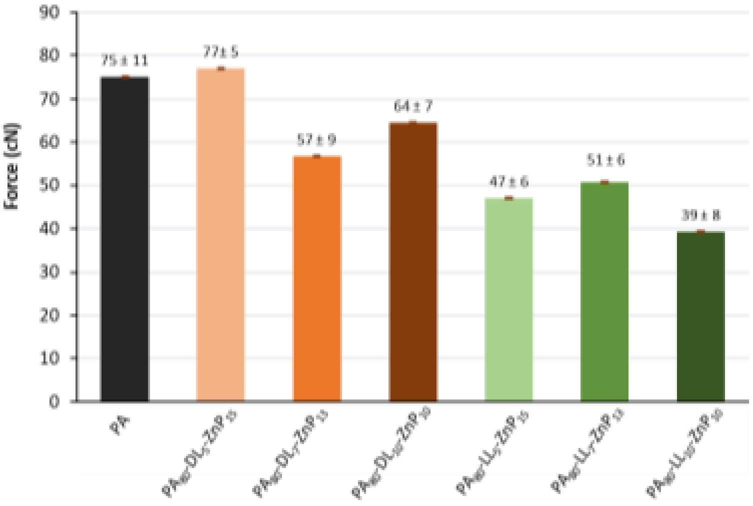

Figure 5.9. Maximum force at breaking point for monofilaments.

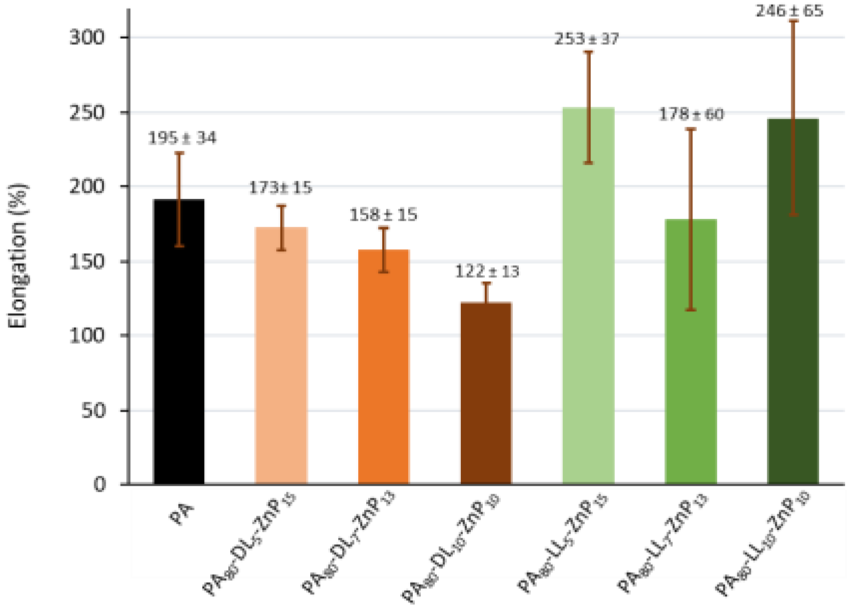

Figure 5.10. Elongation at breaking point for monofilaments.

5.4. Fire behaviour analysis on fabric

Knitted fabrics were produced for all loaded multifilament to prepare samples for fire behaviour testing. Interlock structure of about 1400 ± 50 g/m^2 and thickness of around 3 mm was prepared as described in Chapter 2. A double layer interlock structure was preferred due to its compactness and stability against shrinkage. The influence of different fabric structure on flammability was studied in hybrid viscose blends. It was reported the double layer knitted structure have better flame retardancy than single layer structure (Garvey et al., 1998). Mass loss calorimeter was used to carry out fire testing measurement on fabric samples of 100 mm × 100 mm × 3 mm on a horizontal orientation (Figure 5.11). All tests were performed at 35 kW/m^2. This flux simulates to a heat flux in a mild fire scenario.

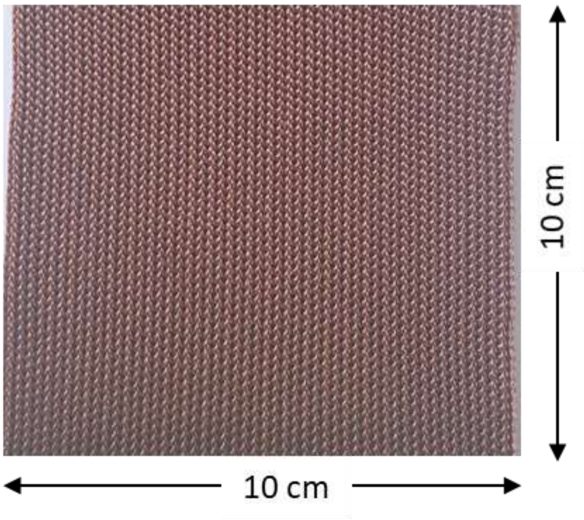

Figure 5.11. knitted fabric structure for fire testing.

HRR and THR curves of fabric from PA and loaded with DL and ZnP are shown in Figure 5.12 (a-b) and residue images of tested samples are shown in Figure 5.13. The averaged results are collected in Table 5.2. The fabric sample of PA ignites after 78s, rapidly increases the HRR and reaches to PHRR about 278 kW/m^2 and then decreases with the total heat released of around 38 MJ/m^2. The PA_{80}-DL_{20} sample delayed TTI to 184s and THR and MARHE are reduced considerably to 17% and 34% compared to PA sample. Furthermore, a visually higher amount of residue is observed due to the presence of DL (Figure 5.13 (c)). However, the HRR and PHRR are not reduced, this indicates that char layer is not capable to reduce the evolution of combustible products. Cayla et al. (2016) also observed the similar behaviour in fabric samples of kraft lignin and PLA blends whereas the HRR and PHRR was not significantly reduced with the lignin addition. Besides, in PA_{80}-ZnP_{20} fabric, the presence of ZnP has no significant reduction in fire properties, except for the THR, which reduce to 15%.

All combinations of DL and ZnP showed postponing in the TTI than that of PA, which is attributed to delaying in the formation of effective gas mixture that can trigger the ignition. In addition, the HRR and PHRR are slightly reduced; at the same time, THR and MARHE greatly influenced in comparison to unfilled PA. For example, PA_{80}-DL_5-ZnP_{15} sample shows the PHRR reduction about 16% and THR around 21% than that of PA, Besides, increasing the lignin content in PA_{80}-DL_7-ZnP_{13} significantly reduces the MARHE up to 54%. This combination gives better fire retardancy compared to the other two formulations. Increasing char residue is observed due to the presence of lignin showing the charring effect.

The cone calorimetry tests carried out at 35 kW/m^2 for these formulations on plate specimen also showed a similar trend in HRR curves. The reduction in PHRR was not significant at lower DL loading content (i.e., 5 and 7 wt%) and the maximum reduction reached 43% with 10 wt% loading of both fillers. It was concluded that the charring effect of DL was less effective than LL blends. The lower reduction of HRR and PHRR indicates that the condensed phase flame retardant action of DL and ZnP is less effective.

Table 5.2. fire testing results on fabric form mass loss calorimeter (heat flux: 35 kW/m^2).

Sample	TTI (s)	PHRR (kW/m^2)	THR (MJ/m^2)	Reduction (%)	MARHE (kW/m^2)	Reduction (%)
PA	78 ± 5	278 ± 2	38 ± 4	-	114 ± 4	-
PA_{80}-DL_{20}	184 ± 68	246 ± 30	31 ± 4	– 17	75 ± 3	–34
PA_{80}-ZnP_{20}	122 ± 21	287 ± 19	32 ± 2	– 15	106 ± 5	–7
PA_{80}-DL_5-ZnP_{15}	209 ± 40	234 ± 1	30 ± 1	– 21	66 ±7	–43
PA_{80}-DL_7-ZnP_{13}	294 ± 42	237 ± 8	32 ± 4	– 16	52 ± 0	–54
PA_{80}-DL_{10}-ZnP_{10}	198 ± 90	247 ± 20	31 ± 0	– 17	75 ± 7	–34

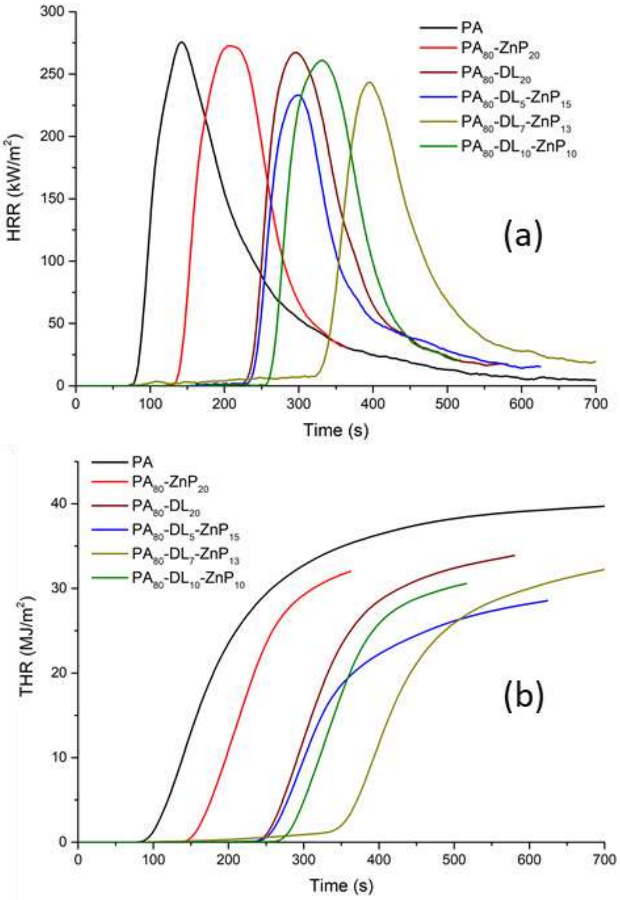

Figure 5.12. Heat release curves for DL and ZnP blends form mass loss calorimeter test at 35 kW/m2, (a) HRR and (b) THR curves.

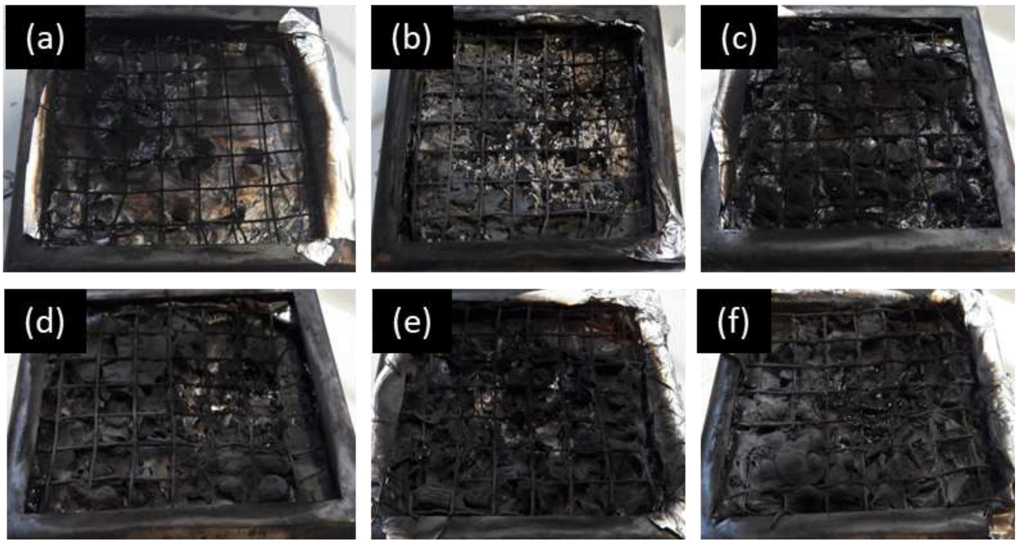

Figure 5.13. Residue images after mass loss calorimeter test (a) PA, (b) PA_{80}-ZnP_{20}, (c) PA_{80}-DL_{20}, (d) PA_{80}-DL_5-ZnP_{15}, (e) PA_{80}-DL_7-ZnP_{13}, (f) PA_{80}-DL_{10}-ZnP_{10}.

5.5. Conclusion

In this chapter, fire retardant PA textiles based on industrial lignin and Phosphinate FR were developed and their fire retardant properties were investigated. Melt fluidity of blends indicated that ternary blends are feasible for the melt spinning and fluidity of the blends remain in the range of fluidity required for the melt spinning set-up (i.e., between 15-30 g/10 min). Spinning trails with AlP and lignin blends were not spinnable due to continuous breakage of multifilament during melt spinning. On the other hand, spinning trails with PA-DL-ZnP and PA-LL-ZnP blends produced continuous multifilament without breaking. PA-DL-ZnP blends produced the multifilaments, which was more or less have a comparable mean diameter to PA multifilaments. However, multifilaments produced from PA-LL-ZnP blends have higher mean diameter about 70-76 µm than PA multifilaments of 60 µm, which is equivalent to a variation of 27%. Tensile tests result showed that PA-DL-ZnP filaments showed a higher value of force at breaking point and higher tenacity as compared to PA-LL-ZnP filaments. Fire testing results with PA-DL-ZnP fabric showed that interaction of DL and ZnP delayed the TTI but has little influence on HRR and PHRR reduction. However, the presence of lignin significantly reduced the THR and MARHE due to the char residue formation showing the charring effect. Among these formulations, best fire-retardant properties were found with PA_{80}-DL_7-ZnP_{13} fabric sample.

References

Cayla, A., Rault, F., Giraud, S., Salaün, F., Fierro, V., Celzard, A., 2016. PLA with intumescent system containing lignin and ammonium polyphosphate for flame retardant textile. Polymers (Basel). 8. https://doi.org/10.3390/polym8090331

Garvey, S.J., Anand, S.C., Rowe, T., Horrocks, A.R., Walker, D., 1998. The effect of fabric structure on the flammability of hybrid viscose blends, in: Fire Retardancy of Polymers. Elsevier, pp. 376–394. https://doi.org/10.1533/9781845698584.4.376

Kun, D., Pukánszky, B., 2017. Polymer/lignin blends: Interactions, properties, applications. Eur. Polym. J. 93, 618–641. https://doi.org/10.1016/J.EURPOLYMJ.2017.04.035

Rault, F., Giraud, S., Salaün, F., Almeras, X., 2015. Development of a halogen free flame retardant masterbatch for polypropylene fibers. Polymers (Basel). 7, 220–234. https://doi.org/10.3390/polym7020220

Sallem-Idrissi, N., Sclavons, M., Debecker, D.P., Devaux, J., 2016. Miscible raw lignin/nylon 6 blends: Thermal and mechanical performances. J. Appl. Polym. Sci. 133, n/a-n/a. https://doi.org/10.1002/app.42963

Sallem-Idrissi, N., Van Velthem, P., Sclavons, M., 2018. Fully Bio-Sourced Nylon 11/Raw Lignin Composites: Thermal and Mechanical Performances. J. Polym. Environ. 26, 4405–4414. https://doi.org/10.1007/s10924-018-1311-7

6. GENERAL CONCLUSION AND FUTURE STUDIES

6.1. General Conclusion

This thesis work was carried out as a part of the SMDTex project into three partner universities; ENSAIT – GEMTEX Laboratory, Politecnico di Torino and Soochow University. Lignin is abundantly available as renewable resources in lignocellulosic biomass and industrial lignin is produced from wood and paper pulping industries as by product and primarily used for energy recovery. However, the biobased character of lignin allows its potential applications in various sectors. Therefore, this Ph.D work aimed at the utilization of lignin as additive (charring agent) for developing biobased flame retardant textile structure. PA was used as polymer matrix for developing flame retarded multifilament and fabric structure. PA has been exploited in various areas including textile applications. However, its low flame-retardant properties and extended dripping limit its potential applications in the textile field. Therefore, it is necessary to flame retard PA in order to widen its areas of application. The entire thesis was divided into five chapters.

The state of the art allowed us to review various FR additives applied to thermoplastic polymers and more specifically to polyamides. Char promoting FRs are found as efficient environmentally friendly non-halogenated FR alternatives. In particular, phosphinate salts (ZnP and AlP) are very effective flame retardants in engineering polymers, because they show their activity in the gas phase as well as in the condensed phase. However, these additives have fairly high cost and exhibit improved FR activity at high loading content (>20 wt%) and therefore have been used in some studied as synergists to reduce their quantity while achieving acceptable fire performance. Literature review study also showed that lignin as biobased material exhibits interesting FR properties, especially because of its charring ability. Since char formation is one of the solutions to confer flame retardancy to the polymers, commercially available lignin revealed as promising FR additive for thermoplastic polymers. Moreover, the addition of FR additive with lignin further improves the fire performance.

Fire retardancy can be accomplished by various methods such as the use of high-performance polymers, grafting of FR molecule into the main chain of the polymer. However, these solutions are costly and difficult to implement in low-cost textile applications. Treatment or finishing of the surface is another method that is easy and cost-effective and applied on synthetic and natural fibres, but treatments are sometimes not durable. Therefore, our choice has been the additive route that consists of mixing FR additive and thermoplastic polymer in the molten stage. Extrusion was chosen as the compounding process. Indeed, it allows incorporating the fire-retardant additives directly in the molten polymer matrix, thus, avoids the durability issue. This method has several advantages such as ease of implementation and low cost. It also allows the possibility to select a wide choice of raw materials with an adaptable mass ratio.

In the first step, the influence of various laboratory and industrial grade lignins and their content on the thermal stability and fire retardancy of PA was investigated. The binary blends based on PA and containing 5, 10, 15, and 20 wt % of different lignins (sulphonated and kraft lignins) were prepared using a twin-screw extruder. SEM morphology showed good interfacial interaction and dispersion state of lignin particles in the polymer phase. TG analyses of the prepared blends showed that the presence of sulphonate group in LL and LS was responsible for the formation of high quantity of char residue (55 – 58 wt% at 600 °C), while, the kraft lignin give rise to the formation of lower char residue (41 – 48 wt%). Furthermore, UL94 vertical flame test showed that 15 wt% is the optimal lignin loading which achieves improved FR properties for LL. Fire behaviour analysis performed by cone calorimetry showed that the blends containing sulphonate lignin (LL and LS) demonstrated significant reductions of PHRR (–51%) and of THR (–23%) due to the formation of a stable char residue (charring effect). Conversely, the microcomposites containing kraft lignins showed the detrimental effect, because formed char residue was not capable of reducing HRR and THR values.

Char forming ability of following lignins was exploited for designing FR formulation. Lignins were combined with commercially available phosphinate FR. In the primary study, LS (laboratory grade lignin) was combined with ZnP. Various formulations of ternary blends including LS with ZnP were prepared by extrusion in order to optimize the ratio to evaluate fire retardant behaviour. TGA showed that the incorporation of lignin in the ternary blends increased the thermal stability of PA, promoting the formation of a stable char residue at the end of the experiments. Besides, the study of evolved gas revealed that ternary blends mainly produces phosphinate ion and hydrocarbons along with the small amount of phosphinic acid during the main degradation stage. Flammability tests showed that the addition of sulphonated lignin LS improved the FR properties due to the char formation and most enhanced results were achieved when 10 wt% LS and ZnP were combined. In addition to this, cone calorimetry results showed the interactions between lignin and ZnP promoted a significant reduction of PHRR and THR. This finding was attributed to the formation of a protective char layer. The most enhanced results were found when 10 wt% of LS and ZnP were combined. Moreover, increasing lignin content also effectively reduced the CO and CO_2/CO yield compared to unfilled PA.

In the next step, for the practical valorization of lignin, low-cost industrial lignins were directly mixed with commercial phosphinates FR for scale-up and production of multifilament. The most produced industrial lignin, i.e., lignosulphonate and kraft lignin were used as carbon source in combination with ZnP and AlP. Dispersion of lignin and FR in PA assessed by SEM showed that ternary blends of ZnP and lignin show uniform dispersion in PA matrix. However, LL and AlP blends show agglomerates about 10 µm. TG analyses showed that the incorporation of lignin in ternary blends increased the thermal stability of PA, promoting the formation of a stable char residue at the end of the tests. The addition of LL favoured the higher char formation due to the presence sulphonate groups and the char residue obtained from ZnP blends was higher than that of AlP containing ternary blends, showing the interaction between ZnP and lignin favour the formation of a stable char residue. Flammability tests showed the combination of LL and ZnP effectively improves FR properties by reducing total combustion time, self-extinction and the V-1 rating was achieved for PA_{80}-LL_{7}-ZnP_{13} and PA_{80}-LL_{10}-ZnP_{10} blends. Conversely, the combination of lignin with AlP did not improve the FR properties, all blends showed V-2 rating. Cone calorimetry results showed the interactions between lignin and phosphinate promoted reduction of PHRR and THR. In particular, the best fire-retardant performance was achieved by combining LL with AlP (i.e., PA_{80}-LL_{10}-AlP_{10}), resulting in a strong reduction of PHRR (– 74 %). The presence of lignin in ternary blends reduced the CO and CO_2/CO yield compared to PA. Particularly, PA_{80}-LL_{10}-ZnP_{10} blend shows minimum CO release without affecting fire performance. The morphology of char residue showed that the formation of compact char layer is primarily responsible for the improved fire-retardant properties.

In the last chapter, industrial lignin and phosphinate FR combinations were used to develop multifilaments using melt spinning process. MFI value showed the feasibility of blends for melt spinning. All the lignin (DL/LL) and ZnP based blends were successfully transformed into multifilaments. However, the spinning of AlP and lignin (DL/LL) mixture was not spinnable and showed the irregular flow of material with certain breakage of filaments. Multifilaments obtained from DL and ZnP have a comparable mean diameter to PA multifilaments (about 60 µm), whereas LL and ZnP blends showed higher mean diameter about 70 – 76 µm with the variation of 27% with respect to PA. Mechanical testing results showed that PA-DL-ZnP filaments have higher tensile strength than PA-LL-ZnP filaments. Fire testing of PA-DL-ZnP fabric showed that the combination of DL and ZnP has little influence on HRR and PHRR reduction. However, the presence of lignin significantly reduced the THR and MARHE due to the char residue formation showing the charring effect.

6.2. Future studies

This PhD work confirms that lignin can be a promising additive in designing the FR system. It also demonstrates that combination with phosphinates improves its FR performance in PA polymer matrix. Several efforts have been undertaken to explain the mode of action of lignin in this polymer and many experiments were carried out for a better understanding. However, many perspectives have emerged in this dissertation. For example, the fire behaviour of lignin and phosphinates (ZnP/AlP) were discussed in detail, but the contribution of lignin as a synergistic agent is still unexplained. Some ratios were found to be more efficient than others when the loading of both additives in ternary blends reached to 10 wt% the cone calorimetry and UL94 tests showed the best results. Further investigation on lignin/phosphinate synergism should be done to know if the effect comes from the "lignin" or the "phosphinate".

Considering the mode of action in the condensed phase, it was directly assumed that during combustion test sulphonate group containing lignin blends likely to decompose by releasing SO_2, thus limiting the heat release and transformed into thermally stable Na_2SO_4 in the condensed phase. This finding might be explained by detecting SO_2 release during combustion test. Another question arises regarding the flame-retardant action in UL94 test, it was assumed that ZnP decomposition release phosphinate compounds in the gas phase that can form $P-O^{\bullet}$ radicals, which may act as radical scavengers and lead to flame inhibition through radical trapping. The evolution of $P-O^{\bullet}$ radical can be investigated by GC-MS analysis. As far as condensed phase mechanism is concerned, it was concluded that fire retardant properties improved due to protective char layer formation. It would be interesting to deepen the study of char formation; the cone calorimeter tests with interrupted at a key moment might give more understanding about char formation. It would also be possible to evaluate the distribution of phosphorus in particular during the formation of char.

In this study, the fire performance of PA-DL-ZnP fabric sample was presented. However, PA-LL-ZnP knitted fabric structures were not prepared due to difficulty in knitting with these multifilament fire performances will be studied. Further experiments would be considered, for knitted structure preparation and fire testing of fabric samples

▪ Replacement of phosphinate by biobased phosphorus source

In future studies to develop fully biobased flame-retardant textile to maintain the good environmental profile of the resulting blends, lignin (as charring agent) can be combined with another biobased compound (acid source). In this regard, phosphinate FR can be replaced by biobased acid source. Phytic acid seems to be a good candidate for this purpose. In fact, phytic acid, a saturated cyclic acid, is the principal storage form of phosphorus in plant seeds and contains high phosphorus content (28 wt%). Its flame retardant effect has been proved in many applications (Cheng et al., 2018; Feng et al., 2017; Laoutid et al., 2018; Zhang et al., 2018). The chemical structure of phytic acid is presented in Figure 6.1.

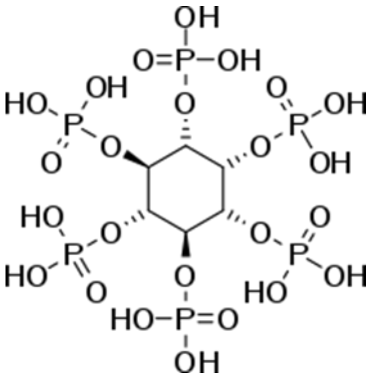

Figure 6.1. Chemical structure of phytic acid.

▪ Thermal stability of phytic acid and lignin combination

Figure 6.2 shows the thermo-oxidative decomposition of the dried phytic acid, LL and the combination of both. The decomposition of phytic acid takes place in several degradation steps that have been reported in the literature (Daneluti and Matos, 2013) and correspond to dehydration, carbonization and char degradation reaction. It was observed that below 600 °C, only dehydration and carbonization reaction take place. Above 600 °C, thermal decomposition of the char takes place leading to a final char residue of about 45 % at 800 °C. In order to evaluate the interest of phytic acid/lignin combination, we studied the thermal behaviour of phytic acid/LL. Dried phytic acid was mixed with an equal amount of LL and mechanically mixed, and then the mixture was dried at 80 °C for 6 hours. From the TGA in air, it was observed that $T_{5\%}$ slightly shifts to higher side but still not stable enough with PA processing condition. This indicates no interaction occurs when they are mixed directly. Thus, they cannot be used as additive in direct form.

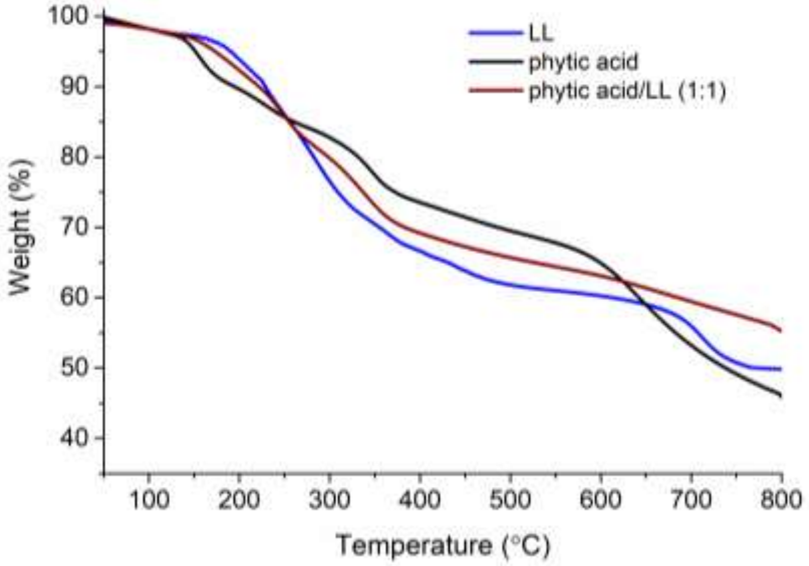

Figure 6.2. TGA of LL, phytic acid and its combination, at 10 °C/min in air.

Phytic acid has a remarkable P/C atomic ratio (1/1) with the unique chelating ability with most metals (Ekholm et al., 2003; Nassar et al., 2015). The application of phytic acid as flame retardant has been widely described, but the application of metal phytate (salt of phytic acid) as flame retardant are limited. Metal phytates are more thermally stable than phytic acid; however, their charring ability depends on the metal cation. L. Costes et al. studied the FR effect of different metallic phytates as biobased phosphorus additives for PLA. Different metallic cations were prepared from Na-phytate. It was found that different metallic cations lead to some difference in the initial decomposition temperature and the formation of char at the end of the test (Costes et al., 2015). Recently, W Yang et al. used Ca-Ma-phytate with CNT for providing mechanical and FR properties for PLA biocomposite. The compounding process was performed at 185 °C using a co-rotating twin-screw extruder (Yang et al., 2018). These studies indicate that it would be interesting to synthesize different metallic phytates and find a suitable one which can be processed with PA in combination with lignin.

References

Cheng, X.W., Guan, J.P., Yang, X.H., Tang, R.C., 2018. Durable flame retardant wool fabric treated by phytic acid and TiO2 using an exhaustion-assisted pad-dry-cure process. Thermochim. Acta 665, 28–36. https://doi.org/10.1016/j.tca.2018.05.011

Costes, L., Laoutid, F., Dumazert, L., Lopez-Cuesta, J.M., Brohez, S., Delvosalle, C., Dubois, P., 2015. Metallic phytates as efficient bio-based phosphorous flame retardant additives for poly(lactic acid). Polym. Degrad. Stab. 119, 217–227. https://doi.org/10.1016/j.polymdegradstab.2015.05.014

Daneluti, A.L.M., Matos, J. do R., 2013. Study of thermal behavior of phytic acid. Brazilian J. Pharm. Sci. 49, 275–283. https://doi.org/10.1590/S1984-82502013000200009

Ekholm, P., Virkki, L., Ylinen, M., Johansson, L., 2003. The effect of phytic acid and some natural chelating agents on the solubility of mineral elements in oat bran. Food Chem. 80, 165–170. https://doi.org/10.1016/S0308-8146(02)00249-2

Feng, Y., Zhou, Y., Li, D., He, S., Zhang, F., Zhang, G., 2017. A plant-based reactive ammonium phytate for use as a flame-retardant for cotton fabric. Carbohydr. Polym. 175, 636–644. https://doi.org/10.1016/j.carbpol.2017.06.129

Laoutid, F., Vahabi, H., Shabanian, M., Aryanasab, F., Zarrintaj, P., Saeb, M.R., 2018. A new direction in design of bio-based flame retardants for poly(lactic acid). Fire Mater. 42, 914–924. https://doi.org/10.1002/fam.2646

Nassar, M., Hiraishi, N., Tamura, Y., Otsuki, M., Aoki, K., Tagami, J., 2015. Phytic acid: An alternative root canal chelating agent. J. Endod. 41, 242–247. https://doi.org/10.1016/j.joen.2014.09.029

Yang, W., Tawiah, B., Yu, C., Qian, Y.F., Wang, L.L., Yuen, A.C.Y., Zhu, S.E., Hu, E.Z., Chen, T.B.Y., Yu, B., Lu, H.D., Yeoh, G.H., Wang, X., Song, L., Hu, Y., 2018. Manufacturing, mechanical and flame retardant properties of poly(lactic acid) biocomposites based on calcium magnesium phytate and carbon nanotubes. Compos. Part A Appl. Sci. Manuf. 110, 227–236. https://doi.org/10.1016/j.compositesa.2018.04.027

Zhang, X., Zhou, X.Y., Cheng, X.W., Tang, R.C., 2018. Phytic acid as an eco-friendly flame retardant for silk/wool blend: A comparative study with fluorotitanate and fluorozirconate. J. Clean. Prod. 198, 1044–1052. https://doi.org/10.1016/j.jclepro.2018.07.103

Appendix

Appendix 1a. MFI values of PA and binary blends with lignin.

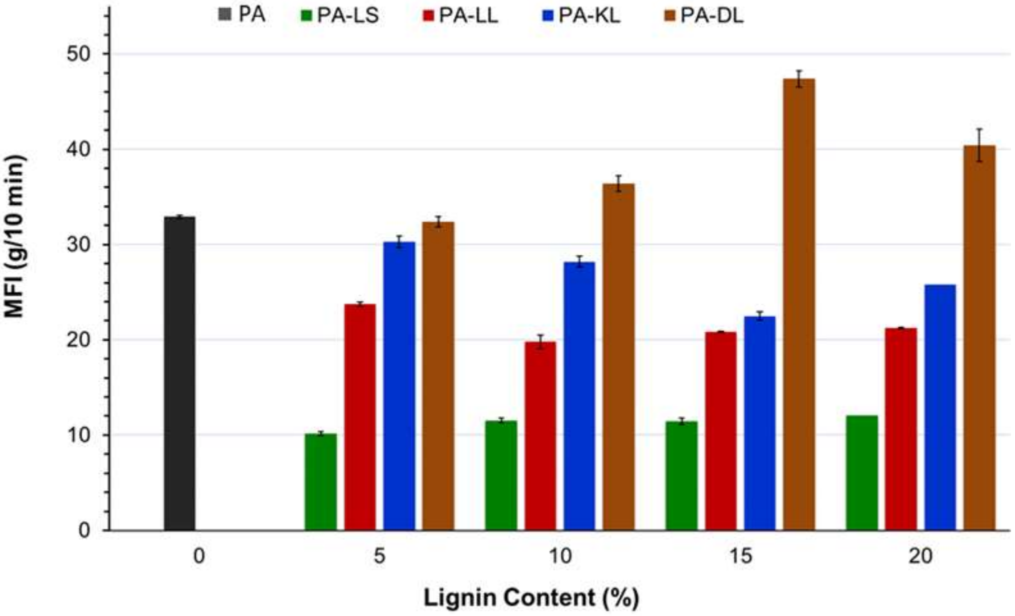

Appendix 1b. MFI values of PA and its ternary blends with LS and ZnP.

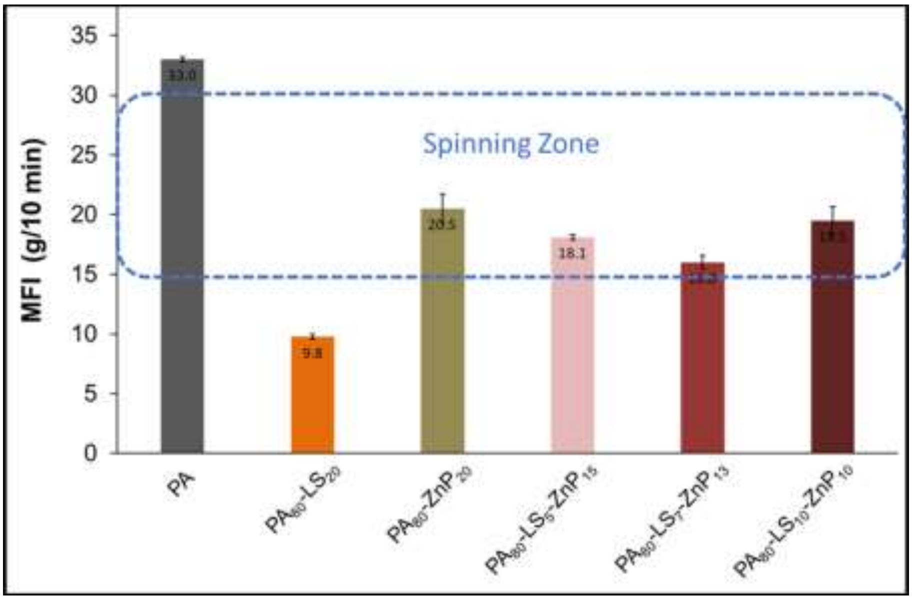

Appendix 2. Tensile test load-elongation curve for binary blends.

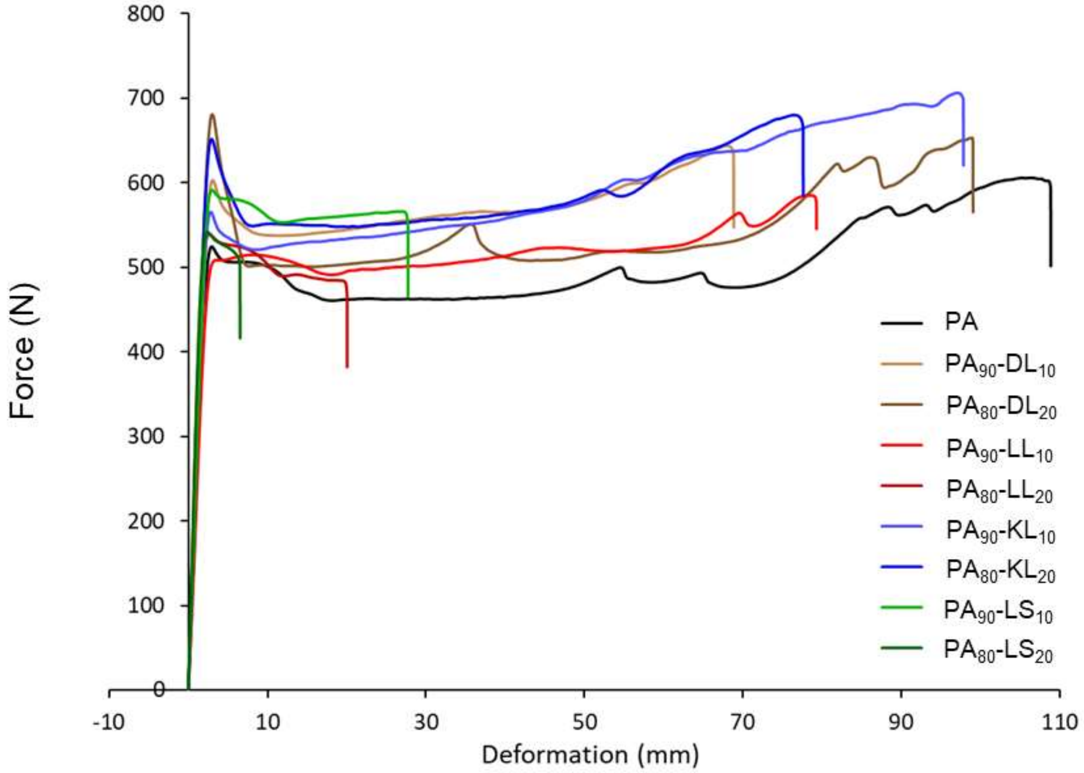

Appendix 3. SEM micrographs of Clariant phosphinate FR, (a) ZnP and (b) AlP.

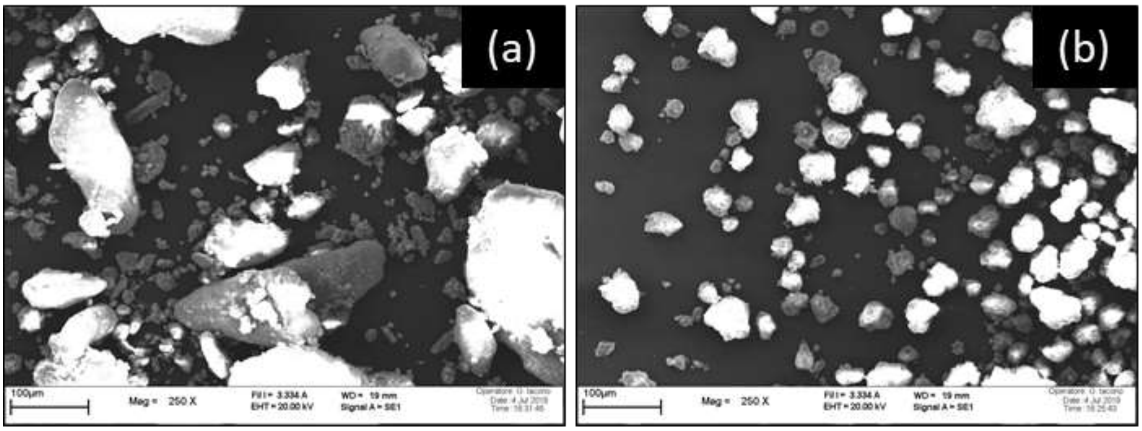

Research Publications

Peer reviewed journal papers

- N. Mandlekar, A. Cayla, F. Rault, S. Giraud, F. Salaün, G. Malucelli, J. Guan. Thermal stability and fire retardant properties of polyamide 11 microcomposites containing different Lignins. *Industrial & Engineering Chemistry Research, 2017, 56, 13704-13714. DOI: 10.1021/acs.iecr.7b03085*
- N. Mandlekar, G. Malucelli, A. Cayla, F. Rault, S. Giraud, F. Salaün, J. Guan. Fire retardant action of zinc phosphinate and polyamide 11 blends containing lignin as a carbon source. *Polymer Degradation and Stability, 2018, 153, 63-74.* doi:org/10.1016/j.polymdegradstab.2018.04.019
- Neeraj Mandlekar, Aurelie Cayla, Francois Rault, Stephane Giraud, Fabien Salaün, Jinping Guan. Valorization of industrial lignin as biobased carbon source in fire retardant system for polyamide 11 blends. *MDPI Polymers, 2019, 11, 180*. doi:10.3390/polym11010180

Conference paper

- N. Mandlekar, A. Cayla, F. Rault, S. Giraud, F. Salaün, G. Malucelli, J. Guan. Intumescent formulations based on lignin and phosphinates for the bio-based textiles. 17th AUTEX world textile conference. *IOP Conf. Series: Materials Science and Engineering, 2017, 254, 052004*. doi:10.1088/1757-899X/254/5/052004

Book chapter

- N. Mandlekar, A. Cayla, F. Rault, S. Giraud, F. Salaün, G. Malucelli, J. Guan. An Overview on the Use of Lignin and Its Derivatives in Fire Retardant Polymer Systems. Book "Lignin - Trends and Applications", *Publication Intech Open, Editor, Matheus Poletto, ISBN 978-953-51-3902-7*. doi.org/10.5772/intechopen.72963

Participation in conferences

Oral presentation

- N. Mandlekar, A. Cayla, F. Rault, S. Giraud, F. Salaün, G. Malucelli, J. Guan. Overview of lignin used as flame retardant additive: Textile applications. Presented at - *Eco-friendly flame retardant material (ECOFRAM) - 2016, Mons, Belgium*.
- N. Mandlekar, A. Cayla, F. Rault, S. Giraud, F. Salaün, G. Malucelli, J. Guan. Intumescent formulations based on lignin and phosphinates for bio-based flame retardant textiles. Presented at - *World Textile Conference (AUTEX) – 2017, Corfu, Greece*.

Poster presentation

- N. Mandlekar, A. Cayla, F. Rault, S. Giraud, F. Salaün, G. Malucelli, J. Guan. Integration of wood waste to develop biobased fire retardant textile structures. Presented at - *9ème Journée des Doctorants – 2016, Université du Lille, Douai, France.*
- N. Mandlekar, A. Cayla, F. Rault, S. Giraud, F. Salaün, G. Malucelli, J. Guan. Utilization of industrial lignin as fire retardant additive in polymer system for the textile applications. Presented at - *Third European Conference on Fire-safe Textiles and plastics – 2017, Ghent, Belgium.*